

TABLE OF CONTENTS

2.0	STRUCTURAL EVALUATION.....	2-1
2.1	Description of Structural Design	2-1
2.1.1	Discussion.....	2-1
2.1.2	Design Criteria.....	2-3
2.1.2.1	Basic Design Criteria	2-3
2.1.2.2	Miscellaneous Structural Failure Modes.....	2-3
2.1.3	Weights and Centers of Gravity	2-4
2.1.4	Identification of Codes and Standards for Package Design.....	2-4
2.2	Materials	2-5
2.2.1	Material Properties and Specifications	2-5
2.2.2	Chemical, Galvanic, or Other Reactions	2-5
2.2.3	Effects of Radiation on Materials	2-5
2.3	Fabrication and Examination.....	2-7
2.3.1	Fabrication	2-7
2.3.2	Examination.....	2-7
2.4	Lifting and Tie-down Standards for All Packages	2-8
2.4.1	Lifting Devices	2-8
2.5	General Considerations	2-9
2.5.1	Evaluation by Test.....	2-9
2.5.2	Evaluation by Analysis.....	2-11
2.6	Normal Conditions of Transport	2-12
2.6.1	Heat.....	2-12
2.6.1.1	Summary of Pressures and Temperatures	2-12
2.6.1.2	Differential Thermal Expansion.....	2-12
2.6.1.3	Stress Calculations	2-12
2.6.1.4	Comparison with Allowable Stresses.....	2-13
2.6.2	Cold	2-13
2.6.3	Reduced External Pressure	2-13
2.6.4	Increased External Pressure.....	2-13
2.6.5	Vibration.....	2-13
2.6.6	Water Spray	2-14A
2.6.7	Free Drop.....	2-14A
2.6.8	Corner Drop	2-15
2.6.9	Compression – Stacking Test	2-15
2.6.10	Penetration	2-15
2.7	Hypothetical Accident Conditions	2-16
2.7.1	Free Drop.....	2-23
2.7.1.1	Technical Basis for the Free Drop Tests	2-23
2.7.1.2	Test Sequence for the Selected Tests	2-24
2.7.1.3	Summary of Results from the Free Drop Tests.....	2-24
2.7.2	Crush.....	2-24
2.7.3	Puncture	2-25

TABLE OF CONTENTS (cont)

2.7.3.1	Technical Basis for the Puncture Drop Tests	2-25
2.7.3.2	Summary of Results from the Puncture Drop Test	2-26
2.7.4	Thermal.....	2-26
2.7.4.1	Summary of Pressures and Temperatures	2-27
2.7.4.2	Differential Thermal Expansion.....	2-27
2.7.4.3	Stress Calculations	2-27
2.7.4.4	Comparison with Allowable Stresses.....	2-27
2.7.5	Immersion – Fissile Material	2-27
2.7.6	Immersion – All Packages	2-28
2.7.7	Summary of Damage	2-28
2.8	Accident Conditions for Air Transport of Plutonium.....	2-29
2.9	Accident Conditions for Fissile Material for Air Transport.....	2-30
2.10	Special Form.....	2-31
2.11	Fuel Rods.....	2-32
2.11.1	Rod Pipe.....	2-32
2.12	Appendices	2-33
2.12.1	References	2-33
2.12.2	Container Weights and Centers of Gravity	2-34
2.12.2.1	Container Weights	2-34
2.12.2.2	Centers of Gravity	2-34
2.12.3	Mechanical Design Calculations for the Traveller XL Shipping Package	2-36
2.12.3.1	Analysis Results and Conclusions	2-38
2.12.3.2	Calculations.....	2-40
2.12.4	Drop Analysis for the Traveller XL Shipping Package	2-67
2.12.4.1	Conclusion and Summary of Results	2-67
2.12.4.2	Predicted Performance of the Traveller Qualification Test Unit.....	2-68
2.12.4.3	Comparison of Test Results and Predictions.....	2-116
2.12.4.4	Discussion of Major Assumptions	2-128
2.12.4.5	Calculations.....	2-129
2.12.4.6	Model Input.....	2-135C
2.12.4.7	Evaluations, Analysis and Detailed Calculations	2-142
2.12.4.8	Accelerometer Test Setup	2-143
2.12.4.9	Bolt Factor of Safety Calculation.....	2-144
2.12.5	Traveller Drop Tests Results.....	2-148
2.12.5.1	Prototype Test Unit Drop Tests	2-148
2.12.5.2	Qualification Test Unit Drop Tests	2-167
2.12.5.3	Certification Test Unit Drop Tests	2-183
2.12.5.4	Application to Higher Contents Weights	2-192
2.12.5.5	Conclusions.....	2-192C

TABLE OF CONTENTS (cont)

2.12.6Supplement to Drop Analysis for the Traveller XL Shipping Package – Clamshell Axial Spacer Structural Evaluation.....	2-201
2.12.6.1Background	2-202
2.12.6.2Conclusions.....	2-202
2.12.6.3Detailed Calculations and Evaluations	2-202
2.12.7Supplement to Drop Analysis for the Traveller XL Shipping Package – Clamshell Removable Top Plate Structural Evaluation	2-212
2.12.7.1Background	2-212
2.12.7.2Conclusions.....	2-214
2.12.7.3Detailed Calculations and Evaluations	2-214
2.12.8Supplement to Drop Analysis for the Traveller XL Shipping Package – Structural Analysis of the Traveller VVER Shipping Package.....	2-219

LIST OF TABLES

Table 2-1	Summary of Traveller STD, Traveller XL and Traveller VVER Design Weights	2-4	
Table 2-2	Safety-Related Materials Used in the Traveller Packages	2-6	
Table 2-3	Summary of Regulatory Requirements	2-9	
Table 2-4	Summary of Traveller Mechanical Analysis	2-11	
Table 2-5	Summary of the Development of the Traveller	2-17	
Table 2-6	Traveller STD, Traveller XL, and Traveller VVER Design Weights	2-34	
Table 2-7	Deleted		
Table 2-8	Deleted		
Table 2-9	Deleted		
Table 2-10	Top Outpack Latch Bolt Minimum Factors of Safety (FS) for 9m Side Dropped	2-77	
Table 2-11	Top Outpack Hinge Bolt Minimum Factors of Safety (FS) for 9m Side Drop	2-78	
Table 2-12	Clamshell Keeper Bolt Minimum Factors of Safety for 9m Side Drop	2-80	
Table 2-13	Clamshell Bottom Plate Bolt Minimum Factor of Safety for 9m Side Drops.....	2-81	
Table 2-14	Clamshell Grooved Top Plate Bolt Minimum Factors of Safety for 9m Side Drops	2-82	
Table 2-15	Clamshell Lipped Top Plate Bolt Minimum Factors of Safety for 9m Side Drops	2-83	
Table 2-16	Top Outpack Latch Bolt Minimum Factors of Safety for 9m CB-Forward of Corner Drops	2-93	
Table 2-17	Top Outpack Hinge Bolt Minimum Factors of Safety for 9m CB Forward of Corner Drops	2-93	
Table 2-18	Clamshell Keeper Bolt Minimum Factors of Safety for 9m CG-Forward-of- Corner Drops	2-94	
Table 2-19	Clamshell Bottom Plate bolt Minimum Factors of Safety for 9m CG-Forward- of-Corner Drops.....	2-95	
Table 2-20	Clamshell Grooved Top Plate Bolt Minimum Factors of Safety for 9m CG-Forward-of-Corner Drops	2-95	
Table 2-21	Clamshell Lipped Top Plate Bolt Minimum Factors of Safety for 9m CG-Forward-of-Corner Drops	2-96	
Table 2-22	Prototype Tests Used to Compare with Analysis	2-117	
Table 2-23	Comparison of Predicted and Actual Deformations for Test 1-1	2-121	
Table 2-24	Initial Velocities 9 Meter Drop and 1 Meter Pin Puncture Analyses	2-136	
Table 2-25	Summary of Elastic Properties	2-142	
Table 2-26	Bolt Strength Summary	2-145	

LIST OF TABLES (cont.)

Table 2-27	Strengths of Various Classifications of Bolts [14]	2-146
Table 2-28	Bolt Strength Ratio	2-147
Table 2-29	Series 1 As-Tested Drop Conditions	2-150
Table 2-30	Measured Decelerations in Prototype Test 1.1	2-156
Table 2-31	Measured Accelerations in Test 1.2	2-158
Table 2-32	Prototype Test Series 2	2-159
Table 2-33	Traveller Prototype Drop Tests Performed in Test Series 3	2-165
Table 2-34	QTU-1 Measured Weight	2-167
Table 2-35	QTU-1 Drop Test Orientations	2-168
Table 2-36	Key Dimensions of QTU-1 Fuel Assembly Before Testing	2-173
Table 2-37	QTU-1 Fuel Assembly Grid Envelope After Testing	2-174
Table 2-38	QTU-1 Fuel Rod Pitch Data After Testing	2-175
Table 2-39	QTU Series 2 As-Tested Drop Conditions	2-175
Table 2-40	QTU-2 Weights	2-176
Table 2-41	Key Dimensions of QTU-2 Fuel Assembly Before Testing	2-181
Table 2-42	QTU-2 Fuel Assembly Grid Envelope After Testing	2-182
Table 2-43	QTU-2 Fuel Rod Pitch Data After Testing	2-183
Table 2-44	Test Weights	2-185
Table 2-45	CTU Drop Test Orientations	2-186
Table 2-46	Fuel Assembly Key Dimension Before Drop Test	2-196
Table 2-47	CTU Fuel Assembly Grid Envelop Dimensions After Testing	2-197
Table 2-48	CTU Fuel Assembly Rod Envelope Data After Testing	2-198
Table 2-49	CTU Fuel Assembly Rod Envelope After Testing	2-199
Table 2-50	CTU Fuel Rod Gap and Pitch Inspection After Testing	2-200
Table 2-51	Dimension and Material Properties of Axial Spacer	2-205
Table 2-52	Aluminum Properties	2-206
Table 2-53	Annealed 304 Stainless Steel Properties	2-206
Table 2-54	Crushable Foam Properties	2-206
Table 2-55	Neoprene (60 durometer) Properties	2-206
Table 2-56	Aluminum Properties for Traveller VVER Analysis	2-232
Table 2-57	Annealed 304 Stainless Steel Properties for Traveller VVER Analysis	2-232
Table 2-58	Crushable Foam Properties for Traveller VVER Analysis	2-233

LIST OF FIGURES

Figure 2-1	Traveller STD Exploded View	2-2
Figure 2-1A	Sample of Clamshell Accelerations Measured During Road Test (May 11, 2004)	2-14
Figure 2-1B	Impact Limiter “Pillow” Assembly	2-22A
Figure 2-1C	Container Bottom End	2-22A
Figure 2-1D	Impact Limiter “Pillow” Assembly	2-22B
Figure 2-1E	Bottom Plate – Viewed from Inside	2-22B
Figure 2-1F	CTU Package Bottom End	2-22C
Figure 2-2	Traveller XL and Traveller STD Dimensions and Center of Gravity (Note: End View is Common to both Models)	2-35
Figure 2-3	Westinghouse Fresh Fuel Shipping Package, the Traveller XL	2-36
Figure 2-4	Internal View of the Traveller Shipping Package	2-37
Figure 2-5	Traveller Lifting Configurations	2-43
Figure 2-6	Lifting Hole Force Detail	2-44
Figure 2-7	Lifting Bracket Fabrication Detail	2-45
Figure 2-8	Hole Tear-out Model and Mohr’s Circle Stress State	2-46
Figure 2-9	Traveller STD Stacked Lifting Configuration	2-48
Figure 2-10a	Forklift Handling XL Model and Assumed Cross Section	2-49
Figure 2-10b	Forklift Pocket Weld Detail	2-50A
Figure 2-10c	Leg Assembly Loading Condition During Inadvertent Tie-Down	2-51
Figure 2-10d	Welding Depiction at Representative Gusset Plate	2-51A
Figure 2-10e	Welding Depiction at Cross Member	2-51B
Figure 2-10f	Lift Eye Loading Assumed Conditions During Inadvertent Tie-Down	2-51C
Figure 2-10g	Vertical Lift Eye Welding Configuration	2-51D
Figure 2-10h	Combined Shear Lift Eye Welding Configuration	2-51F
Figure 2-11	Typical Temperature Dependent Tensile Properties for Tempered 6000 Series Al	2-52
Figure 2-12	Temperature Dependent Tensile Properties for 304 SS	2-53
Figure 2-13	Temperature Dependent Crush Strength for 10 PCF Polyurethane Foam	2-54
Figure 2-14	Temperature Dependent Crush Strength for 20 PCF Polyurethane Foam	2-54
Figure 2-15	Temperature Dependent Crush Strength for 6 PCF Polyurethane Foam	2-55
Figure 2-16	Temperature Dependent Crush Strength for Traveller Foam at 10% Strain	2-55

Figure 2-17	Compression/Stacking Requirement Analysis Model.....	2-58
Figure 2-18	Stacking Force Model on Stacking Bracket.....	2-59
Figure 2-19	Outerpack Section Compression Model.....	2-60
Figure 2-20	Leg Support Section Compression Model.....	2-63
Figure 2-21	Traveller Stiffeners, Legs, and Forklift Pockets.....	2-69
Figure 2-22	Results of Prototype Drop Test	2-70
Figure 2-23	Side Drop Orientation.....	2-70
Figure 2-24	Low Angle Drop Orientation.....	2-71
Figure 2-25	Damage from Prototype Low Angle Drop (Test 1.1).....	2-71
Figure 2-26	Horizontal Drop Orientation.....	2-72
Figure 2-27	Predicted Energy and Work for 9m Horizontal Drop Onto Outerpack Hinges	2-73
Figure 2-28	Predicted Energy and Work Histories for a 9m Horizontal Drop Onto the Outerpack Hinges	2-73
Figure 2-29	Predicted Rigid Wall Force Histories for 9m Horizontal Drops Onto the Outerpack Latches and Hinges.....	2-74
Figure 2-30	De-coupled Impacts for 9 m Horizontal Side Drop.....	2-75
Figure 2-31	Bolts on Prototype Outerpack	2-76
Figure 2-32	Bolt Labels for Right Outerpack	2-77
Figure 2-33	Bolt Labels for Left Outerpack.....	2-79
Figure 2-34	Clamshell Closure Latches and Keeper Bolts	2-79
Figure 2-35	Clamshell Keeper Bolt Labels.....	2-80
Figure 2-36	Clamshell Top and Bottom End Plates.....	2-81
Figure 2-37	Clamshell Bottom Plate Bolt Labels	2-82
Figure 2-38	Clamshell Bottom Plate Bolt Labels	2-83
Figure 2-39	Clamshell Doors	2-84
Figure 2-40	Clamshell Response during Side Drop.....	2-85
Figure 2-41	Clamshell Doors at Bottom Plate	2-85
Figure 2-42	Predicted Response of Clamshell Bottom Plate and Doors During 9m Horizontal Drop onto Outerpack Latches.....	2-86
Figure 2-43	Top Nozzle Analysis Drop Orientation.....	2-87
Figure 2-44	Location of Impact	2-87

LIST OF FIGURES (cont.)

Figure 2-45	Damage to Outerpack During Angled Drop onto Top Nozzle End of Package.....	2-88
Figure 2-46	Predicted Deformation of Outerpack Top Nozzle Impact Limiter.....	2-88
Figure 2-47	Predicted Pin Puncture Orientation after a CG-Forward-of-Corner Test.....	2-89
Figure 2-48	Outerpack Top Separation vs. Drop Angle	2-90
Figure 2-49	Predicted Energy and Work Histories for 9 m CG-over-Corner Drop onto the Top Nozzle End at Various Angles.....	2-91
Figure 2-50	Predicted Rigid Wall Forces	2-92
Figure 2-51	Clamshell Top Plate Geometry	2-96
Figure 2-52	Traveller Drop Orientations Analyzed For Maximum Fuel Assembly Damage	2-97
Figure 2-53	Predicted Energy and Work Histories for a 9m Vertical Drop Onto the Top Nozzle End of the Package	2-99
Figure 2-54	Predicted Energy and Work Histories for a 9m Vertical Drop Onto the Bottom Nozzle End of the Package	2-99
Figure 2-55	Predicted Rigid Wall Histories for 9m Vertical Drops onto the Bottom (QU-1) and Top (QU-8B) Ends of the Package	2-100
Figure 2-56	Predicted Force Between Clamshell and Impact Limiter for 9m Vertical Drops	2-101
Figure 2-57	Predicted Fuel Assembly Accelerations for 9m Vertical Drops	2-102
Figure 2-58	Impact Between Clamshell and Bottom Impact Limiter for Vertical Drop onto Bottom End of Package.....	2-102
Figure 2-59	First Impact Between Clamshell and Top Impact Limiter for Vertical Drop onto Top End of Package.....	2-103
Figure 2-60	Second Impact Between Clamshell and Top Impact Limiter for Vertical Drop onto Top End of Package.....	2-103
Figure 2-61	Third Impact Between Clamshell and Top Impact Limiter for Vertical Drop onto Top End of Package.....	2-104
Figure 2-62	Predicted Temperature and Foam Density Effect on Outerpack/Drop Pad Interface Forces (9m CG-Forward-of-Corner with 18° Rotation Drop onto the Top End of the Package).....	2-105
Figure 2-63	Predicted Temperature and Foam Density Effect on Outerpack/Drop Pad Accelerations (9m CG-Forward-of-Corner with 18° Rotation Drop onto the Top End of the Package).....	2-105
Figure 2-63A	Predicted Temperature and Foam Density Effect on Outerpack/Drop Pad Interface Forces (9m Vertical Drop onto the Bottom End of the Package)	2-106
Figure 2-63B	Predicted Temperature and Foam Density Effect on Fuel Assembly Acceleration (9m Vertical Drop onto the Bottom End of the Package)	2-106

LIST OF FIGURES (cont.)

Figure 2-64	Predicted Energy and Work Histories at Various Temperatures	2-107
Figure 2-65	Pin Drop Orientation	2-108
Figure 2-66	Predicted Outerpack/Pin Interference Forces (1m Drop onto 15mm Diameter Steel Pin)	2-108
Figure 2-67	Predicted Fuel Assembly Accelerations (1m Drop onto 15mm Diameter Steel Pin)	2-109
Figure 2-68	Pin Drop onto Outerpack Hinges	2-109
Figure 2-69	Predicted Outerpack/Pin Interface Forces (1m Drop onto 15mm Diameter Steel Pin)	2-110
Figure 2-70	Predicted Fuel Assembly Accelerations (1m Drop onto 15mm Diameter Steel Pin)	2-110
Figure 2-71	Predicted Energy and Work Histories for a 1 m Horizontal Pin Drop (Pin Underneath the Package CG).....	2-111
Figure 2-72	Predicted Energy and Work Histories for a 1 m Tilted Pin Drop (20° Tilt With TN End Down.....	2-112
Figure 2-73	Predicted Energy and Work Histories for a 1 m Horizontal Pin Drop (Pin Hitting Hinge at Package CG)	2-112
Figure 2-74	Comparison of Predicted Maximum Pin Indentions	2-113
Figure 2-75	Predicted Outerpack/Pin Interface Forces (1 m Drop onto 15 mm Diameter Steel Pin After 9m Drop).....	2-114
Figure 2-76	Predicted Fuel Assembly Accelerations (1 m Drop onto 15mm Diameter Steel Pin after 9 m Drop).....	2-115
Figure 2-77	Predicted Energy and Work Histories (1 m Drop onto 15 mm Diameter Steel Pin after 9 m Drop).....	2-116
Figure 2-78	Prototype Drop Tests Used To Benchmark Analysis.....	2-117
Figure 2-79	Prototype Unit 1 Drop Test	2-118
Figure 2-80	Comparison of Test 1.1 with Analytical Results	2-119
Figure 2-81	Comparison of Test 1.1 with Analytical Results.....	2-120
Figure 2-82	Deformations at End of Package	2-122
Figure 2-83	Internal Deformations at Inside Outerpack	2-123
Figure 2-84	Outerpack Deformations at Bottom Nozzle End of Package	2-124
Figure 2-85	Pin Puncture Deformations.....	2-124
Figure 2-86	Dimensions of Pin Puncture Deformations	2-124

LIST OF FIGURES (cont.)

Figure 2-87	Outerpack Predicted Deformations of Pin Drop	2-125
Figure 2-88	Predicted and Measured Y Accelerations.....	2-126
Figure 2-89	Three Axis Measured Accelerations.....	2-126
Figure 2-90	Predicted and Measured Y Accelerations.....	2-127
Figure 2-91	Predicted and Measured Y Accelerations.....	2-127
Figure 2-92	Measured Primary and Secondary Accelerations	2-128
Figure 2-93	FEA Model Input Files	2-130
Figure 2-94	Outerpack Mesh in Prototype Model.....	2-131
Figure 2-95	Impact Limiter in Prototype Unit Model	2-131
Figure 2-96	Clamshell Mesh in Qualification Unit Model	2-132
Figure 2-97	Fuel Assembly in Both Prototype and Qualification Unit Models.....	2-132
Figure 2-98	Outerpack Hinge Model	2-133
Figure 2-99	FEA Input Files	2-134
Figure 2-100	Outerpack Mesh in Qualification Unit Model.....	2-134A
Figure 2-100A	FE Meshes of Outerpack Legs and Forklift Pockets	2-134A
Figure 2-100B	Lower Outerpack Mesh for Qualification Unit Model.....	2-134B
Figure 2-100C	Qualification Unit Model Mesh Detail.....	2-134C
Figure 2-100D	Upper Outerpack Mesh for Qualification Unit Model	2-134D
Figure 2-101	Impact Limiter Meshes in Qualification Unit Model	2-135
Figure 2-101A	Hinge/Latch Feature in Qualification Unit Model.....	2-135A
Figure 2-102	Clamshell Mesh in Qualification Unit Model	2-135B
Figure 2-102A	Clamshell Top Head in Qualification Unit Model	2-135B
Figure 2-102B	Clamshell Top Nozzle Hold-down Bars in Qualification Unit Model.....	2-135C
Figure 2-102C	Clamshell Hinges and Latches in Qualification Unit Model.....	2-135C
Figure 2-103	Package Drop Angle	2-137
Figure 2-104	Gravity Load Profile	2-138
Figure 2-105	Stress Strain Data for LAST-A_FOAM	2-139
Figure 2-105A	Foam Response at Strains from 0-10%	2-139A
Figure 2-106	Stress-Strain Curves for 304 Stainless Steel.....	2-140
Figure 2-107	Temperature Effects on Tensile Properties of Annealed Stainless Steel.....	2-140

LIST OF FIGURES (cont.)

Figure 2-108	Stress-Strain Characteristics of Aluminum in Clamshell	2-141
Figure 2-109	Temperature Effects on Tensile Properties of Aluminum in Clamshell.....	2-141
Figure 2-110	Accelerometer Locations on Prototype Unit 1	2-144
Figure 2-111	Traveller Prototype Internal View	2-149
Figure 2-112	Traveller Prototype External View	2-150
Figure 2-113	Drop Orientations for Prototype Test Series 1	2-151
Figure 2-114	Traveller Prototype Exterior After Test 1.1.....	2-152
Figure 2-115	Traveller Prototype Interior After Test 1.1.....	2-153
Figure 2-116	Traveller Prototype Exterior After Test 1.2.....	2-154
Figure 2-117	Traveller Prototype Interior After Test 1.2.....	2-155
Figure 2-117A	Accelerometer Locations on Prototype Drop Test	2-155A
Figure 2-118	Clamshell Accelerometer Trace for Prototype Test 1.1	2-156
Figure 2-119	Outerpack Accelerometer Trace for Prototype Test 1.1	2-157
Figure 2-120	Clamshell Accelerometer Trace for Prototype Test 1.2	2-157
Figure 2-121	Traveller Prototype After Test 1.3.....	2-159
Figure 2-122	Drop Orientations for Traveller Prototype Test Series 2.....	2-160
Figure 2-123	Traveller Prototype After Test 2.1	2-161
Figure 2-124	Traveller Prototype After Test 2.2.....	2-162
Figure 2-125	Traveller Prototype After Test 2.3.....	2-163
Figure 2-126	Traveller Prototype Interior After Test Series 2.....	2-164
Figure 2-127	Traveller Prototype Clamshell and Bottom Impact Limiter After Test Series 3.....	2-166
Figure 2-128	Traveller Prototype Clamshell and Bottom Impact Limiter After Test Series 3.....	2-166
Figure 2-129	Drop Orientation for QTU Test Series 1	2-168
Figure 2-130	QTU-1 Outerpack After Test 1.1	2-169
Figure 2-131	QTU-1 Outerpack After Test 1.2.....	2-170
Figure 2-132	QTU-1 Outerpack After Test 1.3.....	2-170
Figure 2-133	QTU-1 Fuel Assembly After Drop and Burn Tests.....	2-171
Figure 2-134	Measurements Made on QTU-1 Fuel Assemblies Before and After Drop Tests	2-172

LIST OF FIGURES (cont.)

Figure 2-135	QTU Test Series 2 Drop Orientations	2-177
Figure 2-136	QTU Outerpack After Test 2.1	2-178
Figure 2-137	QTU Outerpack After Test 2.2	2-178
Figure 2-138	QTU Outerpack After Test 2.3	2-179
Figure 2-139	QTU-2 Clamshell and Fuel Assembly After Drop Tests	2-180
Figure 2-140	Traveller CTU Test Article Internal View	2-184
Figure 2-141	Traveller CTU External View	2-185
Figure 2-142	CTU Drop Test Orientations	2-186
Figure 2-143	Top Nozzle End Outerpack Impact Damage	2-187
Figure 2-144	CTU Outerpack Stiffener After Test 1	2-188
Figure 2-145	CTU Outerpack After Test 2	2-188
Figure 2-146	CTU Outerpack After Test 2	2-189
Figure 2-147	Hinge Separation at Bottom Nozzle End From Test 2	2-189
Figure 2-148	CTU Outerpack After Test 3	2-190
Figure 2-149	CTU Clamshell After Drop and Fire Tests	2-191
Figure 2-150	Outerpack Lid Moderator After Testing	2-191
Figure 2-151	Fuel Assembly Damage Sketch and Pre-test Assembly	2-193
Figure 2-152	CTU Fuel Assembly After Testing	2-194
Figure 2-153	CTU Fuel Assembly Top End After Testing	2-194
Figure 2-154	Cracked Rod From CTU Fuel Assembly	2-195
Figure 2-155	Cracked Rod Locations on CTU Fuel Assembly	2-195
Figure 2-156	Axial Spacer below Fuel Assembly in Traveller XL Clamshell	2-201
Figure 2-157	FEA Model – Axial Spacer	2-204
Figure 2-158	Dynamic Crush Strengths for Foam Materials Utilized in the Traveller	2-207
Figure 2-159	Annealed 304 Stainless Steel Stress-Strain Characteristics	2-207
Figure 2-160	Deformed Model with Axial Spacer at 23 ms (the end of the impact)	2-208
Figure 2-161	Predicted Total End Crushing (mm) with Axial Spacer	2-209
Figure 2-162	Kinetic Energy History (mJ) of the Axial Spacer Model	2-209
Figure 2-163	Fuel Handling Tool Grappled to a 17x17 Top Nozzle (in blue) within the Opened Outerpack and Clamshell	2-213
Figure 2-164	Fuel Handling Tool Shown Attached to a 17x17 XL Fuel Assembly and Behind the Overhanging Shear Lip	2-213
Figure 2-165	Traveller Top End Plate FEA Model	2-215
Figure 2-166	RTP Model at Beginning of Impact (0 ms) and End of Impact (33 ms)	2-216
Figure 2-167	Rigid Wall Impact Force History of RTP Model	2-217
Figure 2-168	Kinetic Energy History of RTP Model (mJ vs s)	2-217
Figure 2-169	Comparison of Simulated Top Nozzle Damage (left) to Drop Test (right)	2-218

LIST OF FIGURES (cont.)

Figure 2-170	Traveller VVER Exploded View	2-220
Figure 2-171	Traveller VVER Clamshell Top Detail.....	2-220
Figure 2-172	Cross-Section views of Traveller XL and Traveller VVER Shipping Packages.....	2-221
Figure 2-173	XL and VVER Clamshell Lengths Shown with the Outerpack Lid Removed	2-222
Figure 2-174	Similarity of XL and VVER Clamshell Extrusions	2-223
Figure 2-175	Identical Hardware for XL and VVER Clamshell Quarter-turn Latches.....	2-223
Figure 2-176	Traveller VVER Clamshell Top Plate Assembly	2-224
Figure 2-177	VVER Fuel Assembly Installed - Top Nozzle Region	2-225
Figure 2-178	VVER Fuel Assembly Installed - Bottom Nozzle Region.....	2-225
Figure 2-179	Puncture Plate Distance from Ground During Impact	2-227
Figure 2-180	Traveller VVER Clamshell Model Showing Key Components	2-228
Figure 2-181	Traveller VVER Finite Element Model	2-229
Figure 2-182	Traveller VVER Model with Clamshell Walls and End Limiter Cover Plate Hidden	2-230
Figure 2-183	Traveller VVER Top Plate Assembly Showing Integral Axial Clamp and Rubber Pad	2-230
Figure 2-184	Comparison of Dynamic Crush Strengths of the Foams Components	2-233
Figure 2-185	Annealed 304 Stainless Steel Stress-strain Characteristics.....	2-234
Figure 2-186	Traveller XL Shown in a Top-down Impact Orientation.....	2-235
Figure 2-187	Top Down 9m Impact of Traveller VVER Package in 5 ms Increments	2-236
Figure 2-188	Kinetic Energy Plot for VVER Model.....	2-237
Figure 2-189	Deformed Shape of Model at 25ms	2-238
Figure 2-190	Max. Plastic Strain in the Clamshell Main Walls	2-238
Figure 2-191	Slap-down Model	2-241
Figure 2-192	Model with Upper Outerpack Hidden to Show VVER Clamshell	2-241
Figure 2-193	Outerpack Max. Longitudinal Bending Load History	2-242
Figure 2-194	Slight Plastic Strain in Clamshell Extrusion	2-243
Figure 2-195	Traveller VVER Top Plate "Shear lip"	2-244

2.0 STRUCTURAL EVALUATION

This section presents the structural design criteria, weights, mechanical properties of material, and structural evaluations which demonstrate that the Traveller series of packages meet all applicable structural criteria for transportation as defined in 10 CFR 71¹ and TS-R-1².

2.1 DESCRIPTION OF STRUCTURAL DESIGN

The structural evaluation of the standard length Traveller (Traveller STD) and the longer length Traveller (Traveller XL) packages was performed with various tests and computer simulation using finite element analysis. Since the Traveller VVER utilizes the same Outerpack as the Traveller XL and recent design changes (e.g., the removable top plate) were evaluated using a benchmarked finite element model, the VVER package was also analyzed using finite element computer simulation. The results of the computer simulations and testing are provided in the following sections. Supporting analyses and analyses of not-tested structural aspects are also provided. See Figure 2-170 for an exploded view of the Traveller VVER package.

The Traveller shipping package consists of two major fabricated components: 1) an Outerpack assembly, and 2) a Clamshell assembly. The Outerpack consists of a stainless steel outer shell for structural strength, a layer of rigid polyurethane foam for thermal and impact protection, and a stainless steel inner shell for structural strength. Polyethylene blocks are affixed to the inner shell of the Outerpack for criticality safety. See Section 6, Criticality Evaluation, for full criticality safety description. The Clamshell consists of an aluminum container to structurally enclose the contents. Neutron absorber panels are affixed to the inner faces of the Clamshell. Rubber shock mounts separate and isolate the Clamshell from the Outerpack assembly. See Figure 2-1 for an exploded view of the Traveller STD package.

2.1.1 Discussion

The designs of the Traveller STD and Traveller XL unirradiated fuel shipping packages are the same except for length (and therefore weight). The Traveller VVER design is a hexagonal Clamshell mounted inside a Traveller XL Outerpack. Any reference to the Traveller XL Outerpack is applicable to Traveller VVER Outerpack for structural considerations. Details of the packages, including dimensions, and materials can be found in Section 1, General Information. Both packages consist of an Outerpack, and a Clamshell. Positive closure of the Outerpack is accomplished by means of high strength stainless steel bolts. The number of bolts is the same for the XL and STD designs, thus the loading per bolt is lower for the STD design. There are 48 bolts $\frac{3}{4}$ -inch bolts in the Outerpack, 24 attaching the hinge sections to the lower Outerpack and 24 attaching the upper Outerpack to the hinge sections. To remove the upper Outerpack, the 24 bolts must be removed. In the preferred approach, the Outerpack is opened when it is in a vertical orientation by removing the 12 bolts attaching the upper Outerpack to the hinges on one side. This allows the upper Outerpack to be opened on the other hinge sections, like a door. The design loadings for both

1. Title 10, Code of Federal Regulations, Part 71 (10 CFR 71), Packaging and Transportation of Radioactive Material, January 1, 2004 Edition
2. TS-R-1 1996 Edition (Revised), Regulations for the Safe Transport of Radioactive Material.

packages are below the ultimate design loads for the Outerpack bolts. The worst case forces for the package are presented in Section 2.12.3.2.2, Horizontal Side Drops, and a discussion regarding the design allowable is presented in Section 2.12.3.7, Evaluation, Analysis and Detailed Calculations, and Section 2.12.3.9, Bolt Factor of Safety Calculation. Further evidence of the adequacy of the Outerpack bolts is demonstrated through 9m drop testing whereby only one (1) Outerpack bolt failed in a total of nine (9) 9m drop tests. The single bolt that failed did so as a result of direct impact with the drop pad. The Clamshell is closed using 1/4-turn nuts which lock latches on the doors of the assembly.

The Outerpack bolts and the Clamshell closure mechanisms have been subjected to the drop conditions of 10 CFR 71 and TS-R-1 without failure. Therefore, these designs are more than adequate to withstand the loads experienced during normal conditions of transport.

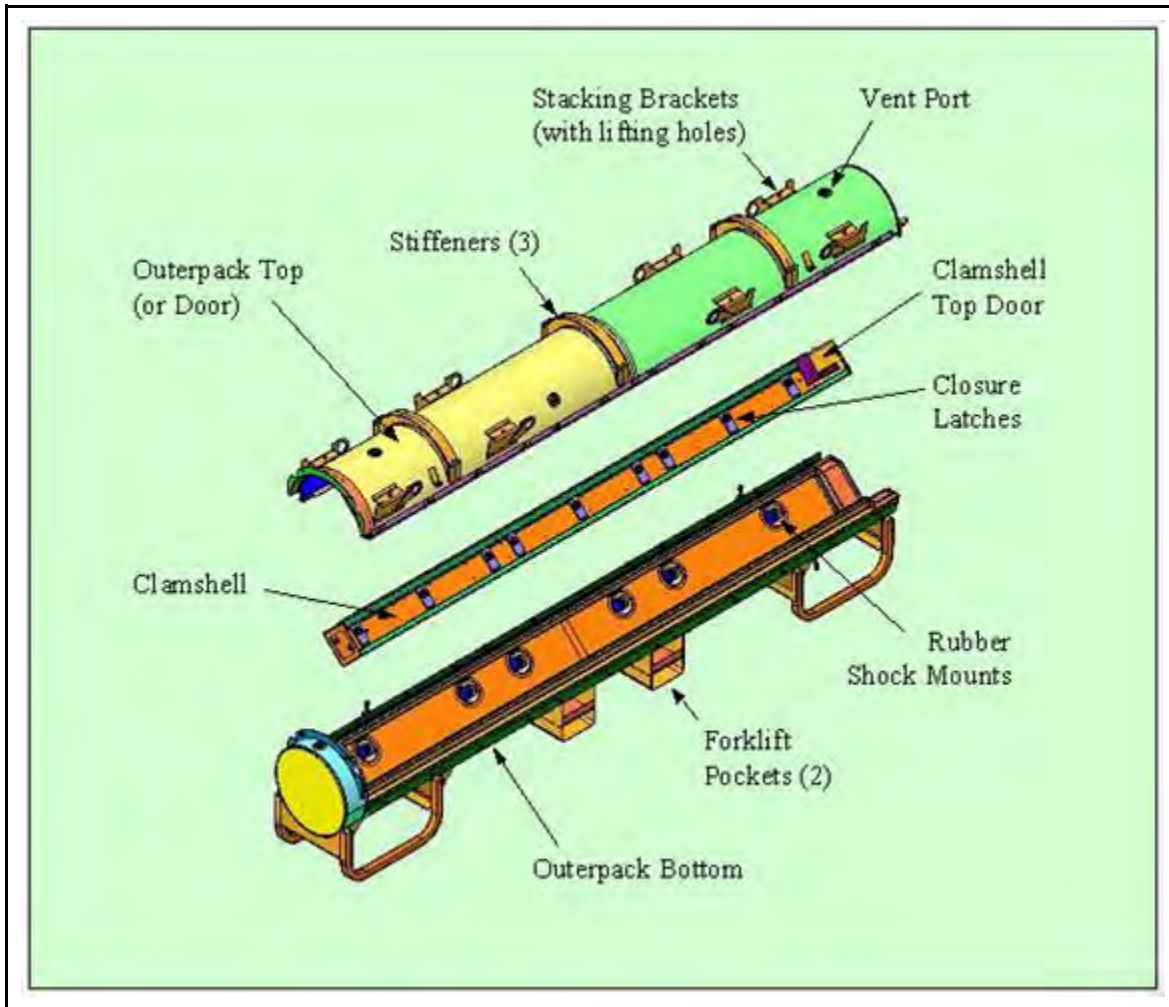


Figure 2-1 Traveller STD Exploded View

Closure of the Outerpack is provided by (12) $\frac{3}{4}$ -10UNC hex head bolts, which allows the top half of the Outerpack assembly to swing open on a series of hinges. The Outerpack top half or “door” may be opened in either direction, depending on which bolts are removed. Optionally, the top Outerpack assembly may also be completely removed by removal of (24) $\frac{3}{4}$ -10UNC hex head bolts. Closure of the Traveller STD and Traveller XL Clamshells are provided by latch assemblies that are secured with nine (9) $\frac{1}{4}$ -turn nuts, and eleven (11) $\frac{1}{4}$ -turn nuts, respectively.

The Traveller packages are not pressure sealed from the ambient environment, therefore, no differential pressures can occur within the package.

Handling of the packages is performed using the forklift pockets on the lower Outerpack. Handling may also utilize the lifting holes in the stacking brackets on the upper Outerpack.

Standard fabrication methods are utilized to fabricate the Traveller series of packages. Visual weld examinations are performed on all welds of the Traveller packages in accordance with AWS D1.6. and ASME Section III, Subsection NF-5360, for stainless steel and aluminum respectively.

2.1.2 Design Criteria

2.1.2.1 Basic Design Criteria

Evidence of performance for the Traveller XL package is achieved by (1) empirical evaluations using full-scale packages and (2) large-strain capable Finite Element Analysis (FEA). The Traveller XL is bounding due to its increased weight and length when compared to Traveller STD. The criteria that was used for impact evaluation is a demonstration that the containment and confinement systems maintain integrity throughout Normal Conditions of Transport (NCT) and Hypothetical Accident Condition (HAC) certification testing. That is, it is necessary to demonstrate that there is no release of material, no loss of moderator or neutron absorber, no decrease in Outerpack geometry, and no increase in Clamshell geometry. The as-found condition of the package (packaging and contents) is the baseline configuration for the criticality safety evaluation that can be found in Chapter 6, Criticality Evaluation.

A detailed discussion related to Traveller XL design criteria, can be found in Appendix 2.12.3, Mechanical Design Calculations for the Traveller XL Shipping Package.

2.1.2.2 Miscellaneous Structural Failure Modes

2.1.2.2.1 Brittle Fracture

The primary structural materials of the Traveller packages are austenitic stainless steel (ASTM A240 Type 304 SS) and 6000 Series aluminum (extruded components 6005-T5, all else 6061-T6). These materials do not undergo a ductile-to-brittle transition in the temperature range of interest [i.e., down to -40°F (-40°C)], and thus do not require evaluation for brittle fracture.

2.1.2.2.2 Fatigue

Because the shells of the Outerpack are constructed of ductile stainless steel and they are formed into a very stiff body with low resulting stresses, no structural failures of the Outerpack due to fatigue will occur. Because the Clamshell is structurally isolated from the Outerpack through the rubber shock mounts, no Clamshell fatigue will occur. The Clamshell is, for practical purposes, decoupled from the Outerpack through the rubber shock mounts. These rubber shock mounts also provide excellent damping to the Clamshell.

2.1.2.2.3 Buckling

For normal condition and hypothetical accident conditions, the Clamshell which structurally encloses the fuel, will not buckle due to free or puncture drops. This behavior has been demonstrated via full-scale testing of the bounding Traveller XL package.

2.1.3 Weights and Centers of Gravity

The Traveller XL weight bounds the Traveller STD and Traveller VVER weight as shown in Table 2-1. The calculated weight breakdown for the major individual subassemblies, including the shipping components for both packages, is listed below. For licensing purposes, the maximum bounding Traveller XL design weight is assumed to be 5,230 lb (2,372 kg). The general, Traveller structural analysis applicable to STD, XL and VVER is located in Section 2.12.2. The Traveller VVER specific structural analysis is located in Section 2.12.8.

Table 2-1 Summary of Traveller STD, Traveller XL, Traveller VVER Design Weights			
	Traveller STD	Traveller XL	Traveller VVER
Max. Fuel Assembly Weight, lb (kg)	1650 (748)	1971 (894)	1850 (839)
Max. Tare Weight, lb (kg)	2850 (1293)	3255 (1476)	3255 (1476)
Design and Licensing Basis Gross Weight, lb (kg)	4500 (2041)	5230 (2372)	5105 (2316)

The center of gravity of both Traveller packages is approximately at the geometric center of the Outerpack, i.e., approximately 23 inches above ground level, at the axial mid-station for both packages. Appendix 2.12.2, Container Weights and Centers of Gravity, shows the overall dimensions, locations of the centers of gravity for both packages, and detailed major component weights.

2.1.4 Identification of Codes and Standards for Package Design

The Traveller packages are evaluated with respect to the general standards for all packaging specified in 10 CFR §71.43, and TS-R-1 (paragraphs 606 – 649, as applicable). The fabrication, assembly, testing, maintenance, and operation will be accomplished with the use of generally accepted codes and standards such as ASME, ASTM, AWS. Special processes will be documented with procedures that will be evaluated and approved.

2.2 MATERIALS

2.2.1 Material Properties and Specifications

Mechanical properties for the materials used for the structural components of the Traveller packages are provided in this section. Temperature-dependent material properties for structural components are primarily obtained from Section II, Part D, of the ASME Boiler and Pressure Vessel (B&PV) Code. The analytic evaluation of the Traveller packages is via computer simulation (ANSYS/LS-DYNA[®]), only the material properties specific to the analysis portion and computer simulation portion of the evaluation are given. Table 2-2 lists the materials used in the Traveller packages and summarized key properties and specifications. More detailed material properties can be found in Appendix 2.12.3, Mechanical Design Calculations for the Traveller XL Shipping Package, and Appendix 2.12.4, Drop Analysis for the Traveller XL Shipping Package.

All materials used in the fabrication of the Certification Test Unit (CTU) meet 10 CFR 71 and TS-R-1 requirements. However, simulated neutron absorber plates were affixed to the inner faces of the Clamshell. These were fabricated from 1100-T0 aluminum (“dead soft” aluminum). These component plates did not contain boron, and were used to simulate the mechanical and thermal properties of the neutron absorber plates. The 1100-T0 aluminum was used due to its low mechanical properties. In production units, the actual neutron absorber plates will have insignificant differences in the material properties compared to the material used in the prototypes and CTU package.

2.2.2 Chemical, Galvanic, or Other Reactions

The Traveller series of packages are fabricated from ASTM A240 Type 304 stainless steel, 6000-series aluminum, borated 1100-series aluminum, polyurethane foam, and polyethylene sheeting. The stainless steel Outerpack does not have significant chemical or galvanic reactions with the interfacing components, air, or water.

The aluminum Clamshell is physically isolated, and environmentally protected, by the Outerpack and therefore will have negligible chemical or galvanic reactions with the interfacing components, air, or water. In addition, the Type 304 stainless steel fasteners which attach various Clamshell components represent a very small area ratio (cathode-to-anode ratio), which will render the reaction insignificant. Therefore, the requirements of 10 CFR §71.43(d), TS-R-1 (613) are met.

The Outerpack hinge bolts are zinc plated for the purpose of improving galling resistance which can be a significant problem when stainless steel fasteners are inserted in stainless steel threaded holes. The plating is not required for chemical or galvanic protection.

2.2.3 Effects of Radiation on Materials

There are no materials used in the Traveller packages which will be adversely affected by radiation under normal handling and transport conditions.

Table 2-2 Safety-Related Materials Used in the Traveller Packages			
Material	Critical Properties	Reference Specifications/Codes	Comments
304 Stainless Steel	UTS: 75 ksi (517 MPa) YLD: 30 ksi (206 MPa) τ_{allow} : 18 ksi (124 MPa) E: 29.4 E6 psi (203 GPa)	ASTM A240 ASTM A276	Fully annealed material and not subject to brittle fracture.
6005-T5 Aluminum	UTS: 38 ksi (262 MPa) YLD: 35 ksi (241 MPa) τ_{allow} : 21 ksi (145 MPa) E: 10 E6 psi (69 GPa)	ASTM B221 ASTM B209	Reference standard UNS A96005
6061-T6 Aluminum	UTS: 38 ksi (262 MPa) YLD: 35 ksi (241 MPa) τ_{allow} : 21 ksi (145 MPa) E: 10 E6 psi (69 GPa)	ASTM B221 ASTM B209	Reference standard UNS A96061
Polyurethane Closed Cell Foam	Densities: 6 ± 1 pcf (0.096 ± 0.016 gm/cm ³), 10 ± 1 pcf (0.16 ± 0.016 gm/cm ³), 20 ± 2 pcf (0.32 ± 0.016 gm/cm ³) Crush Strengths: See Appendix 2.12.3	Westinghouse Specification PDSHIP02 ASTM D1621-94 ASTM D1622-93 ASTM D2842	Burn Characteristics verified by ASTM F-501, with exceptions noted in PDSHIP02.
UHMW Polyethylene	Specific Gravity: > 0.93 Molecular Wt: >3 million	ASTM D4020	N/A
Borated Aluminum Laminate Composite	Minimum areal densities: Borated Al Composite: 0.024 g/cm ²	Westinghouse Specification PDSHIP04 ASTM E748	The minimum areal densities are defined for the finished plate or laminate final thickness of $0.125" \pm 0.006"$ (3.175 mm ± 0.153 mm). No structural credit is taken for the neutron poison plates.
Ceramic Insulation (Paper and Felt)	Max. use temp: >1800°F (982°C) Conductivity: ≤ 1.2 Btu-in/hr-ft ² @ 500°F, (0.173 W/m-K @ 260°C)	N/A	The paper thickness is 0.0625" (1.59 mm), and the blanket thickness is 0.25" (6.35 mm)

2.3 FABRICATION AND EXAMINATION

2.3.1 Fabrication

The Traveller packages (XL, VVER and STD) are manufactured using standard fabrication techniques. No exotic materials or processes are required. Safety related items which are needed for criticality safety purposes have specific manufacturing specifications which clearly delineate all necessary codes, standards, and specifications required to meet design intent. All fabrication specifications are listed on the engineering drawings.

The fabrication processes of the Traveller include basic processes such as cutting, rolling, bending, machining, welding, and bolting. All welding is performed in accordance with ASME Section IX.

The manufacturing flow of the Traveller units includes fixturing of the inner and outer shells of the upper and lower Outerpack assemblies. Individual closure components are then aligned and welded in place. Sub-assemblies such as the forklift pockets, leg structures and stacking brackets are assembled in a parallel manner and appended to the main assemblies at appropriate times. Upon welding closure of the assemblies, the upper and lower Outerpack assemblies are secured together and poured with polyurethane foam material. Pouring of this material is tightly controlled through the foam manufacturing specification.

When the Traveller is filled with foam, it is ready for final assembly and installation of the Clamshell which has followed a parallel fabrication process. One difference for the Clamshell is that the faces are manufactured extrusions as opposed to “off-the-shelf” material. The extrusions are fabricated to industry standard specifications. Upon integration of the Clamshell to the Outerpack, final assembly and light grit blasting conclude the manufacturing process.

2.3.2 Examination

Manufacture of all Traveller packages shall be performed in accordance with strict Quality Assurance (QA) requirements. Included in the manufacture of the packages are examinations to verify that each package is being built to the required specifications. These examinations include the following:

1. Receipt inspections whereby the received components are visually inspected for workmanship, overall part quality, dimensional compliance, and material certification compliance.
2. All welds (which shall be performed by qualified welders/processes) shall be visually examined by a qualified inspector in accordance with AWS D1.6 and ASME Section III, Subsection NF-5360, for stainless steel and aluminum respectively.
3. Examinations which evaluate form, fit, and function shall be performed on each package to verify its operability and assess its overall quality.

2.4 LIFTING AND TIE-DOWN STANDARDS FOR ALL PACKAGES

2.4.1 Lifting Devices

The lifting criteria is governed by 10 CFR §71.45(a) and TS-R-1 (607). 10 CFR §71.45(a) states that any lifting attachment that is a structural part of the package must be designed with a minimum safety factor of three against yielding when used to lift the package in its intended manner. In addition, it must be designed so that failure of any lifting device under excessive load would not impair the ability of the package to meet other requirements of 10 CFR 71. The following calculations are based on the features of the Traveller XL package which bounds the Traveller STD for these requirements. Lifting and tie-down are described in detail in Appendix 2.12.3, Mechanical Design Calculations for the Traveller XL Shipping Package. |

2.5 GENERAL CONSIDERATIONS

The Traveller package structural evaluation consists of a combination of mechanical design calculations, finite element analysis, and testing. Table 2-3 shows the regulatory requirements and the means by which satisfactory compliance was demonstrated.

Table 2-3 Summary of Regulatory Requirements				
Requirement Description	US NRC	TS-R-1	Applicable Condition	Means Demonstrated
Lifting attachments	10 CFR 71.45(a)	TS-R-1, § 607	General Package Standard	Mech. Design Calc.
Tie-Down devices	10 CFR 71.45(b)(1,2)	TS-R-1, § 636	General Package Standard	Mech. Design Calc.
Design temperatures between –40°F (–40°C) and 158°F (70°C)	10 CFR 71.71(c)(1,2)	TS-R-1, § 637 and 676	General Package Standard	Mech. Design Calc.
Internal/External Pressure	10 CFR 71.71(c)(3,4)	TS-R-1, § 615	Normal transport condition	Mech. Design Calc.
Vibration	10 CFR 71.71(c)(5)	TS-R-1, § 612	Normal transport condition	Mech. Design Calc.
Water spray	10 CFR 71.71(c)(6)	TS-R-1, § 721	Normal transport condition	Mech. Design Calc.
Compression/Stacking test	10 CFR 71.71(c)(9)	TS-R-1, § 723	Normal transport condition	Mech. Design Calc.
Penetration	10 CFR 71.71(c)(10)	TS-R-1, § 724	Normal transport condition	Mech. Design Calc.
Immersion	10 CFR 71.73(c)(6)	TS-R-1, § 729	Accident transport condition	Mech. Design Calc.

2.5.1 Evaluation by Test

The development of the Traveller packages included mechanical scoping tests to quantify the critical characteristics of the components or subsystems of the design. These scoping tests included:

1. Outerpac Hinge Strength-to-Failure Testing
2. Hinge Alignments Tests
3. Foam Pouring Tests
4. Foam Burn Tests (pail type)
5. Clamshell Hinge Strength-to-Failure Testing
6. Clamshell Weld Tests

7. Clamshell impact tests
8. Impact limiter testing including “pillow” impact testing

The scoping tests provided designers with performance data. However, proof of performance in the Traveller package was obtained through full-scale testing. As such, these tests were not required to be performed in accordance with full QA standard. However, all full-scale Traveller XL packages were fabricated and tested under all QA requirements.

The development of the Traveller consisted of essentially three (3) full-scale test campaigns. These campaigns consisted of what are called the Prototype units (2), the Qualification Test Units (QTU) (2), and finally the Certification Test Units (CTU) (1). In general, these packages are very similar. The overall configuration of the Outerpack and Clamshell remain essentially identical throughout the design evolution. With each test campaign, the design was modified to increase structural or thermal margin, or to reduce excess design margin when appropriate. The significant design changes from Prototype to CTU were:

1. The reduction in Outerpack shell thicknesses from 11 gage (0.120", 0.30 cm) to 12 gage (0.105", 0.27 cm),
2. The adjusting of polyurethane foam densities (first a lowering of density for structural reasons, then an increase for improve thermal performance),
3. The addition of a thin stainless steel covering of the moderator blocks,
4. The replacement of short individual Outerpack hinges with a continuous Outerpack hinge,
5. A redesign of the Clamshell head attachment configuration, and finally,
6. A reduction in the number and size of the Outerpack hinge bolts.

The purpose of the computer simulation was to assist in evaluating these minor changes and predict performance of the modified packages. The computer simulation was also used to show the impact of initial test conditions (temperature of package) and manufacturing variability (foam density tolerances, skin thickness variations, etc.). These factors showed negligible effects on the overall performance of the packages. Details can be found in Appendix 2.12.4, Drop Analysis for the Traveller XL Shipping Package. |

A summary of the development and testing of the Traveller XL full-scale test packages is described in Table 2-5, and the detailed results of each test are described in Appendix 2.12.5, Traveller Drop Test Results. |

2.5.2 Evaluation by Analysis

Analysis consisted of mechanical design calculations and finite element analysis. Mechanical design calculations are described in detail in Appendix 2.12.3. Finite element analysis, utilizing LS-DYNA software, is described in detail in Appendix 2.12.4.

Table 2-4 gives a summary of the regulatory requirements that are demonstrated through mechanical design calculations

Table 2-4 Summary of Traveller Mechanical Analysis		
Requirement Description	Allowable Design Value(s) or Acceptance Criteria	Component Calculated Value vs. Allowable
Lifting attachments	Tensile Yield Stress, $\sigma_y < 30$ ksi Shear Yield Stress, $\tau_y < 18$ ksi Weld shear Yield Stress, $\tau_y < 12$ ksi Hoist Screw Shear Stress, $\tau < 72$ ksi Coupling Nut Shear Stress, $\tau < 18$ ksi Hoist Ring Tensile Stress, $\tau < 130$ ksi	Hole tear-out (4-pt. lifting) XL: $\tau = 5,230$ psi < 18 ksi STD: $\tau = 6,364$ psi < 18 ksi Weld shear (4-pt. lifting) XL: $\tau = 7,565$ psi < 12 ksi STD: $\tau = 9,205$ psi < 12 ksi Forklift XL Bending: $\sigma = 17,528$ psi < 30 ksi STD Bending: $\sigma = 26,260$ psi < 30 ksi XL Weld shear: $\tau = 3,533$ psi < 12 ksi STD Weld shear: $\tau = 6,080$ psi < 12 ksi Hoist Ring Assembly Bolt shear: $\tau = 50,619$ psi < 72 ksi Coupling Nut Shear Stress: $\tau = 17,671$ psi < 18 ksi Hoist ring tensile: $\sigma = 35,659$ psi < 130 ksi
Tie-Down	Weld shear Yield Stress, $\sigma_y < 12$ ksi	Leg Assembly Weld shear: $\tau = 11,648$ psi < 12 ksi Lift Eyes Weld shear (vertical): $\tau = 7,158$ psi < 12 ksi Weld shear (combined): $\tau = 7,173$ psi < 12 ksi
Temperatures Effects	No brittle fracture No impact from Differential Thermal Expansion (DTE)	No brittle fracture No DTE Impact
Internal/External Pressure	Compressive Yield Stress, $\sigma_y < 30$ ksi	No stress developed
Vibration	No impact on structural performance $f_{natOP} > f_{nat TRANS}$	No impact, 23 Hz > 3.7 -8 Hz
Water spray	No impact on structural performance	No impact
Compression/Stacking	Weld shear Yield Stress, $\tau_y < 12$ ksi Compressive Yield Stress, $\sigma_y < 30$ ksi Elastic Stability (Critical Buckling), $F < P_{cr}$	Stacking Bracket: Weld shear: $\tau = 4,729$ psi < 12 ksi Bending: $\sigma = 1,827$ psi < 30 ksi Outerpack Buckling: Buckling: 26,150 lb $< 78,583$ lb Leg Support Buckling: Buckling: 3,269 lb $< 71,978$ lb
Penetration	No perforation of outer skin	Bounded by 1.0m HAC pin-puncture; No perforation of outer skin.
Immersion	Compressive Yield Stress, $\sigma_y < 30$ ksi	No stress developed

2.6 NORMAL CONDITIONS OF TRANSPORT

2.6.1 Heat

The thermal evaluation for the heat test is described and reported in Section 3, Thermal Evaluation.

2.6.1.1 Summary of Pressures and Temperatures

There is no pressure seal in the Traveller series of packages. Therefore, there is no pressure build up within the package. Maximum temperature for the following sections were evaluated to 158°F (70°C) and minimum temperatures to -40°F (-40°C).

2.6.1.2 Differential Thermal Expansion

The effects differential thermal expansion for the Traveller series of packages is negligible due to the design of the package. The most significant differential is between the aluminum Clamshell and the fuel assembly, and is less than 0.25 inches. The differential thermal expansion is accommodated by rubber-cork spacers between the Clamshell and fuel assembly.

Ultra-high Molecular Weight (UHMW) polyethylene does have a significantly higher coefficient of thermal expansion (CTE) when compared to Type 304 stainless steel. For this reason, the moderator panels are segmented along their lengths to accommodate the differential thermal expansion between the polyethylene and the inner stainless steel shells of the Outerpack. Additionally, oversized holes in the polyethylene panel are used to accommodate the effects of both temperature extremes.

See Appendix 2.12.3, Mechanical Design Calculations for the Traveller XL Shipping Package, for detailed differential thermal expansion calculations. |

2.6.1.3 Stress Calculations

The Traveller packages are fabricated from relatively thin sheet metal parts which are not subject to thermal gradients generated from the interior of the package. The packages are also not sealed to the environment, therefore pressure stress is negated. The most significant stress potential occurs from the differential expansion rates of the bolted polyethylene moderator panels to the inner steel shells of the Outerpack. This potential stress is also negated by design, whereby the panels are made in sections and the bolt clearances and gaps between panels are adequately sized to allow unrestrained growth and contraction.

Successful testing of full scale Traveller XL packages indicates that the stresses associated with differential thermal expansion of the various packaging components are negligible.

2.6.1.4 Comparison with Allowable Stresses

As discussed in Section 2.6.1.3, Stress Calculations, further evaluation of stresses associated with differential thermal expansion for the various Traveller package components is not required.

2.6.2 Cold

The materials used in construction of the Traveller packages are not degraded by cold at -40°C (-40°F). Stainless steel and aluminum exhibit no brittle fracture at these temperatures. Therefore, the requirements of 10 CFR §71.71(c)(2) and TS-R-1 (618) are satisfied.

2.6.3 Reduced External Pressure

Since the Traveller series of packages are not sealed against pressure, there can not be any significant differential pressure. *See Appendix 2.12.3.2.4.1 for additional explanation.*

2.6.4 Increased External Pressure

Since the Traveller series of packages are not sealed against pressure, there can not be any significant differential pressure. *See Appendix 2.12.3.2.4.1 for additional explanation.*

2.6.5 Vibration

The package must be evaluated to consider the effects of normal vibration on the design performance. The isolation system is designed to dampen normally induced vibrations from transport, and is not fundamental to the safe operation of the package. However, the Outerpak must maintain its structural integrity during transport to maintain a safe transport condition as specified in 10 CFR §71.71(5), TS-R-1 (612). Typical attachment to a transport conveyance for the Traveller packages includes nylon straps or chain mounted both over the package and on the gusset tray connected to the support legs pointed inboard. The loading configuration can be modeled as a simply supported beam. Furthermore, the Outerpak is conservatively modeled considering only the outer shell at the first mode of vibration. The typical natural frequency range for transportation vehicles, $f_{nat \text{ TRANS}}$, is 3.7-8 Hz. The natural frequency of the Outerpak can be determined from: l

$$f_{natOP} = a\sqrt{(EIg/l^3)/m}$$

where $a=1.57$ (primary mode coefficient assuming hinge-hinge end conditions for additional conservatism), $E = 29.4E6$ psi, $I = 634 \text{ in}^4$, $m = 2834$ pounds, $g = 386.4 \text{ in/s}^2$ and $l = 226.2 \text{ in}$. Substituting values:

$$f_{natOP} = 1.57 \sqrt{[(29.4E6)(634)(386.4)/(226.2)^3] / 2834} \text{ 1/s (Hz)}$$

$$f_{natOP} = 1.57 \sqrt{220} \text{ Hz}$$

$$f_{natOP} = 23 \text{ Hz}$$

Since the natural frequency of the Outerpack is greater than the natural frequency typical of a transportation vehicle, resonance of the Outerpack is not expected and normally induced vibrations will not preclude the package from performing its design function.

The rubber shock mounts effectively isolate and dampen loads and vibrations to the Clamshell and its contents. No resonant vibration conditions which could fatigue the Clamshell shall occur during normal conditions of transport.

There are several natural frequencies of the shock mount system depending on direction of movement. The dominant frequency is for vertical movement. This frequency is between 5.9 and 6.7 Hz (for Traveller XL) depending on the weight of the fuel assembly being transported. The fore and aft pitch frequency is slightly higher (6.9-7.9 Hz) but has a lower amplitude. Road tests have been performed with the suspension system to measure amplitudes during shipping. Figure 2-1A is characteristic of the results seen. When the truck travels over a bump, the clamshell initially sees relatively large accelerations (2-3 g's) but this oscillation quickly damps out to accelerations less than 1 g. This 300 mi trip involved approximately five and a half hours on the road with 1.4×10^5 total cycles.

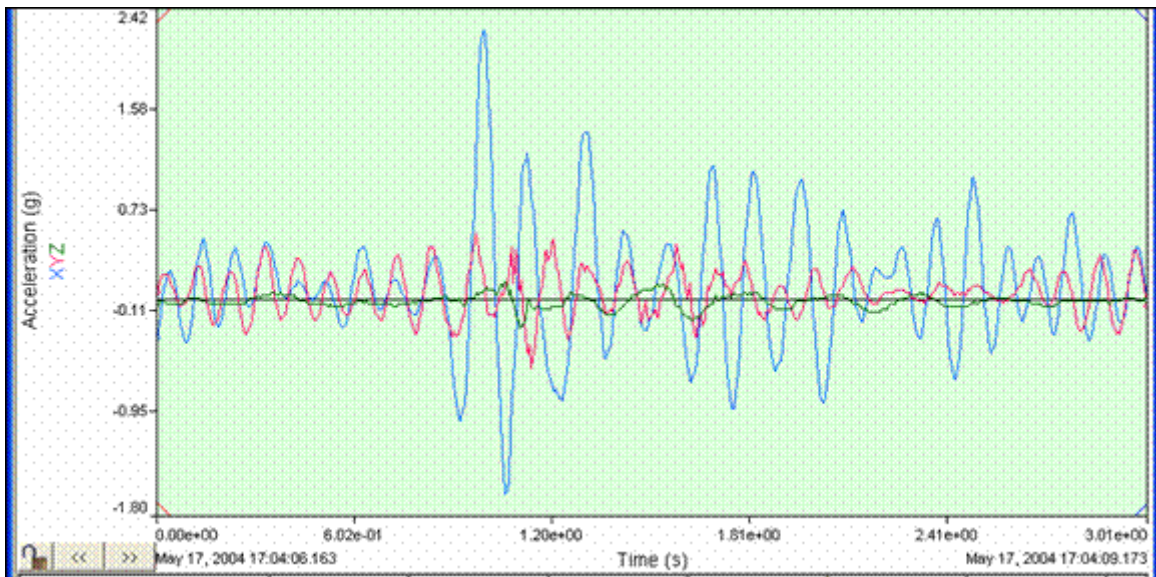


Figure 2-1A Sample of Clamshell Accelerations Measured During Road Test (May 11, 2004)

2.6.6 Water Spray

The materials of construction utilized for the Traveller packages are such that the water spray test identified in 10 CFR §71.71(c)(6), TS-R-1 (721), will have negligible effect on the package. Further, the Traveller Outerpack is cylindrical, and is specifically shaped to negate water collection. Since the Outerpack shell is fabricated from ASTM A240 Type 304 SS, the water spray will not impact the structural integrity of the package.

2.6.7 Free Drop

Since the gross weight of the bounding Traveller XL package is approximately 5,000 kg (11,000 lb), a 1.2 m (4 feet) free drop is conservatively required per 10 CFR §71.71(c)(7), TS-R-1 (722). As discussed in Appendix 2.12.5, Traveller Drop Test Results, 1.2 m drops were performed on the Traveller CTU as an initial condition for subsequent Hypothetical Accident Condition (HAC) tests.

The Traveller packages are well protected during drop testing. In particular, the leg structure including fork lift structure, stacking structure, and upper Outerpack stiffener I-beam structure, all protect the Traveller during impact. Traveller CTU free drop testing and engineering evaluations indicated that this testing have negligible impact on the integrity of the package. However, the orientation selected for the free drop testing was a low angle slap-down, approximately 10 degrees, with the package inverted. The basis for selection of this orientation was that this orientation offered the greatest opportunity to stress the welded joints at the ends of the package. Detailed descriptions of the test results are given in Appendix 2.12.5, Traveller Drop Test Results. Examinations following the prototypic and CTU testing proved the ability of the Traveller packaging to maintain its structural and criticality control integrity. Therefore, the requirements of 10 CFR §71.71(c)(7) are satisfied.

This page intentionally left blank.

2.6.8 Corner Drop

The corner drop test does not apply, since the gross weight of the package exceeds 100 pounds (50 kg), as specified in 10 CFR §71.71(c)(8) or 100 kg (221 lb) as specified in TS-R-1 (722).

2.6.9 Compression – Stacking Test

The compressive load requirement of 10 CFR §71.71(c)(9), TS-R-1 (723) is satisfied by the Traveller packages. Details of the analysis can be found in Appendix 2.12.3, Mechanical Design Calculations for the Traveller XL Shipping Package.

2.6.10 Penetration

The 1 m (40 inch) drop of a 1 ¼-inch (3.2 cm) diameter, 6 kg (13 pound), hemispherical end steel rod, as specified in 10 CFR §71.71(c)(10), TS-R-1 (724), is of negligible consequence to the Traveller series of packages. This conclusion is due to the fact that the Traveller packages are designed to minimize the consequences associated with the much more limiting case of a 1 m (40 inch) drop of the entire package onto a puncture rod, as discussed in Section 2.7.3, Puncture. The 12-gauge (2.7 mm) minimum thickness of the outer shell of the Outerpak is not damaged by the penetration event. Therefore, the requirements of 10 CFR §71.71(c)(10), TS-R-1 (724), are satisfied.

2.7 HYPOTHETICAL ACCIDENT CONDITIONS

When subjected to the hypothetical accident conditions as specified in 10 CFR §71.73, the Traveller package meets the performance requirements specified in Subpart E of 10 CFR 71, and TS-R-1 (726-737 as applicable). This conclusion is demonstrated in the following subsections, where the most severe accident condition is addressed and the package is shown to meet the applicable design criteria. The method of demonstration is through both computer analysis and by testing. The loads specified in 10 CFR §71.73 are applied sequentially, per Regulatory Guides 7.8 and 7.9 (draft).

The Traveller XL Certification Test Unit (CTU) test results are summarized in Section 2.7.7, Summary of Damage, with details provided in Appendix 2.12.5, Traveller Drop Test Results. Additional full-scale test results conducted prior to the certification tests are also included in Appendix 2.12.5. These tests describe the improvements to the Traveller XL design, substantiate the basis for the most severe hypothetical accident condition, and were used to validate the computer simulations.

The following table summarizes the development of the Traveller XL shipping package from the first prototype through the Certification Test Unit, or CTU. As can be seen, satisfying the thermal test requirements proved more difficult than expected. However, the culmination of the development effort has yielded a shipping package that has been thoroughly tested and meets the requirements of both 10 CFR 71 and TS-R-1.

Table 2-5 Summary of the Development of the Traveller			
Traveller XL	Test Sequence(s)	Structural Performance	Fire/Thermal Performance
Prototype-1 Drop testing: Jan 27-28, 2003 Burn Testing: Feb 28, 2003	Objective: FEA validation - 9 m low angle slap down (14.5 degrees) - 9 m high angle (71 degrees) - 1 m pin puncture (through CG, low angle) - 35 minute pool fire burn test.	- Outerpack – <u>Satisfied</u> requirements. Minor, local damage only. - Clamshell – <u>Satisfied</u> requirements for 9 m low angle test. <u>Failed</u> requirements for 9 m high angle test. <u>Satisfied</u> 1 m pin puncture test.	Outerpack <u>failed</u> to prevent ignition of polyethylene sheets in one location. Clamshell temperature away from interior combustion <u>satisfied</u> fire requirements.
<p>Comments:</p> <p>The Traveller XL Prototype-1 demonstrated robust structural performance, except for the Clamshell head(s) attachment which was not adequate. The most probable root cause of ignition of polyethylene sheeting was polyurethane foam combustion products entering the inside of the Outerpack as a result of holes drilled into inner Outerpack shell for thermocouples. No seals were used in the Outerpack for conservatism.</p> <p>Fire testing failed to prevent ignition of the combustible materials in the Outerpack. However, the components not adjacent to the internal fire remained well within thermal limitations, thus, demonstrating that the Outerpack had sufficient thermal resistance to external heat flow into package.</p> <p>Design Changes as a Result of Testing:</p> <p>Additional bolts were added to secure the top Clamshell head for Prototype-2 testing (see below).</p> <p>The package was subjected to the applicable tests for Normal and Hypothetical Accident conditions as described below. Following this series, the package was modified again to assess the robustness of the design. The center Outerpack hinge bolts were removed (1 of 3 bolts) from each hinge section. The number of locking pins on the Clamshell latches was also reduced, from 18 to 12.</p>			
Prototype-2 Drop Testing: Jan 30, 2003 Burn Testing: N/A	- 1.2 m low angle slapdown (20 degrees) - 1 m pin puncture (through CG, low angle) - 9 m high angle (72 degrees) Bolts and locking pins removed (described above) - 9 m end drop (bottom end down) - 9 m horizontal (feet down) - 9 m horizontal (side down)	- Outerpack – <u>Satisfied</u> requirements for all 9 m drops and pin puncture tests. Minor, local damage only. - Clamshell – <u>Satisfied</u> requirements for first 9 m drop. Bottom head separated in second 9 m drop (bottom end drop) because the fuel assembly was not properly seated against bottom Clamshell head as a result of prior drop. No other significant damage.	- Prototype 2 was not subjected to HAC fire testing.

Table 2-5 Summary of the Development of the Traveller (cont.)			
Traveller XL	Test Sequence(s)	Structural Performance	Fire/Thermal Performance
<p>Comments:</p> <p>The performance of the Prototypes (1 & 2) associated with the first testing campaign clearly demonstrated the robustness of the Overpack and Clamshell (except for the Clamshell head attachments). In all, six (6) drops were performed on 2 full-scale prototypes from 9 m. The Outerpack retained its overall integrity and functionality. Most importantly, all design features important to criticality safety performed as intended. Moderator blocks and simulated neutron absorber plates remained intact and attached to their respective structural components.</p> <p>Design Changes as a Result of Testing:</p> <p>Based on the robust structural performance of the Prototype units, several design changes were made to the Traveller XL for subsequent testing in the second test campaign. The Traveller units fabricated for the second campaign were called the Qualification Test Units, or QTUs. A total of two units were fabricated and tested. The significant changes to the QTUs were as follows:</p> <ol style="list-style-type: none"> 1. The Outerpack stainless steel shells were reduced from 11 gauge (0.1196 in., 3.04 mm) to 12 gauge (0.1046 in., 2.66 mm). This change was made primarily to lower weight and reduce excessive structural margin. 2. The hinge bolts were reduced in both number and size, from ten 7/8" (2.22 cm) diameter bolts to ten 3/4" (1.91 cm) bolts. This change was made to reduce excessive design margin. 3. A total of 2 seal materials were added to the design to act as: 1) an environmental seal, and 2) to minimize hot gases from entering the Outerpack seams. 4. The Outerpack leg structure, circumferential stiffeners, stacking brackets, and forklift pocket structures were changed. These changes were made for simplified manufacturing purposes and to reduce excessive design margin. 5. The polyurethane foam density of the center section of the package was reduced from 11 pcf to 10 pcf. The axial limiter foam sections of the package were also reduced from 16 pcf to 14 pcf. This change was made to lower the impact deceleration, and therefore loads experienced by the Clamshell. 6. The Clamshell extrusions were made thicker, from a nominal 0.375" (0.95 cm) to 0.438" (1.11 cm). This change was made primarily to eliminate welding of the heads to the extrusions. Bolted connections were utilized to attach the heads. 7. The welded simulated poison plates were redesigned for a bolted connection. This change was made to reduce the distortion of the aluminum Clamshell extrusions due to welding. 8. The Clamshell door locking latches were redesigned for quarter-turn nuts. This change was made for manufacturing and aesthetic purposes. 9. The Clamshell axial restraint system for restraint of the fuel assembly was redesigned. This change was made to simplify the fuel handling. 			

Table 2-5 Summary of the Development of the Traveller (cont.)			
Traveller XL	Test Sequence(s)	Structural Performance	Fire/Thermal Performance
QTU-1 Drop Testing: Sep 11, 2003 Burn Testing: Sep 15, 2003	<ul style="list-style-type: none"> - 1.2 m low angle slapdown (10 degree) - 9 m high angle (72 degrees) - 1 m pin-puncture (83 degrees at bottom end) - 37 minute pool-fire burn test. 	<ul style="list-style-type: none"> - Outerpack – <u>Satisfied</u> requirements for both drops and pin puncture tests. Minor, local damage only. - Clamshell – <u>Satisfied</u> requirements for both drops and pin puncture tests. 	<u>Failed</u> to prevent ignition of the polyethylene sheeting inside the Outerpack. Temperatures inside the Outerpack exceeded design limits. The package was extinguished approximately 1 hour after the conclusion of the pool fire testing.
<p>Comments:</p> <p>The Traveller XL QTU-1 demonstrated robust structural performance. No Outerpack bolts failed. The Outerpack did not separate, and the pin puncture did not perforate the inner or outer shells nor did it effect the Clamshell in any detrimental way.</p> <p>One hour after the pool fire, the package burning was extinguished. Upon inspection of the QTU-1 unit, it was determined that excessive distortion of the Outerpack shells between the hinges, allowed sufficient hot gases to ignite the polyethylene sheeting on the top half of the Outerpack. The burnt polyethylene sheeting was directly in line with the gaps in between the hinges. The burnt zones (4) were located only on the upper half of the Outerpack. This is most likely due to the flanges on the mating Outerpack halves which preferentially directs incoming gases to the upper portion of the Outerpack.</p> <p>Design Changes as a Result of Testing:</p> <p>Based on unsuccessful fire testing of the QTU-1 unit, the QTU-2 unit was modified for improved thermal performance. Since the QTU-2 had already been drop tested in accordance with 10 CFR 71, and TS-R-1 requirements, only minor modifications were deemed acceptable. Only changes considered for the QTU-2 were ones that would not have affected the drop characteristics and performance. The changes made to the QTU-2 unit subsequent to drop testing are listed as follows:</p> <ol style="list-style-type: none"> 1. The 10 short Outerpack hinge sections were removed and replaced with 8 (four per side) long hinge sections that butted together forming a continuous hinge covering essentially all of the Outerpack mating seams. 2. The polyethylene moderator sheeting (both top and bottom sections) was covered with 26 gage stainless steel sheet metal. This sheet material was welded to the inner shells of the Outerpack along the sides of the covers, the ends (both top and bottom) were sealed with adhesive. The coverings therefore, were not completely welded closed. 			
QTU-2 Drop Testing: Sep 11, 2003 Burn Testing: Oct 20, 2003	<ul style="list-style-type: none"> - 1.2 m low angle slapdown (10 degrees) - 9 m end drop (bottom end down) - 1 m pin puncture (22 degrees through CG) - 32 minute pool-fire burn test. 	<ul style="list-style-type: none"> - Outerpack – <u>Satisfied</u> requirements for both drops and pin puncture tests. Minor, local damage only. - Clamshell – <u>Satisfied</u> requirements for both drop tests and thermal tests. No failures were noted in any structure, or fasteners. The maximum temperature of the Clamshell and its contents never exceeded design limits 	<ul style="list-style-type: none"> - <u>Failed</u> to prevent ignition of the polyethylene sheeting inside the Outerpack. However, the maximum temperature of the Clamshell and contents remained below 200°C. The package was extinguished approximately 7 hours after the conclusion of the pool fire testing.

Table 2-5 Summary of the Development of the Traveller (cont.)			
Traveller XL	Test Sequence(s)	Structural Performance	Fire/Thermal Performance
<p>Comments:</p> <p>The Traveller XL QTU-2 demonstrated robust structural performance. No Outerpack bolts failed. The Outerpack did not separate, and the pin puncture did not perforate the inner or outer shells nor did it effect the Clamshell in any detrimental way.</p> <p>Seven hours after the pool fire, the package burning was extinguished. During this seven hour period there was continuous low level smoldering. Upon inspection of the QTU-2 unit, it was determined that ignition occurred at the bottom end of the package. This was most likely caused by distortion of the Outerpack halves in the area of the bottom end where the impact limiter warped away from the top Outerpack half during the fire. The continuous hinge sections also did not cover the last 3 inches of the Outerpack seams on both sides of the package, which may have allowed additional hot gases to enter the package. The hot gas ingress occurred at a location where there was exposed polyurethane foam (the inner axial limiter foam) due to the thin stainless steel limiter cover being punched out by the Clamshell. This was an expected consequence of the bottom end drop.</p> <p>The long sheet metal covers which were welded along their sides but applied adhesive at the ends did not perform as anticipated. The covers distorted during the testing and opened the adhesive joint. This allowed the polyethylene moderator to ignite. The areas around the shock mounts also were not covered with sheet metal thus exposing the moderator to the conditions inside the Outerpack. These exposed areas showed signs of burning in post-test examinations.</p> <p>The QTU-2 test demonstrated that the polyethylene sheeting must be completely welded, or “canned”, by sheet metal to prevent ignition. However, this test was further evidence that the “bulk” heating of the inside of the Outerpack was acceptable, even with burning occurring within the Outerpack. This is a result of the fact that there is insufficient oxygen to support large amounts of burning. It was estimated that over the 7.5 hours of total burning, only about 10-15% of the moderator material was consumed.</p> <p>Design Changes as a Result of Testing:</p> <p>Based on the structural success of the QTU units and the thermal failures of the units, several changes were made to the design. These changes are listed below:</p> <ol style="list-style-type: none"> 1. The 26 gage moderator sheet metal covers were redesigned so that the polyethylene was completely encapsulated by sheet metal. This mandated the use of sheet metal “cones” around each shock mount. Additionally, thin ceramic insulating material was incorporated between the moderator sheet and the metal covers, around the cones, and over a length of 30 inches at both the top and bottom ends. The ceramic “paper” is nominally 0.06 inches (0.15 cm) in thickness. Ceramic felt was also incorporated to fill the voids under the shock mount cones and at the ends of the moderator sheets. 2. The thin sheet metal impact limiter cover which were design to be punched out by high angle Clamshell impacts were redesigned to have thicker (0.25", 0.64 cm) puncture-resistant plates. These “pillows” were separate structures that were tested in a separate series of mechanical and thermal tests prior to CTU testing. The purpose of the pillows was to prevent polyurethane foam from becoming exposed to the inside of the outerpack, even in end drops. The pillow also incorporated a thick (0.25", 0.64 cm) plate at its base to act as a heat capacitor for incoming heat during the fire testing. Finally, the void space between the pillow and the outer sections of the impact limiters was filled with ceramic felt and paper to further reduce the heat load to the pillows and the internal contents of the Outerpack. 3. The foam density within the inner section of the impact limiters, or pillows, was reduced from 7 pcf to 6 pcf to allow more crushing of the foam. This change was made to lower the impact forces on the Clamshell and its contents. 			

Table 2-5 Summary of the Development of the Traveller (cont.)			
Traveller XL	Test Sequence(s)	Structural Performance	Fire/Thermal Performance
<p>4. The four (4) long Outerpack hinge sections were lengthened to cover all of the Outerpack seams. There existed a nominal 3 inch (7.6 cm) uncovered section at the bottom end.</p> <p>5. The bottom limiter cover which curves around the bottom impact limiter was extended an additional 1.5 inches axially. Ribs (or lips) were added to this cover, and to the bottom limiter, to further reduce the ingress of hot gases.</p> <p>6. The foam density in the outer sections of impact limiters was increased from 14 pcf to 20 pcf to reduce the heat flow through these sections.</p> <p>7. The polyethylene moderator sheets were redesigned for manufacturing purposes.</p> <p>8. The silicone rubber Omega seal, was replaced with acrylic impregnated fiberglass braided tubing. This change was made to eliminate a potential source of combustion inside the Outerpack.</p> <p>The design changes listed above were retrofitted onto the QTU-1 unit (which had already been burned). The QTU-1 unit was then instrumented and taken through a series of fire tests in an effort to quantify the thermal design margins associated with these design changes. This testing was considered necessary to quantify the thermal design margins before the final Certification Test Unit (CTU) test article was tested. The modified unit was tested twice. It was first burned for 40 minutes, then it was re-burned for another 30 minutes the following day. The results of the tests were excellent. The impact limiter pillow temperature never exceeded 120°C, and the data confirms the primary heating to the inside of the Outerpack is by conduction.</p> <p>Based on the successful testing of the modified QTU-1 article, the design changes were incorporated in the manufacturing of the Traveller XL CTU package.</p>			
CTU Drop Testing: Feb 5, 2004 Burn Testing: Feb 10, 2004	<ul style="list-style-type: none"> - 1.2 m low angle slapdown (9 degrees) - 9 m end drop (bottom end down) - 1 m pin puncture (21 degrees through CG, directly onto Outerpack hinge) - 32 minute pool-fire burn test. 	<ul style="list-style-type: none"> - Outerpack – <u>Satisfied</u> requirements for both drops and pin puncture tests. Minor, local damage only. - Clamshell – <u>Satisfied</u> requirements for both drop tests and thermal tests. The Clamshell retained its shape and remained closed and latched after drop testing. 	Clamshell – <u>Satisfied</u> requirements for fuel containment and criticality safety. The Clamshell and its contents remained below a maximum of 150°C.
<p>The Traveller XL CTU demonstrated robust structural performance. No Outerpack bolts failed and the Outerpack retained its circular pre-test shape. The Outerpack did not separate, and the pin puncture did not perforate the inner or outer shells nor did it affect the Clamshell in any detrimental way. Minor weld failures on the Outerpack, in the region near the impact, were observed in post-test examinations. These failures had negligible effect on the performance of the CTU. The two (2) quick release pins on the cover lips detached during the drop test, therefore, they could not be used where they were intended, in the burn test (as such, they were not re-installed for the burn testing).</p>			

Table 2-5 Summary of the Development of the Traveller (cont.)			
Traveller XL	Test Sequence(s)	Structural Performance	Fire/Thermal Performance
<p>The impact limiter pillows performed as intended, however, they did not crush as much as intended due to the inherent axial flexibility of the 17x17 XL fuel assembly. The moderator sheeting remained completely contained within the sheet metal covering. A small brown spot was observed on the back side of one moderator sheet attached to the Outerpack top half. A very small amount of flow occurred away from the hot spot. This melt spot was small, affecting only a few cubic centimeters of material.</p> <p>The Clamshell was found intact and closed, and the simulated poison plates maintained their attached position with very little distortion. Minor damage was observed at the location of the impact with the pillow, however, the damage had negligible effect on the performance of the Clamshell. All closure nuts remained intact with no signs of distortion or stress.</p> <p>The most significant observation from the post-test examinations were 20 cracked fuel rod bottom end plug welds. These cracks occurred in the regions corresponding to the corners of the bottom nozzle. At these corners, the buckled bottom nozzle has steep faces (in excess of 45 degrees), which was exacerbated by the characteristically long legs of the 17XL assembly. The angled faces apply a side force to the local fuel rods as they are decelerated in the impact. The largest crack occurred in a fuel rod located in the outermost row within the assembly. The crack in the rod had a maximum width of approximately 0.075" (1.91 mm). This width is not sufficiently large enough for loss of fuel from the rod. Further, in all cases of cracked rods, the bottom end plugs did not separate. Therefore, fuel pellets are prevented from exiting any of the cracked rods.</p> <p>Design Changes as a Result of Testing:</p> <p>The CTU satisfied the HAC drop-test and burn-test requirements in all aspects. However, as with any development program, improvements can be envisioned after every series of tests. Based on the results of the CTU tests, several minor changes shall be incorporated into production units to enhance the performance of the package. There changes do not change the performance or characteristics of the package, but merely improve the safety margin of the package by incorporating rather obvious improvements as listed below. The basis for the change is also listed below:</p> <ol style="list-style-type: none"> 1. The studs which hold the moderator blocks to the upper Outerpack half failed during the drop testing. The moderator remained contained within the sheet metal covering. However, the number of 3/8" (0.95 cm) diameter studs shall be increased by 50% on the top Outerpack assembly only. 2. The bottom impact limiter pillow is welded at the top plate to the Outerpack inner plate. This weld is design to break in a high angle impact. It performed well in the drop test, however, it did not completely break. This joint shall be redesigned with a small groove cut into the inner plate to form a weakened break point. The break shall therefore not necessarily occur at the weld location. 3. The quick release pins used to secure the bottom end seam flange cover failed during drop testing but had negligible effect on the performance (intended for thermal performance only). Therefore, they were not used in the thermal test and will not be used in production units. <p>The figure below (Figure 2-1B) shows the impact limiter, or Pillow, assembly (shown without insulation). This assembly is shown installed in the Traveller package bottom (the configurations are the same for STD and XL packages) in Figure 2-1C. The weld between the bottom plate (yellow) and the puncture plate (red) is also shown. During testing this weld failed as expected, however, it did not completely allow the components to separate. This design change weakens the bottom plate by reducing its thickness to a nominal 0.025" thickness, as shown in Figures 2-1D and 2-1E. A .25 inch wide channel was added to weaken the part.</p>			

Table 2-5 Summary of the Development of the Traveller
(cont.)

Traveller XL	Test Sequence(s)	Structural Performance	Fire/Thermal Performance
--------------	------------------	------------------------	--------------------------

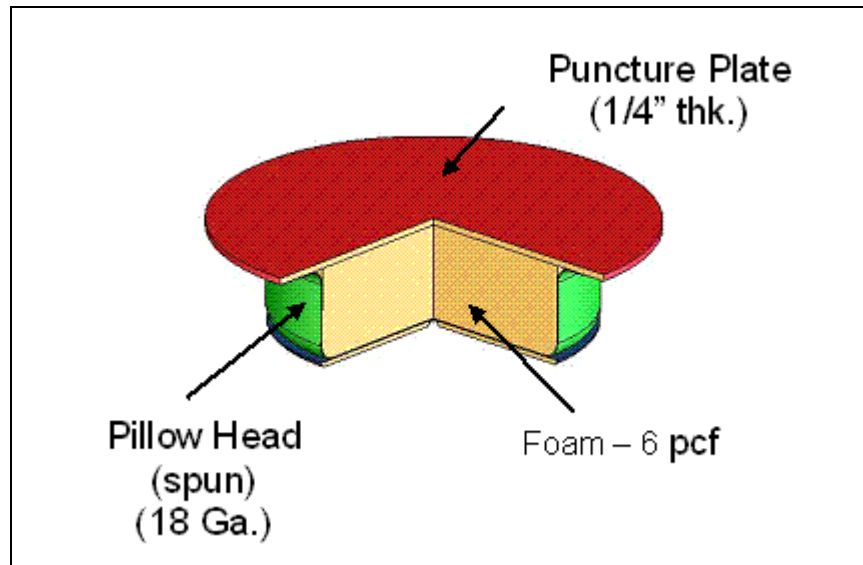


Figure 2-1B Impact Limiter "Pillow" Assembly

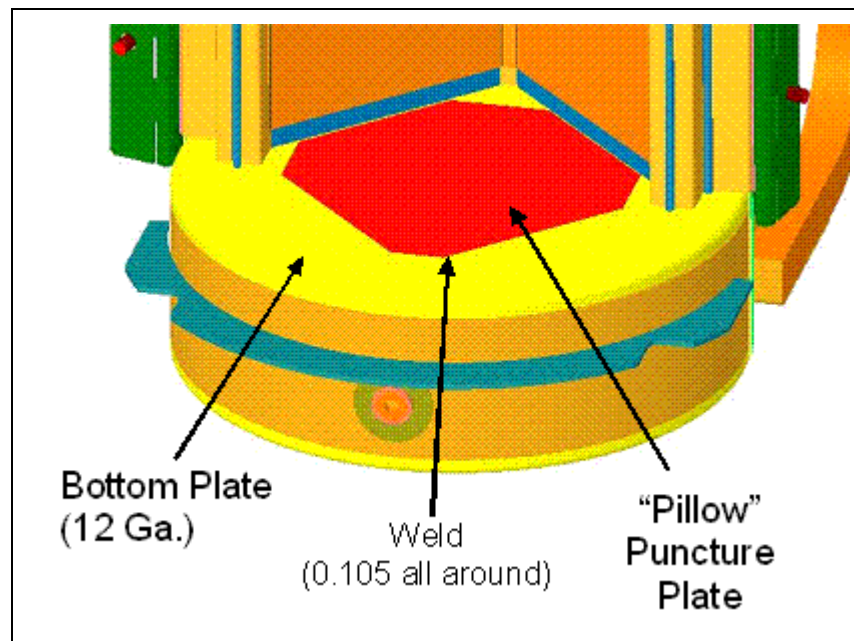


Figure 2-1C Container Bottom End

Table 2-5 Summary of the Development of the Traveller
(cont.)

Traveller XL	Test Sequence(s)	Structural Performance	Fire/Thermal Performance
--------------	------------------	------------------------	--------------------------

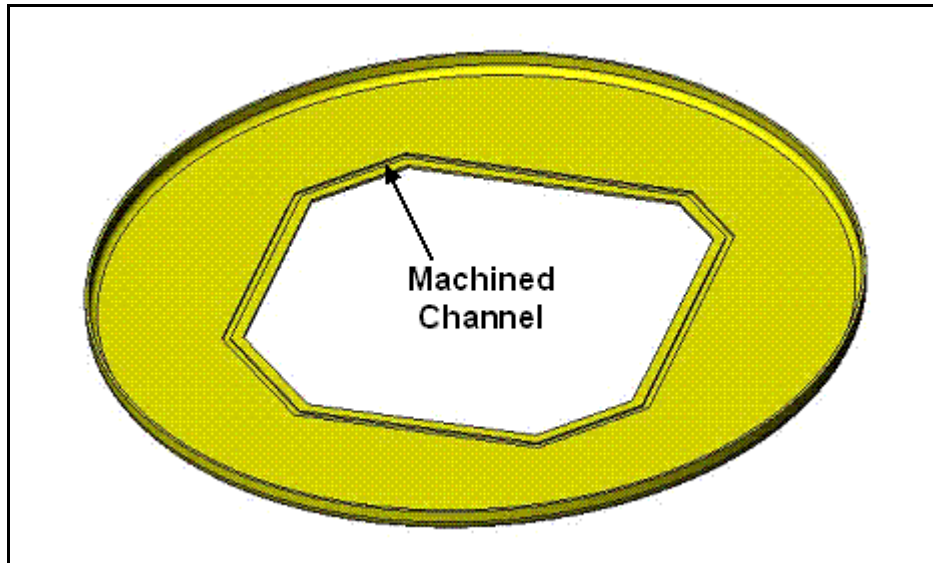


Figure 2-1D Impact Limiter "Pillow" Assembly

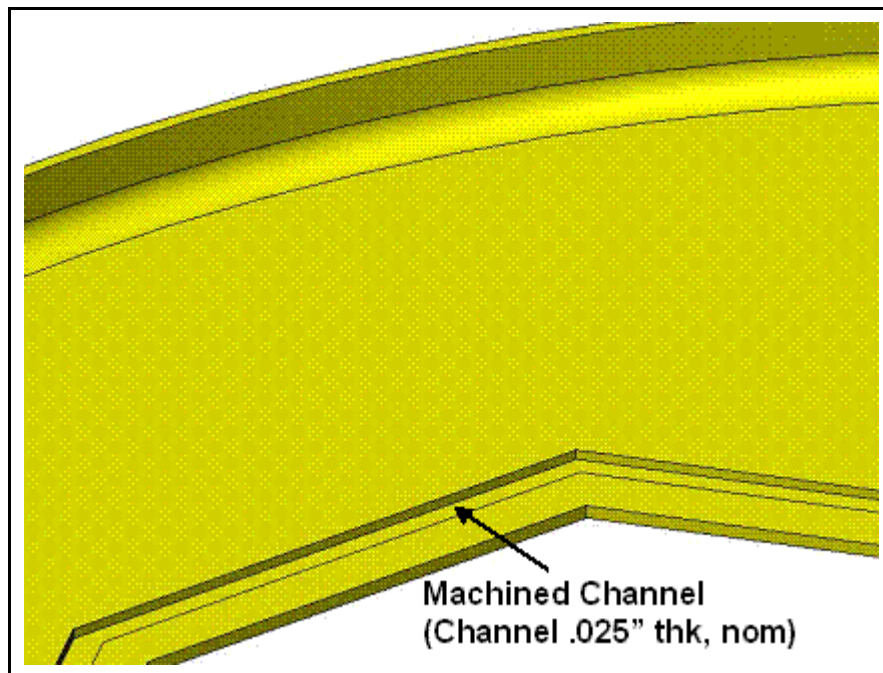
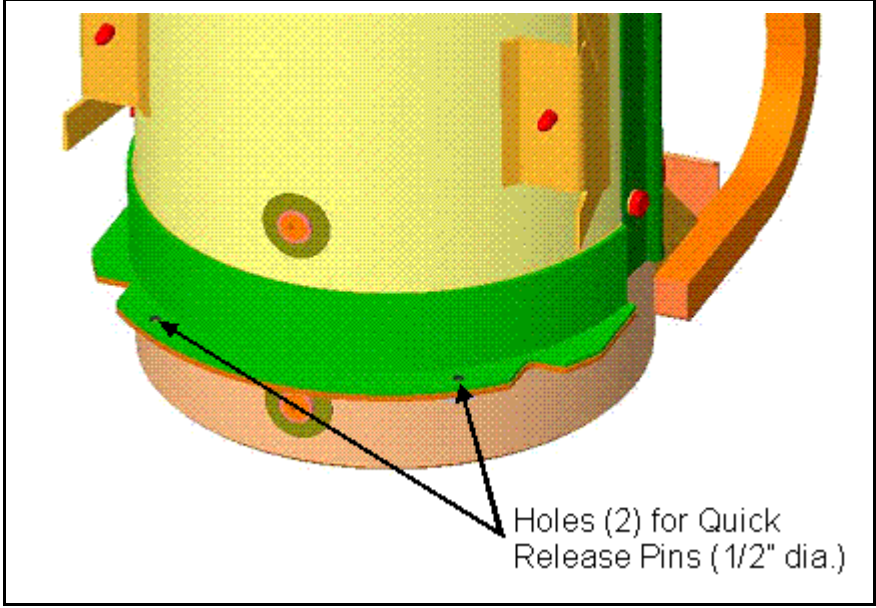


Figure 2-1E Bottom Plate - Viewed from Inside

Table 2-5 Summary of the Development of the Traveller (cont.)			
Traveller XL	Test Sequence(s)	Structural Performance	Fire/Thermal Performance
<p>The CTU design included a pinned connection (2 quick release pins – 0.5" diameter) between Outerpack halves at the bottom end of the package. Quick release pins were designed to help prevent the halves from warping and opening a gap locally during fire testing. Figure 2-1F shows the location of the quick release pins. During drop testing, the pins failed, therefore, they could not be used in the fire testing</p>			
 <p>Holes (2) for Quick Release Pins (1/2" dia.)</p>			
<p>Figure 2-1F CTU Package Bottom End</p>			

This page intentionally left blank.

2.7.1 Free Drop

Subpart F of 10 CFR 71, TS-R-1 (727) requires that a 9-meter (30 foot) free drop be considered for the Traveller series of packages. The free drop is to occur onto a flat, essentially unyielding, horizontal surface, and the package is to strike the surface in an orientation for which the maximum damage is expected. The free drop is addressed by test, in which the most severe orientation is used. The free drop precedes both the puncture and fire tests. The ability of the Traveller packages to adequately withstand this specified drop condition is demonstrated via drop testing of the full-scale Traveller XL Certification Test Unit (CTU). The Traveller XL variant bounds the shorter and lighter Traveller STD design. Simulations using finite element analysis are performed to demonstrate the response of the package to free drop tests with the Clamshell axial spacer and removable top end plate.

2.7.1.1 Technical Basis for the Free Drop Tests

To properly select a worst case package orientation for the 9 m (30 feet) free drop event, the foremost item that could potentially compromise the criticality control integrity of the Traveller series of packages must be clearly identified.

The criticality control integrity may be compromised by four methods: 1) excessive movement of the fuel rods such that they form a critical geometry, 2) damage/destruction of the neutron absorber and polyethylene sheeting, 3) degradation of the neutron absorber/polyethylene sheeting and/or 4) other structural damage that could affect the nuclear reactivity of an array of packages.

For the above considerations, testing and FEA predictive methodology must include orientations that affect the Clamshell geometry and integrity. Throughout the development of the Traveller XL, minor design changes were made to optimize the structural and thermal performance of the package.

A total of nine (9) 30 foot (9 m) free drops were performed using full-scale prototypes at a variety of orientations to determine the most severe orientation and to assist in benchmarking the computer simulation model. Based on these tests, and the predictions of the analytic analyses, it was determined that the most severe 9 m free drop orientation was a bottom-end down drop due to; 1) the relatively high deceleration, 2) the greatest opportunity for lattice expansion of the fuel, and 3) the greatest opportunity for fire damage as a result of the subsequent pool-fire thermal testing.

The bottom-down end drop causes the greatest damage to the axial impact limiters, or “pillows.” These pillows were incorporated as a re-design from QTU-2 testing whereby the Clamshell punched through the plate covering the inner section of the axial impact limiter. This exposed foam later burned within the interior of the Outerpack and ignited the moderator panels. The concept of a puncture plate was redesigned to incorporate a “puncture resistant” plate. The inner foam limiter was therefore protected by the puncture resistant plate (1/4" thk, 0.64 cm), and was enclosed by a spun metal “can” welded to the plate to completely seal the pillow assembly. CTU test results confirmed that no polyurethane foam was exposed as a result of the bottom-down end impact.

The long bottom nozzle “legs” associated with the Westinghouse 17x17 XL fuel assembly are considered the most severe because they allow considerable strain of the bottom nozzle (particularly the flow plate, or

adapter plate) during a bottom-down end drop. The bowed adapter plate offers the greatest opportunity to damage fuel rods during the impact.

The top-down end drop produces significantly lower deceleration due to buckling of the axial clamp bolts. As these buckle, considerable energy is absorbed, thus lower the buckling of the top nozzle. By comparison, the bottom-down end drop is more severe.

2.7.1.2 Test Sequence for the Selected Tests

Analyses indicated and testing demonstrated that the puncture tests did not cause any damage to the package that would lead to further damage in the fire test, and neither did they compromise package containment or confinement. Therefore either order in which the 9m drop test and the puncture test are performed is equally valid.

TS-R-1, para 727, states that the drop test sequence shall be such that, upon completion, the specimen will have suffered such damage as to lead to maximum damage in the thermal test that follows. The TS-R-1 advisory document, TS-G-1.1, expands on this, saying that the assessment of maximum damage should consider what affect the drops have on package containment, shielding, and confinement. TS-G-1.1 further cautions that the most damaging package orientation may not be a flat impact onto the bar top surface, but an angle in the range 20°–30° range, because such an angle causes tearing of the outer skin as well as puncturing.

Section 2.7.3.1 discusses the technical basis for the puncture test, indicating that the greatest possibility of cumulative damage to this package occurs when the pin puncture is located within the area of impact of the 9m drop. Thus, maximum damage would occur when the puncture test follows the 9m drop test. During the Traveller development period, several test specimens were subjected to puncture drops onto different parts of the package in an effort to determine which location was most damaging. In one instance the drop test sequence was altered to assess whether or not a different order would cause more damage. As mentioned above, it was found that the puncture tests did not cause any damage to the package that would jeopardize either package containment or confinement. Therefore either order in which the 9m drop test and the puncture test are performed is equally valid.

Section 2.7.3.2 summarizes the results from the puncture drop tests. The several puncture tests are described in detail in the SAR and are summarized below.

Test Specimen	SAR	Test Sequence	Inspection Results
FEA Analysis	2.12.3.2.7	Two cases modeled: – Horizontal drop onto belly – Horizontal drop onto hinge	<ul style="list-style-type: none"> • Predicted unlikely that the outer shell would be penetrated in either case • (Good agreement between FEA results and prototype test results)
Prototype I	2.12.4.1	(1) 9m Drop – Bottom nozzle drop – 71° angle CG over corner on hinge (2) Puncture – Package at 20° angle upside down over center of gravity	<ul style="list-style-type: none"> • Outerpak outer skin was locally indented 1.63" • Impact punch zone width was 10.5" • Pin did not perforate the outer skin • Internal inspection findings – small dent about 7/16" to 1/2" and 15" wide resulted from the pin puncture test • Moderator blocks were not impacted by the pin test.

Test Specimen	SAR	Test Sequence	Inspection Results
Prototype II	2.12.4.1	(1) Puncture – Drop onto package side – Package at 20° angle, CG (2) 9m Drop – Top nozzle drop – 72° angle CG over corner	<ul style="list-style-type: none"> • Outerpac outer skin was locally indented about 2" • Impact punch zone was 10" tall and 14" wide • Pin did not perforate the inner and outer shell • Moderator blocks and neutron poison plates maintained position
Qualification Test Unit I	2.12.4.2.1	(1) 9m Drop – Top nozzle drop – 72° angle CG over corner (2) Puncture – Drop onto top nozzle end – Package at 83° angle – Dropped on hinge to add to damage from 9m drop	<ul style="list-style-type: none"> • Indention was approximately 1-1/2" deep • Additional tearing of the joint was noted which resulted in measured tear of approximately 1-1/8" • Moderator blocks and neutron poison plates maintained position
Qualification Test Unit II	2.12.4.2.2	(1) 9m Drop – Bottom nozzle drop – 90° angle (2) Puncture – Drop onto underbelly of package – Package at 22° angle	<ul style="list-style-type: none"> • Damage zone was 9" long x 6" wide x 2-7/8" deep • Moderator blocks and neutron poison plates maintained position
Certification Test Unit	2.12.4.3	(1) 9m Drop – Bottom nozzle drop – 90° angle (2) Puncture – Drop onto side of package, onto hinge – Package at 21° angle	<ul style="list-style-type: none"> • 6" length of hinge dented length to a maximum depth of 1.375" • Hinge separation of 1/2" from package about 7-1/2" from the impact point towards the top nozzle end • Hinge knuckles were not compromised • Moderator blocks and neutron poison plates maintained position

2.7.1.3 Summary of Results from the Free Drop Tests

Successful HAC free drop testing of the Traveller XL CTU certification unit indicates that the various structural features are adequately designed to withstand the 9 m (30 foot) free drop event. The most important result of the testing program was the demonstrated ability of the bounding Traveller XL package to maintain its criticality safety integrity.

Significant results of the free drop tests, including the thermal test, are as follows:

1. There was no breach or distortion of the Clamshell aluminum container.
2. There was no evidence of melting or material degradation on the polyethylene sheeting.
3. The Outerpack remained closed and structurally intact.
4. A small number of rods (20) were cracked during drop testing (only seen in bottom-end drops).
5. Rod damage has been at the end of the rods only. No damage anywhere else.
6. None of the end plugs have separated from the rods.
7. No pellet material is lost from the cracked rods.

Further details of the free drop test results are provided in Appendix 2.12.5, Traveller Drop Test Results. |

2.7.2 Crush

The crush test specified in 10 CFR §71.73(c)(2), TS-R-1 (727) is required only when the specimen has mass not greater than 500 kg (1,100 pounds), an overall density not greater than $1,000 \text{ kg/m}^3$ (62.4 lb/ft^3), and radioactive contents greater than 1,000 A2, not as special form. The gross weights of the Traveller packages are greater than 500 kg (1,100 pounds). Therefore, the dynamic crush test of 10 CFR §71.73(c)(2), TS-R-1 (727) is not applicable to the Traveller series of packages.

2.7.3 Puncture

Subpart F of 10 CFR 71 requires performing a puncture test in accordance with the requirements of 10 CFR §71.71(c)(3), TS-R-1 (727). The puncture test involves a 1 m (40 inch) drop onto the upper end of a solid, vertical, cylindrical, mild steel bar mounting on an essentially unyielding, horizontal surface. The bar must be 15 cm (6 inches) in diameter, with the top surface horizontal and its edge rounded to a radius of not more than 6 mm (1/4 inch). The minimum length of the bar is to be 20 cm (8 inches). The ability of the bounding Traveller XL packages to adequately withstand this specified drop condition is demonstrated via testing of numerous full-scale Traveller XL prototypes and the Certification Test Unit (CTU).

2.7.3.1 Technical Basis for the Puncture Drop Tests

To properly select a worst case package orientation for the puncture drop test, items that could potentially compromise criticality integrity of the Traveller package must be clearly identified. For the Traveller XL package design, the foremost item to be addressed is the integrity of the Clamshell and the neutron moderation and absorption materials (i.e., neutron absorber plate and polyethylene sheeting).

The integrity of the Clamshell and the criticality control features may be compromised by two methods: 1) breach of the Clamshell boundary, and 2) degradation of the neutron moderation/control materials due to fire.

For the above reasons, testing must consider orientations that attack the Outerpack closure assembly, which may result in an excessive opening into the interior for subsequent fire event, and/or the Clamshell which contains the fuel assembly. Based on prototype testing and computer simulations of the pin puncture event, the pin puncture has insufficient energy to cause significant damage to the Outerpack hinge closure system nor to the Clamshell (including components within the Clamshell).

The greatest possibility of cumulative damage to the package occurs when the pin puncture is located within the area of impact of the 9m drop. These locations further attack the welded joints adjacent to the crushed area between the Outerpack outer shell and the end cap. Many pin puncture locations were tested in prototype testing, and all had insignificant impact on the structural and thermal performance of the package. See Table 2-2 above, and Appendix 2.12.5, Traveller Drop Test Results, for more information regarding pin puncture testing.

Based on the above discussion, the Traveller XL CTU was specifically evaluated at a “new” location. The pin puncture was located such that the pin impacted directly on an Outerpack hinge at a low impact angle. This test had not previously been performed, and it was desired to test the hinge’s ability to take a pin impact and still perform its important function of thermally protecting the seam between Outerpack bottom and top assemblies. The thermal protection offered by the hinge is described in more detail in Section 3.

2.7.3.2 Summary of Results from the Puncture Drop Test

Successful HAC puncture drop testing of the CTU indicates that the various Traveller XL packaging features are adequately designed to withstand the HAC puncture drop event. The most important result of the testing program was the demonstrated ability of the bounding Traveller XL to maintain its structural integrity. Significant results of the puncture drop testing are as follows:

1. Minor damage to the Outerpack and Outerpack hinge
2. No affect on the structural or thermal performance of the package.
3. There was no evidence of separation of the Outerpack seam which would allow hot gases to enter the Outerpack.
4. No evidence of movement occurred that would have significantly affected the geometry or structural integrity of the Clamshell.
5. There was no evidence of loss of contents from the Clamshell due to the puncture events.
6. There was no evidence of deterioration of the polyethylene sheeting in the subsequent fire event.
7. There was no evidence of deterioration of the borated-aluminum sheeting (simulated) in the subsequent fire event.

Further details of the puncture drop test results are provided in Appendix 2.12.5, Traveller Drop Test Results. |

2.7.4 Thermal

Subpart F of 10 CFR 71, TS-R-1 requires performing a thermal test in accordance with the requirements of 10 CFR §71.71(c)(4), TS-R-1 (728). To demonstrate the performance capabilities of the Traveller packaging when subjected to the HAC thermal test specified in 10 CFR §71.71(c)(4), TS-R-1 (727), a full-scale CTU was burned in a fully engulfing pool fire. The test unit was subjected to a 9 m (30 foot) free drop, and a 1.2 m (4 foot) puncture drop, prior to being burned, as discussed above. Further details of the thermal performance of the Traveller XL CTU are provided in Section 3, Thermal Evaluation.

Type K thermocouples were installed on the exterior surface of the packaging (each side, top, and bottom) to monitor the package's temperature during the test. In addition, passive, non-reversible temperature indicating labels were installed on the Clamshell, fuel assembly, and inner surfaces of the Outerpack.

The CTU was exposed to a minimum 800°C (1,475°F), 30-minute pool fire. As discussed in Appendix 2.12.5, Traveller Drop Test Results, the package was orientated such that the Outerpack was on its side. This orientation offered the greatest opportunity for formation of a chimney and thus result in maximum combustion of the Outerpack foam and degradation of the polyethylene sheeting. |

Following the minimum 30-minute fire, the CTU was allowed to cool naturally in air, without any active cooling systems.

2.7.4.1 Summary of Pressures and Temperatures

The accident case pressure is assumed to be 0 psig since the Outerpack and Clamshell are not sealed.

The peak temperatures for the Clamshell, as recorded by five (5) temperature indicating strips, was 104°C (217°F). No loss of material was observed in the polyethylene material.

2.7.4.2 Differential Thermal Expansion

Fire testing of a full-scale Traveller XL package indicates that the stresses associated with differential thermal expansion of the various components are negligible.

2.7.4.3 Stress Calculations

Successful fire testing of a full-scale Traveller XL CTU package, as well as prior tested prototypes, indicates that the stresses associated with differential thermal expansion of the various packaging components are negligible.

2.7.4.4 Comparison with Allowable Stresses

As discussed in Section 2.7.4.3, Stress Calculations, further evaluation of stresses associated with differential thermal expansion for the various Traveller package components is not required.

Successful HAC thermal testing of the CTU indicates that the various Traveller packaging design features are adequately designed to withstand the HAC thermal test event. The most significant result of the testing program was the demonstrated ability of the Traveller XL CTU to maintain its criticality control integrity, as demonstrated by post-test inspection of; the moderator and poison materials, the remaining polyurethane foam, and the integrity of the Clamshell.

Further details of the thermal test results are provided in Appendix 2.12.5, Traveller Drop Tests Results and Section 3, Thermal Evaluation.

2.7.5 Immersion – Fissile Material

Subpart F of 10 CFR 71 requires performing an immersion test for fissile material packages in accordance with the requirements of 10 CFR §71.73(c)(6), TS-R-1 (733). Because of the seal configuration (see Section 1, General Information), the Traveller STD and Traveller XL packages are not leak-tight under external overpressure. Under the immersion test, water will fill all internal void space. Because of the pressure equalization, the packaging structure is therefore not subjected to loading during these tests.

2.7.6 Immersion – All Packages

Subpart F of 10 CFR 71 requires performing an immersion test for fissile material packages in accordance with the requirements of 10 CFR §71.73(c)(6), TS-R-1 (729). Because of the seal configuration (see Section 1, General Information), the Traveller STD and Traveller XL series of packages are not leak-tight under external overpressure. Under the immersion test, water will fill all voids. Because of the pressure equalization, the packaging structure is therefore not subjected to loading during these tests.

As the package model criticality study assumes the worst-case flooding scenario, the Traveller XL CTU is exempted from this water immersion test.

2.7.7 Summary of Damage

As discussed in the previous sections, the cumulative damaging effects of the free drops, puncture drop, and thermal tests were satisfactorily withstood by the Traveller XL CTU. Subsequent examinations of the CTU confirmed that integrity of the criticality control components was maintained throughout the test series. The geometry of the Clamshell remained essentially unchanged from the pretest condition. In addition, the Fuel Assembly was well protected and experienced damage that was within acceptance criteria. Therefore, the requirements of 10 CFR §71.73, TS-R-1 (726-729) have been adequately satisfied.

2.8 ACCIDENT CONDITIONS FOR AIR TRANSPORT OF PLUTONIUM

Not applicable.

2.9 ACCIDENT CONDITIONS FOR FISSILE MATERIAL FOR AIR TRANSPORT

Application to be made at a later date.

2.10 SPECIAL FORM

The contents of the Traveller series of packages do not classify as special form material.

2.11 FUEL RODS

In the Traveller XL and STD packages, the fuel rods within the package provide containment for the nuclear fuel. This containment was successfully demonstrated in 3 full-scale test campaigns comprising a total of nine (9) 30 foot free drops, and the corresponding 1.3 meter free-drops and pin puncture tests. These tests resulted in 100% containment of the fuel pellets within rod of every fuel assembly.

For all 9-meter drop test orientations except for the bottom-down end drop (long axis of package aligned with the gravity vector), every fuel rod survived with no damage except slight to moderate buckling of the cladding. Rod pressure test sampling was routinely performed on these fuel assemblies. Except for the bottom-down end drop, all of the rods sampled remained intact and pressurized. All rods visually appeared in excellent condition.

A total of two (2) full-scale Traveller XL packages (QTU-2 and CTU) were tested in a bottom-down end drop orientation. Both of these fuel assemblies (dummy Westinghouse 17x17 XLs) experienced a small percentage of rods with cracked welds in the location of the bottom end plug. In the worst case assembly (CTU), post-test inspection of the fuel assembly indicated that approximately 7.5% of the fuel rods were visibly cracked at the end plug weld zone. The average magnitude of the crack widths measured approximately 0.030 inches (0.76 mm) encompassing about one-half of a rod diameter. This minor cracking is considered insignificant since fuel pellets of diameter 0.374 inches (9.50 mm) are approximately 12.5 times larger than the average visible crack widths. A crack width of 0.075 inches (1.91 mm) was the largest observed. This width is not sufficient for fuel pellets to escape. Therefore, the containment system satisfies its requirement of containing loss of fuel.

Due to the nature of the bottom-down end impact, the fuel rod array is tightly packed and forced into the bottom nozzle. As the bottom nozzle buckles, the rods located nearest the corners of the adapter plate experience a side loading due to the deformed shape of the plate. This moment is sufficient to crack the weld, however, it is clearly not sufficient to completely break off the bottom end plug since the array of rods is so tightly packed. No complete separation of the bottom end plug was observed in any fuel rods for both fuel assemblies. Therefore, the fuel pellets are safely contained within each fuel rod. Further details can be found in Appendix 2.12.5, Traveller Drop Tests Results.

2.11.1 Rod Pipe

The Traveller Clamshell is primarily designed to transport PWR fuel assemblies. To accommodate loose fuel rods, a rod pipe has been designed. It is a 304 stainless steel rod pipe with a maximum diameter of 6.625 inches (6" Schedule 40 pipe), maximum length 200 inches, and a maximum loaded weight of 1650 lbs.

The loose rod pipe is a relatively rigid structure as compared to a fuel assembly. The rod pipe is a single structural member closed by rigid mechanisms. Because the fuel assembly is less stiff than the rod pipe, the fuel assembly is more likely to deform plastically from localized buckling.

The rod pipe is fit to conform into the clamshell axially with a rubber spacer, and is restrained laterally by the bent flanges with foam rubber "clamps" similar to retraining a fuel assembly at the spacer grid locations.

The TRAVELLER response to the 9-meter HAC drop test resulted in the kinetic energy due to the combined mass of the fuel assembly and clamshell being absorbed by the outerpack impact limiter and minor fuel assembly buckling. As a result, the strain damage to the fuel assembly was minimal, and the clamshell retained its pre-test geometry and its structural integrity even though the full stroke of the impact limiter was not utilized. When subject to the 9-meter impact test described in 10CRF71.73, the rod pipe is expected to utilize the full stroke of the impact limiter due to their rigidity. The resulting applied impact force to the rod pipe is expected to be less than that imparted to the fuel assembly. Furthermore, the rod pipe is expected to act in a coupled manner similar to the fuel assembly and result in similar load paths. With the maximum mass of 1650 pounds, the rod pipe will have less impact energy imparted on their rigid structure as well. The maximum rod pipe mass is less than the maximum fuel assembly mass used in the 9-meter impact test. Therefore, the performance of the TRAVELLER packaging with rod pipe contents would be similar to and bounded by the performance of the TRAVELLER packaging that was demonstrated by the 9-meter HAC drop with the fuel assembly contents.

This page intentionally left blank.

2.12 APPENDICES

2.12.1 References

None.

2.12.2 Container Weights and Centers of Gravity

2.12.3 Mechanical Design Calculations for the Traveller XL Shipping Package

2.12.4 Drop Analysis for the Traveller XL Shipping Package

2.12.5 Traveller Drop Test Results

2.12.6 Supplement to Drop Analysis for the Traveller XL Shipping Package – Clamshell Axial Spacer Structural Evaluation

2.12.7 Supplement to Drop Analysis for the Traveller XL Shipping Package – Clamshell Removable Top Plate Structural Evaluation

2.12.8 Supplement to Drop Analysis for the Traveller XL Shipping Package - Structural Analysis of the Traveller VVER Shipping Package

2.12.2 Container Weights and Centers of Gravity

2.12.2.1 Container Weights

This section provides the Traveller XL, VVER and STD weight breakdown to establish design and licensing weights, and centers of gravity for each package. The Design and Licensing Basis Gross Weight is calculated from the Nominal Total Weight plus the 2.3% manufacturing uncertainty. The maximum tare weight is the Design and Licensing Basis Gross Weight less the maximum fuel assembly weight. Maximum tare and Design and Licensing weights are rounded up to the nearest tenth after the maximum tare weight is determined.

Table 2-6 Traveller STD, Traveller XL, and Traveller VVER Design Weights			
	Traveller STD	Traveller XL	Traveller VVER
Nominal Outerpack Weight, lb (kg)	2368 (1074)	2670 (1211)	2670 (1211)
Max. Fuel Assembly Weight, lb (kg)	1650 (748)	1971 (894)	1850 (839)
Nominal Clamshell Weight, lb (kg)	378 (171)	467 (212)	463 (210)
NOMINAL TOTAL WEIGHT, lb (kg)	4396 (1994)	5108 (2317)	4983 (2260)
DESIGN and LICENSING BASIS GROSS WEIGHT, lb (kg)	4500 (2041)	5230 (2372)	5105 (2316)
DESIGN TARE WEIGHT, lb (kg)	2850 (1293)	3255 (1476)	3255 (1476)

2.12.2.2 Centers of Gravity

This section provides the location of the center of gravity for empty Traveller XL/VVER and Traveller STD packages.

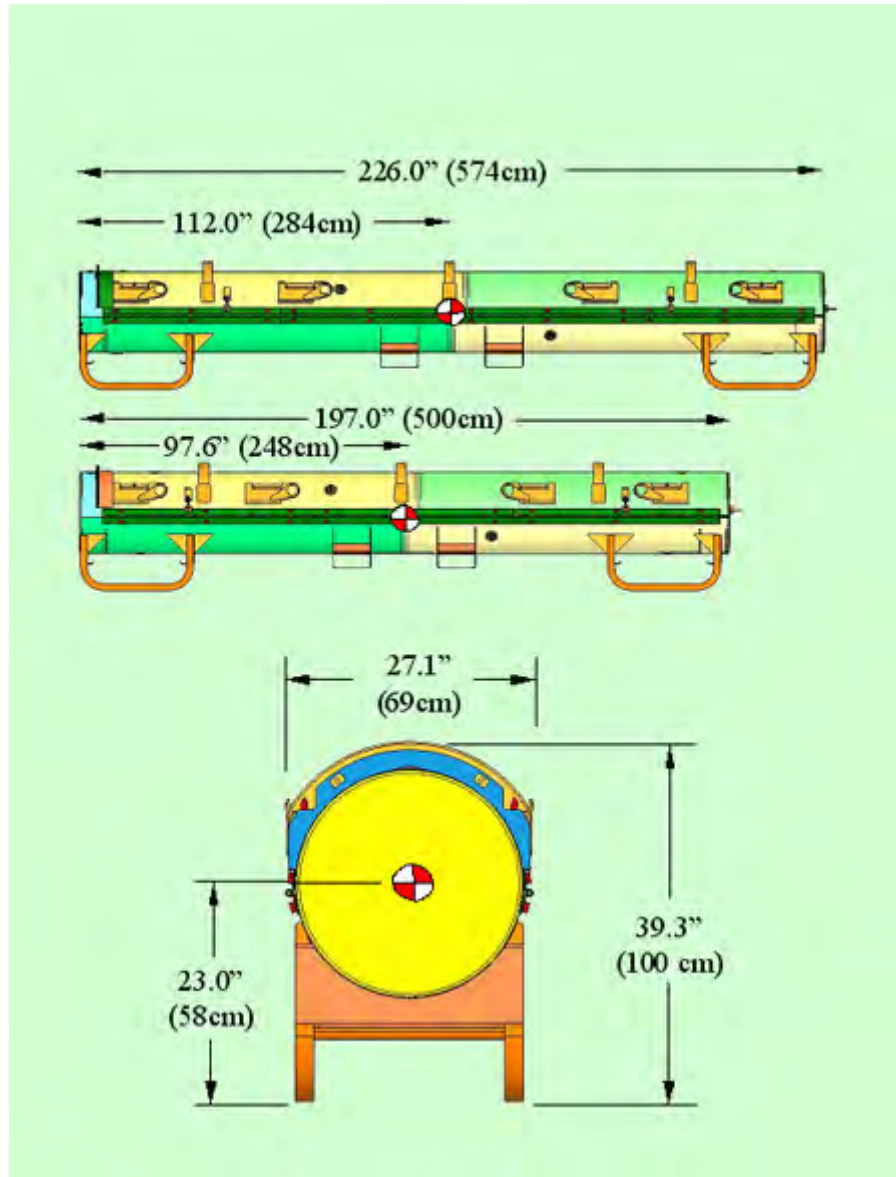


Figure 2-2 Traveller XL/VVER and Traveller STD Dimensions and Center of Gravity
(Note: End View is Common to both Models)

2.12.3 Mechanical Design Calculations for the Traveller XL Shipping Package

During Traveller package development, normal transport and hypothetical accident condition testing were performed to demonstrate package compliance to test conditions described in 10 CFR 71 and TS-R-1. For those requirements not demonstrated by testing, a mechanical analysis was performed to demonstrate package compliance. This section outlines the non-tested requirements to be satisfied and provides an analysis for each requirement.

The Traveller XL package is depicted in Figure 2-3. The exterior view of the Outerpack is shown. The internal packaging including the Clamshell is shown in Figure 2-4. The Traveller XL package structurally and mechanically bounds the Traveller VVER and Traveller STD packages because the XL is more massive than either the VVER or STD (except in the case of stacking where a double stacked Traveller STD bounds the Traveller XL and Traveller VVER). Additionally, the computer simulations and full-scale testing of the Traveller XL units demonstrate a robust design with considerable safety margins with respect to all structural and mechanical requirements.

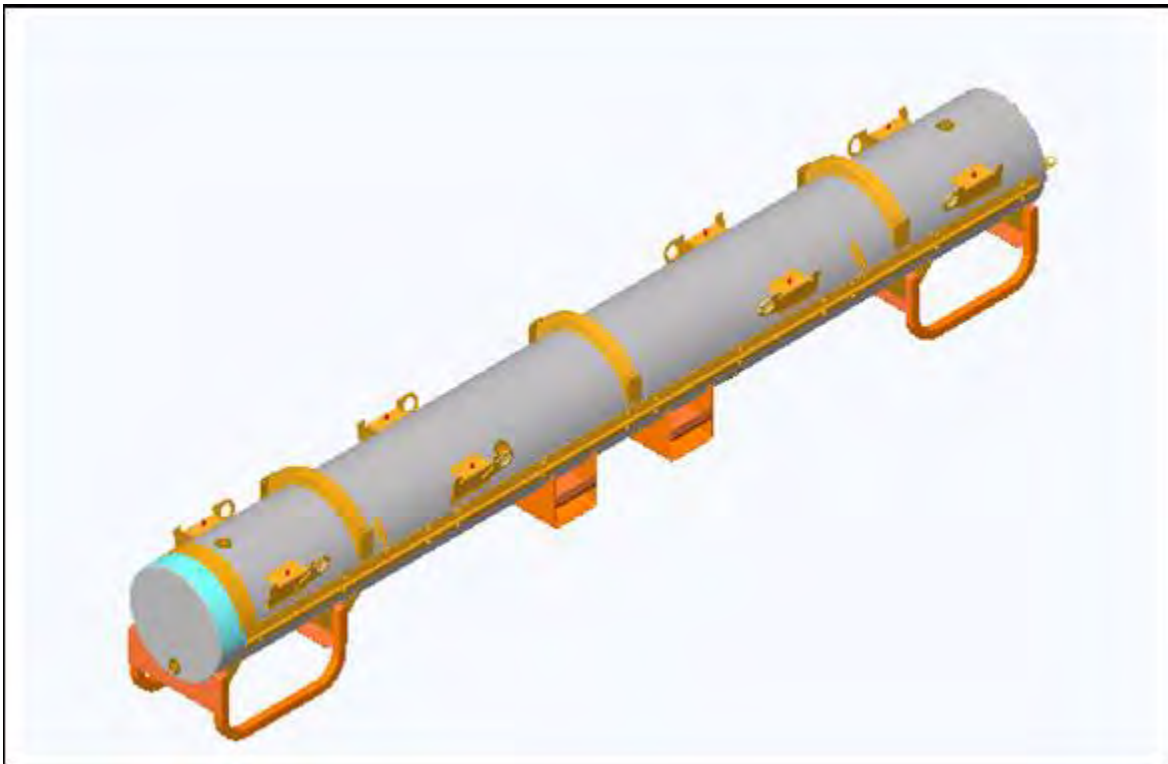


Figure 2-3 Westinghouse Fresh Fuel Shipping Package, the Traveller XL

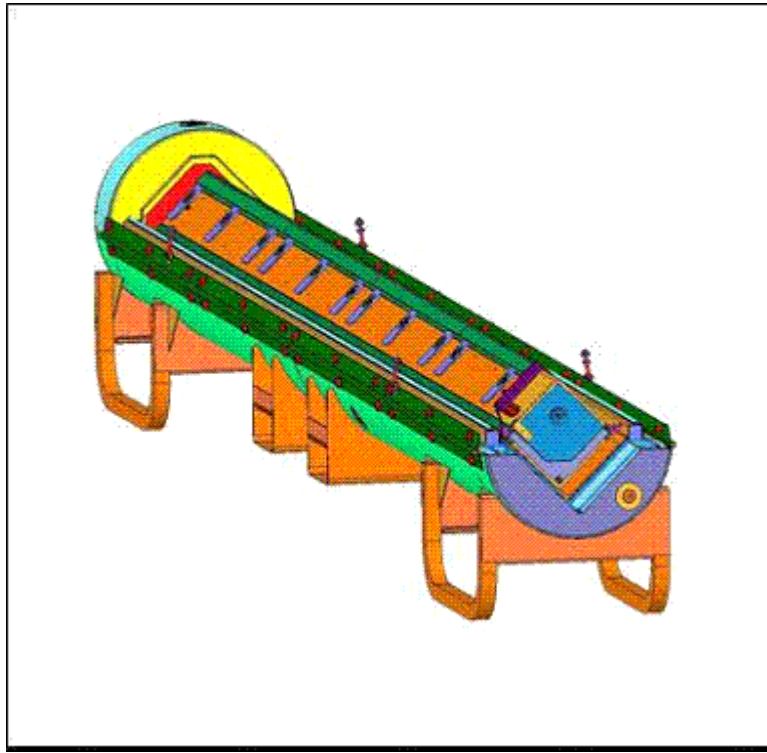


Figure 2-4 Internal View of the Traveller Shipping Package

2.12.3.1 Analysis Results and Conclusions

These analyses were performed to demonstrate Traveller XL package compliance to the mechanical requirements described in 10 CFR 71 and TS-R-1 for which no formal testing was conducted. These calculations bound the lighter, shorter Traveller STD unit. The applicable requirements were summarized in Table 2-3. The results of the design calculations (where applicable), acceptance criteria, and conditional acceptance shown in Table 2-4. Based on the results in Table 2-4, the Traveller package is shown to be compliant to mechanical requirements described in 10 CFR 71 and TS-R-1

Table 2-7 has been deleted.

Table 2-8 has been deleted.

Assumptions

The calculations to determine the maximum Outerpack allowable stresses for yield, shear, and weld shear are based on the properties of ASTM A240 Type 304 Stainless Steel. It is further assumed that the weld consumable possess greater mechanical properties than that of the base metal. Hence, the mechanical properties of the base metal will be employed for weld stress analysis. The reference drawings included in this analysis represent the Certification Test Unit (CTU) Traveller XL, which was fabricated for the drop and fire tests.

Acceptance Criteria

The Traveller package was structurally evaluated to demonstrate compliance to the conditions described in Table 2-3. The package's Outerpack structure is composed of ASTM A240 Type 304 Stainless steel. The mechanical properties are of listed below:

- Tensile strength, Minimum: 75 ksi
- Yield strength, Minimum: 30 ksi

For mechanical analysis where tensile, shear, or weld shear stresses were determined, the acceptance criteria was as follows:

- Maximum allowable tensile yield stress, $\sigma_y = 30$ ksi
- Maximum allowable shear stress, $\tau_{\max} = .6\sigma_y = 18$ ksi
- Maximum allowable weld shear stress, $\tau_{\text{weld}} = .4\sigma_y = 12$ ksi

The material constant Young's Modulus for 304 Stainless steel is:

$$E = 29.4E6 \text{ psi}$$

2.12.3.2 Calculations

Nine mechanical conditions were evaluated for Traveller package. These conditions are outlined in Table 2-3. Standard engineering methods were used for these calculations.

2.12.3.2.1 Input

The design loads were determined according to the criteria described in 10 CFR 71 and TS-R-1, 1996 where appropriate. The Traveller XL package weight bounds the Traveller STD design as shown in Table 2-6. The total weights for each Traveller design include shipping components where applicable.

Table 2-9 has been deleted.

Lifting – The lifting criteria is governed by 10 CFR 71.45(a) and TS-R-1, Paragraph 607. 10 CFR 71.45(a) states that any lifting attachment that is a structural part of the package must be designed with a minimum safety factor of three against yielding when used to lift the package in its intended manner. In addition, it must be designed so that failure of any lifting device under excessive load would not impair the ability of the package to meet other requirements of 10 CFR 71. The applied loads to the package lifting attachments are then:

For the case of Traveller XL:

$$F_l = 3W_{XL}$$

$$F_l = 3(5,230) \text{ lb}$$

$$F_l = 15,690 \text{ lb for the Traveller XL}$$

For the case of stacked Traveller STD:

$$F_l = 3W_{2STD}$$

$$F_l = 3(2 \times 4,500) \text{ lb}$$

$$F_l = 27,000 \text{ lb}$$

Tie-Downs – The tie-down requirements are described in 10 CFR 71.45(b)(1,2) and TS-R-1, Paragraph 636. 10 CFR 71.45 states that a system of tie-downs that is a structural part of the package must be capable of withstanding, without generating stress in excess of its yield strength, a static force applied to the center of gravity having the following components:

- Vertical: 2 g
- Axial: 10 g
- Transverse: 5 g

Thus, the applied tie-down loads for the Traveller are:

- Vertical: 10,460 lb
- Axial: 52,300 lb
- Transverse: 26,150 lb

Design Temperatures between -40°F (-40°C) and 158°F (70°C) – The package must account for temperatures ranging from -40°F (-40°C) to 158°F (70°C) per TS-R-1 (637), and from -40°F (-40°C) to 100°F (38°C) per 10 CFR 71.71(c)(1,2). Thus, the bounding temperature range to consider for package design is -40°F (-40°C) to 158°F (70°C). The analysis of the Traveller package will consider the effects of temperature on thermally induced stress.

Internal/External Pressure – The package must account for the effects of external pressure conditions. The effects of reduced and increased external pressure are described in 10 CFR 71.71(c)(3,4) and TS-R-1 (615). The reduced external pressure is 25 kPa (3.5 psi) absolute, and the increased external pressure is 140 kPa (20 psi) as stated in 10 CFR 71.71.

Water Spray – A water spray test is required for the Traveller package to consider the effects of excessive rainfall on the structural integrity of the package. The water spray test is described by 10 CFR 71.71(c)(6) and TS-R-1 (721). The water spray test is to simulate a rainfall rate of approximately 5 cm/hr (2 in/hr) for at least one hour.

Compression/Stacking Test – The Traveller package must be subjected to a static compression test per by 10 CFR 71.71(c)(9) and TS-R-1 (723). Both regulations require that the applied load be the greater of the following:

An equivalent load of five times the mass of the package or the equivalent of 13 kPa (2 psi) multiplied by the vertically projected area of the package. Evaluating each case:

Case 1

The applied stacking force for case 1 is:

$$Fs = 5W_{XL}$$

$$Fs = 5(5230) \text{ lb}$$

$$Fs = 26,150 \text{ lb}$$

Case 2

The applied stacking force for case 2 is:

$$Fs = (Length)(OD)(P)$$

$$Fs = (226.2)(27.1)in^2(2)psi$$

$$Fs = 12,260 \text{ lb}$$

Thus, the applied stacking load is $Fs = 26,150 \text{ lb}$.

Penetration – The penetration test is an impact test described by 10 CFR 71.71(c)(10) and TS-R-1 (724). The package must be subject to the impact of the hemispherical end of a vertical steel cylinder of 3.2 cm (1.25 in) diameter and a mass of 6 kg (13 lb) dropped from 1 m (40 in) onto the surface of the package that is expected to be the most vulnerable to puncture.

Immersion – The immersion test is a hypothetical accident condition test that evaluates the effects of static water pressure head on the structural integrity of the package. The test condition is described by 10 CFR 71.73(c)(6) and TS-R-1 (729). The regulations state that the package must be immersed under a head of water of at least 15 m (50 ft) for at least 8 hours in the most damaging orientation. For demonstration purposes, an external gauge pressure of 150 kPa (21.7 psi) is considered to meet the test conditions.

2.12.3.2.2 Lifting

Traveller XL Four Point Lift – The Traveller package is crane lifted using a 4-point lift with attachment points located on the stacking bracket. Figure 2-5 shows a sample package with the lifting configurations. The assumed sling angle is 30°. The applied load, $F_l = 15,690$ lb.

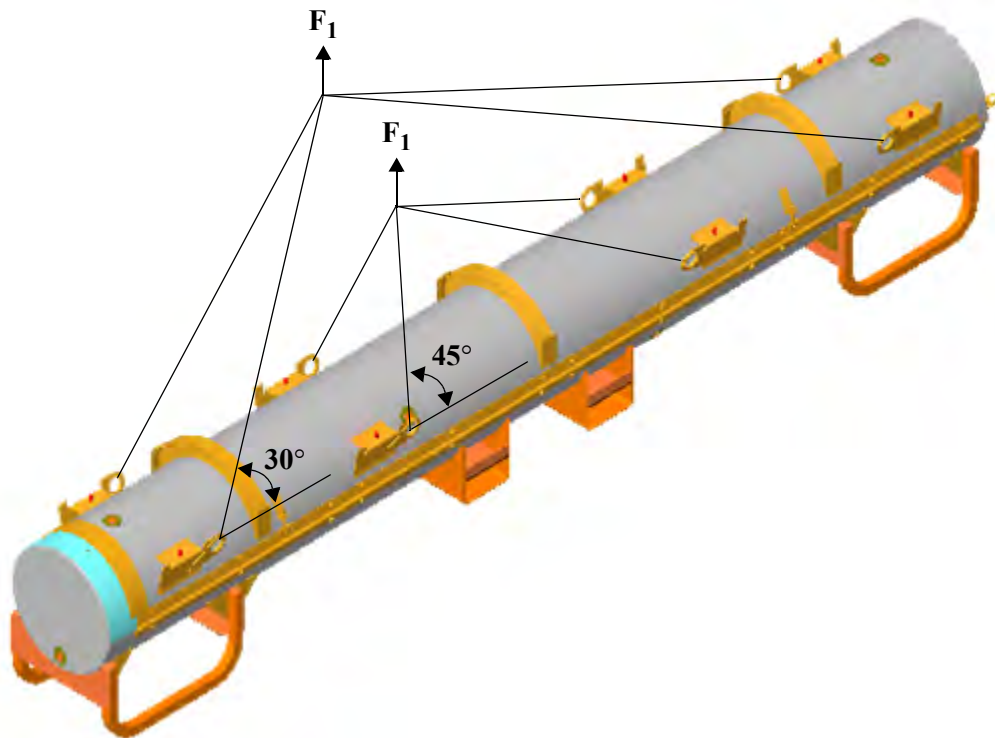


Figure 2-5 Traveller XL Lifting Configurations

Based on the lifting configuration, the applied load transferred to each lifting hole, F , is:

$$F = \frac{F_l}{4 \sin 30}$$

$$F = \frac{15,690}{4} / .5 \text{ lb}$$

$$F = 7,845 \text{ lb/hole}$$

The applied forces and resultant components for a single lifting hole are shown in Figure 2-6.

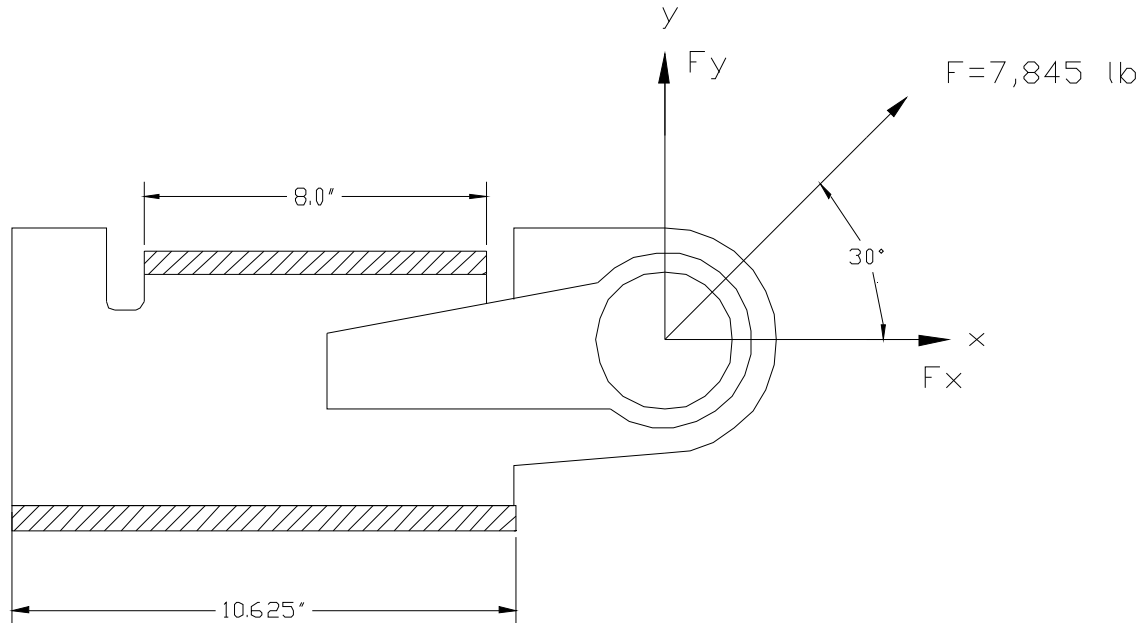


Figure 2-6 Lifting Hole Force Detail

The resulting force components are then:

$$F_x = F(\cos 30)$$

$$F_x = 7,845(0.866) \text{ lb}$$

$$F_x = 6,794 \text{ lb, and}$$

$$F_y = F(\sin 30)$$

$$F_y = 7,845(0.50) \text{ lb}$$

$$F_y = 3,923 \text{ lb}$$

The lifting bracket consists of ASTM A276 SS plate with an attached lifting eye. The lifting eye is 0.25" thick ASTM A276 SS plate and is reinforced with a 0.25" plate doubler. A lifting bracket detail is shown in Figure 2-7.

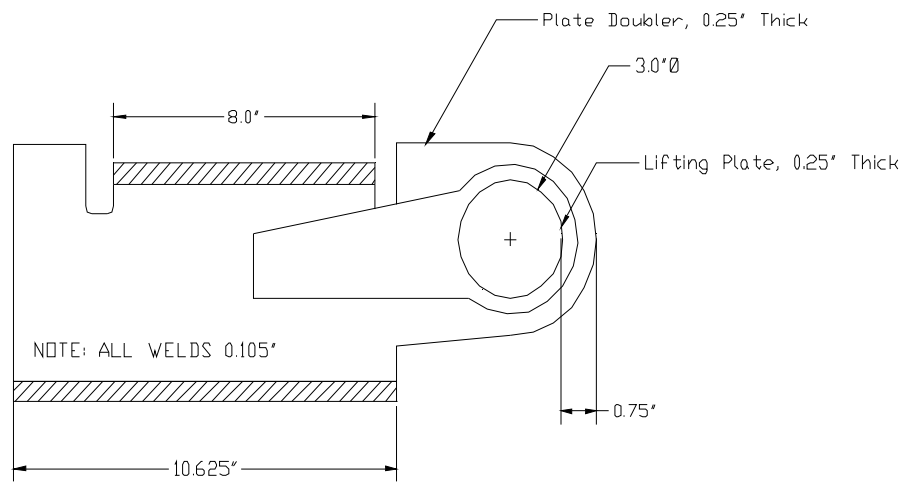


Figure 2-7 Lifting Bracket Fabrication Detail

The lifting analysis consists of two calculations: 1) hole tear-out and, 2) weld strength.

The hole tear-out is assumed to occur at the minimum 0.75" section of material in the lifting eye plate. From Table 2-4, the maximum allowable Shear Yield Stress, τ_y is 18 ksi. The stressed area is the minimum thickness of 0.5" times the section width of the tear out, 0.75" and double shear is assumed. Thus,

$$A = 2(.75)(.5) \text{ in}$$

$$A = 0.75 \text{ in}$$

The elemental volume stress state is described by the Mohr's Circle as shown in Figure 2-8. The resulting stress on the element due to applied load of 7,500 lbs is:

$$\sigma_x = F / A$$

$$\sigma_x = 7,845 / .75 \text{ psi}$$

$$\sigma_x = 10,460 \text{ psi}$$

The maximum shear stress on the element is then:

$$\tau_{\max} = \sqrt{\left[\frac{(\sigma_{x'} - \sigma_{y'})}{2}\right]^2 + \tau_{x'y'}^2}$$

$$\tau_{\max} = \sqrt{\left[\frac{(10,460 - 0)}{2}\right]^2 + 0^2}$$

$$\tau_{\max} = 5,230 \text{ psi}$$

Shear tear-out of the hole is not expected since $\tau_{\max} = 5,230 \text{ psi} < \tau_{\text{allow}} = 18,000 \text{ psi}$.

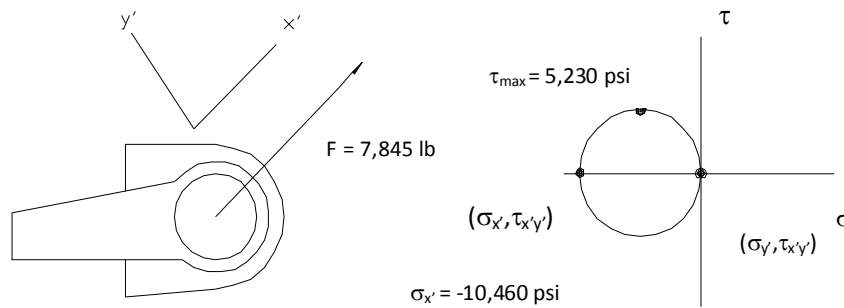


Figure 2-8 Hole Tear-out Model and Mohr's Circle Stress State

- The weld attaching the lift plates to the Outerpack shell are required to demonstrate that they are adequate to preclude local weld yielding. The analysis assumes that one of the wire ropes is non-functional and three of the four welds bear the lifting load. The weld shear stress is found by $\tau_{\text{weld}} = F/A$, where F is the applied vertical or horizontal load and A is the weld area. The assumed weld area is:

$$A = hl \sin 45, \text{ where } l \text{ is } (.75)(10.625+8") = 13.97" \text{ from Figure 2-6, and } h \text{ is the weld thickness, } 0.105".$$

The applied loads are $F_x = 6,794 \text{ lbs}$ in the vertical direction and $F_y = 3,923$ in the horizontal direction. The weld stresses are then:

$$\tau_x = F_x/A \text{ and } \tau_y = F_y/A$$

Substituting values,

$$\tau_x = 6,794 / (.105)(13.97)(.707) \text{ psi}$$

$$\tau_x = 6,551 \text{ psi, and}$$

$$\tau_y = \frac{F_y}{A}$$

$$\tau_y = 3,923 / (.105)(13.97)(.707) \text{ psi}$$

$$\tau_y = 3,783 \text{ psi}$$

The stresses τ_x and τ_y are perpendicular to each other, and the resulting weld shear stress is:

$$\tau = \sqrt{(\tau_x^2 + \tau_y^2)}$$

$$\tau = \sqrt{(6,551^2 + 3,783^2)}$$

$$\tau = 7,565 \text{ psi}$$

The welds are sufficient to prevent local yielding since $\tau_{\max} = 7,565 \text{ psi} < \tau_{\text{allow}} = 12,000 \text{ psi}$.

Traveller STD Four Point Lift – The Traveller STD package may be crane lifted using a 4-point lift with attachment points located on the inner stacking bracket. Figure 2-9 shows sample STD packages with the lifting configuration. The assumed sling angle is 45° since the inner lifting brackets are utilized. The applied load is $F_l = 27,000 \text{ lb}$ from Section 2.12.3.2.1. The methodology is the same as for the Traveller XL since the load path and structure is assumed nearly identical. However, the force components are greater:

$$F = \frac{F_l}{4 \sin 45}$$

$$F = \frac{27,000}{4 \cdot .707} \text{ lb/hole}$$

$$F = 9,546 \text{ lb/hole}$$

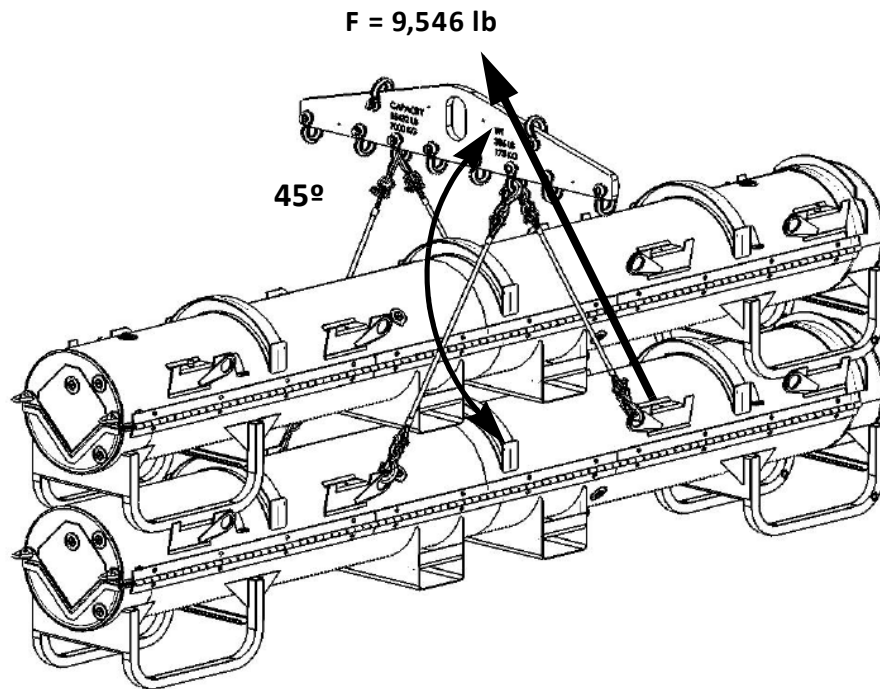


Figure 2-9 Traveller STD Stacked Lifting Configuration

Substituting into the force component geometric relationships:

$$F_x = F_y = 6,750 \text{ lb}$$

These resultant forces result in the following hole tear-out and weld shear loads using the same equations shown for the Traveller XL and substituting Traveller STD values:

Hole tear-out

$$\tau_{\max} = 6,364 \text{ psi}$$

Shear tear-out of the hole is not expected since $\tau_{\max} = 6,364 \text{ psi} < \tau_{\text{allowx}} = 18,000 \text{ psi}$.

Weld Shear

$$\tau = 9,205 \text{ psi}$$

The welds are sufficient to prevent local yielding since $\tau_{\max} = 9,205 \text{ psi} < \tau_{\text{allowx}} = 12,000 \text{ psi}$.

Forklift Analysis – During package lift by a forklift, only the center portion of the package is supported by the forklift extension arms. Consequently, the package is subject to a bending load due to the unsupported weight of the package. The loading conditions include a single Traveller XL and two stacked Traveller STDs.

For the bending evaluation, the Traveller package is conservatively modeled as a cantilever beam with the length equal to half of the overall Traveller length. For XL, $L_f = 113.1$ inches and the design lifting load is distributed over the length of the package as shown in Figure 2-10a. The outer shell is the only assumed structure of the package carrying the bending load. This calculation is repeated for Traveller STD with $L_f = 98.6$ inches. The design weights are calculated in Section 2.12.3.2.1. as 15,690 and 27,000 pounds for Traveller XL and two Traveller STD stacked, respectively.

The forklift pockets weldments are also subjected to a shear load during lifting as the forks will apply a normal force along the top plate as shown in Figure 2-10b. Both the Traveller XL and Traveller STD doubled stacked conditions are evaluated.

Bending

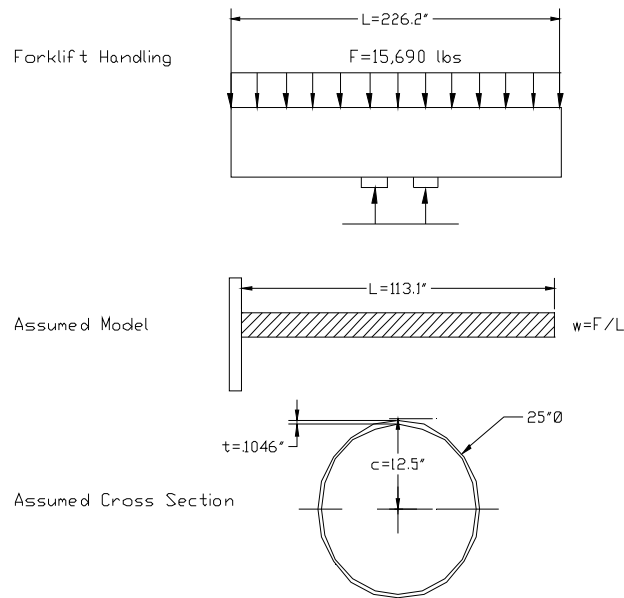


Figure 2-10a Forklift Handling XL Model and Assumed Cross Section

The bending stress can be determined from the classic flexure equation:

$$\sigma = \frac{Mc}{I}, \text{ where}$$

c is the distance from the neutral axis to the outer fibers, M is the applied bending moment, and I is the moment of inertia of the section.

The applied moment is given by:

$$M = \frac{wL^2}{2}$$

where w equals F/L from Figure 2-10a. The value for w is:

$$w = \frac{F}{L}$$

$$w = \frac{15,690}{113.1} \text{ lb/in} = 139 \text{ lb/in}$$

Thus,

$$M = \frac{(139)(113.1)^2}{2} \text{ in-lb}$$

$$M = 889,017 \text{ in-lb}$$

The moment of inertia for the shell, I, is calculated as follows:

$$I = \frac{\pi}{4}(R_o^4 - R_i^4)$$

where $R_o = 12.5"$ and $R_i = (12.5 - .1046)"$, $R_i = 12.395"$.

Thus,

$$I = \frac{\pi}{4}(12.5^4 - 12.395^4) \text{ in}^4$$

$$I = 634 \text{ in}^4$$

The bending stress is then:

$$\sigma = \frac{(889,017)(12.5)}{634} \text{ psi}$$

$$\sigma = 17,528 \text{ psi}$$

Forklift loading is not expected to impact the XL package by bending since $\sigma = 17,528 \text{ psi} < \sigma_{yield} = 30,000 \text{ psi}$.

In the case of the Traveller STD stacked:

$$w = \frac{27,000}{98.6} \text{ lb/in} = 274 \text{ lb/in}$$

$$M = \frac{(274)(98.6)^2}{2} \text{ in-lb}$$

$$M = 1,331,909 \text{ in-lb}$$

The bending stress is then:

$$\sigma = \frac{(1,331,909)(12.5)}{634} \text{ psi}$$

$$\sigma = 26,260 \text{ psi}$$

Forklift loading is not expected to impact the STD package by bending since $\sigma = 26,260 \text{ psi} < \sigma_{\text{yield}} = 30,000 \text{ psi}$.

As previously noted, the model conservatively assumes the outer shell is loaded, and the actual Outerpack structure with foam would provide even greater margin against bending.

Weld Shear

The forklift pocket (Item 01 in Figure 2-10b) weldments are also subjected to a shear load during lifting as the forks will apply a normal force along the top plate (Item 02) bottom surface as shown in Figure 2-10b. There are two cases to be evaluated: Traveller XL and Traveller STD doubled stacked. The applied forces are:

$$F_l = 15,690 \text{ lb for the Traveller XL}$$

$$F_l = 27,000 \text{ lb for two Traveller STDs stacked}$$

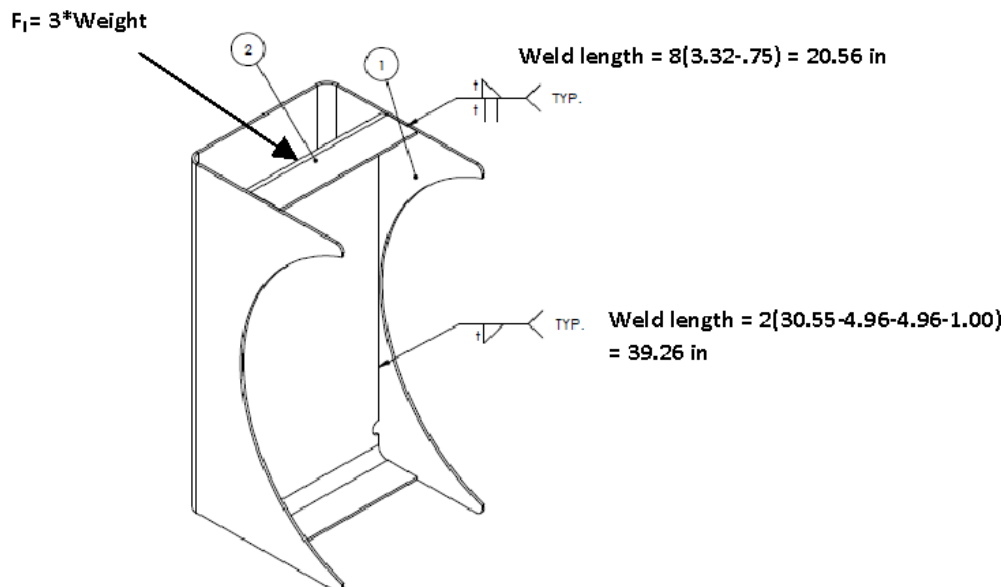


Figure 2-10b Forklift Pocket Weld Detail

The assumed weld area is:

$$A = hl \sin 45, \text{ where } l \text{ is } (20.56'' + 39.26'') = 59.82'' \text{ and } h \text{ is the weld thickness, } 0.105''.$$

The weld stresses are then:

$$\tau_{XL} = F_{XL} / A \text{ and } \tau_{STD} = F_{STD} / A$$

Substituting values for Traveller XL,

$$\tau_{XL} = 15,690 / (.105)(59.82)(.707) \text{ psi}$$

$$\tau_{XL} = 3,533 \text{ psi}$$

The welds are sufficient to prevent local yielding since $\tau_{XL} = 3,533 \text{ psi} < \tau_{allowx} = 12,000 \text{ psi}$.

Substituting values for Traveller STD,

$$\tau_{STD} = 27,000 / (.105)(59.82)(.707)$$

$$\tau_{STD} = 6,080 \text{ psi}$$

The welds are sufficient to prevent local yielding since $\tau_{STD} = 6,080 \text{ psi} < \tau_{allowx} = 12,000 \text{ psi}$.

Bolts

During package lift for fuel loading and unloading, the package is hoisted using the two rings attached to the top nozzle end of the Outerpack top. The hoist rings attach to the Outerpack using two 3/8-16 UNC Grade 8 Medium-Carbon socket head cap screws per hoist ring into a welded nut. The four screws are subject to shear loading in the most limiting case. The screws are fabricated to a minimum proof load of 120,000 psi. The load per bolt is the design lifting load of 15,690 pounds distributed by the four bolts. Thus, the load per bolt is 3,923 pounds. The allowable axial stress is the yield stress of 120,000 psi and the allowable shear stress is .6Sy, 72,000 psi. The stressed area is 0.0775 in². The applied stress is then:

$$\tau = F / A$$

$$\tau = 3,923 / .0775 \text{ psi}$$

$\tau = 50,619$ psi, which is less than the allowable shear stress of 72,000 psi as well as the axial allowable stress of 120,000 psi and is acceptable.

Coupling Nut

When the package is vertical, the coupling nut will be subject to a shear load. The nut is 3/8-16 and the material is 304 stainless steel. The allowable shear stress is 18,000 psi.

The stressed area of the internal thread is found by:

$$A = .7845(D - \frac{.9743}{n})^2 \text{ where } D \text{ is the nominal diameter } 0.375 \text{ inches, and } n \text{ is the number of threads per inch; } 16.$$

$$A = .0775 \text{ in}^2$$

The shear area A_n is found by:

$$A_n = (3.1416)(n)(Le)(Ds \text{ min}) \left[\frac{1}{2n} + .57735(Ds \text{ min} - En \text{ max}) \right] \text{ in}^2$$

where:

n =	16
Le =	0.269
Ds_min =	0.364
En_max =	0.340

Thus, $A_n = 0.222 \text{ in}^2$. The shear stress is then:

$$\tau = F / A$$

$$\tau = 3,923 / .222 \text{ psi}$$

$\tau = 17,671$ psi, which is less than the allowable material shear stress of 18,000 and is acceptable.

Hoist Ring

After the package is in the vertical position, the hoists will be loaded in tension. The applied tensile stress for normal up-ending is found from $\sigma = P/A$. The load per 3/8 inch diameter hoist ring is:

$$P = 15,690/2 \text{ lbs}$$

$$P = 7,845 \text{ lbs}$$

The tensile stress per hoist ring is:

$$\sigma = 7,845/[2][(\pi)(0.375^2)/4]$$

$$\sigma = 7,845/0.22 \text{ psi}$$

$$\sigma = 35,659 \text{ ksi.}$$

Since the allowable tensile yield strength is 130 ksi minimum, the hoist ring satisfies the lifting requirements.

2.12.3.2.3 Tie-Down Analysis

The Traveller packages are secured to the transport conveyance by means nylon straps (or chains) across the top of the Outerpack, and by chains that are passed through the leg assembly tray and connected inboard to the conveyance tie-down point. Thus, there are no structural devices designed for tie-down. However, it is possible that the leg assembly or the eight lift eyes could be inadvertently used for tie-downs. According to 10CFR71.45 these component require analysis to demonstrate that the inadvertent tie-down locations have the strength capability to that required for a tie-down device (or be rendered inoperable).

Leg Assembly

In the event that the leg assemblies are used as tie-downs and not rendered inoperable for tie-down, the two leg assemblies on the Outerpack base will be loaded. A depiction of this loading configuration is shown in Figure 2-10c.

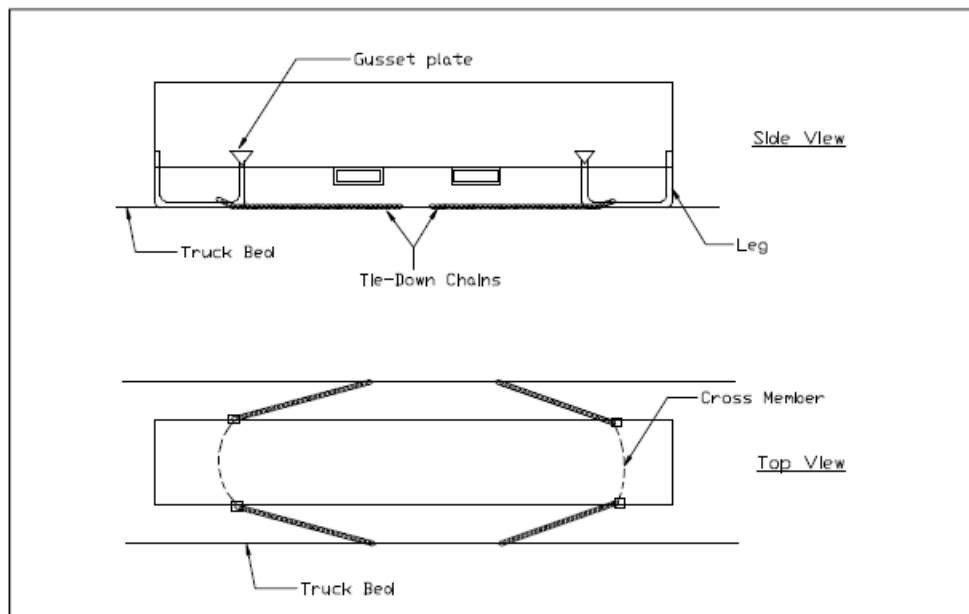


Figure 2-10c Leg Assembly Loading Condition During Inadvertent Tie-Down

The chains are assumed to be attached to each leg pair near the truck bed base so that the resulting chain angle (from the side perspective) is small enough to constitute an axially applied resultant load. For this loading condition, both leg pairs are loaded in the axial direction. The resultant applied force is the vector summation of the vertical, axial, and transverse components:

$$F = \sqrt{F_x^2 + F_y^2 + F_z^2}$$

$$F = \sqrt{52,300^2 + 26,150^2 + 10,460^2} \text{ lbs}$$

$$F = 59,401 \text{ lbs for both pairs.}$$

Therefore, the applied load for a single leg pair is .5F, or 29,701 lbs.

The leg assembly is attached to the Outerpack using a gusset plate, and also by an arced cross. Two gusset plates (6 inches wide each) are welded to the Outerpack base by a continuous 0.10 inch fillet weld on the outside of the skin. Thus, for single leg pair loading, the total weld length of the cross member section is 12+12, or 24 inches (Figure 2-10d).

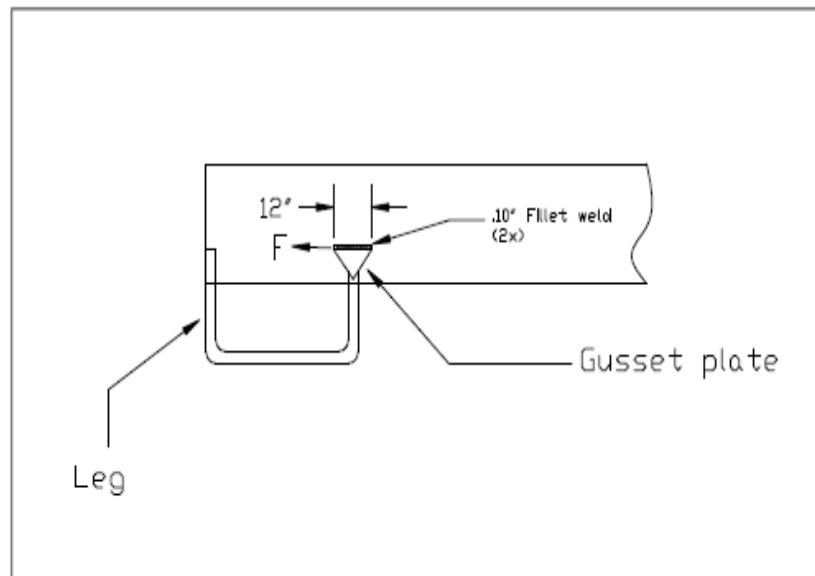


Figure 2-10d Welding Depiction at Representative Gusset Plate

The cross members are curved 7 gage plates welded to the Outerpack base using minimum 0.10 fillet welds, 1 inch long at 12 places per side as shown in Figure 2-10e. Thus, the total weld length each cross members is 12 inches.

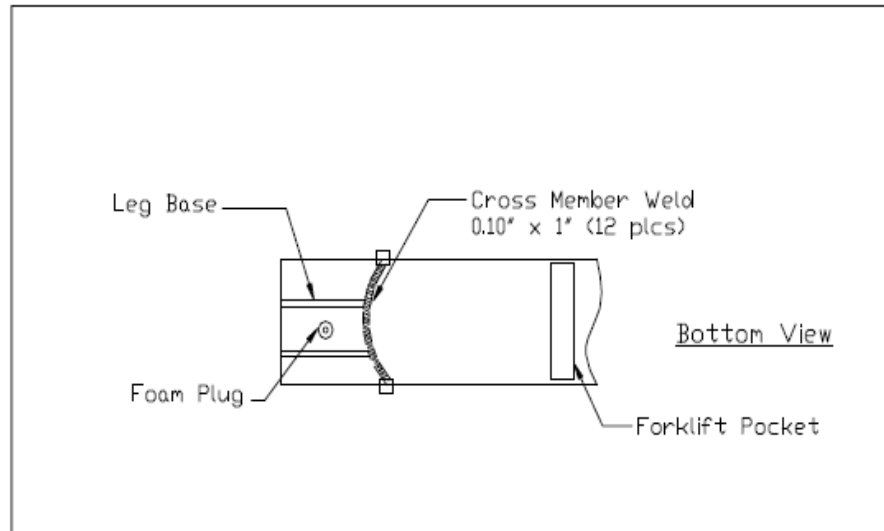


Figure 2-10e Welding Depiction at Cross Member

Weld Shear Analysis

The leg assembly is attached to the Outerpack shell by both the gusset and cross member welds. These welds are required to demonstrate that they are adequate to preclude local yielding. Axial loading of the resultant force results in a shear load on the welds.

The weld shear stress is found by:

$$\tau_{weld} = F/A,$$

where F is the applied vector shear load of 29,701 lbs and A is the weld area.

The weld area is:

$$A = hl \sin 45^\circ, \text{ where } l \text{ is } 24 + 12 = 36'', \text{ and } h \text{ is the weld thickness, } 0.10''.$$

$$A = (0.10)(36)(.707) \text{ in}^2$$

$$A = 2.55 \text{ in}^2$$

The weld shear stress is then:

$$\tau_{weld} = \frac{29,701}{2.55} \text{ psi}$$

$$\tau = 11,648 \text{ psi}$$

Thus, the welds are sufficient to prevent local yielding since $\tau_{weld} = 11,648 \text{ psi} < \tau_{allowx} = 12,000 \text{ psi}$.

Lift Eyes

In the event that the lift eyes are used as tie-down, the normal system of tie down would include eight (8) point loads (Figure 2-10f). The analysis will assume that one of the chains fails per side, so the applied load is for six (6) lift eyes. The chains may be angled at an assumed 30 degrees or vertical as shown in Figure 2-10f.

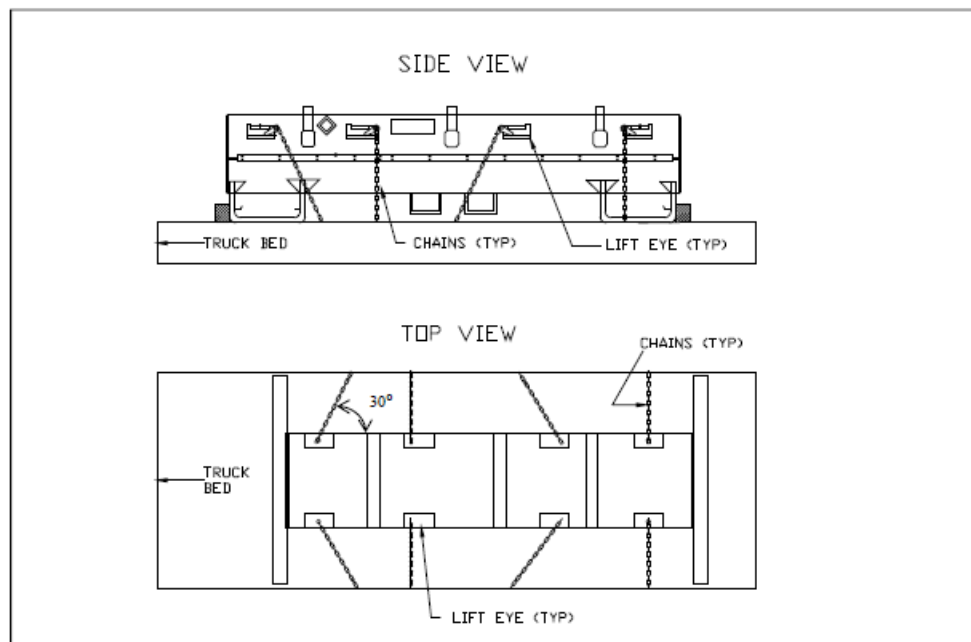


Figure 2-10f Lift Eye Loading Assumed Conditions During Inadvertent Tie-Down

The applied load is a combined vector load to the center of gravity of a single package. For this loading condition, each attached lift eye is loaded with 1/6th of the total load. The resultant applied force is the vector summation of the vertical, axial, and transverse components:

$$F = \sqrt{F_x^2 + F_y^2 + F_z^2}$$

$$F = \sqrt{52,300^2 + 26,150^2 + 10,460^2} \text{ lbs}$$

$$F = 59,401 \text{ lbs.}$$

Therefore, the applied load for a single lift eye is .167F, or 9,900 lbs.

Weld Shear Analysis - Vertical Direction

The lift eye is fillet welded to the Outerpack shell. The top and bottom part of the lift eyes are welded at 8 inches and 10.63 inches, respectively. Thus, the total weld length for the top and bottom weld subject to shear is 18.63 inches. A depiction of the loading configuration and lift eye sketch is shown in Figure 2-10g for the vertical chain orientation.

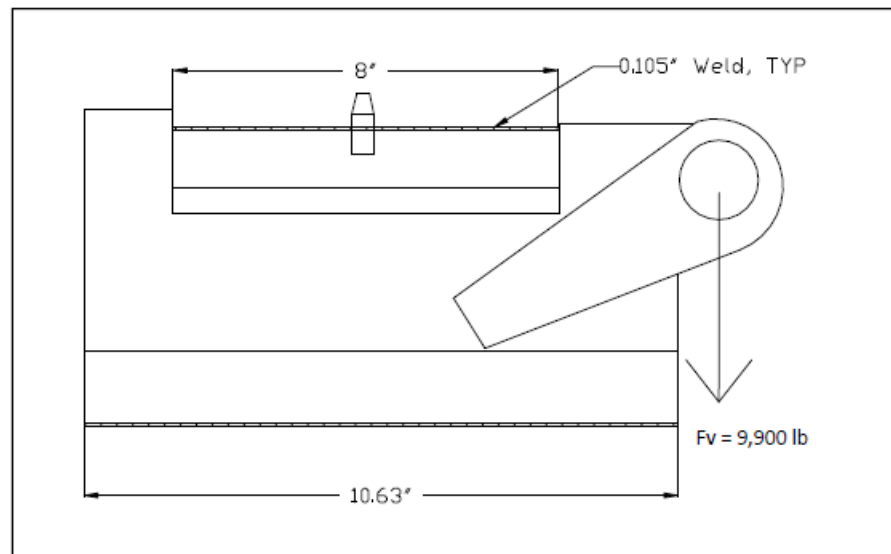


Figure 2-10g Vertical Lift Eye Welding Configuration

These welds are required to demonstrate that they are adequate to preclude local yielding for the vertical direction.

The weld shear stress is found by:

$$\tau_{weld} = F/A,$$

where F is the applied vector shear load of 9,900 lbs and A is the weld area. The weld area is:

$$A = hl \sin 45, \text{ where } l \text{ is } 18.63'', \text{ and } h \text{ is the weld thickness, } 0.105''.$$

$$A = (0.105)(18.63)(.707) \text{ in}^2$$

$$A = 1.38 \text{ in}^2$$

The weld stress is then:

$$\tau_{weld} = 9,900 / 1.38 \text{ psi}$$

$$\tau = 7,158 \text{ psi}$$

Thus, the welds are sufficient to prevent local yielding since $\tau_{weld} = 7,158 \text{ psi} < \tau_{allow} = 12,000 \text{ psi}$.

Weld Shear Analysis - Combined Shear

A depiction of the combined shear loading configuration and lift eye sketch is shown in Figure 2-10h for the angled chain orientation. Since there are horizontal and axial components, the principal shear force will be calculated. The vector stress components are shown pictorially below:

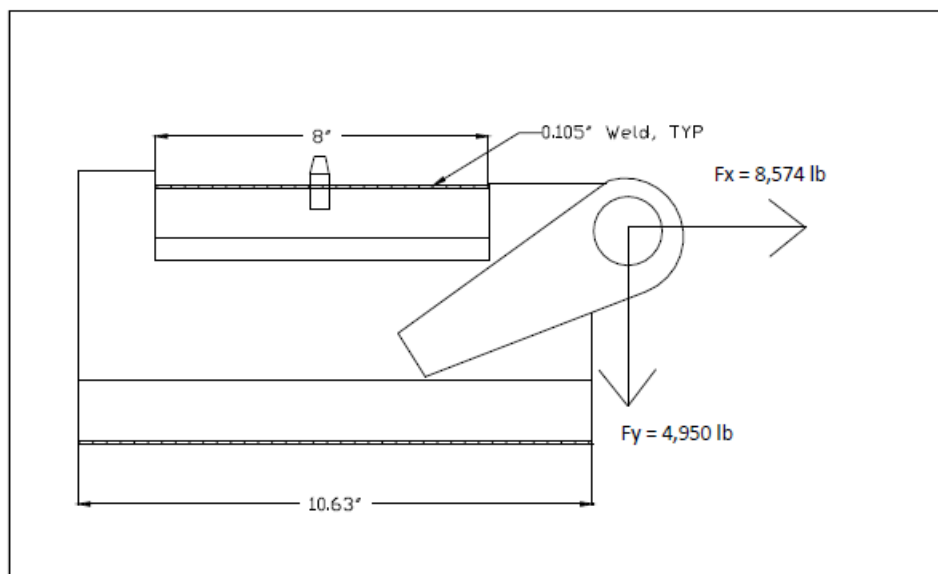
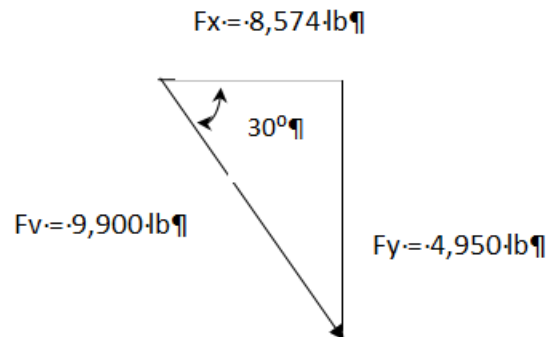


Figure 2-10h Combined Shear Lift Eye Welding Configuration

The x-direction weld shear stress is found by:

$$\tau_{weld\ x} = \frac{F_x}{A},$$

where F is the applied vector shear load of 9,900 lbs and A is the weld area.

The weld area is:

$$A = hl \sin 45^\circ, \text{ where } l \text{ is } 18.63", \text{ and } h \text{ is the weld thickness, } 0.105".$$

$$A = (0.105)(18.63)(.707) \text{ in}^2$$

$$A = 1.38 \text{ in}^2$$

The weld stress is then:

$$\tau_{\text{weld}} x = 8,574 / 1.38 \text{ psi}$$

$$\tau_{\text{weld}} x = 6,213 \text{ psi}$$

The y-direction weld shear stress is found by:

$$\tau_{\text{weld}} y = Fx / A,$$

where F is the applied vector shear load of 9,900 lbs and A is the weld area.

The weld area is:

$$A = hl \sin 45^\circ, \text{ where } l \text{ is } 18.63", \text{ and } h \text{ is the weld thickness, } 0.105".$$

$$A = (0.105)(18.63)(.707) \text{ in}^2$$

$$A = 1.38 \text{ in}^2$$

The weld stress is then:

$$\tau_{\text{weld}} y = 4,950 / 1.38 \text{ psi}$$

$$\tau_{\text{weld}} y = 3,586 \text{ psi}$$

Therefore, the principle shear stress is:

$$\tau = \sqrt{(\tau_x^2 + \tau_y^2)}$$

$$\tau = \sqrt{(6,213^2 + 3,586^2)}$$

$$\tau = 7,173 \text{ psi}$$

The welds are sufficient to prevent local yielding since $\tau_{\max} = 7,173 \text{ psi} < \tau_{\text{allow}} = 12,000 \text{ psi}$.

2.12.3.2.4 Design Temperature Analysis –40°F (-40°C) and 158°F (70°C)

The materials of construction of the Traveller Outerpak include ASTM A240 Type 304 Stainless Steel for the shells and low density, closed cell polyurethane impact limiter/thermal insulator (10 pcf along the axis, 6 pcf inside the top and lower pillows, and 20 pcf between the top and lower pillows). The Clamshell is comprised of ASTM B209/B221 Type 6005-T5 Aluminum. As demonstrated in the below sections, the package is suitable for transport operations over the required design temperature range.

Brittle Fracture – Aluminum alloys, including 6005-T5 Aluminum, do not exhibit a ductile-to-brittle temperature transition; consequently, neither ASTM nor ASME specifications require low temperature Charpy or Izod tests of aluminum alloys. Thus, brittle fracture of the aluminum components is not expected. Austenitic steels such as 304 Stainless Steel have a Face Centered Cubic (FCC) structure and consequently exhibit a ductile-to-brittle transition at cryogenic temperatures near -297°F (-183°C). Thus, brittle fracture of the stainless steel components is not expected.

Mechanical Properties For Design Temperature Range – The range of tensile and yield strength of 6005 series Aluminum over the design temperature range will not preclude the package from performing its intended design function. Figure 2-11 provides the temperature dependent yield and tensile strengths typical for a 6000-series aluminum up to approximately 212°F (100°C). Furthermore, the recommended operating temperature of aluminum alloys for structural applications is up to a temperature of 400°F (204°C), which is well below the maximum design temperature of 158°F (70°C).

The range of tensile and yield strength of 304 stainless steel over the design temperature range will not preclude the package from performing its intended design function. Figure 2-12 provides the temperature dependent yield and tensile strengths for 304 SS up to approximately 194°F (90°C).

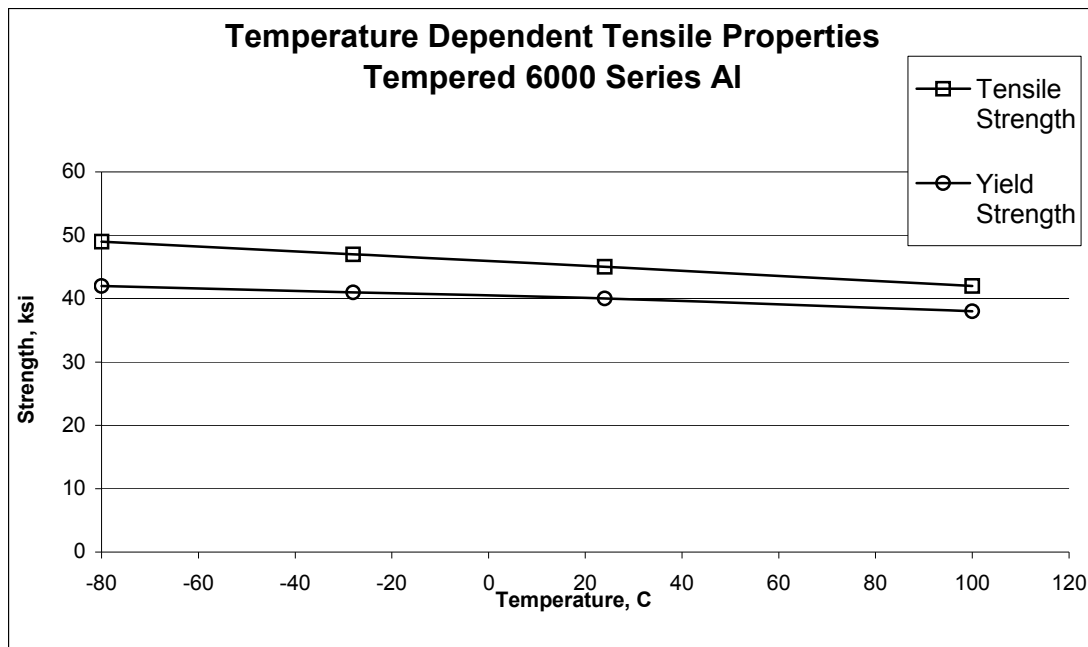


Figure 2-11 Typical Temperature Dependent Tensile Properties for Tempered 6000 Series Al

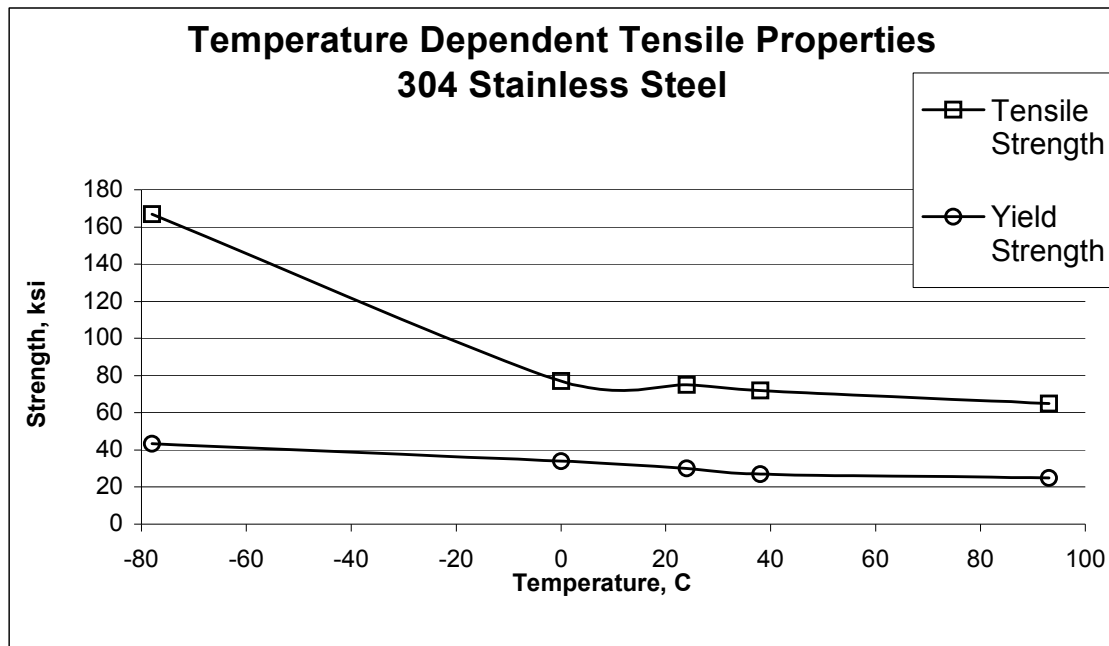


Figure 2-12 Temperature Dependent Tensile Properties for 304 SS

Temperature Evaluation of Foam – The foam is used as a crushable impact limiter and a special thermal insulator. This section only considers the mechanical properties since the thermal functions are evaluated in Section 3, Thermal Evaluation. The foam exhibits a general increase in compressive strength as temperature decreases. Figures 2-13, 14 and 15 show the compressive strength for the 10 pcf (pound per cubic foot), 20 pcf, and 6 pcf foam as a function of temperature, respectively. Of interest is the area under each temperature curve from 0-60% strain (the recommended energy absorption operation range of the foam). For each foam density, the temperature range considered does not significantly impact the energy absorption characteristics. Also, Figures 2-15 show that the compressive strength difference between -29°C and 24°C are relatively similar indicating at -40°C the behavior of the foam will not significantly change. Figure 2-16 provides the temperature dependent strength of each foam density at 10% strain from -54°C to 82°C. The curves show essentially a linear increase in crush strength as temperature decreases. Therefore, the impact properties of the foam are acceptable for use in the temperature range from -40°F (-40°C) to 158°F (70°C).

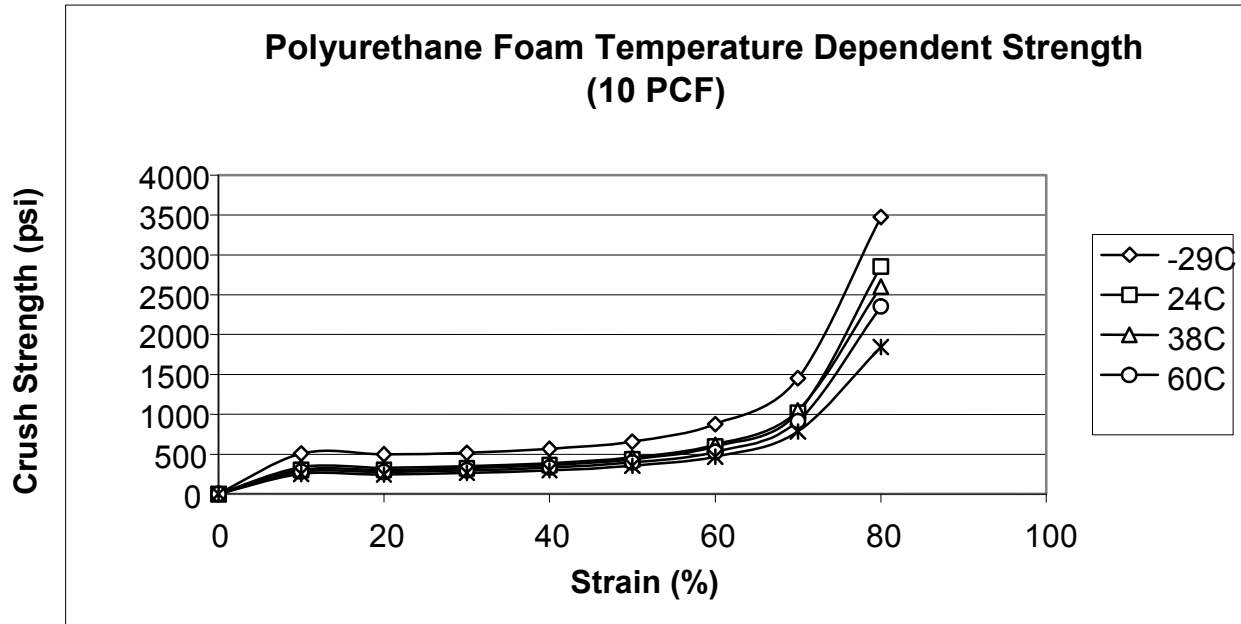


Figure 2-13 Temperature Dependent Crush Strength for 10 PCF Polyurethane Foam

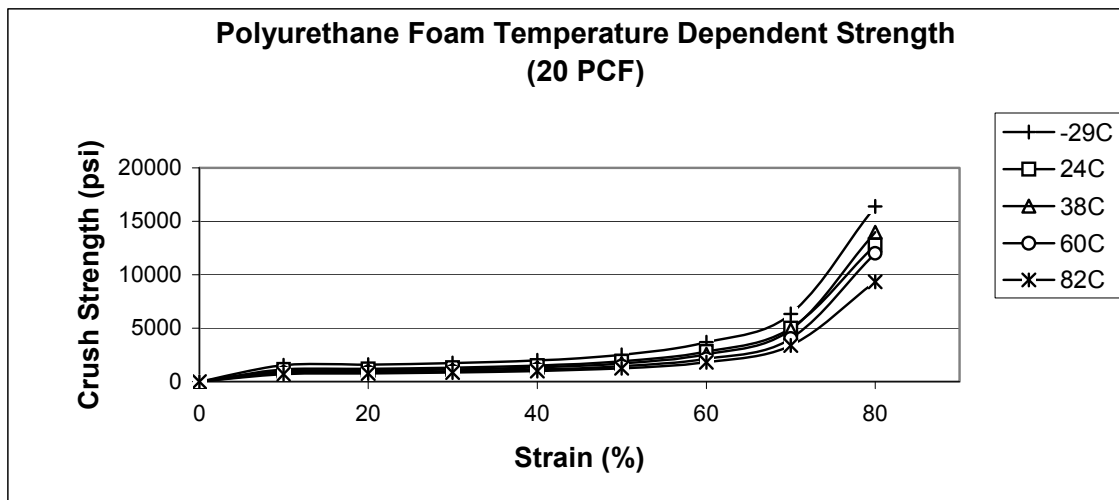


Figure 2-14 Temperature Dependent Crush Strength for 20 PCF Polyurethane Foam

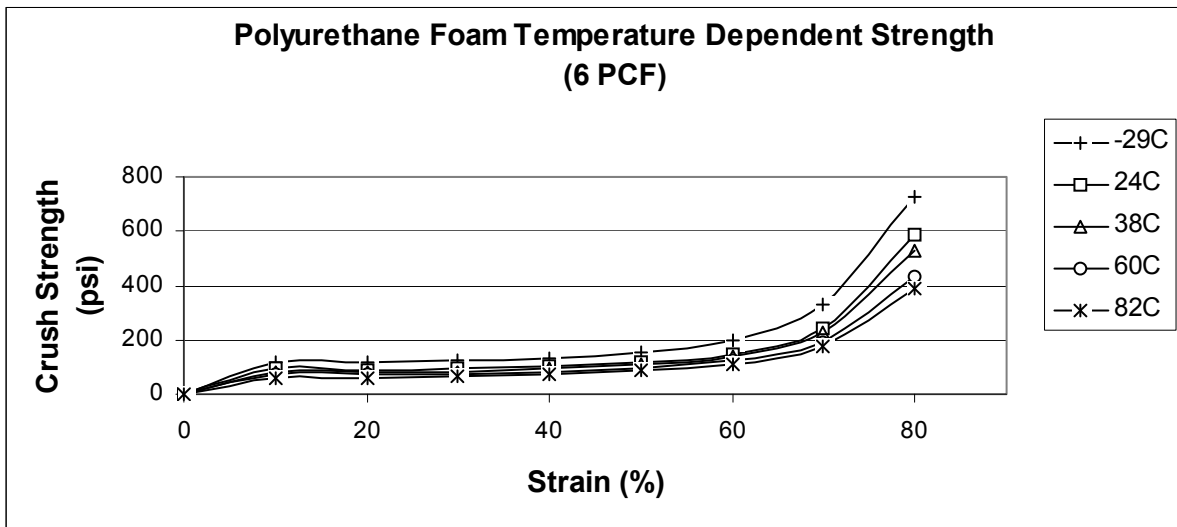


Figure 2-15 Temperature Dependent Crush Strength for 6 PCF Polyurethane Foam

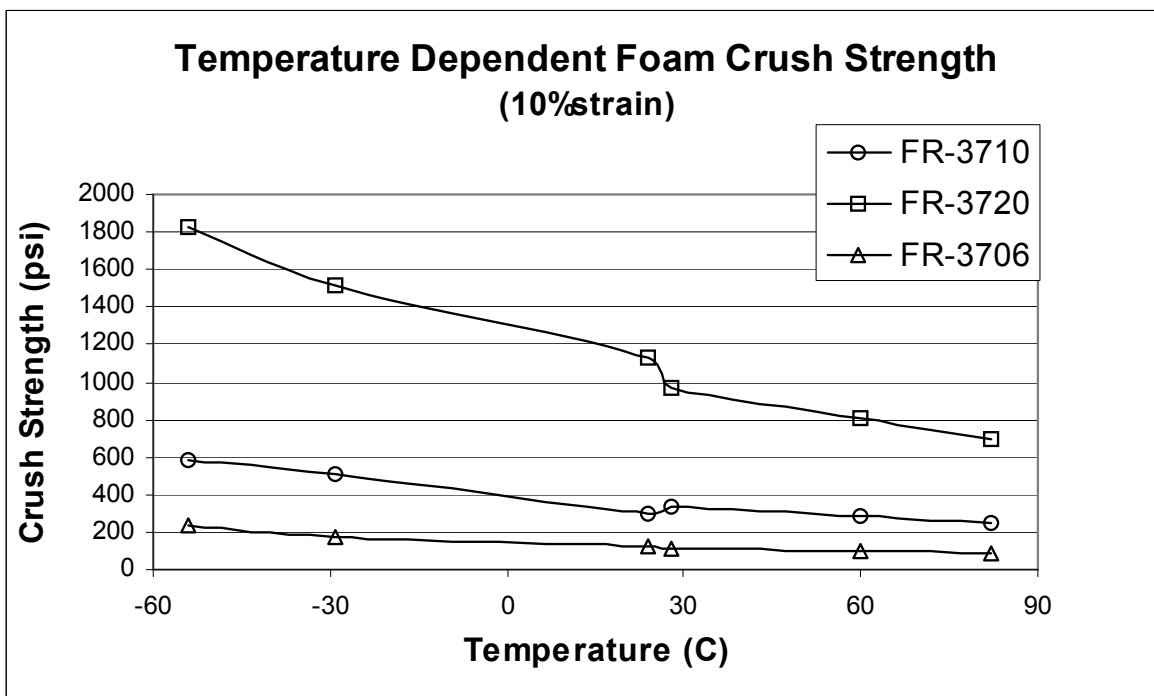


Figure 2-16 Temperature Dependent Crush Strength for Traveller Foam at 10% Strain

Differential Thermal Expansion – Differential thermal expansion (DTE) is expected to only impact the fuel assembly and Clamshell interface. The Outerpack is not under physical constraints and can accommodate thermal growth. Differential thermal expansion between the foam and the stainless steel shells of the Outerpack is easily accommodated by the elastic properties (low modulus value) of the foam.

However, the Ultra-high Molecular Weight (UHMW) polyethylene does have a significantly higher coefficient of thermal expansion (CTE) when compared to 304 stainless steel. For this reason, the moderator panels are segmented along their lengths to accommodate the differential thermal expansion between the polyethylene and the inner stainless steel shells of the Outerpack. Holes in the polyethylene segments are used to attach the panels to the inner Outerpack shells using threaded studs. These studs must not be loaded by the individual panel differential thermal expansion, or contraction. For this reason, each hole drilled into the polyethylene panel is significantly large to preclude thermally induced stresses in the bolt studs. The following calculation addresses this case.

The polyethylene moderator blocks are attached by 0.375 inch diameter weld studs on the inner skin of the on the Outerpack. The weld studs penetrate the moderator blocks through 0.563 inch diameter holes. The blocks are mounted with a nominal gap, block to block, of 0.260 inches. The coefficients of thermal expansions are:

- 304 stainless steel 9.6 μ in/in-°F
- UHMW polyethylene 72 – 111 μ in/in-°F

Using the worst difference in expansion coefficients, 100 μ in/in-°F, the gaps between the blocks will accommodate heat up from 70° to 167°F. In addition, there is an additional 0.094 inch of clearance between the weld studs and each side of the holes in the polyethylene that will allow blocks with less than nominal clearance to slide in a direction to provide uniform clearance along the length of the Traveller.

Because the polyethylene's coefficient of expansion is much greater than stainless steel, interference between moderator blocks is not an issue when temperature drops. Instead, it is the interference between the blocks and the weld studs. Based on nominal clearances and a maximum distance of 17.0 inches from outboard hole-to-outboard hole, the package temperature can drop from 70°F to -41°F before the polyethylene is stressed. Most of the moderator blocks have significantly smaller distances between the outboard holes (6.5 to 12.5 inches) allowing them to accommodate larger temperature changes.

See Licensing drawings for additional details.

Analyzing the DTE between the fuel assembly and the Clamshell is evaluated assuming fuel loading is performed at 70°F (21°C) and shipped to a cold environment of -40°F (-40°C) since the aluminum will tend to contract more than the fuel assembly. The thermal growth is found by the familiar equation:

$\Delta L = \alpha(\Delta T)L_o$, where ΔL is the total growth, L_o CS is the original length of the Clamshell (202 inches), L_o FA is the original length of the fuel assembly (188.86 inches, per drawing 1453E86), ΔT is the temperature change (110°F), and α is the coefficient of thermal expansion.

For Aluminum, $\alpha = 13 \mu\text{in/in-}^\circ\text{F}$. For Zircalloy, $\alpha = 2.79 \mu\text{in/in-}^\circ\text{F}$.

The differential thermal growth between the Clamshell and the fuel assembly is then:

$$\begin{aligned} \text{DTE} &= \{\Delta L = \alpha(\Delta T)L_{o_{CS}} \text{ Al}\} - \{\Delta L = \alpha(\Delta T)L_{o_{FA}} \text{ Zirlo}\} \\ &= \{13\text{e-}6 \times 110 \times 202\} \text{ inches} - \{2.79\text{e-}6 \times 110 \times 188.86\} \text{ inches} \\ &= 0.29 - 0.058 \text{ inches} \end{aligned}$$

Thus,

$$\text{DTE} = 0.23 \text{ inches (the fuel assembly grows 0.23 inches relative to the Clamshell).}$$

The combined thickness of the base cork rubber and axial clamp cork rubber is 0.50 inches and can accommodate the growth due to differential thermal expansion. Thus, DTE is not a concern. Since the total differential growth associated with the XL Clamshell is greater than the STD Clamshell, it is the bounding calculation.

2.12.3.2.4.1 Internal/External Pressure

The Traveller package utilizes silicone rubber or fiberglass seals to preclude dust and other contaminants from entering the package. These seals are not continuous, and do not form an airtight pressure boundary. The package does not maintain a boundary between pressure gradients and is not designed to be pressurized during transport. Thus, internal/external reduced pressure will not impact the structural integrity of the package.

2.12.3.2.4.2 Vibration

The package must be evaluated to consider the effects of normal vibration on the design performance. The isolation system is designed to dampen normally induced vibrations from transport, and is not fundamental to the safe operation of the package. However, the Outerpack must maintain its structural integrity during transport to maintain a safe transport condition. Typical package attachment to a transport conveyance for the Traveller includes nylon straps or chain mounted both over the package and on the gusset tray connected to the support legs pointed inboard. The loading configuration can be modeled as a simply supported beam. Furthermore, the Outerpack is conservatively modeled considering only the outer shell at the first mode of vibration. The typical natural frequency range for transportation vehicles, $f_{\text{nat TRANS}}$, is 3.7-8 Hz. The natural frequency of the Outerpack can be determined from.

$$f_{\text{natOP}} = a \sqrt{(EIg/l^3)/m}$$

where $a=1.57$ (primary mode coefficient assuming hinge-hinge end conditions for additional conservatism), $E=29.4\text{E}6$ psi, $I=634$ in⁴, $m = 2,834$ pounds, $g = 386.4$ in/s² and $l = 226.2$ in (distance from gusset tray to gusset tray). Substituting values:

$$f_{\text{natOP}} = 1.57 \sqrt{[(29.4\text{E}6)(634)(386.4)/(226.2)^3]/(2,834)} \text{ 1/s (Hz)}$$

$$f_{natOP} = 1.57 \sqrt{220} \text{ Hz}$$

$$f_{natOP} = 23 \text{ Hz}$$

Since the natural frequency of the Outerpack is greater than the natural frequency typical of a transportation vehicle, resonance of the Outerpack is not expected and normally induced vibrations will not preclude the package from performing its design function.

2.12.3.2.5 Water Spray

The Traveller Outerpack is cylindrical, and shaped so that water will not be collected. Since the shell is fabricated of 304 SS, the water spray will not impact the structural integrity of the package.

2.12.3.2.6 Compression/Stacking test

The Traveller package must demonstrate elastic stability for a 5 g static load. No credit is taken for the circumferential stiffeners or the forklift support tubes. The analysis assumes the stacking load is uniformly distributed over the four outermost stacking brackets on the Outerpack. Figure 2-17 depicts the shell compression/stacking model.

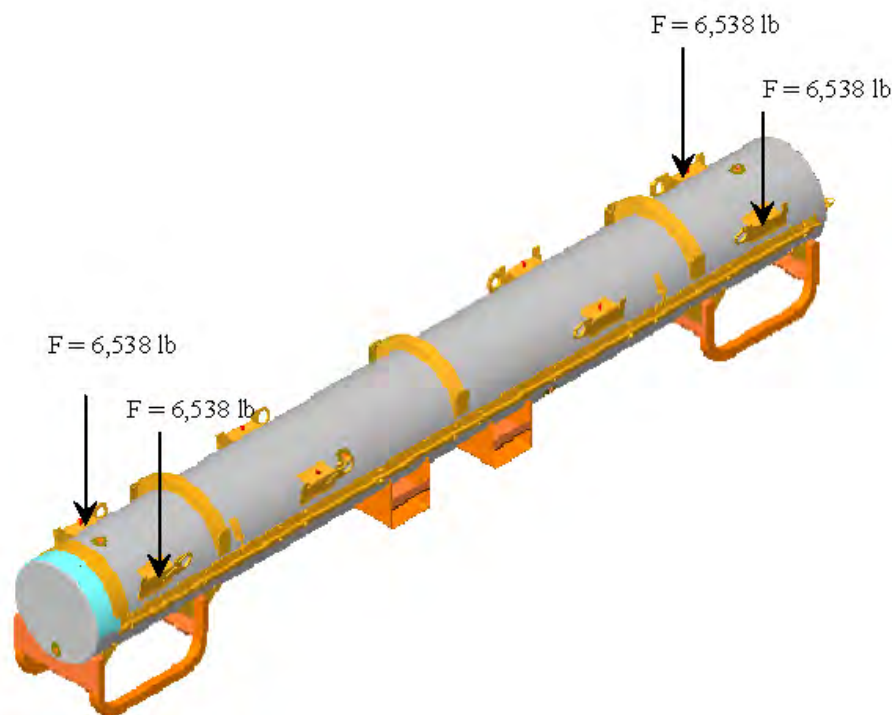


Figure 2-17 Compression/Stacking Requirement Analysis Model

The applied stacking force for the stacking test was determined to be:

$$F_s = 26,150 \text{ lb from Section 2.12.3.2.1.}$$

The load path is assumed to follow through the welds of the stacking brackets, through the Outerpack side, and then to the leg supports. This assumption is based on the package stacking configuration or the placement of weight on the package top. Each loaded section will be analyzed for its structural integrity.

Stacking Bracket – The stacking bracket is expected to experience a shear load on the weld during stacking. The loading configuration for a single bracket is shown in Figure 2-18.

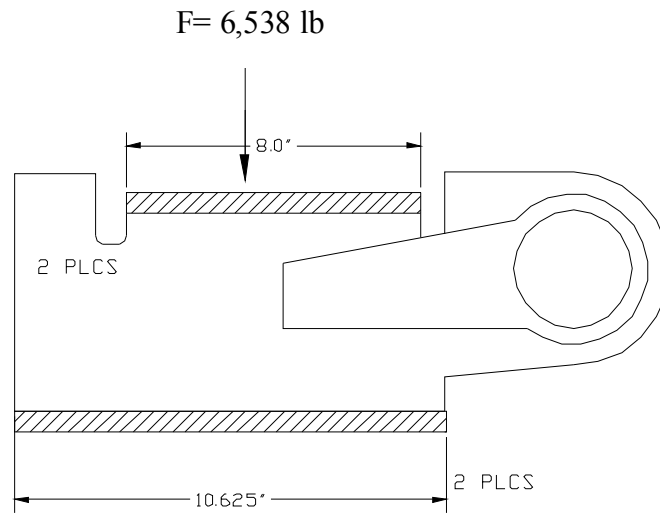


Figure 2-18 Stacking Force Model on Stacking Bracket

The load on each stacking bracket is found by dividing the applied load of 26,150 pounds by the four brackets that support the load:

$$F = 26,150 \text{ lb}$$

$$F = 6,538 \text{ lb}$$

The weld shear stress is found by $\tau_{\text{weld}} = F/A$, where F is the applied vertical or horizontal load and A is the weld area. The assumed weld area is the total weld area of each bracket and is found by:

$$A = h l \sin 45, \text{ where } l \text{ is } (10.625'' + 8'') = 18.625'' \text{ from Figure 2-18 and } h \text{ is the weld thickness, } 0.105''.$$

The weld stress is then:

$$\tau = F/A$$

Substituting values,

$$\tau = 6,538 / (.105)(18.625)(.707) \text{ psi}$$

$\tau = 4,729$ psi, which is less the allowable weld shear stress of 12 ksi.

2.12.3.2.6.1 Outerpack Section

The stacking bracket is expected to experience a compressive load through the package side cross section during stacking as the force follows the projected load path. The loading configuration and model for the Outerpack section is shown in Figure 2-19.

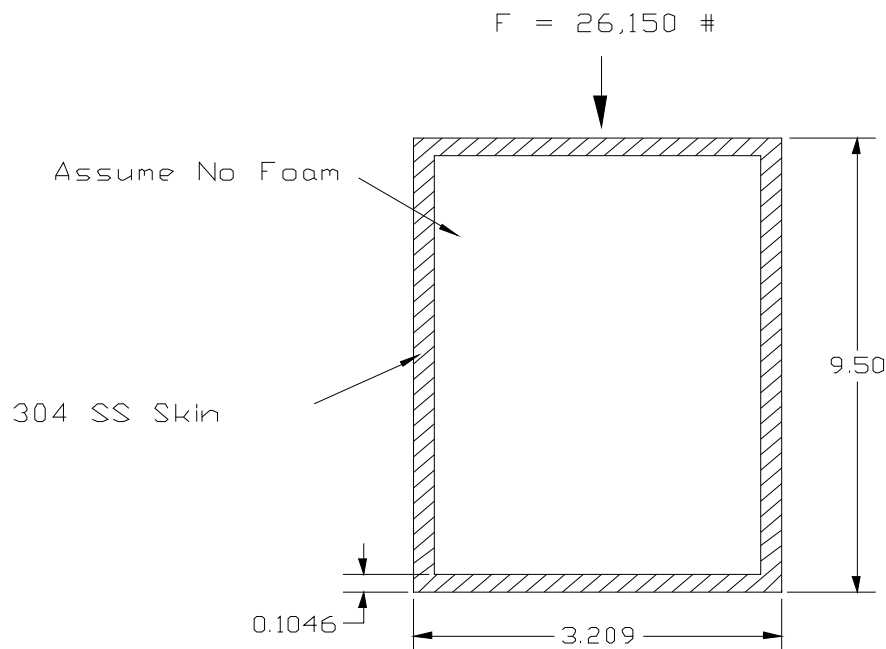


Figure 2-19 Outerpack Section Compression Model

The evaluation first examined the slenderness ratio of this section to determine if buckling is applicable. The model conservatively assumed no structural credit for the foam. In addition, the model assumed the force path section is from the base of the stacking bracket to the top of the support leg. The cross section consisted of a rectangular section of dimensions 9.50" x 3.209" with a wall thickness of 0.1046". The critical buckling load will be calculated and compared to the actual load to determine elastic stability of the Outerpack section.

The slenderness ratio, SR, can be expressed as:

$$SR = l / k$$

where l is the effective length, 9.50 inches, and the radius of gyration, k, is:

$$k = \sqrt{I / A}$$

For the Outerpak section, the moment of inertia, I, and the cross section area, A are:

$$I = (wl^3 - w_i l_i^3) / 12 \text{ in}^4$$

$$I = (3.209\{9.50\}^3 - 3.0\{9.29\}^3) / 12 \text{ in}^4$$

$$I = 28.8 \text{ in}^4$$

$$A = wl - w_i l_i \text{ in}^2$$

$$A = (3.209\{9.50\} - 3.0\{9.29\}) \text{ in}^2$$

$$A = 2.62 \text{ in}^2$$

Thus, the value for k is:

$$k = \sqrt{28.8 / 2.62} \text{ in}$$

$$k = 3.32 \text{ in}$$

The corresponding slenderness ratio is then:

$$SR = 9.50 / 3.32 \text{ in/in}$$

$$SR = 2.86$$

The limiting slenderness ratios for columns are as follows:

Long Columns

$\left(\frac{l}{k}\right)_1 = \sqrt{\frac{2\pi^2 CE}{\sigma_y}}$ where the end condition C is conservatively assumed to be unity, E is Young's Modulus, and σ_y is the tensile yield stress.

Substituting values:

$$\left(\frac{l}{k}\right)_1 = \sqrt{\frac{2\pi^2(29.4E6)}{30000}}$$

$$\left(\frac{l}{k}\right)_1 = 139$$

Short Columns

$$\left(\frac{l}{k}\right)_2 = .282\sqrt{\frac{AI^2}{\pi^2 I}}$$

Substituting values:

$$\left(\frac{l}{k}\right)_2 = .282\sqrt{\frac{2.62(9.50)^2}{\pi^2 28.8}}$$

$$\left(\frac{l}{k}\right)_2 = .257$$

Thus, $.257 < 2.86 \text{ (SR)} < 139$ and the Outerpack section is considered an intermediate column. The critical load for this column is given by:

$$P_{cr} = A\left(\sigma_y - \left\{\frac{\sigma_y l}{2\pi k}\right\}^2 \frac{1}{CE}\right)$$

$$P_{cr} = 2.62(30000 - \left\{\frac{30000 \cdot 9.50}{2\pi \cdot 3.32}\right\}^2 \frac{1}{29.4E6})$$

$$P_{cr} = 78,583 \text{ lb}$$

Since the actual load of 26,150 pounds is less than the critical buckling load of 78,583 pounds, the Outerpack section is considered stable during compression from stacking.

2.12.3.2.6.2 Leg Support

The leg support is expected to experience a compressive load through the straight top cross section during stacking as the force follows the projected load path. The loading configuration and model for the leg support section is shown in Figure 2-20. There are eight (8) leg sections of 2"x2"x.120" 304 SS tubing of approximately 10" length. The expected load for each leg section is 26,150/8 pounds, or 3,269 pounds.

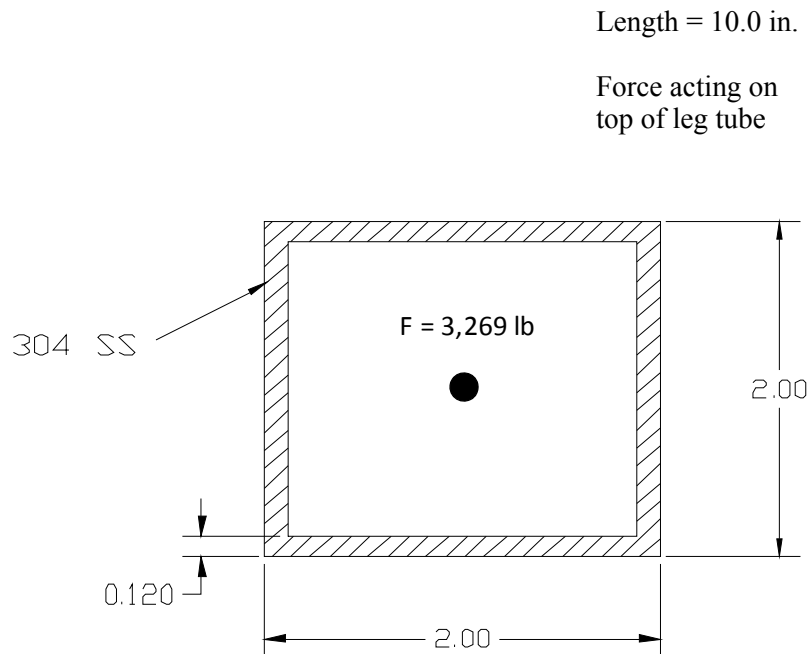


Figure 2-20 Leg Support Section Compression Model

The evaluation will first consider the slenderness ratio of this section to determine if buckling is applicable. The critical buckling load will be calculated and compared to the actual load to determine elastic stability of the leg support section.

The slenderness ratio, SR, is:

$$SR = l / k$$

where l is the effective length, 10.0 inches, and the radius of gyration, k , is:

$$k = \sqrt{I / A}$$

For the Outerpack section, the moment of inertia, I, and the cross section area, A are:

$$I = (wl^3 - w_i l_i^3) / 12 \text{ in}^4$$

$$I = (2.0 \{10.0\}^3 - 1.76 \{10.0\}^3) / 12 \text{ in}^4$$

$$I = 20 \text{ in}^4$$

$$A = wl - w_i l_i \text{ in}^2$$

$$A = (2.0 \{10.0\} - 1.76 \{10.0\}) \text{ in}^2$$

$$A = 2.4 \text{ in}^2$$

Thus, the value for k is:

$$k = \sqrt{20 / 2.4} \text{ in}$$

$$k = 2.9 \text{ in}$$

The corresponding slenderness ratio is then:

$$SR = 10.0 / 2.9 \text{ in/in}$$

$$SR = 3.4$$

The limiting slenderness ratios for columns is:

Long Columns

$\left(\frac{l}{k}\right)_1 = \sqrt{\frac{2\pi^2 CE}{\sigma_y}}$ where the end condition C is conservatively assumed to be unity, E is Young's Modulus, and σ_y is the tensile yield stress.

Substituting values:

$$\left(\frac{l}{k}\right)_1 = \sqrt{\frac{2\pi^2 (29.4E6)}{30000}}$$

$$\left(\frac{l}{k}\right)_1 = 139$$

Short Columns

$$(l/k)_2 = .282 \sqrt{\frac{Al^2}{\pi^2 I}}$$

Substituting values:

$$(l/k)_2 = 0.282 \sqrt{\frac{2.4(10.0)^2}{\pi^2 20}}$$

$$(l/k)_2 = .31$$

Thus, $.31 < 3.4 \text{ (SR)} < 139$ and the leg support section is considered an intermediate column. The critical load for this column is:

$$P_{cr} = A \left(\sigma_y - \left\{ \frac{\sigma_y}{2\pi} \frac{1}{k} \right\}^2 \frac{1}{CE} \right)$$

$$P_{cr} = 2.4 \left(30,000 - \left\{ \frac{30,000}{2\pi} \frac{10.0}{2.9} \right\}^2 \frac{1}{29.4E6} \right)$$

$$P_{cr} = 71,978 \text{ lb}$$

Since the actual load of 3,269 pounds is less than the critical buckling load of 71,978 pounds, the leg support section is considered stable during compression from stacking.

2.12.3.2.7 Penetration

The penetration test can be characterized as a localized impact event on the outer skin of the Outerpack. The energy imparted onto the outer skin is equal to the potential energy of the falling pin:

$PE = mgh$, where the mass of the pin is 13 lb and the drop height is 40 inches. To obtain correct units of energy, the gravitational constant g_c must be used in the energy equation. Thus,

$$PE_{\text{penetration}} = \frac{(13)(40)(32.2)}{32.2} \text{ in-lb (ft*s}^2\text{)/ft*s}^2$$

$$PE_{\text{penetration}} = 520 \text{ in-lb.}$$

By comparison, the energy locally imparted to the outer skin from the pin-puncture drop test is determined from the dropped package mass and the drop height. The mass of the package is 5,230 lb, and the drop height is 40 inches. Thus,

$$PE_{pin} = \frac{mgh}{g_c} = mh$$

$$PE_{pin} = (5,230)(40) \text{ in-lb.}$$

$$PE_{pin} = 209,200 \text{ in-lb.}$$

Pin puncture drop tests have demonstrated that the outer skin was not perforated as a result of impact onto the pin. Since the impact energy of the pin puncture drop test is approximately 400 times greater than that of the pin penetration, the pin puncture drop test bounds the pin penetration. Thus, the pin penetration impact is not expected to result in any significant structural damage to the Outerpack.

2.12.3.2.8 Immersion Analysis

The Traveller package uses silicone rubber or fiberglass seals for thermal protection and to preclude dust and other contaminants from entering the package. The seals are not continuous around the perimeter of the package and do not form a pressure boundary. In the event of water submersion, the inner portion of the package will fill with water creating equal hydrostatic pressure on the Outerpack and Clamshell surfaces. This condition would not result in a stress gradient through the Outerpack or Clamshell. Thus, immersion will not impact the structural integrity of the package.

2.12.4 DROP ANALYSIS FOR THE TRAVELLER XL SHIPPING PACKAGE

The primary method for evaluating the performance of the Traveller under hypothetical accident condition scenarios was actual testing of full-scale prototype packages. During the development program eighteen drop tests were conducted using a variety of orientations. Most of the drops were from greater than 9m. The drop tests are summarized in Table 2-5 and reported in detail in Section 2.12.4.

To supplement the actual test data, a finite element analysis (FEA) study was conducted using two models that were developed for the Traveller XL package. The first FEA model was based on the design of the two prototypes that were tested in January 2003. The second FEA model was based on the design of the two Qualification Test Units that were tested in September 2003. The QTU (actual package and FEA model) incorporated the modifications that were made to the design as a result of the prototype test results.

The objectives of the drop analysis effort were:

- Demonstrate that the first model acceptably predicted actual test results. This was accomplished by comparing the permanent mechanical deformations that resulted from the actual prototype drops with those predicted by the FEA model.
- Assist in the evaluation of test results. Because the FEA prototype model acceptably predicted actual test results, it could be used with confidence as a tool to evaluate possible changes to the packaging design in order to finalize a design that would pass the hypothetical drop tests.
- Assist in planning final tests. The FEA results, combined with the data obtained by prototype drop testing, were used to establish drop orientations for the qualification test unit (QTU) and certification test unit (CTU) tests.

Limitations were observed in the FEA process. For example, mesh density limitations meant that actual stress and strain predicted values could not be considered highly accurate. The models could identify regions of high stress and strain but could not accurately predict component failure unless predicted values were significantly above or below failure points. Instead, the models were developed to evaluate relative deformations, decelerations and energy absorption between drop orientations. The analyses provided a qualitative means for comparing predicted stresses and strains for different drop orientations to allow intelligent selection of drop orientations for testing. The Traveller program utilized extensive full-scale tests to prove the acceptability of the Traveller design. These tests results are described in sections 2.12.4 below and the results are compared with the FEA in this section.

2.12.4.1 Conclusion and Summary of Results

2.12.4.1.1 Conclusion

Analysis indicates that the Traveller XL shipping package complies with 10 CFR 71 and TS-R-1 requirements, respectively for all drop orientations. Test orientations which are most challenging are a 9 meter vertical drop with the bottom end of the package hitting first as shown in Figure 2-52A and a 9 meter

CG-forward-of-corner drop onto the TN end of package with an 18° forward rotation, Figures 2-44 and Figure 2-45. The former has the greatest potential to damage the fuel assembly and the latter is most damaging to the shipping package itself. Based on this analysis, successful drop tests in these two orientations are adequate to demonstrate that the Traveller XL design meets/exceeds the HAC drop test requirements.

2.12.4.1.2 Summary of Results

Analyses were conducted for horizontal side drops, center-of-gravity-over-corner onto the top nozzle drops, and vertical drops onto the top nozzle and bottom nozzle. A significant amount of analytical data is presented in the following sections. Below is an summary of the major points in the order presented:

Determination of Most Damaging Orientations

- The most damaging orientation for the outerpack may not be most damaging for the fuel assembly. Because of the robust design of the packaging, drop orientations that were most damaging to the fuel assembly took precedence.
- Analysis of drop orientations most damaging to the outerpack focused on three orientations: horizontal drop onto the side, vertical end drop (top and bottom nozzle end), and near-vertical drop (center-of-gravity over corner).
- Analysis of drop orientations most damaging to the fuel assembly focused on the vertical end drop (top and bottom nozzle end).

Most Damaging Orientations to Outerpack

- Horizontal drop onto the side gave highest predicted outerpack loads.
- CG forward of corner onto top predicted to be most damaging to outerpack because of potential damage that might compromise package ability to survive the thermal test.
- Damage to the Traveller XL shipping package from the HAC drop tests is predicted to be minor and primarily involves localized deformations in the region of impact. Both the Outerpack and Clamshell structures remain intact and closed.

Most Damaging Orientations to Fuel Assembly

- Bottom nozzle end drop predicted to be more damaging than top nozzle end drop.
- Fuel assembly damage is predicted to be confined to the top or bottom region depending on drop orientation. This damage primarily involves localized buckling and deformation of the nozzles.

Temperature and Foam Density Effects

- Temperature and foam density have a minor effect on drop performance of the Traveller XL package.
- For the orientation predicted most damaging to the Outerpack, a package with nominal foam density and dropped at “normal temperature” (75°F) experiences 8.5 and 13.7% higher loads than, respectively, one containing low density foam and dropped at 160°F or one containing high density foam and dropped at -40°F, Figure 2-62.
- Fuel assemblies in packages containing the highest allowable density foam and dropped at the lowest temperature extreme will experience accelerations that are very similar to those in packages with lowest allowable density foam and dropped at the highest temperature extreme, Figure 2-63. However, the accelerations at these extremes are only 5% greater than for a package dropped at 75°F containing nominal density foam.
- Bottom nozzle end drop predicted to be more damaging than top nozzle end drop.

Pin Puncture

- Analysis indicates that the Traveller XL is capable of withstanding the 1 m pin puncture test. The steel outer skin should not be ruptured.
- A maximum indentation of 67 mm is predicted for the 1 m pin puncture test when the package is impacted from underneath and dropped horizontally with its CG directly above the pin. during this test.

Comparison of Prototype Test Results to Analysis Predicted Results.

- There was good overall agreement between predicted and actual drop performance. This is evident by comparisons of predicted and actual permanent deformations, failed parts, and measured and predicted accelerations at specific positions on the Outerpack and Clamshell.

Bolt Factor-of-Safety Calculations.

- The Traveller XL shipping package will survive the HAC drop tests in any orientation with few or no closure bolt failures. Horizontal side drops onto the hinges or latches, Figures 26A and B, result in the highest hinge/latch bolt loads. The analyses indicate ten $\frac{3}{4}$ -10 stainless steel bolts/side are sufficient to ensure the Outerpack remains closed during such drops. The minimum predicted factor of safety for the Outerpack latch and hinge bolts is 1.12.

[Rev 2 redistributed this information in Section 2.12.3.1 above.]

2.12.4.2 Predicted Performance of the Traveller Qualification Test Unit

2.12.4.2.1 Most Damaging Drop Orientations

A primary objective of this study was to determine the worst case drop orientation(s) for the HAC drop tests. This requirement is to drop test the shipping package in orientations that most damage: a) the shipping package, and b) the fuel assembly. It was quickly realized that the most damaging orientation for the shipping package, would not necessarily be the same for the fuel assembly. Based on the robust performance of the Traveller XL drop units during testing, orientations that were most severe to the fuel assembly became more significant.

Determination of the worst case orientation for the shipping package was facilitated by the Traveller XL computer analysis and results of the prototype tests. Many orientations can be eliminated from consideration due to inherent design features of the Traveller. For example, the circumferential stiffeners on the upper Outerpak, and the legs/forklift pocket structure, Figure 2-21, greatly reduce the crushing of the Outerpak since they crush prior to impact of the main body of the Outerpak. Drop orientations where one or the other

of these structures directly contacts the drop pad, Outerpack damage is reduced in comparison to orientations where these features are not impacted. This is because the energy absorbed in crushing these features cannot be absorbed by the Outerpack.

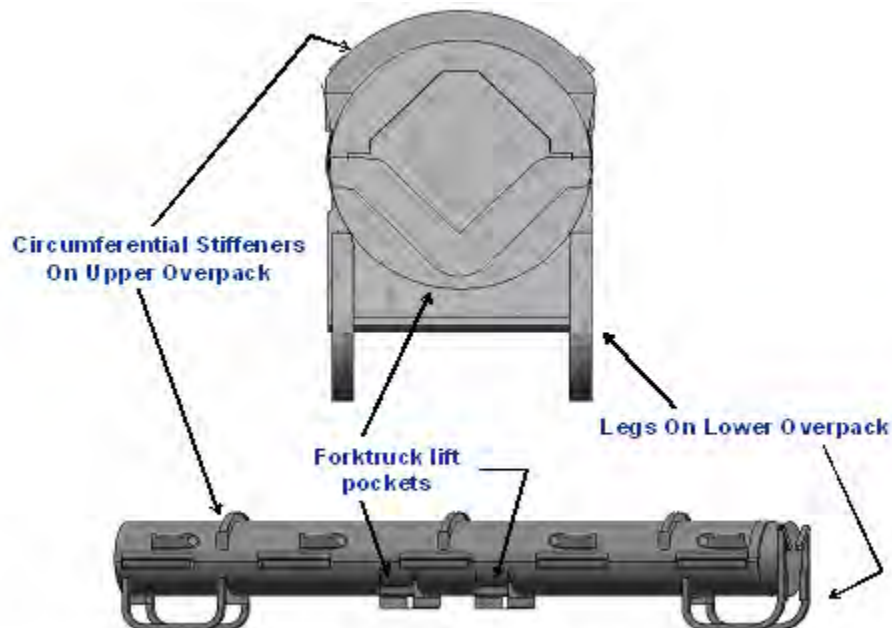


Figure 2-21 Traveller Stiffeners, Legs, and Forklift Pockets

Test results supported this hypothesis. Indeed, in the two available tests of relevance, these features absorbed almost all the energy and very little damage was incurred by the Outerpack. For example, Prototype-1, Test 1.1 was a low angle slap down test resulting in extensive crushing of the upper Outerpack stiffeners, Figure 2-22. Aside from this crushing, very little Outerpack damage was incurred. Prototype-2, Test 3.2 was the second example. In this test, the Outerpack was dropped horizontally onto its legs from 9 m. This resulted in significant crushing of the Outerpack legs and feet, Figure 2-22B, and the forklift supports, not shown. However, the Outerpack was otherwise not significantly damaged.

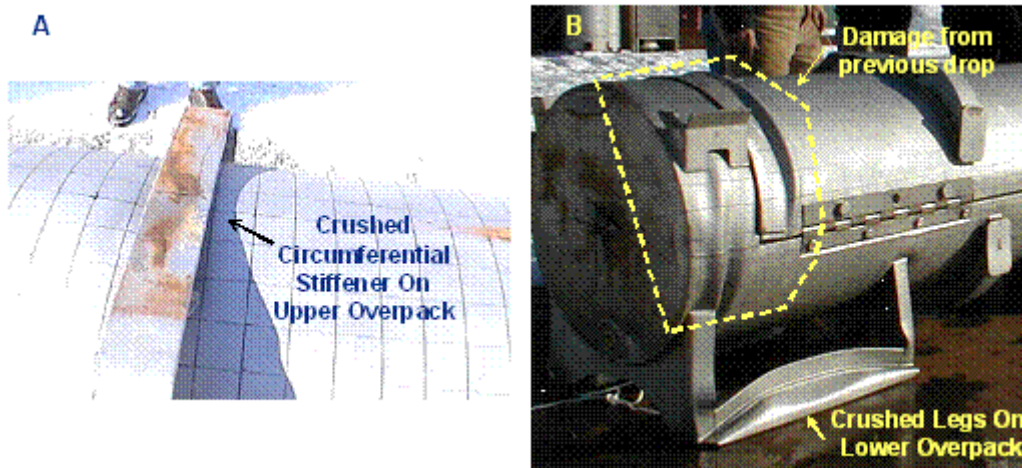


Figure 2-22 Results of Prototype Drop Test

Alternately, neither the stiffeners, nor legs hit first for orientations in which the Outerpack ZX plane defined in is perpendicular to the impact surface, Figure 2-23. Such orientations include side drops or slap downs onto the hinged sides of the Outerpack and vertical drops onto the either end of the package. Thus, our analysis of the most damaging Outerpack orientations focused on these orientations.

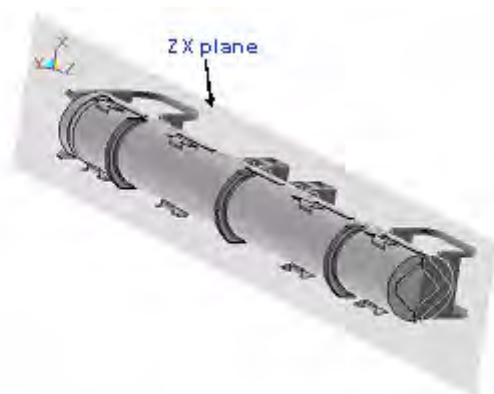


Figure 2-23 Side Drop Orientation

Determining which drop orientations in the ZX plane most damage the shipping package was also facilitated by the Traveller XL design itself. In particular, “slap down” drops, low- to medium-angle impacts where one end of the package hits before the other, as shown in Figure 2-24, divide the impact energy primarily between the top and bottom impact limiters. Generally, this energy is absorbed in a manner that induces relatively little damage for this design. An example of the damage associated with a 15° slap down is shown in Figure 2-25. This figure reflects the damage obtained in Test 1.1 of the Prototype test campaign.



Figure 2-24 Low Angle Drop Orientation

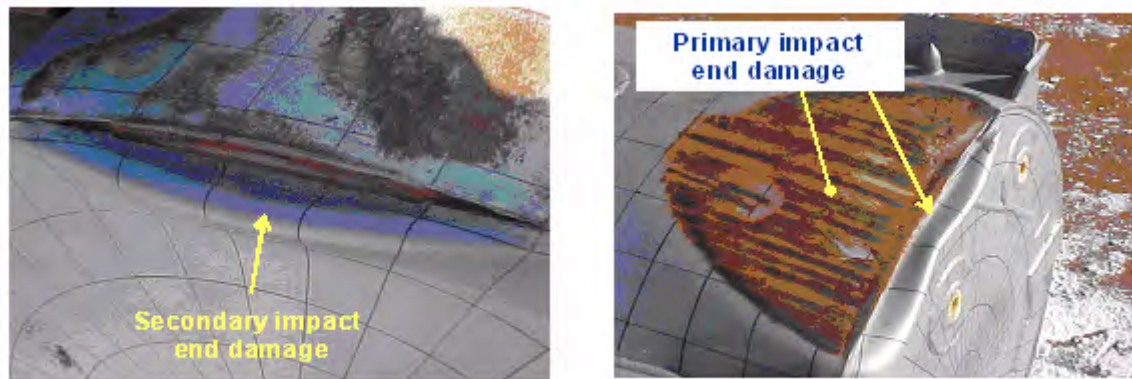


Figure 2-25 Damage from Prototype Low Angle Drop (Test 1.1)

The shipping package may be dropped in some orientations outside the ZX plane and still not be protected by its stiffeners and legs/forklift pocket structure, Figure 2-21. In vertical and nearly vertical orientations, the impact limiter will hit the drop pad first. In these cases, the primary impact energy may be entirely absorbed by the impact limiters and Outerpak walls with little, if any, being channeled into the stiffeners or legs. Indeed, the stiffeners and legs provide no benefit unless the shipping package actually falls over for a secondary impact.

Thus, analysis of orientations most damaging to the Outerpak was focused on horizontal drops onto the Outerpak side (i.e., onto the hinges/latches), vertical drops (onto either end of the package) and nearly vertical drops.

2.12.4.2.2 Horizontal Side Drops

The two possible orientations for a horizontal side drop test involve either a drop onto the opening or latched side of the Outerpack, Figure 2-26A, or a drop onto the permanently (or semi-permanently) hinged side, Figure 2-26B.

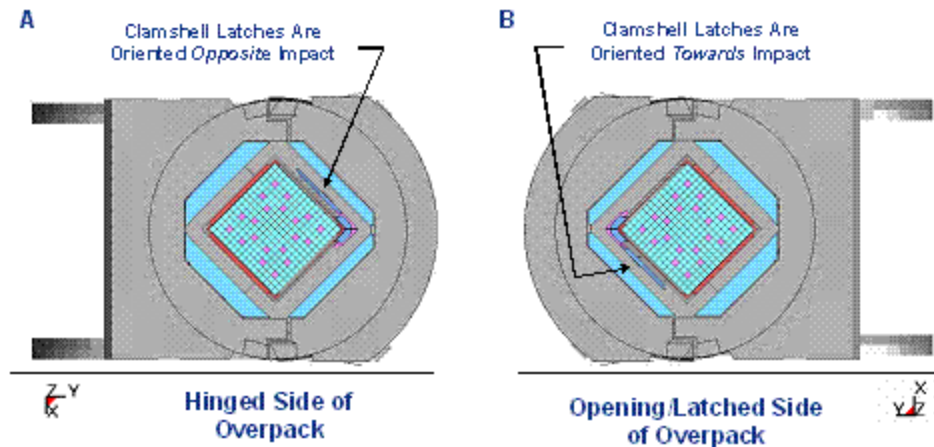


Figure 2-26 Horizontal Drop Orientation

Energy and Work Histories – Global energy and work for the Outerpack horizontal side drops are shown in Figures 2-27 and 2-28. The similarity of these two drops is reflected in these plots. Both plots (as do all the 9.14m (30ft) drops reported herein for the qualification unit) have an initial total energy (TE) of 204 kJ. This value correctly reflects the initial velocity (v) of 13.4 m/s applied to the 2,270 kg (5,005 lb) package mass (m) since our simulation is initiated at the end of Outerpack free fall from 9.14 m (30 ft.); the total energy is comprised only of kinetic energy (KE), and $KE = \frac{1}{2}mv^2$. Total energy remains nearly constant throughout both drop simulations. This reflects the relatively small overall deformations predicted for this drop, i.e., the almost negligible external work done by the package under gravity loading. In both simulations, the event was essentially completed within 10 milliseconds as seen by the flattening of the kinetic energy and internal energies after that time. Moreover, acceptable levels of hourglass, sliding, and stonewall energies were obtained although the sliding energy ultimately reached 10% of the internal energy. This latter issue is not critical since it occurs after the maximum Outerpack/drop pad force has been reached.

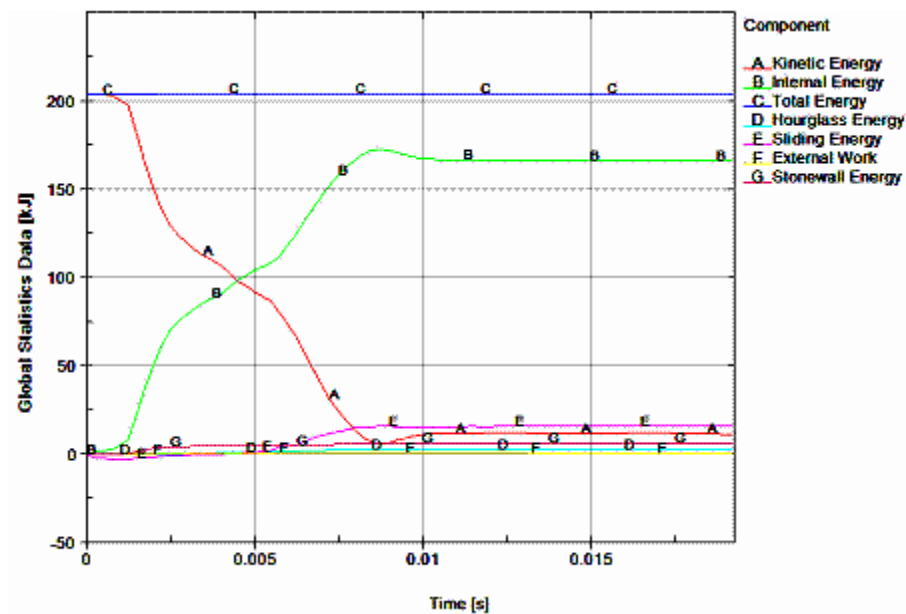


Figure 2-27 Predicted Energy and Work for 9m Horizontal Drop Onto Outerpack Hinges

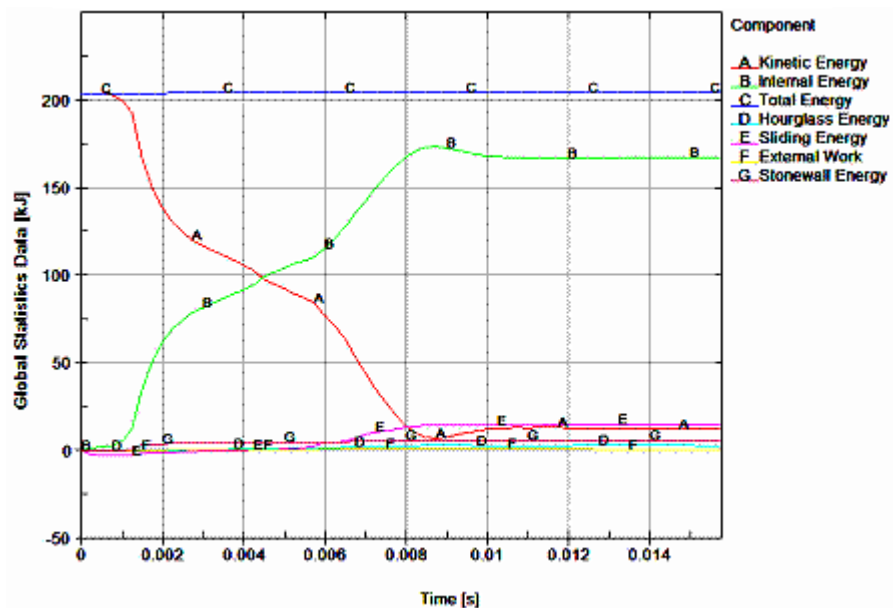


Figure 2-28 Predicted Energy and Work Histories for a 9m Horizontal Drop Onto the Outerpack Hinges

Rigid Wall Forces – Neglecting the very soft shock mounts that tie them together, the Traveller XL shipping package consists of an essentially de-coupled Outerpack and Clamshell/fuel pair. Indeed, the predicted drop scenario consists of the Outerpack crushing onto the pad while the Clamshell/fuel assembly continues falling until it hits the inner surfaces of the Outerpack. Then the Outerpack, Clamshell, and fuel assembly crush further onto the pad. This scenario is reflected in the rigid wall force history shown in Figure 2-29.

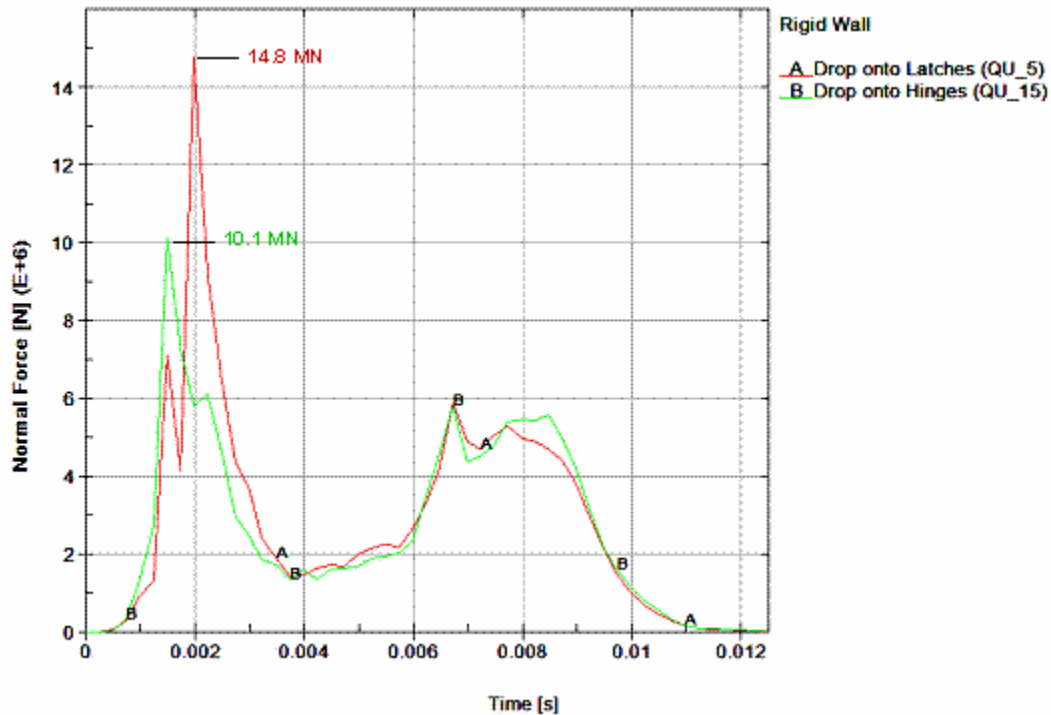


Figure 2-29 Predicted Rigid Wall Force Histories for 9m Horizontal Drops Onto the Outerpack Latches and Hinges

In Figure 2-30A, the initial impact between the Outerpack and pad is seen in the first 4 milliseconds, peaking at approximately 1.5 milliseconds for the drop onto hinge (run QU_15) and 2.0 milliseconds for the drop onto latches (run QU_5). This disparity is attributed to slight errors in the model geometrical definition (rather than to any actual non-symmetry within the design itself). Further, we postulate resolution of this disparity would lower the predicted forces for the drop onto Outerpack latch simulation (run QU_5) and increase those for the simulated drop onto the Outerpack hinges (run QU_15). However, we choose not to resolve this difference but simply used the QU_5 predictions as a bounding and conservative case. At approximately 4.0 milliseconds, the force between the Outerpack and drop pad has decreased and it appears the Outerpack might soon rebound. However, the Clamshell/fuel assembly then contacts the inner surface of the Outerpack and drives it into back into the drop pad, Figure 2-30B.

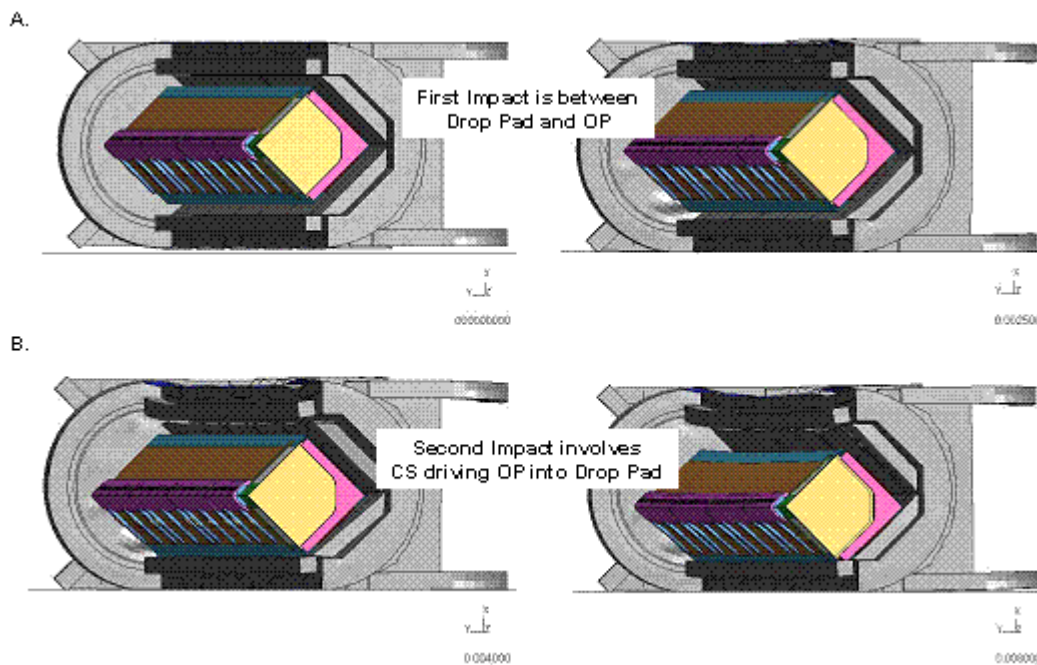


Figure 2-30 De-coupled Impacts for 9 m Horizontal Side Drop

The forces between the Outerpack and drop pad during the first portion of a horizontal side drop are the highest predicted forces for any orientations analyzed. However, these forces are so high because the deformations (i.e., cushioning) are small. Thus, despite the high forces, the package (Outerpack and Clamshell) should be relatively undamaged provided its components remain closed. For the Outerpack, this requires that the majority of the Outerpack latch/hinge bolts do not fail. In the case of the Clamshell, the latch bolts, the top and bottom end plate bolts, and, as will be described, the lipped/groove interfaces between the Clamshell end plates themselves (top end) and between the Clamshell doors and plate (bottom end) must not be comprised. During Prototype testing the robustness of these features was confirmed, as no Outerpack bolts failed, and the Clamshell latches remained closed.

Note that the Clamshell cross-sectional shape is predicted to stay essentially unchanged during the horizontal side drops, Figure 2-30. This is due in large part to the moderator blocks which form a “cradle” for the Clamshell. These moderator blocks prevent the Clamshell from radically changing shape as might otherwise happen since three of the Clamshell edges are either hinged or latched. This is an important structural benefit of the conformal shape of the interior of the Outerpack.

Outerpack Hinge Bolts – The Outerpack hinges are secured to the Outerpack with Type 304 stainless steel bolts, Figure 2-31. The bolts securing the bottom flange of the hinge (or latch) to the lower Outerpack are not removed during normal operation. Thus, the number of bolts used in this area is not critical from a user/operation standpoint. However, the bolts securing the top half of the latch to the upper Outerpack must be removed whenever the package is opened. Thus, the desire is to minimize the number of these bolts while

still insuring the package is not compromised during HAC drop tests. As such, the development of the Traveller XL design started with three 7/8" diameter (2.2 cm) for each hinge segment. A total of five (5) hinge segments per Outerpack side were utilized. The second Prototype unit therefore was tested with only 2 of 3 bolts in each hinge section (10 per side) to verify that design margins were present in the design.

Based on the successful testing of 10 bolts per side, evaluations were initiated to determine if smaller 3/4" diameter (1.91 cm) bolts had sufficient strength to sustain impact loads. These were shown to be acceptable. The QTU-1 and QTU-2 units were dropped with ten 3/4" (1.91 cm) bolts on each side.

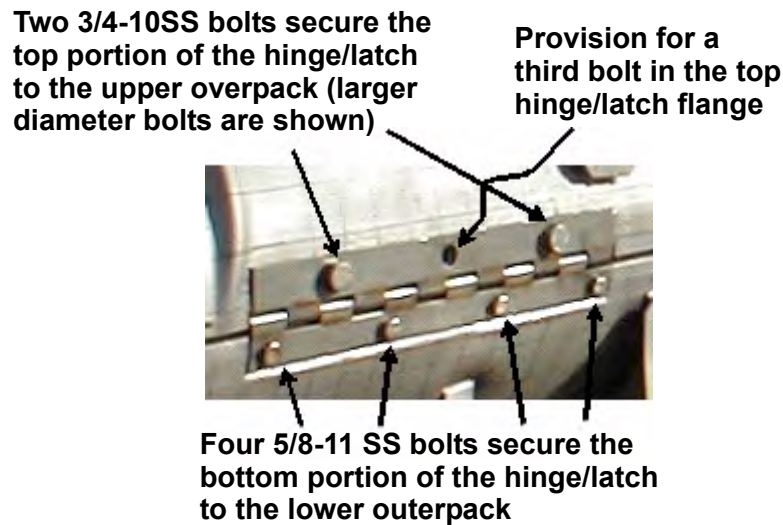


Figure 2-31 Bolts on Prototype Outerpack

Prototype-2, Test 3.3 was a side drop in which two 7/8-9 stainless steel bolts were used to secure the top portion of the hinge to the upper Outerpack and four 5/8-11 stainless steel bolts were used to secure the bottom hinge flange to the lower Outerpack. In this test, no bolts were broken. Our analyses indicate two 3/4-10 stainless steel bolts/latch and hinge are sufficient to insure the Outerpack remains closed during the 9m side drop. This is seen by reviewing the predicted safety factors of the top latch bolts when the package is dropped on its latching side, Figure 2-26B. As shown in Table 2-10, the minimum factor-of-safety (FS) for the top Outerpack latch bolts was 2.15 based on the bolt minimum tensile (125 ksi). This minimum was calculated for a latch bolt when the Outerpack was dropped onto its latched side, Figure 2-26B.

Table 2-10 Top Outerpack Latch Bolt Minimum Factors of Safety (FS) for 9m Side Dropped		
ID (Figure 2-32)	FS/Time	
	Dropped On OP Latches (Figure 2-30B)	Dropped On OP Hinges (Figure 2-30A)
B917	2.22/0.0082 s	2.20/0.0077 s
B921	2.15/0.0065 s	2.21/0.0065 s
B923	2.16/0.0065 s	2.17/0.0065 s
B927	2.20/0.0062 s	2.18/0.0065 s
B929	2.19/0.0057 s	2.19/0.0062 s
B933	2.19/0.0067 s	2.20/0.0077 s
B935	2.20/0.0067 s	2.16/0.0065 s
B939	2.18/0.0065 s	2.18/0.0065 s
B941	2.21/0.0085 s	2.23/0.008 s
B945	2.32/0.0045 s	2.43/0.0045 s



Figure 2-32 Bolt Labels for Right Outerpack

Hinge bolt FS for horizontal 9m side drops on the latched and hinged side of the Outerpack are shown in Table 2-10. If the shipping package were exactly symmetrical, FS for the hinge bolts calculated for a drop on the Outerpack hinges would correspond with those for the latch bolts when the package was dropped onto the latches, etc. However, this was not the case as can be seen by comparing the results shown in Table 2-10 with those in Table 2-11. This small irregularity is primarily attributed to slight errors in the model geometrical definition and to a lesser extent on actual non-symmetry within the design itself. The analysis indicates little likelihood of compromising the Outerpack closure during a 9m side drop.

Table 2-11 Top Outerpack Hinge Bolt Minimum Factors of Safety (FS) for 9m Side Drop		
ID (Figure 2-33)	FS/Time	
	Dropped On OP Latches (Figure 2-30B)	Dropped On OP Hinges (Figure 2-30A)
B947	2.34/0.0025 s	2.20/0.0077 s
B951	3.05/0.0027 s	2.21/0.0065 s
B953	2.58/0.0022 s	2.17/0.0065 s
B957	2.93/0.0022 s	2.18/0.0065 s
B959	2.82/0.0017 s	2.19/0.0062 s
B963	3.19/0.0017 s	2.20/0.0077 s
B965	2.52/0.0022 s	2.16/0.0065 s
B969	2.22/0.0117 s	2.18/0.0065 s
B971	2.52/0.0055 s	2.23/0.008 s
B975	2.54/0.0032 s	2.43/0.0045 s

For the CTU and production designs, minor changes to the design were made to improve burn test performance, as well as simplify manufacturing. To ensure a conservative design, two additional bolts were added on each side of the Outerpack full-length hinge sections. Therefore, the CTU and production packages utilize 12 bolts per side per hinge leaf. This change allowed the reduction of the planned high strength (125 ksi ultimate strength) bolt to be replaced with a lower strength bolt, since there are more bolts, and since the 70 ksi bolts were marginal in performance. It should also be noted that the Prototype-2 package was dropped on its side from 9 m and showed no visible signs of strain on any of the bolts. One explanation for this may be that friction is ignored in the calculation of bolt factors of safety.

The increase in number of bolts, 20%, ($= 12/10$) and the increase in strength of the allowable bolt material, ASTM A193 Class 1 B8, of 7% ($= 75 \text{ ksi}/70 \text{ ksi} - 1$) causes the factors of safety of the worst bolt in a side drop to be reduced from 2.15 to 1.12. Since this is the greatest loading for any orientation, all bolts have an adequate safety margin.



Figure 2-33 Bolt Labels for Left Outerpack

Clamshell Keeper Bolts – The inner Clamshell is restrained during shipment by eleven (11) quarter-turn latches as shown in Figure 2-34. This design was incorporated after Prototype testing, primarily for improved handling characteristics. One half of the latch, the latch handle, is welded to the one Clamshell door hinge. The portion of the latches which is physically turned to allow opening and closing is attached to the opposite door is called the “keeper.” Each keeper is attached to the Clamshell door with ½-13 stainless steel bolts.

Factors-of-safety for the Clamshell keeper bolts are shown in Table 2-12. The analyses indicate that these bolts are unlikely to fail during side drops onto either the Outerpack latches or Outerpack hinges. Further, the modeling of the fuel assembly as a rigid structure likely makes little difference to these predictions since the fuel rods would not be expected to buckle in this drop orientation.

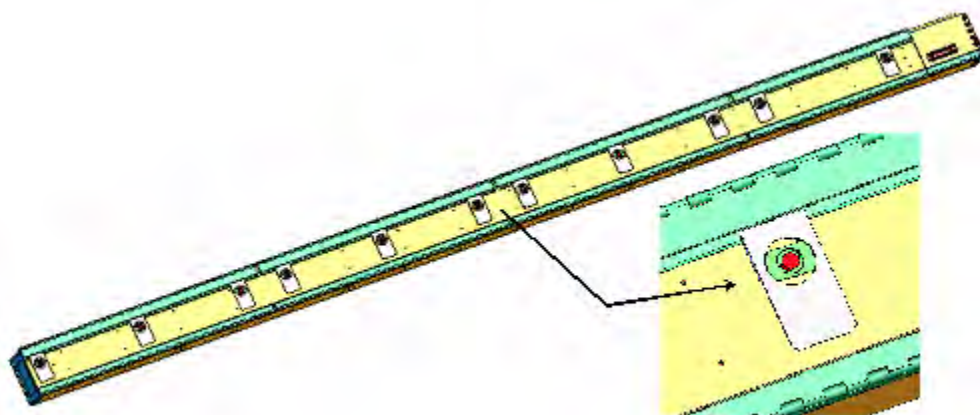


Figure 2-34 Clamshell Closure Latches and Keeper Bolts

Table 2-12 Clamshell Keeper Bolt Minimum Factors of Safety for 9m Side Drop		
ID (Figure 2-35)	FS/Time	
	Dropped On OP Latches (Figure 2-30B)	Dropped On OP Hinges (Figure 2-30A)
B6271277	2.10/0.0067 s	1.72/0.006 s
B6271278	2.15/0.007 s	1.72/0.0085 s
B6271279	3.17/0.0062 s	3.36/0.0075 s
B6271280	2.12/0.0072 s	4.40/0.01 s
B6271281	2.90/0.008 s	4.03/0.0092 s
B6271282	2.50/0.0082 s	2.48/0.0067 s
B6271283	3.70/0.0055 s	2.16/0.0067 s
B6271284	2.56/0.007 s	1.84/0.0062 s
B6271285	1.93/0.0072 s	2.64/0.008 s
B6271286	2.62/0.0072 s	3.00/0.0082 s
B6271287	1.94/0.0075 s	2.29/0.0082 s

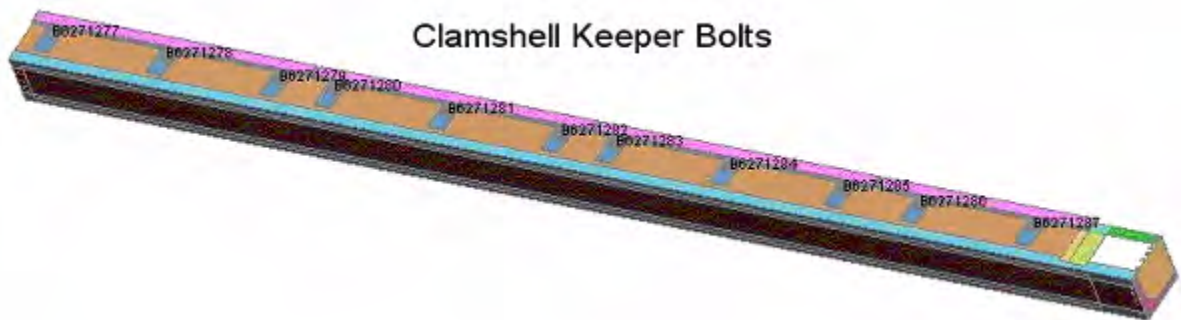


Figure 2-35 Clamshell Keeper Bolt Labels

Clamshell Top and Bottom Plate Bolts – In addition to the Clamshell latch bolts, there are thirty ½-13 stainless steel bolts securing the Clamshell top and bottom end plates. The twenty bolts securing the top end plate are distributed five per side as shown in Figure 2-36A. These bolts are not removed during normal operation and are permanently adhered to the plates. The ten bolts securing the bottom end plate are distributed equally to the two walls of the Clamshell V-shaped bottom extrusion as shown in Figure 2-36B. These bolts are also permanently adhered.

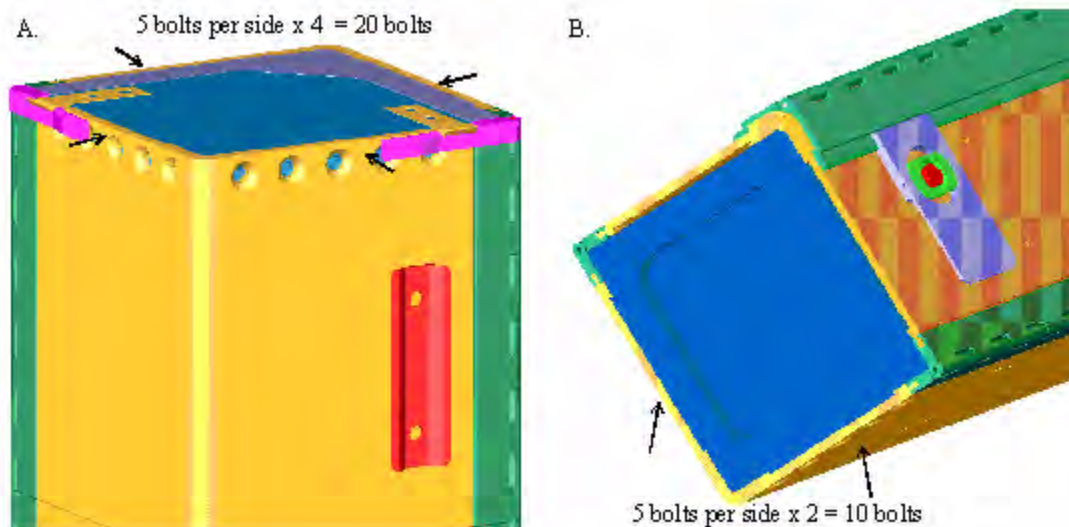


Figure 2-36 Clamshell Top and Bottom End Plates

The analyses indicates that none of the Clamshell bolts at the top and bottom ends will fail during a side drop on either the Outerpack latches or Outerpack hinges. This is evident from the minimum factors of safety shown in Tables 2-14, 2-15 and 2-16. (Our modeling of the fuel assembly as a rigid structure likely makes little difference to these predictions since the fuel rods would not be expected to buckle in this drop orientation.)

Table 2-13 Clamshell Bottom Plate Bolt Minimum Factor of Safety for 9m Side Drops		
ID (Figure 2-37)	FS/Time	
	Dropped on OP Latches (Figure 2-30B)	Dropped on OP Hinges (Figure 2-30A)
B6168785	2.39/0.0047 s	2.33/0.0107 s
B6168786	2.84/0.0070 s	4.29/0.0065 s
B6168787	6.40/0.0092 s	6.96/0.0062 s
B6168788	9.56/0.0092 s	6.26/0.0062 s
B6168789	6.62/0.0190 s	3.96/0.0060 s
B6168794	3.84/0.0062 s	5.43/0.0102 s
B6168793	19.4/0.0050 s	7.61/0.0102 s
B6168792	13.5/0.0087 s	7.88/0.0102 s
B6168791	4.37/0.0065 s	3.57/0.0055 s
B6168790	2.41/0.0060 s	2.48/0.0050 s

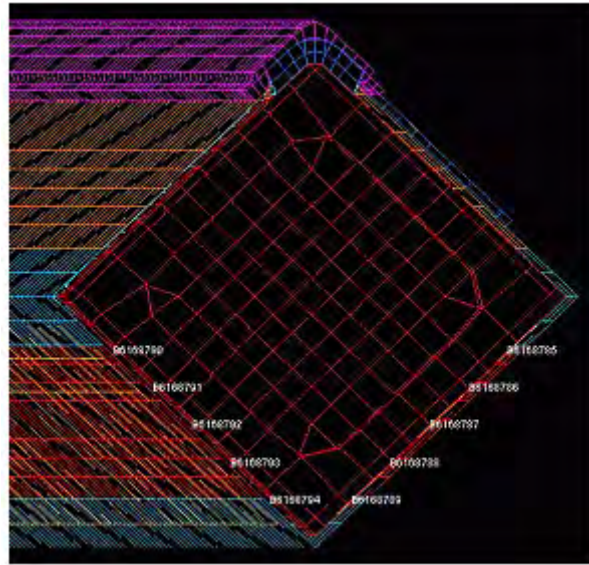


Figure 2-37 Clamshell Bottom Plate Bolt Labels

Table 2-14 Clamshell Grooved Top Plate Bolt Minimum Factors of Safety for 9m Side Drops		
ID (Figure 2-38)	FS/Time	
	Dropped on OP Latches (Figure 2-30B)	Dropped on OP Hinges (Figure 2-30A)
B6168781	4.19/0.006 s	5.21/0.0052 s
B6168780	21.1/0.0065 s	12.67/0.0057 s
B6168779	32.1/0.0077 s	21.22/0.0057 s
B6168778	17.5/0.0095 s	33.37/0.007 s
B6168773	2.29/0.0065 s	2.73/0.005 s
B6168774	2.25/0.0062 s	4.97/0.0087 s
B6168775	3.88/0.0075 s	33.54/0.0092 s
B6168776	24.5/0.0057 s	52.4/0.0077 s
B6168777	13.2/0.0057 s	54.49/0.009 s
B6168769	2.99/0.0052 s	4.77/0.006 s

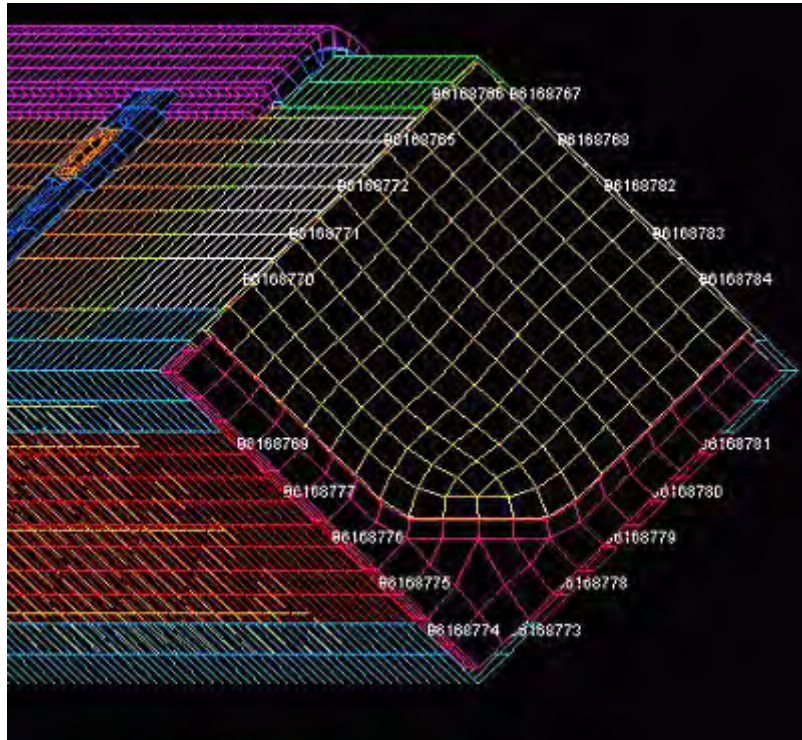


Figure 2-38 Clamshell Bottom Plate Bolt Labels

Table 2-15 Clamshell Lipped Top Plate Bolt Minimum Factors of Safety for 9m Side Drops		
ID (Figure 2-38)	FS/Time	
	Dropped on OP Latches (Figure 2-30B)	Dropped on OP Hinges (Figure 2-30A)
B6168770	2.32/0.005 s	3.38/0.0077 s
B6168771	5.65/0.005 s	10.4/0.006 s
B6168772	5.95/0.005 s	11.6/0.007 s
B6168765	9.29/0.0085 s	18.8/0.0065 s
B6168766	7.27/0.0057 s	7.99/0.007 s
B6168767	6.54/0.007 s	6.58/0.006 s
B6168768	9.68/0.007 s	11.7/0.006 s
B6168762	9.14/0.007 s	9.16/0.006 s
B6168783	6.18/0.0085 s	5.65/0.0122 s
B6168784	4.22/0.008 s	2.25/0.0047 s

Clamshell Top End Plate Joint – One goal of the Traveller package design was to minimize the time and effort associated with loading and unloading the fuel. This necessitated the number of bolts that had to be removed during these operations be as kept as low as possible. To accomplish this, the top end of the Clamshell consists of two interlocking plates as shown in Figure 2-39. One of these plates is grooved and is permanently attached to the V-shaped lower portion of the Clamshell, Figure 2-36A. The other has a lip and is permanently attached to an upper housing above the Clamshell doors, Figure 2-39. This groove-and-lip design should indeed facilitate rapid loading and unloading, however, the joint must not separate to any significant extent during the HAC drop tests that the fuel rods might slip out of the Clamshell.

Fortunately, our analysis indicates that the separation during impact is small, Figure 2-40. Furthermore, the separation is transient/temporary as can be seen by the reduction in the separation distance in the later stages of the analysis, Figure 2-40B compared with Figure 2-40A. These predicted results were obtained from the analysis of the Outerpack drop onto its latches. In this case, the Clamshell latches are positioned underneath the fuel, towards the ground, Figure 2-26B. Analysis of the Outerpack drop onto its hinges yielded similar results although the predicted separation of this joint was slightly less.

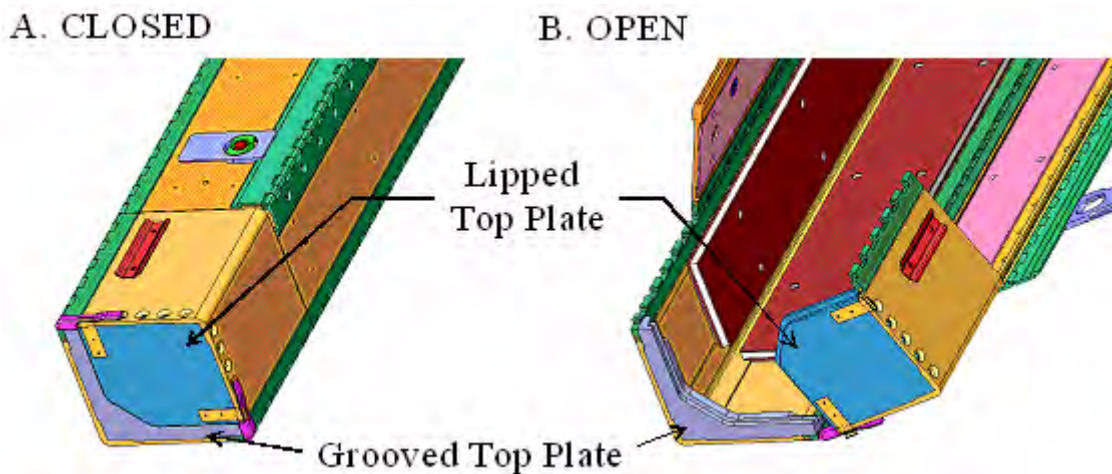


Figure 2-39 Clamshell Doors

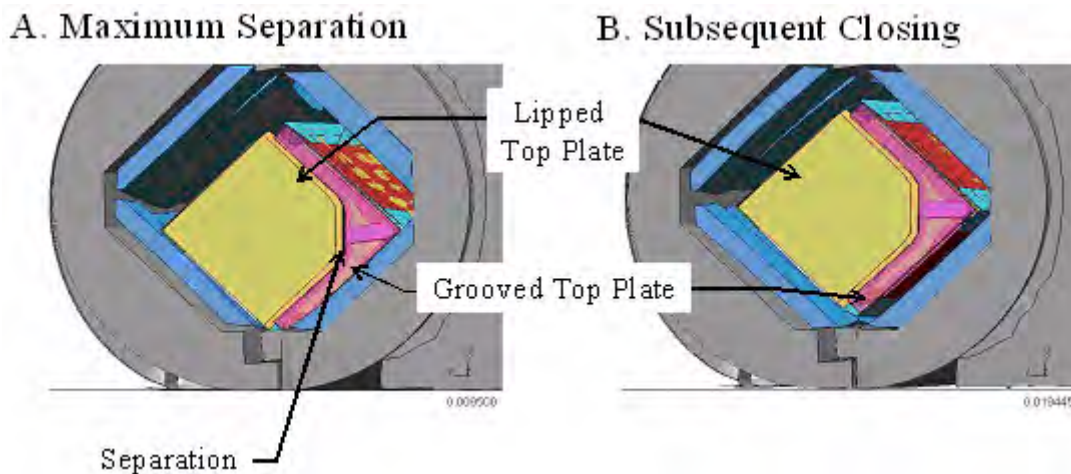


Figure 2-40 Clamshell Response during Side Drop

Clamshell Bottom End Plate/Door Joints – In keeping with the goal of minimizing the time and of loading and unloading the fuel, no bolts must be removed at the bottom end of the Clamshell during these operations. To accomplish this, the bottom Clamshell plate and doors have an interlocking feature consisting of a lip on the bottom end plate and corresponding grooves in both Clamshell doors, Figure 2-41. As described previously for the top end, these joints also do not separate to the extent that a fuel rod could slip through the opening

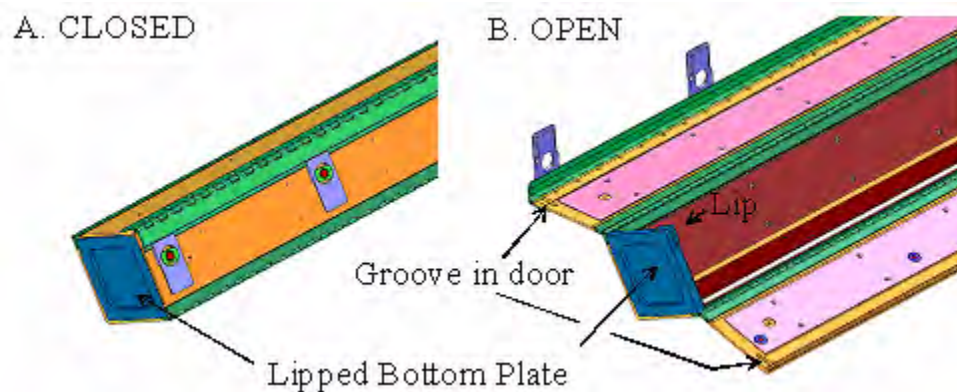


Figure 2-41 Clamshell Doors at Bottom Plate

A small separation of one of these joint during impact is predicted, Figure 2-42. Because the separation is at the upper joint is small, it is not possible that a fuel rod could slip through this joint. Furthermore, the other joint is predicted to remain closed and the bottom end plate should remain intact. These predicted results were obtained from the analysis of the Outerpack drop onto its latches. In this case, the Clamshell latches are positioned underneath the fuel, towards the ground, Figure 2-26B. As with the joint at the top Clamshell plate, the predicted separation of this joint was slightly less for a drop onto the Outerpack hinges.

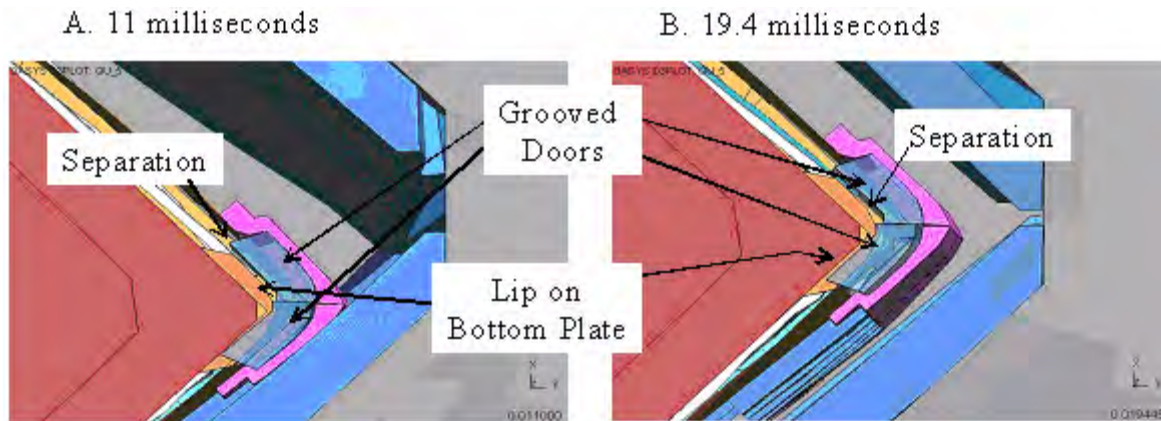


Figure 2-42 Predicted Response of Clamshell Bottom Plate and Doors During 9m Horizontal Drop onto Outerpack Latches

2.12.4.2.3 “CG-over-Corner” and “CG-forward-of-Corner” Drops onto Top Nozzle End of Package

As indicated in Figure 2-43, almost vertical orientations may result in the package center of gravity (CG) being positioned directly above the impacting corner of the package. When this occurs, the drop is designated as a “CG-over-corner” impact. In a CG-over-corner impact, the shipping package will initially continue translating in the direction of impact without rotating. However, deformation of the impacted corner may eventually result in the package tilting and falling over.



Figure 2-43 Top Nozzle Analysis Drop Orientation

CG-over-corner impacts direct all the drop energy to only a portion of the impact limiter. Thus, except for a specific feature of the Traveller XL package, a CG-over-corner impact (either onto the top or bottom end of the package) would probably be the most damaging “nearly vertical” drop. However, as subsequently shown, some drops onto the top nozzle at angles that put the CG forward of the impact corner, i.e., in the “fall” direction of Figure 2-44, are predicted to be more damaging. This is because the resulting deformation involves the Outerpack top corner bending about an (imaginary) axis between the knuckles of the first hinge and latch Figure 2-45.

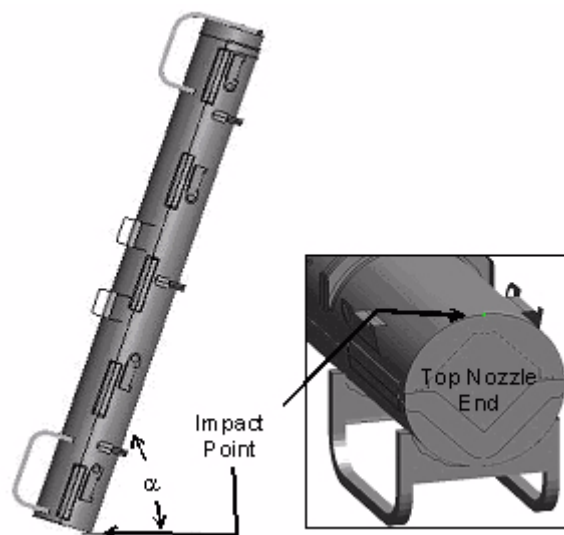


Figure 2-44 Location of Impact

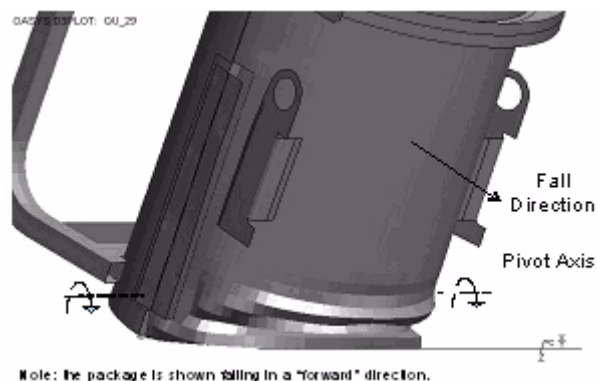


Figure 2-45 Damage to Outerpack During Angled Drop onto Top Nozzle End of Package

The most damaging drop orientation for the Outerpack is a top nozzle down, CG-forward-of-corner configuration having an 18° rotation ($\alpha=72^\circ$), see Figure 2-44. With smaller rotations, the detrimental opening of the Outerpack seam is predicted to be less despite a greater amount of energy being absorbed by the impact limiter. This is because portions of both the upper and lower Outerpack assemblies contact the drop pad and this significantly reduces their relative motion. With larger rotations, Outerpack seam opening is also predicted to be less. This is because the pivot axis moves well in front of the hinge knuckles in Figures 2-45 and 2-46.

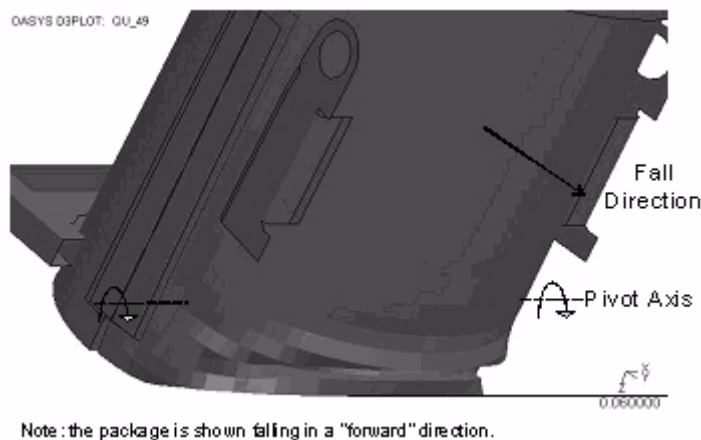


Figure 2-46 Predicted Deformation of Outerpack Top Nozzle Impact Limiter

For the subsequent 1 meter pin puncture drop, the premise is that this is the worst possible additional damage for the Outerpack seam to be further opened. Thus, the most damaging pin puncture orientation following a CG-forward-of-corner test is clearly one where the damaged face of the Outerpack is perpendicular to the pin as depicted in Figure 2-47. The combination of these scenarios; a high angle drop followed by a pin puncture in the location of the initial impact was the basis for the QTU-1 unit testing.

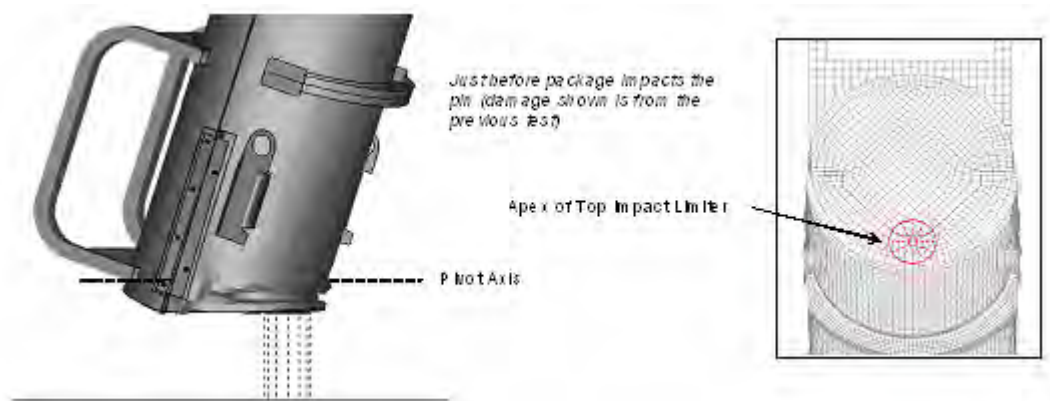


Figure 2-47 Predicted Pin Puncture Orientation after a CG-Forward-of-Corner Test

The FEA of the pin drop incorporated package deformations and stresses calculated to result from the 9m drop. The methodology for including the deformation and stresses involved defining the nodal coordinates in the pin puncture model as the deformed nodal positions of the previous analysis plus a rigid-body-rotation to locate the “model with previous damage” to the proper position/orientation for the pin puncture test. The element stresses were extracted from the first analysis and included as initial stresses in the second analysis.

Finally, from a computation standpoint, it was not practical to compute the secondary impact. This is because the secondary impact is preceded by a lengthy free-fall. Long (multi-day) computations would have been required to run an analysis through the free-fall and secondary impact. Fortunately, secondary impacts for such nearly vertical drops as this are known not to cause much additional damage. This is especially so for the Traveller XL design which will be protected by the circumferential stiffeners on the upper Outerpac. Thus, not having predictions of the secondary impact should be no limitation.

“Worst Case Drop Angle” Determination – As previously discussed, our damage criterion for the CG-forward-of-corner drops onto the top nozzle end of the package was the degree of separation between the upper and lower Outerpac assemblies. Three orientations: 11, 18, and 25° were investigated and it was determined that an angle of 18° resulted in the most separation, Figure 2-48.

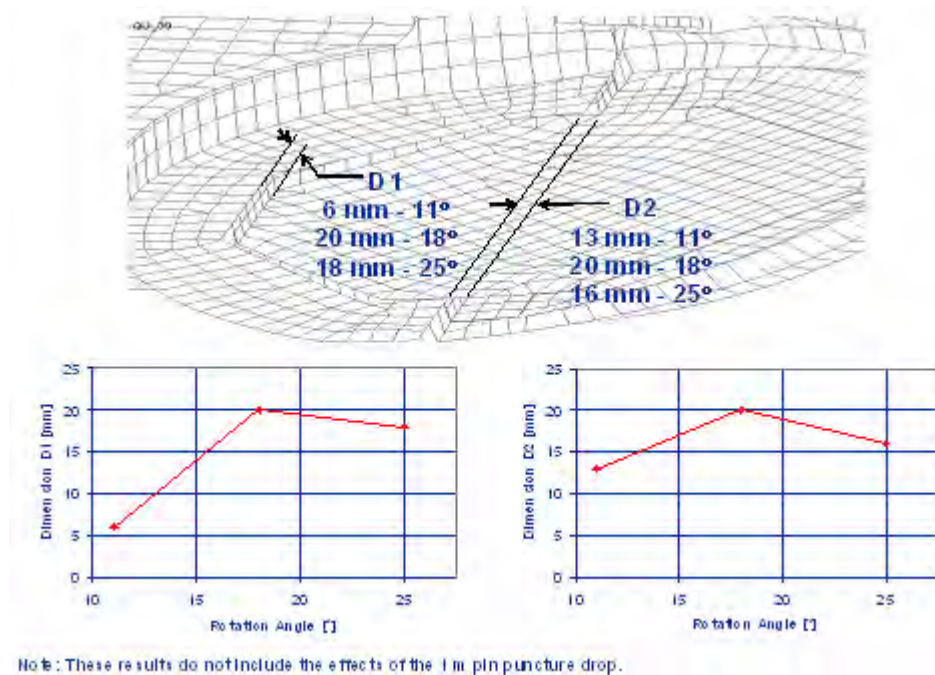


Figure 2-48 Outerpack Top Separation vs. Drop Angle

Energy and Work Histories – Predicted global energy and work histories for the primary impact of three CG-forward-of-corner drops onto the top nozzle end of the package are shown in Figure 2-49. These plots were obtained for forward rotations of 11, 18, and 25°, respectively. As before, the initial total energy (TE) of 204 kJ and increases slightly during the run in concert with the external work due to gravity. In each of these plots, the internal energy (IE) and kinetic energy (KE) traces become flat between 50-60 milliseconds into the impact event. This indicates completion of the primary impact and initiation of rollover. (Rollover and secondary impact were not numerically investigated as previously justified.) Note as drop rotation angle decreases, the internal energy absorbed by the Outerpack is predicted to increase. However, as explained earlier, this should not result in the largest Outerpack seam opening. Finally, hourglass, sliding and stonewall energies are low in each plot. This indicates overall numerically sound analyses. However, late in the analysis, hourglass energy does reach 4.1% of the total energy. While this is a low percentage, the hourglass error is concentrated in the XL pins (PID 10764) and the Clamshell cushioning pads (PIDS 2003 and 2013) in the vicinity of impact. An investigation of this error which involved using fully integrated elements found the energy previously dissipated as hourglass deformation was now (correctly) forced into the bottom impact limiter. This had only a marginal effect on the predicted force in the primary impact of Figure 2-50 and Figure 2-62. However, it did reduce predicted FA accelerations by about 17% (from the 47.3 g's shown in Figure 2-63 to 39.3 g's.). This latter effect was not significant enough to change any conclusions within the report.

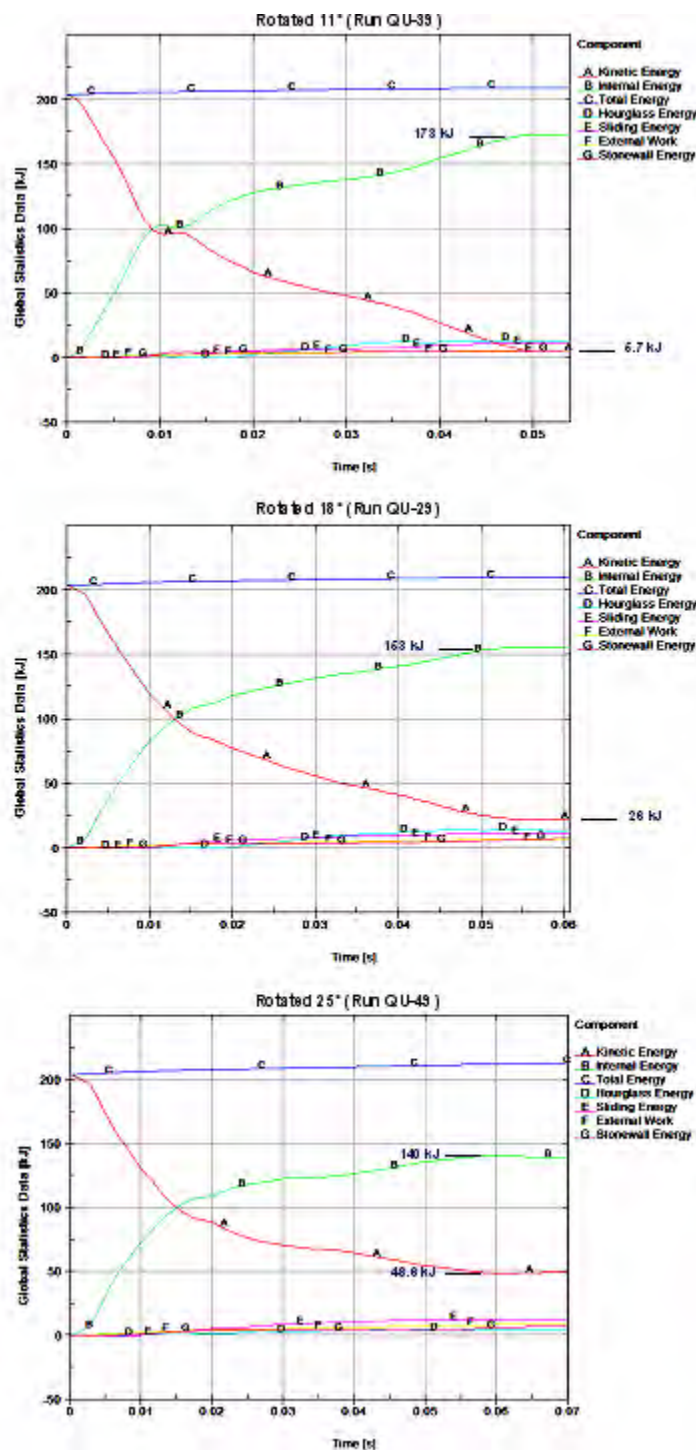


Figure 2-49 Predicted Energy and Work Histories for 9 m CG-over-Corner Drop onto the Top Nozzle End at Various Angles

Rigid Wall Forces – The predicted rigid wall force histories are shown in Figure 2-50 for CG-forward-of-corner drops on to the top end of the package rotated 11, 18, and 25°. These plots show only the primary impact (since the secondary impact due to fall-over was not calculated). The primary impact is divided into two separate events. From impact onset to approximately 25 milliseconds, the Outerpack impacts the drop pad while the Clamshell is still in free-fall. (This is due to the de-coupling between Outerpack and Clamshell previously discussed in section 2.1.1.1.1.) Secondly, the Clamshell hits the inner surfaces of the Outerpack and drives it back into the drop pad from approximately 25 milliseconds into the impact until about 70 milliseconds. Figure 2-50 shows the highest predicted loads for the Outerpack in these three orientations will be encountered at an 11° rotation. This agrees with the previous prediction that as drop rotation angle decreases, the internal energy absorbed by the Outerpack increases.

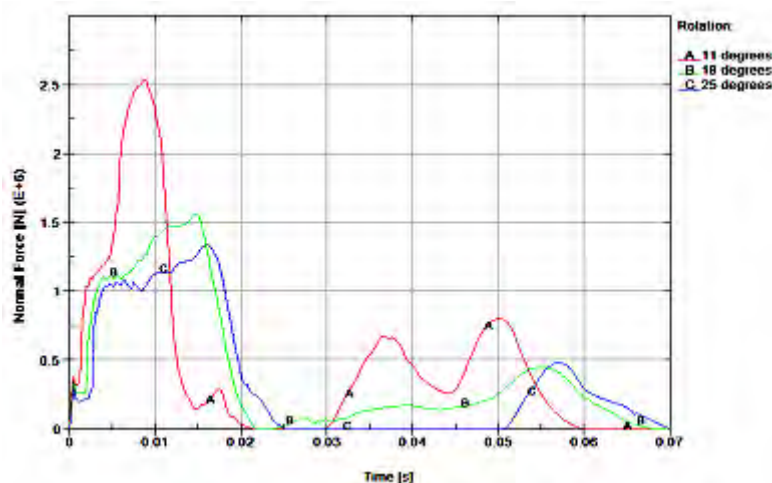


Figure 2-50 Predicted Rigid Wall Forces

As previously stated, the primary concern with CG-forward-of-corner drops onto the top nozzle end of the package is whether or not the thermal integrity needed to protect against the 30 min burn test will be compromised. It was shown that the deformation most likely to induce such damage is greatest when the Traveller XL package is rotated approx. 18° forward from a vertical orientation Figure 2-48. The main concern with the higher loads sustained and additional energy absorbed by the Outerpack at smaller rotation angles is if this jeopardized the Outerpack bolts. This issue is addressed in the following section.

Outerpack Hinge/Latch Bolts – The analysis indicates there is little likelihood of the Outerpack latch and hinge top bolts failing during a 9m CG-forward-of-corner drop onto the top end of the package. This is evident from the relatively high predicted factors of safety for these bolts, Tables 2-16 and 2-17.

Table 2-16 Top Outerpack Latch Bolt Minimum Factors of Safety for 9m CB-Forward of Corner Drops			
ID (Figure 32)	FS/Time		
	11° Forward Rotation	18° Forward Rotation	25° Forward Rotation
B917	3.80/0.0143 s	7.57/0.0102 s	5.08/0.0105 s
B921	3.94/0.014 s	6.89/0.0247 s	6.19/0.0102 s
B923	3.10/0.0225 s	2.63/0.0245 s	3.87/0.0245 s
B927	3.28/0.0227 s	2.70/0.0247 s	4.04/0.0262 s
B929	2.61/0.012 s	2.29/0.0112 s	2.36/0.0147 s
B933	2.45/0.0065 s	2.25/0.0112 s	2.38/0.0147 s
B935	2.22/0.0117 s	2.22/0.0072 s	2.22/0.008 s
B939	2.22/0.0117 s	2.22/0.0072 s	2.22/0.0075 s
B941	2.23/0.0032 s	2.23/0.0052 s	2.23/0.0057 s
B945	2.22/0.0057 s	2.23/0.0077 s	2.23/0.0097 s

Table 2-17 Top Outerpack Hinge Bolt Minimum Factors of Safety for 9m CB Forward of Corner Drops			
ID (Figure 33)	FS/Time		
	11° Forward Rotation	18° Forward Rotation	25° Forward Rotation
B947	3.59/0.014 s	6.37/0.0337 s	5.13/0.0105 s
B951	3.73/0.014 s	7.49/0.0232 s	6.17/0.0135 s
B953	2.95/0.0225 s	3.04/0.0245 s	4.19/0.0322 s
B957	3.19/0.0225 s	3.26/0.0245 s	4.30/0.0322 s
B959	2.65/0.0065 s	2.32/0.0115 s	2.34/0.0147 s
B963	2.51/0.0065 s	2.27/0.011 s	2.40/0.0122 s
B965	2.21/0.0062 s	2.21/0.0243 s	2.21/0.0077 s
B969	2.22/0.006 s	2.21/0.0235 s	2.23/0.0072 s
B971	2.20/0.006 s	2.20/0.0095 s	2.20/0.0110 s
B975	2.22/0.0055 s	2.23/0.0072 s	2.23/0.0077 s

It should also be noted that the latch and hinge bolts nearest impact were predicted to have the smallest (although still very adequate) safety factors. This is logical.

Clamshell Keeper Bolts – Our analysis indicates there is little likelihood of the Clamshell keeper bolts failing during a 9m CG-forward-of-corner drop onto the top nozzle end of the package. This is evident from the relatively high predicted factors of safety for these bolts, Table 2-18.

Table 2-18 Clamshell Keeper Bolt Minimum Factors of Safety for 9m CG-Forward-of-Corner Drops			
ID (Figure 35)	FS/Time		
	11° Forward Rotation	18° Forward Rotation	25° Forward Rotation
B6271277	5.86/0.0255 s	8.71/0.038 s	10.86/0.0237 s
B6271278	5.75/0.027 s	4.79/0.0285 s	4.43/0.0277 s
B6271279	22.6/0.029 s	8.46/0.0287 s	6.63/0.0237 s
B6271280	17.4/0.0258 s	10.89/0.026 s	3.29/0.0225 s
B6271281	13.38/0.023 s	12.31/0.0522 s	7.96/0.024 s
B6271282	19.48/0.0455 s	8.13/0.0375 s	8.85/0.0282 s
B6271283	16.85/0.0207 s	5.41/0.0332 s	5.78/0.0258 s
B6271284	33.54/0.0285 s	8.89/0.0392 s	7.3/0.0252 s
B6271285	17.56/0.0405 s	11.32/0.0132 s	11.69/0.0197 s
B6271286	14.73/0.016 s	9.67/0.0415 s	8.09/0.024 s

It should be noted that the keeper bolt nearest impact was predicted to have the smallest (although still very adequate) safety factor.

Clamshell Top and Bottom Plate Bolts – The analyses indicate that none of the Clamshell bolts at the top and bottom ends will fail during a 9m CG-forward-of-corner drop onto the top nozzle end of the package. This is evident from the minimum factors of safety shown in Tables 2-19, 2-20 and 2-21. (The modeling of the fuel assembly as a rigid structure likely makes little difference to these predictions since the fuel rods would not be expected to buckle in this drop orientation.)

Table 2-19 Clamshell Bottom Plate bolt Minimum Factors of Safety for 9m CG-Forward-of-Corner Drops			
ID (Figure 37)	FS/Time		
	11° Forward Rotation	18° Forward Rotation	25° Forward Rotation
B6168785	2.36/0.0495 s	2.38/0.0245 s	2.50/0.0197 s
B6168786	8.27/0.0497 s	5.85/0.0243 s	4.48/0.0235 s
B6168787	100.3/0.0262 s	94.5/0.0225 s	60.8/0.0235 s
B6168788	97.8/0.0262 s	112/0.0515 s	89.5/0.0235 s
B6168789	51.1/0.0227 s	27.0/0.0230 s	43.3/0.0437 s
B6168794	40.2/0.0222 s	31.0/0.0317 s	27.7/0.0317 s
B6168793	99.9/0.0262 s	83.3/0.0305 s	59.3/0.0385 s
B6168792	100.7/0.0618 s	86.7/0.0202 s	44.2/0.0402 s
B6168791	11.2/0.0412 s	6.55/0.0202 s	7.69/0.0200 s
B6168790	2.84/0.0412 s	2.43/0.0205 s	2.33/0.0280 s

Table 2-20 Clamshell Grooved Top Plate Bolt Minimum Factors of Safety for 9m CG-Forward-of-Corner Drops			
ID (Figure 38)	FS/Time		
	11° Forward Rotation	18° Forward Rotation	25° Forward Rotation
B6168781	2.33/0.0182 s	2.29/0.0187 s	2.31/0.0197 s
B6168780	3.86/0.0397 s	5.32/0.0200 s	4.32/0.0200 s
B6168779	2.84/0.049 s	6.08/0.0510 s	12.06/0.0217 s
B6168778	2.31/0.039 s	2.34/0.0447 s	2.37/0.0470 s
B6168773	2.25/0.0367 s	2.26/0.0430 s	2.26/0.0410 s
B6168774	2.23/0.0367 s	2.22/0.0427 s	2.22/0.0410 s
B6168775	2.31/0.0387 s	2.30/0.0435 s	2.32/0.0467 s
B6168776	2.91/0.0485 s	5.39/0.0555 s	9.58/0.0465 s
B6168777	7.04/0.0495 s	6.20/0.0467 s	4.84/0.0205 s

Table 2-21 Clamshell Lipped Top Plate Bolt Minimum Factors of Safety for 9m CG-Forward-of-Corner Drops			
ID (Figure 38)	FS/Time		
	11° Forward Rotation	18° Forward Rotation	25° Forward Rotation
B6168770	1.76/0.0165 s	1.81/0.0180 s	1.77/0.0195 s
B6168771	1.79/0.0207 s	1.77/0.0177 s	1.75/0.0197 s
B6168772	1.78/0.0360 s	1.76/0.0477 s	1.80/0.0117 s
B6168765	1.76/0.0350 s	1.76/0.0170 s	1.73/0.0135 s
B6168766	1.77/0.0125 s	1.77/0.0150 s	1.72/0.0125 s
B6168767	1.78/0.0200 s	1.75/0.0150 s	1.72/0.0127 s
B6168768	1.77/0.0362 s	1.76/0.0152 s	1.76/0.0277 s
B6168762	1.76/0.0362 s	1.77/0.0510 s	1.76/0.0187 s
B6168783	1.77/0.0192 s	1.77/0.0155 s	1.77/0.0202 s

Clamshell Top End Plate Joint – The analyses indicate the Clamshell top end plate joint (Figure 2-39) will separate slightly, but not come completely apart during CG-forward-of-corner impacts. In particular, the lip on the top plate is predicted to remain within the groove in the V-shaped top plate along both edges but slip completely out in the middle. This is shown in Figure 2-51 for the CG-forward-of-corner drop rotated 11°. It should be noted that this separation is predicted to be permanent, not transient. It should also be noted that predicted deformations were similar but lesser for CG-forward-of-corner drops rotated 18° and 25°. However, in these latter two orientations, the lip on the top plate is predicted to remain within the groove in the V-shaped top plate along its entire length. **This extent of deformation was not observed in full-scale testing of Traveller XL prototypes and is therefore conservative.**

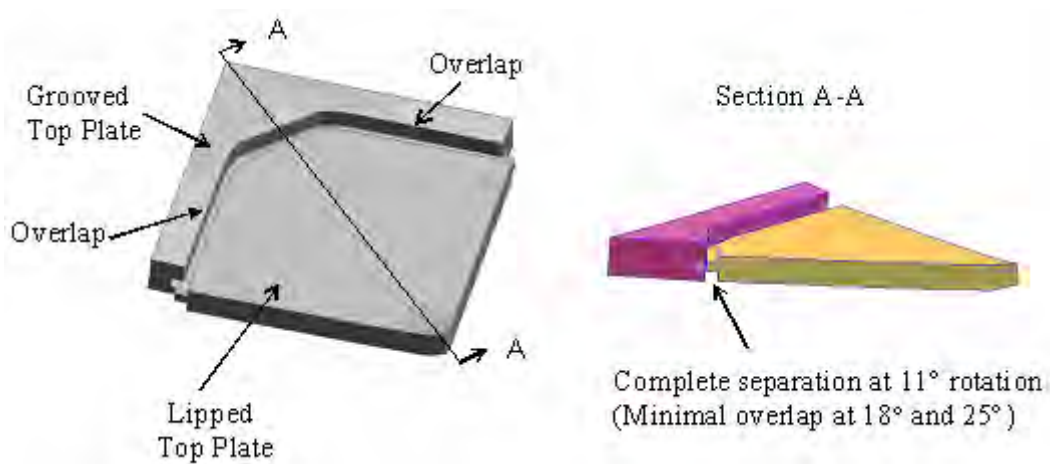


Figure 2-51 Clamshell Top Plate Geometry

Clamshell Bottom End Plate/Door Joints – The analyses indicated the Clamshell bottom end plate is minimally loaded during CG-forward-of-corner drops onto the top end of the shipping package. These trivial loads are not reported herein.

In summary, horizontal side drops onto the Outerpack hinges/latches result in the highest predicted Outerpack loads. Even so, a CG-forward-of-corner drop onto the top nozzle end of the package with 18° forward rotation, Figure 2-48 is predicted most damaging to the Outerpack. This is because the predicted opening of the seam between the upper and lower Outerpack assemblies may compromise the ability of the Traveller XL shipping package to withstand the 30 minute HAC burn test. Drop tests are described in Appendix 2.12.5 and the fire tests are described in Section 3, all of which demonstrate that this is not a serious concern.

2.12.4.2.4 Orientation Predicted Most Damaging to the Fuel Assembly

Determining the drop orientation most damaging to a fuel assembly is greatly facilitated by the geometry of the assembly itself. In particular, the fuel rods within a fuel assembly are very long (4.4 m or more), slender (approx. 9 mm), and relatively flexible. Thus, they are quite susceptible to buckling. For this reason, our hypothesis is that drop orientations which impart the highest axial loads to the assembly are most damaging. Buckling of the fuel rods is also of paramount importance with respect to criticality safety. For criticality safety, fuel rods must not be allowed to buckle in a configuration which results in an unsafe nuclear condition. See Section 6 for a complete description of the criticality safety of the Traveller packages.

Obviously, highest axial loads are generated by vertical or nearly vertical loadings. Near-vertical orientations may impart higher loads to a portion of the fuel rods than the average load applied to a fuel rod in truly vertical drops. However, in these orientations, the adjacent rods or Clamshell structure will provide lateral support. Thus, our focus was entirely on (truly) vertical drops for fuel assembly damage, Figure 2-52. Vertical orientations result in higher impact loads because the larger footprint impacts the ground and therefore the system is stiffer than a high angle orientation where the initial contact is a point which “grows” a footprint.

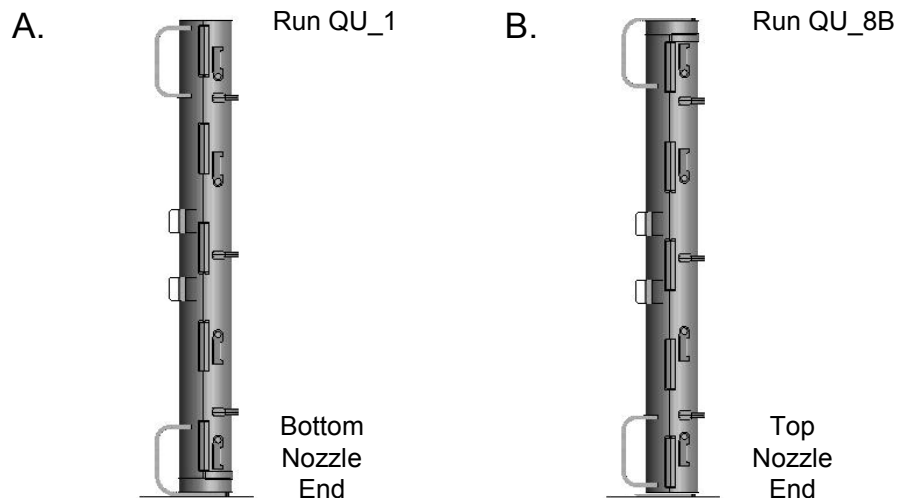


Figure 2-52 Traveller Drop Orientations Analyzed For Maximum Fuel Assembly Damage

The tendency of the fuel rods to buckle proved a severe modeling limitation because post-buckling behavior was simply beyond our current modeling capability. Post-buckling involves one or more buckled fuel rods impacting a nearby rod or Clamshell wall. These collisions involved a large momentum transfer because the fuel rods are so heavy. In our model, the mesh of the walls and nearby rods was simply not capable of properly absorbing this energy. The result was the analysis aborted almost immediately once any fuel rods buckled. This was due to “negative volumes” (highly distorted solid elements) which resulted from the inability of the Clamshell walls, as meshed, to properly absorb the momentum transferred from the fuel rods. This occurred in all analyses we attempted and often with as much as 30 percent of the drop energy not yet absorbed. The mesh of the surrounding structure was simply not capable of properly absorbing this energy. Successful resolution of this problem would have required significantly finer meshes of both the fuel rods and surrounding structure and perhaps many other changes. From a practical standpoint, this level of analysis is beyond the capabilities of current computer systems. Rather, the fuel rods and associated fuel assembly structure (i.e., the grids), except for the top and bottom nozzles, were converted into a rigid part using the LS-DYNA[®] deformable-to-rigid option. This prevented the fuel rods from buckling and eliminated the associated problems with negative volumes allowing an analysis that absorbed all the available energy.

This approach prevented any associated loading of the structure surrounding the sides of the fuel assembly (the Clamshell walls), forfeiting the ability to predict the maximum loads and stresses on the Clamshell walls and latches in regions adjacent to the fuel rods. Since the fuel nozzles and other structures near the Clamshell top and bottom ends were kept deformable, Clamshell loads and stresses at the ends of the Clamshell were still fairly accurate. Further, the energy not transferred to the Clamshell walls was now forced into other structures – primarily the fuel assembly nozzles (which were kept deformable) and the end impact limiters in the case of axial drops. Thus, our analyses should be non-conservative for Clamshell regions adjacent to the fuel rods, accurate for the Clamshell top and bottom ends, and probably overly conservative for the displacements in the Outerpack impact limiters.

2.12.4.2.5 Vertical Drops

Our analysis determined that a vertical drop onto the bottom end of the package would be more damaging to the fuel assembly than a drop onto the top end. This is because the Clamshell is subjected to larger impact forces and the fuel assembly must withstand larger accelerations.

Energy and Work Histories – Global energy and work for vertical drops onto the top and bottom end of the package are shown in Figures 2-53 and 2-54, respectively. As before, both plots have an initial total energy (TE) of 204 kJ. The total energy rises slightly, reflecting the external work done by the package under gravity loading. Hourglass, sliding, and stonewall energies were small relative to the total energy. This indicates a good overall numerical analysis was obtained in both simulations.

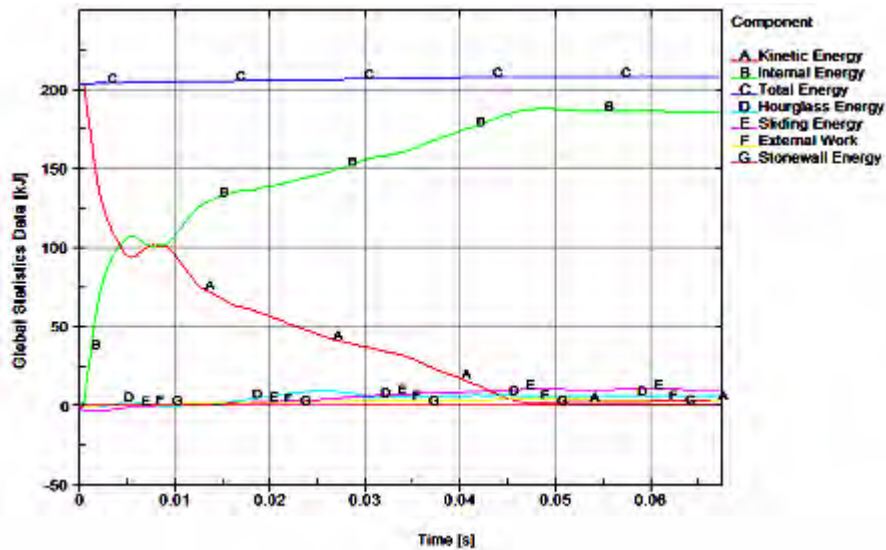


Figure 2-53 Predicted Energy and Work Histories for a 9m Vertical Drop Onto the Top Nozzle End of the Package

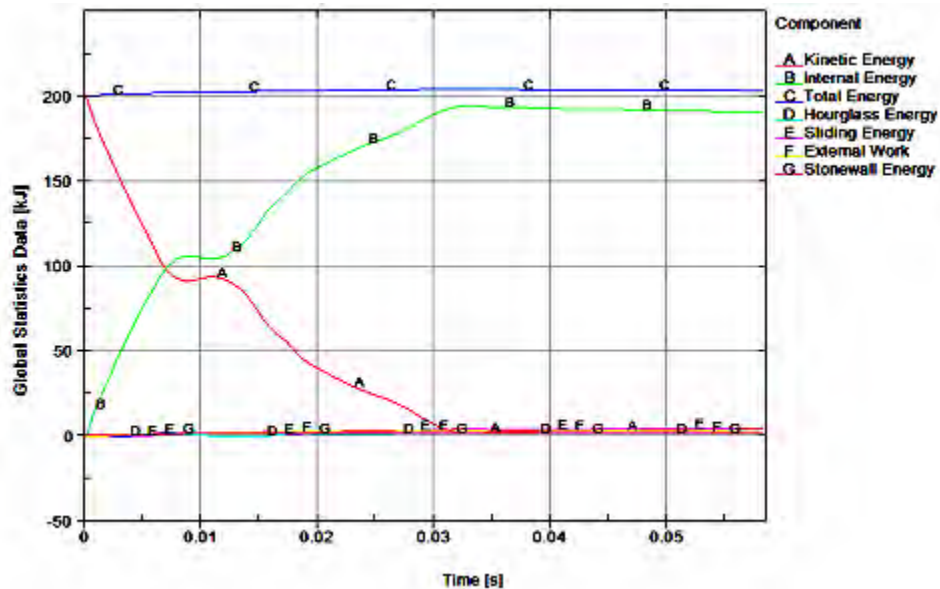


Figure 2-54 Predicted Energy and Work Histories for a 9m Vertical Drop Onto the Bottom Nozzle End of the Package

Rigid Wall Forces – Predicted force histories between the Outerpack and drop pad are shown in Figure 2–49 for top and bottom end vertical drops. The near de-coupling of the Clamshell and Outerpack is clearly evident in both simulations. In the drop onto the bottom end of the package, the initial impact between

Outerpack and drop pad has a 12 milliseconds (approx.) duration. The Clamshell is not involved in this impact as it is still in free-fall (neglecting the small forces of the shock mounts.) At approximately 15 milliseconds into the simulation, the Clamshell contacts the inner surface of the bottom impact limiter and pushes it back into the drop pad. The Clamshell and Outerpack impact further into the drop pad while the fuel assembly is now essentially decoupled from the Clamshell and still in free-fall. As the Outerpack and Clamshell begin to re-bound (at ~25 milliseconds into the simulation) the fuel assembly impacts the Clamshell and all three components (Outerpack, Clamshell and fuel assembly) crash back into the drop pad. The shipping package begins to rebound at approximately 31 milliseconds into the simulation and has left the drop pad after 45 milliseconds. A similar scenario is evident for the vertical drop onto the top nozzle end of the package.

Referring to Figure 2-55, it is noted that the predicted maximum Outerpack load for the top end drop is more than 2X that for the bottom end drop (5.1 versus 2.5 MN, respectively). This shows the higher cushioning capability of the bottom impact limiter design. Further, this indicates that bolts in the Outerpack hinges and latches in the vicinity of impact will be loaded more significantly in a vertical drop onto the top end of the package. Finally, the predicted 5.1 MN load on the Outerpack for a vertical top end drop is still 2-3X less than that predicted for horizontal side drops, Figure 2-29.

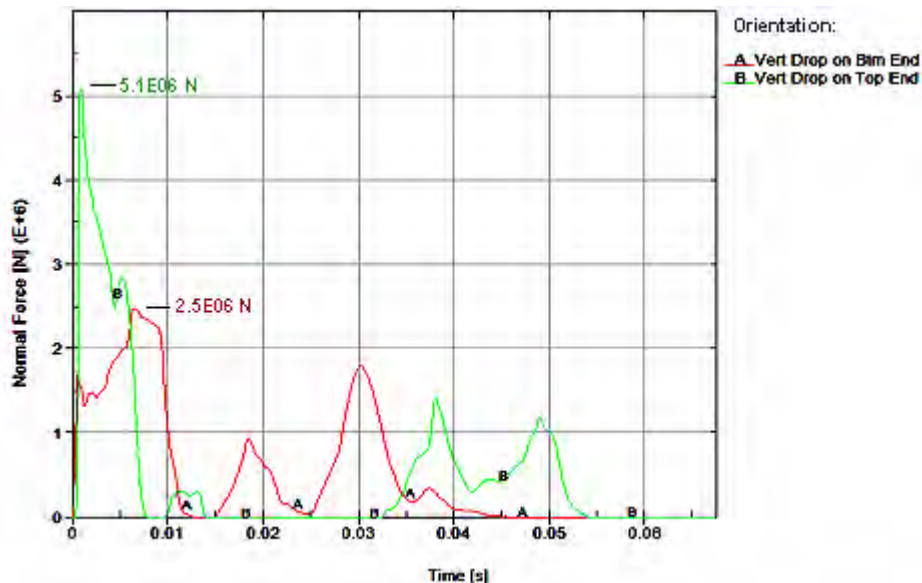


Figure 2-55 Predicted Rigid Wall Histories for 9m Vertical Drops onto the Bottom (QU-1) and Top (QU-8B) Ends of the Package

Clamshell Loads and Accelerations – The force between Clamshell and impact limiter was determined for vertical drops by specifying contacts between the CS top and bottom plates and the innermost impact limiter covers. For drops onto the top end of the package, this required defining contacts between the two CS top plates (the grooved and the lipped plate) and the innermost plate of the top impact limiter and summing

the predicted forces. This technique was only used for vertical drops because these are the only drop orientations in which the Clamshell impacts into only one surface.

Results are shown in Figure 2-56 (for the primary impact only as previously explained.) Note that the force is zero until almost 9 milliseconds into the drop simulation (which starts right before the Outerpack hits the drop pad. This is the time it takes the Clamshell to fall through the approximate 120 mm sway space separating the Clamshell and inner and the top and bottom impact limiters.

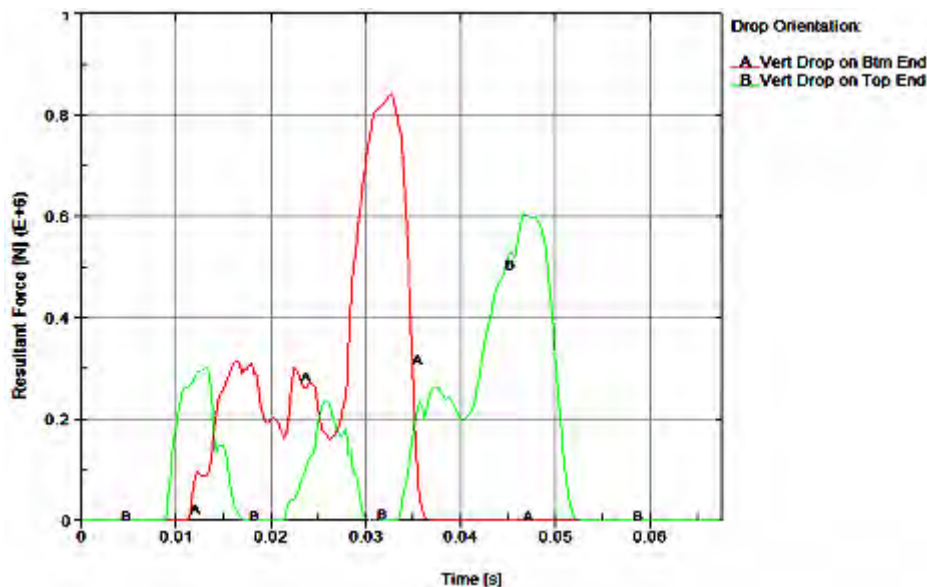


Figure 2-56 Predicted Force Between Clamshell and Impact Limiter for 9m Vertical Drops

Note also in Figure 2-56 that drops onto the bottom end of the package are more severe for the Clamshell than those onto the top end. Indeed, predicted CS loads for vertical drops onto the top and bottom end of the package are, respectively, 605 and 843 kN. These loads resulted in higher accelerations for the fuel assembly (FA) as well. As shown in Figure 2-57, predicted FA accelerations are 102 and 126 g's, respectively, for drops onto the bottom and top ends of the package.

The predicted sequence for a drop onto the bottom nozzle end of the package is shown in Figure 2-58. Impact between the Clamshell and inside covering of the bottom impact limiter occurs at approximately 13 milliseconds into the simulation; the maximum load between CS and bottom impact limiter is predicted to occur at approx. 33 milliseconds; and, the Clamshell is in full rebound by 40 milliseconds. Note the predicted crushing of the bottom nozzle legs shown in Figure 2-58.

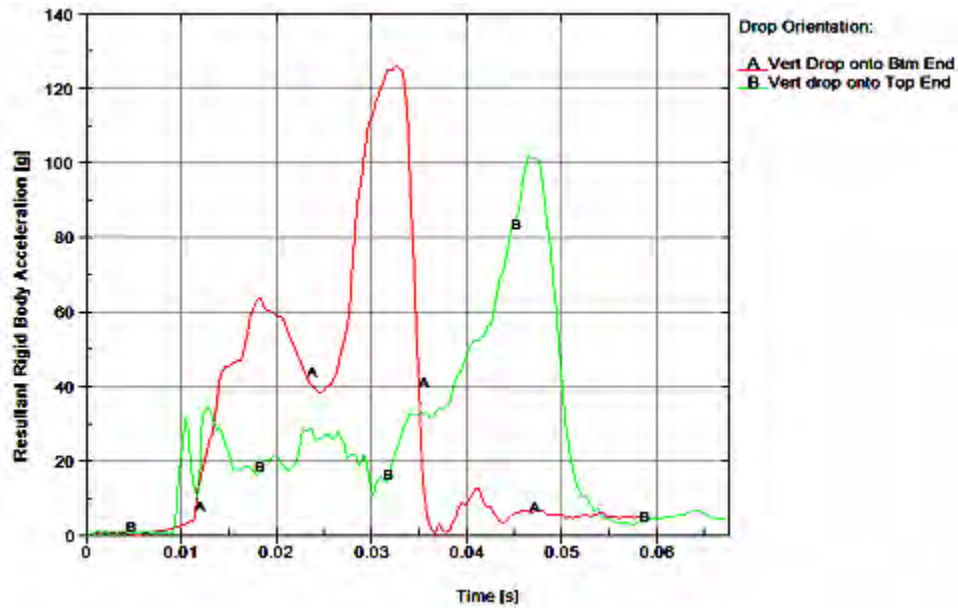


Figure 2-57 Predicted Fuel Assembly Accelerations for 9m Vertical Drops

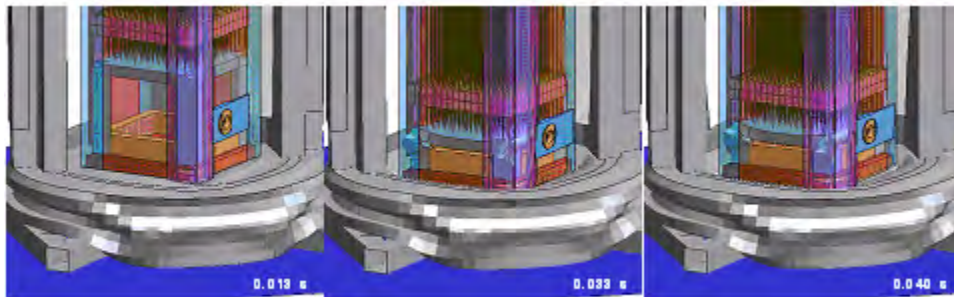


Figure 2-58 Impact Between Clamshell and Bottom Impact Limiter for Vertical Drop onto Bottom End of Package

It is interesting to note the Clamshell and top impact limiter are predicted to collide three times during the primary impact of top end drops. These impacts are depicted in Figures 2-59, 2-60 and 2-61. As shown in Figure 2-59, the first impact involves the Clamshell hitting the top impact limiter from free-fall (at ~9 milliseconds) and the XL pins and top nozzle hold-down posts buckling under the load of the fuel assembly until the top nozzle slides off the hold-down posts (at ~17 milliseconds.) The Clamshell now begins to rebound and leaves the top impact limiter. However, as shown in Figure 2-60, the fuel assembly

continues its downward motion and the top nozzle contacts the midsection of the hold-down posts at about 21.5 milliseconds. At approximately 30.5 milliseconds, Figure 2-60, the hold-down posts are predicted to break near their connection to the cross member connecting them. Then, the fuel assembly pushes the Clamshell back into the top impact limiter. This momentarily removes the fuel assembly loading from the Clamshell and it no longer is pushed into the Outerpack. However, the FA continues falling and the top nozzle begins pushing into the cross member at approximately 33.5 milliseconds. The FA continues its downward fall until motion is arrested at approximately 53 milliseconds, Figure 2-61.

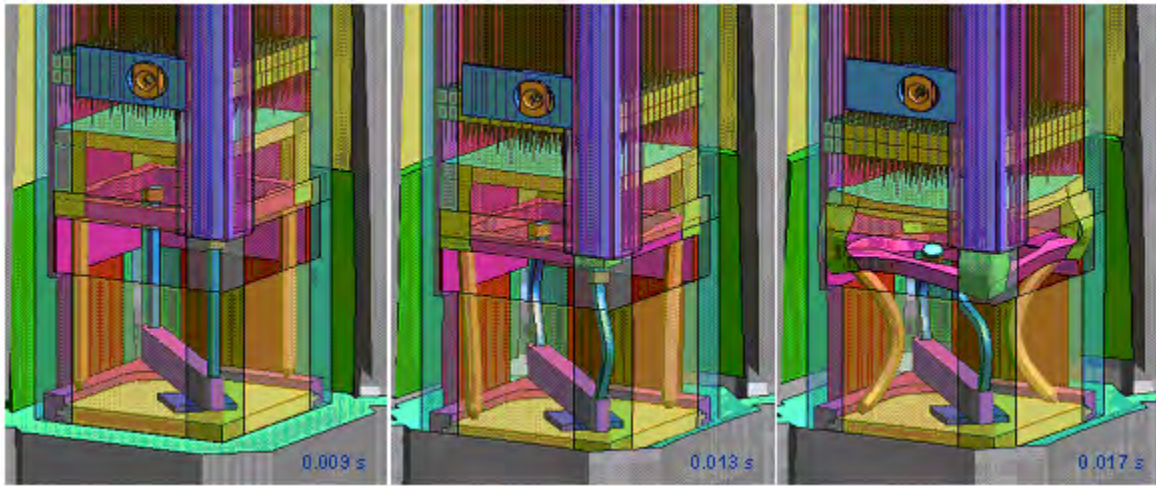


Figure 2-59 First Impact Between Clamshell and Top Impact Limiter for Vertical Drop onto Top End of Package

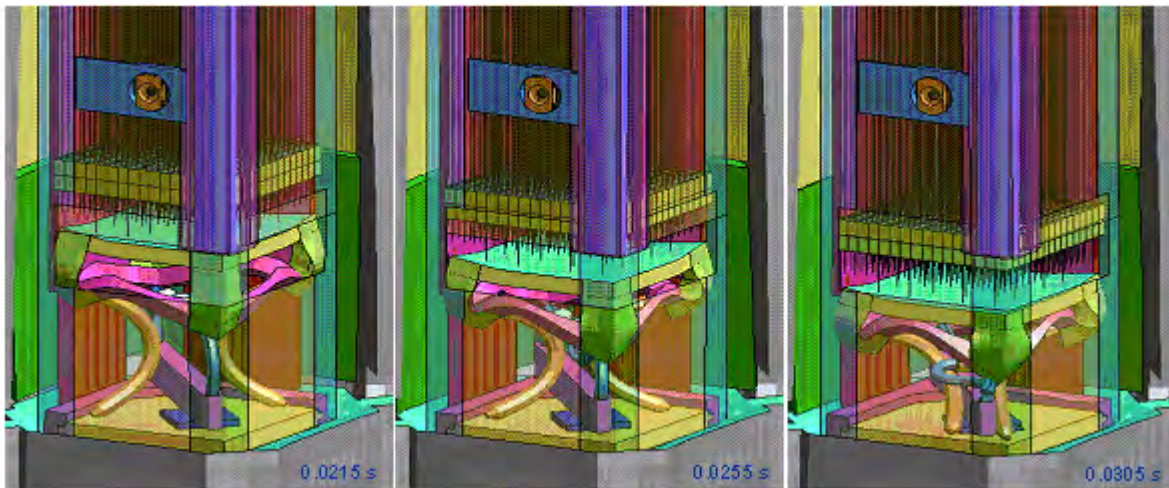


Figure 2-60 Second Impact Between Clamshell and Top Impact Limiter for Vertical Drop onto Top End of Package

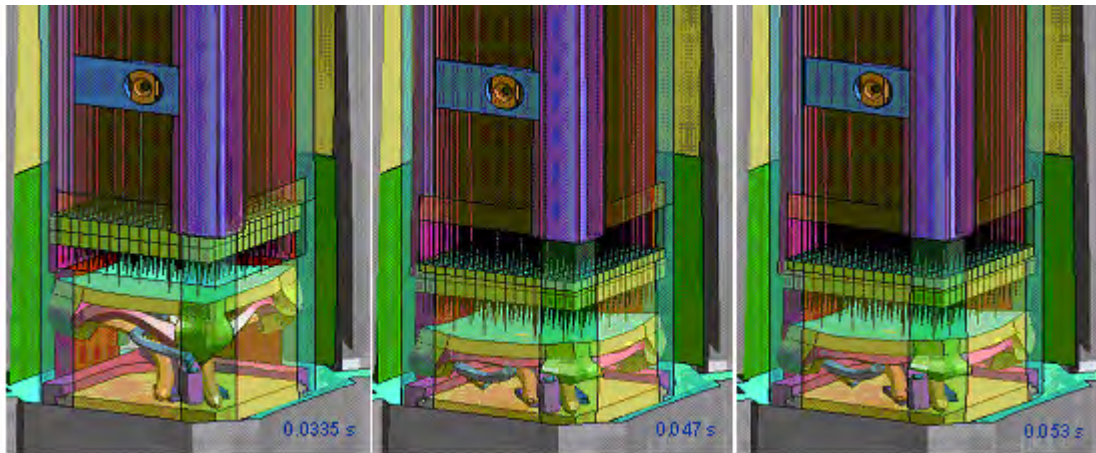


Figure 2-61 Third Impact Between Clamshell and Top Impact Limiter for Vertical Drop onto Top End of Package

From the results shown in this section, we conclude that a CG-forward-of-corner drop onto the top nozzle end of the package with an 18° forward rotation, Figures 2-44 and 2-45 is most damaging to the Outerpack. Further, as also shown, we conclude that the drop most damaging to a fuel assembly is a vertical one onto the bottom nozzle end of the package, Figure 2-52A. Thus, successful drop tests in these two orientations are an adequate demonstration that the Traveller XL design meets/exceeds the HAC drop test requirements.

2.12.4.2.6 Temperature and Foam Density Effects

The Traveller XL package must be capable of passing the HAC drop tests at any temperature within the range -40 to 160°F. Furthermore, foam crush strength is also directly related to foam density. The drop orientation previously determined most damaging to the Outerpack was selected to study the effect of temperature and density (the 9 meter CG-forward-of-corner drops onto the TN end of package with an 18° forward rotation, Figure 2-44). Our finding is that a Traveller XL package with nominal foam density and at “normal temperature” (75°F) experiences slightly higher Outerpack loads when dropped in this orientation compared with packages containing low density foam and dropped at 160°F or containing high density foam and dropped at -40°F, see Figure 2-62. In particular, the predicted maximum Outerpack load for the 75°F temperature/nominal density scenario is 1.69 MN. This is 8.5% more than the maximum load predicted for the -40°F/high density scenario and 13.7% more than that for the 160°F/low density scenario. Our analyses also indicates fuel assemblies in packages containing the highest allowable density foam and dropped at the lowest temperature extreme will experience accelerations that are very similar to those in packages with lowest allowable density foam and dropped at the highest temperature extreme, see Figure 2-63. However, the accelerations at these extremes are only 5% greater than for a package dropped at 75°F containing nominal density foam. Thus, temperature and foam density have a minor effect on drop performance of the Traveller XL package.

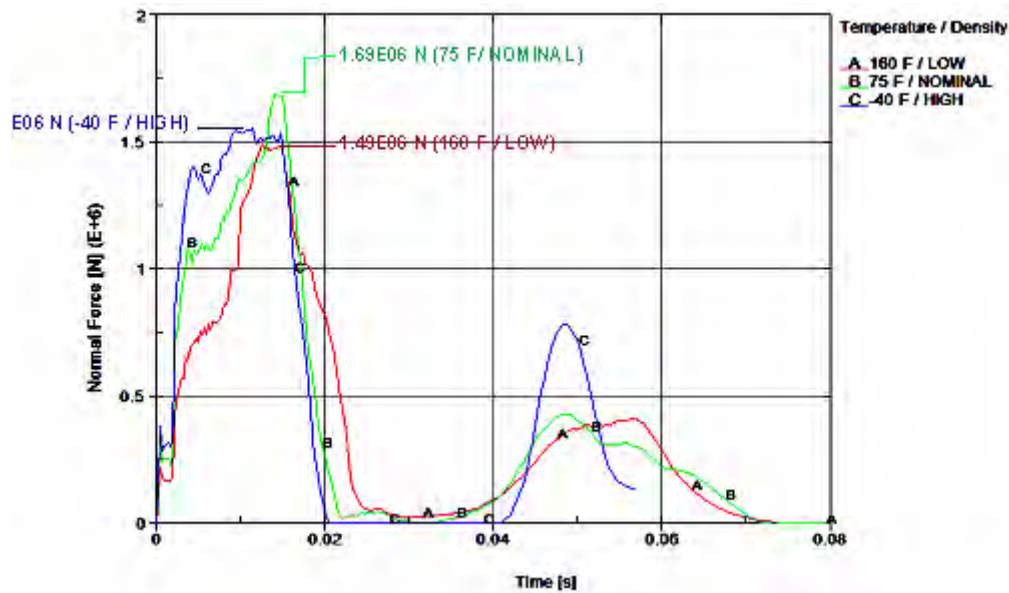


Figure 2-62 Predicted Temperature and Foam Density Effect on Outerpack/Drop Pad Interface Forces (9m CG-Forward-of-Corner with 18° Rotation Drop onto the Top End of the Package)

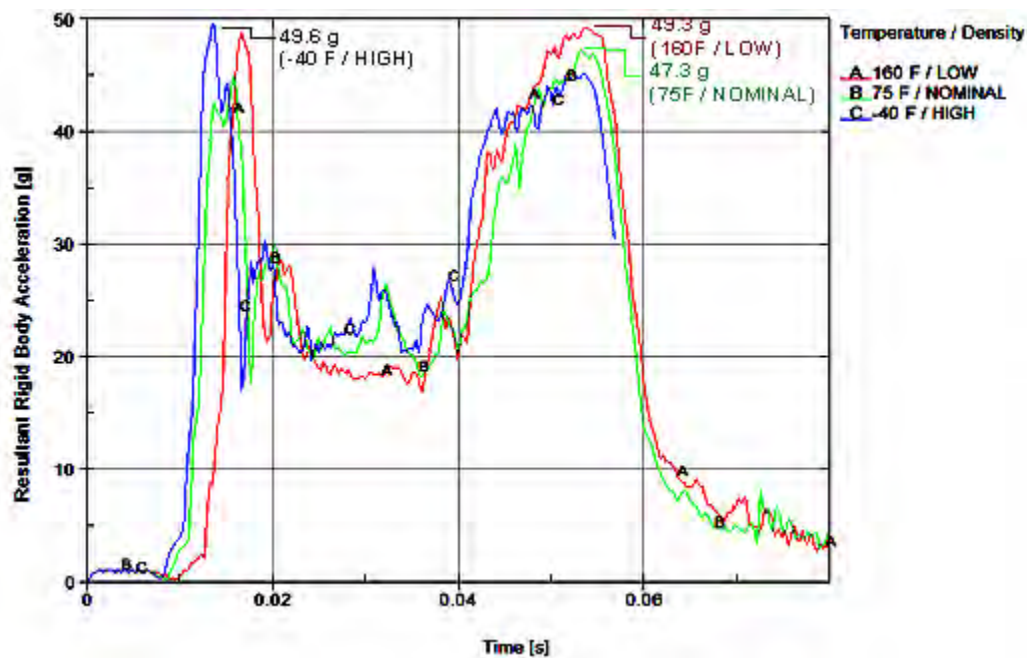


Figure 2-63 Predicted Temperature and Foam Density Effect on Outerpack/Drop Pad Accelerations (9m CG-Forward-of-Corner with 18° Rotation Drop onto the Top End of the Package)

In addition, the 9 meter vertical bottom-end down drop was analyzed using material properties for -40°C (-40°F) with foam density at the upper end of the tolerance band and 71°C (160°F) with foam density at the lower end of the tolerance band. The predicted results were compared with each other and with those at 24°C (75°F) and nominal foam density previously reported in Section 2.12.3.2.5. The results support the conclusions obtained from analysis of the 9 meter CG-forward-of-corner drops: temperature and variation in foam density due to manufacturing tolerances have only a minor effect on the drop performance of the Traveller package.

Temperature/foam tolerance effects for the 9 meter vertical drop onto the bottom nozzle end of the package were evaluated for the three previously noted conditions. Both predicted outerpack/drop pad force histories and fuel assembly accelerations were compared as shown in Figures 2-63A and 2-63B.

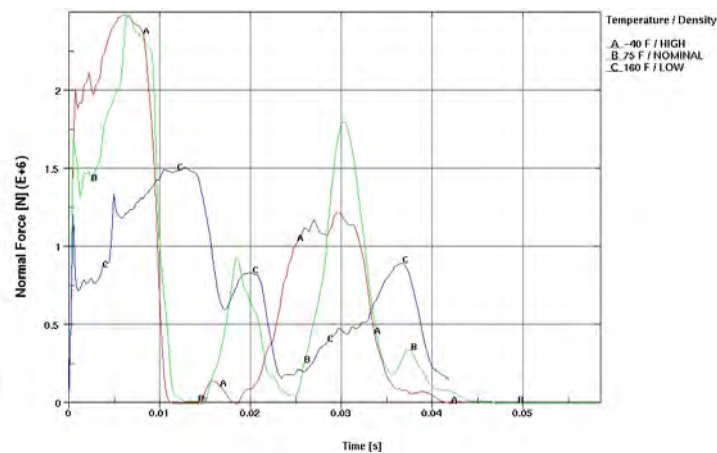


Figure 2-63A Predicted Temperature and Foam Density Effect on Outerpack/Drop Pad Interface Forces (9m Vertical Drop onto the Bottom End of the Package)

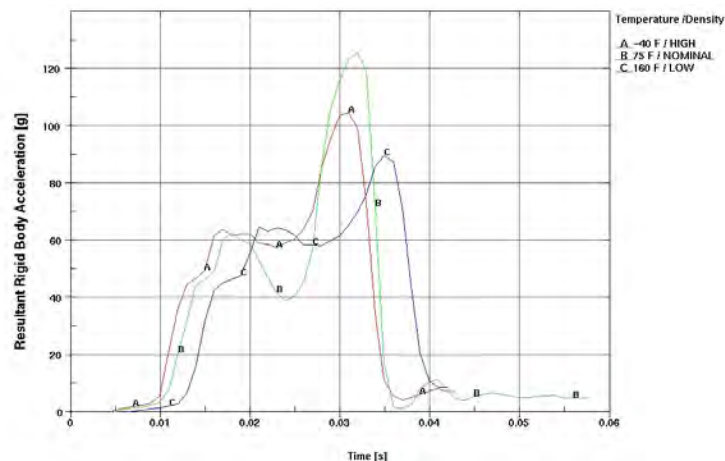


Figure 2-63B Predicted Temperature and Foam Density Effect on Fuel Assembly Acceleration (9m Vertical Drop onto the Bottom End of the Package)

Both of these figures predict that the highest forces occur when the package is 24°C (75°F) with the package having nominal foam density. (This does not necessarily mean that a package dropped at 24°C/75°F having foam densities at either the high or low end of the tolerance band would have had lower outerpack/drop pad forces and lower FA accelerations since that was not investigated.) In particular, the predicted maximum outerpack load for the 75°F (24°C)/nominal foam density scenario was 2.5E6 N. This was equal to that predicted for -40°C (-40°F) with foam density at the upper end of the tolerance band and about 67% greater than the 1.5E6 N load predicted for 71°C (160°F) with foam density at the lower end of the tolerance band. Moreover, a maximum FA acceleration of 126 g's was predicted for drops at 24°C (75°F) with the package having nominal foam density. This was approximately 20% higher than the 105 g's predicted for the -40°C (-40°F) with foam density at the upper end of the tolerance band scenario and approximately 40% higher than the 90.1 g's predicted for 71°C (160°F) with foam density at the lower end of the tolerance band case.

Energy and Work Histories – The predicted global energy and work histories for the package at 75°F containing nominal density foam was previously shown in Figure 2-29 (18° rotation.) This information is repeated in Figure 2-64 along with the corresponding results for a package dropped at 160°F with low density foam and at -40°F and high density foam. Although not discernable from these graphs, the initial total energies were slightly different for the three runs. In particular, the initial energy for the 160°F/low foam density run was 202 kJ, 204 kJ for the 75°F/nominal foam density run, and 205 kJ for the -40°F/high foam density run. These slight differences were obviously a result of the slight differences in predicted weight. Hourglass, sliding, and stonewall energies were small relative to the total energy. This indicates good overall numerical analyses.

2.12.4.2.7 Pin Puncture

In addition to the 9m drops, the package must survive a “pin puncture” test. The pin puncture test involves dropping the shipping package onto a flat-headed (15 cm diameter with 6 mm chamfer all around) steel pin from a 1 m height. The orientation of the package and location of pin impact must be chosen to achieve the greatest damage to the package.

The pin damage investigation consisted of two approaches. First, the pin drop was analyzed, based on maximum impact forces imparted to the Outerpack. Then, the cumulative damage that a pin drop could cause following a 9 m drop was studied. The latter study was naturally based on the 9 m drop predicted to cause the most Outerpack damage.

Maximum Loads – Our analysis indicates the shipping package will be subjected to the higher loads when dropped in a horizontal orientation, Figure 2-65A, compared to an inclined one Figure 2-65B. For example, when the package is tilted 20° (with the top nozzle end of the package towards the ground), our analysis predicts the maximum impact load is 561 kN. This is 10% less than the 624 kN load predicted for a fully horizontal drop Figure 2-66.

This page intentionally left blank.

|

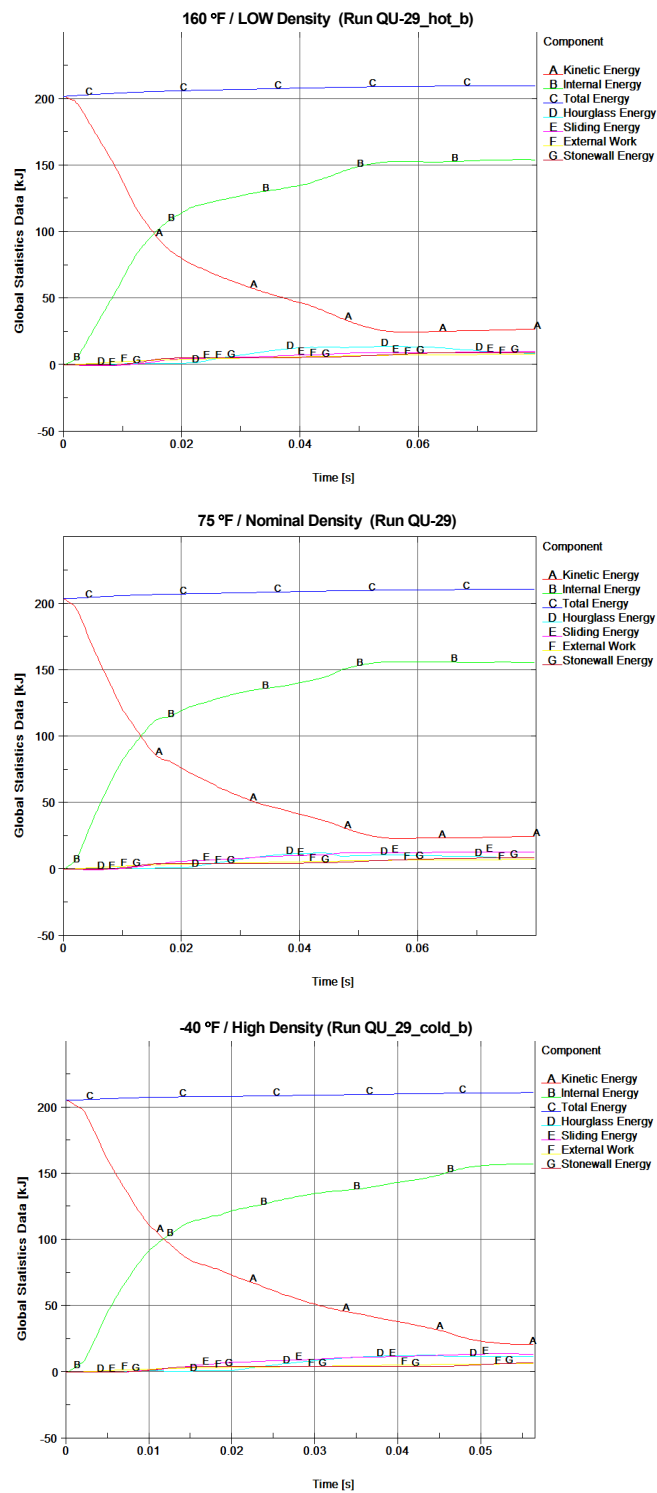


Figure 2-64 Predicted Energy and Work Histories at Various Temperatures

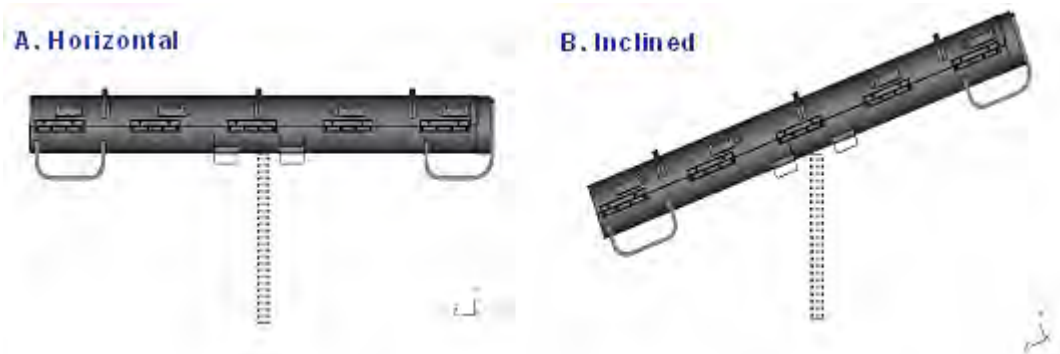


Figure 2-65 Pin Drop Orientation

A comparison of predicted fuel assembly accelerations is shown in Figure 2-67. Note the fuel assembly is predicted to experience approximately 9% higher accelerations in a fully horizontal pin drop than one inclined at 20 degrees.

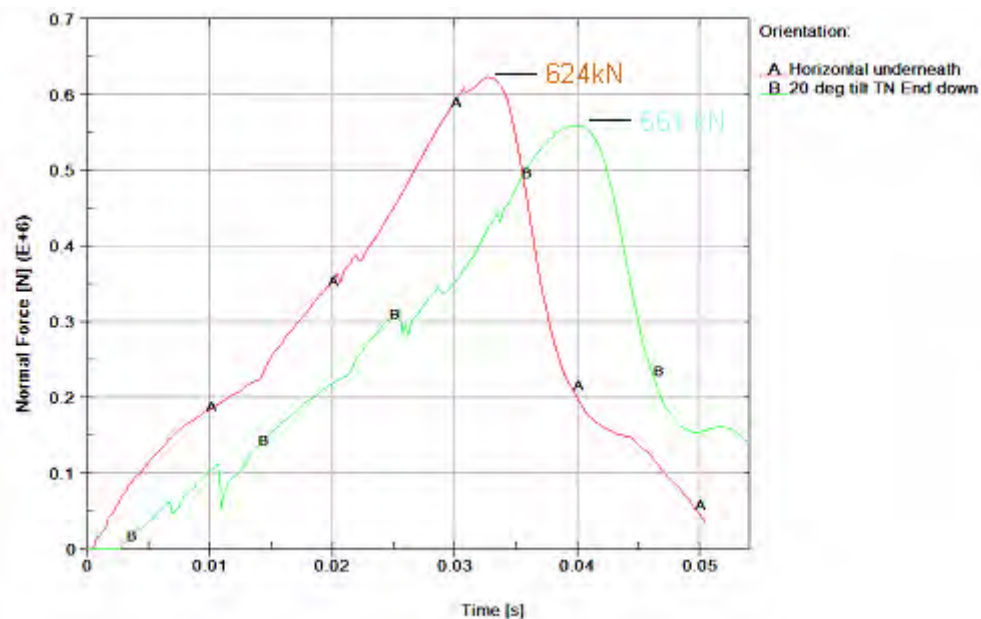


Figure 2-66 Predicted Outerpack/Pin Interference Forces (1m Drop onto 15mm Diameter Steel Pin)

Thus, a fully horizontal pin puncture drop produces higher Outerpack loads and fuel assembly accelerations than inclined pin puncture drops.

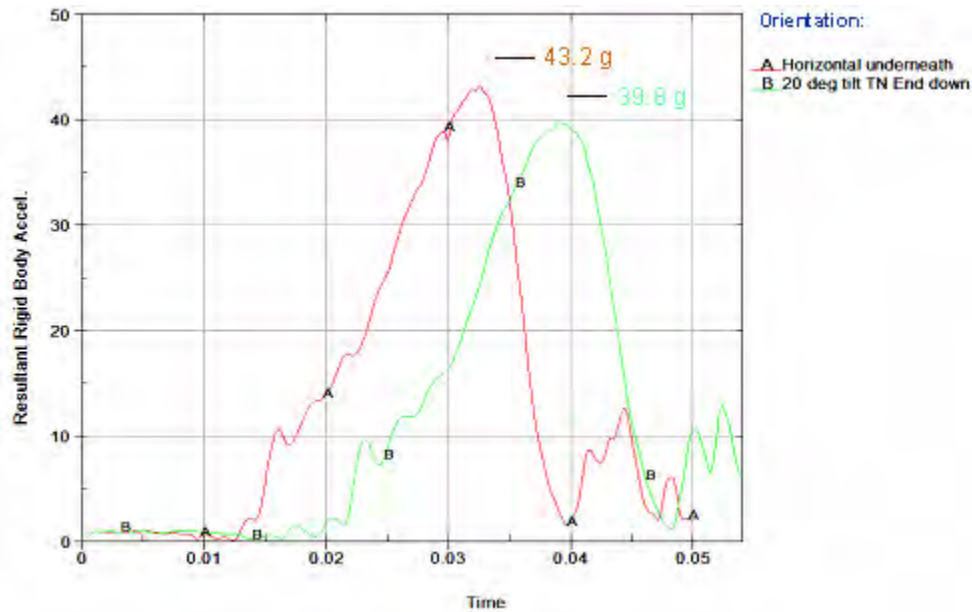


Figure 2-67 Predicted Fuel Assembly Accelerations (1m Drop onto 15mm Diameter Steel Pin)

Worst Horizontal Pin Drop – Two axial rotations were compared when studying the horizontal pin puncture drops. These were the previously described orientation in which the pin impacts the shipping package from underneath, Figure 2-65A, and one where the pin impacts the Outerpack hinges, Figure 2-68. In both cases, the pin was positioned directly under the package CG.

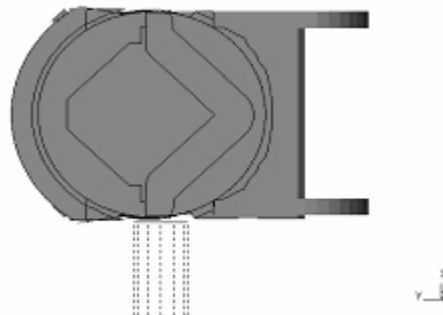


Figure 2-68 Pin Drop onto Outerpack Hinges

Interestingly, predicted Outerpack loads were practically the same for a horizontal pin puncture to the underneath side of the Outerpack and a pin impact directly to a hinge, Figure 2-69. However, there was less cushioning for the fuel assembly in the latter drop. This is evident from the predicted fuel assembly accelerations of 43.2 g's for the impact to the underneath region of the Outerpack and 82.1 g's for the hinge impact, Figure 2-70.

In fact, all of these pin puncture orientations were tested using full-scale Traveller XL units. In all cases, the pin puncture tests were passed without any puncturing of the outer skins of the units, nor any detrimental effects to the Clamshell/fuel assembly, or criticality safety aspects of the package.

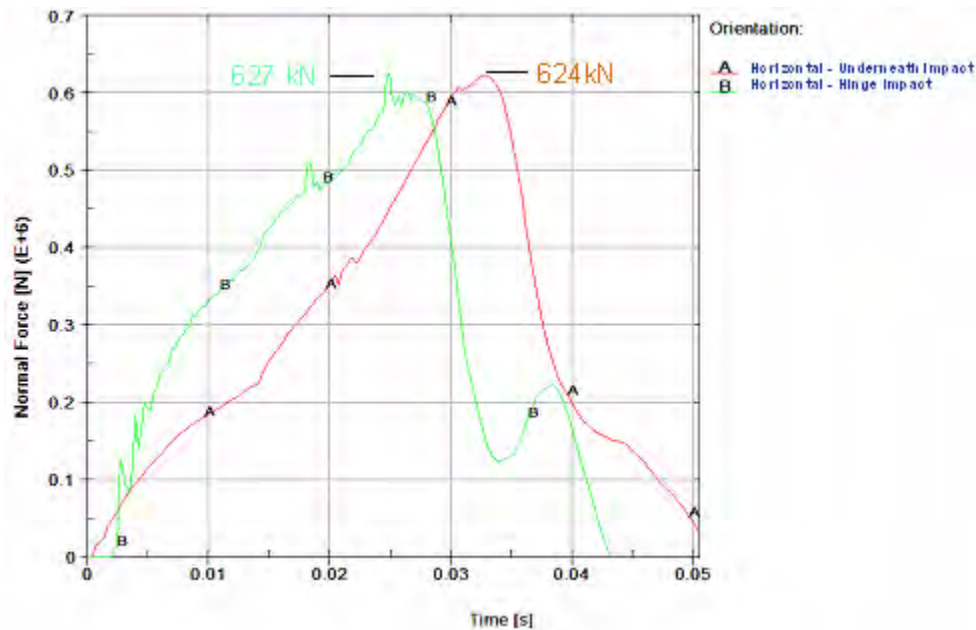


Figure 2-69 Predicted Outerpack/Pin Interface Forces (1m Drop onto 15mm Diameter Steel Pin)

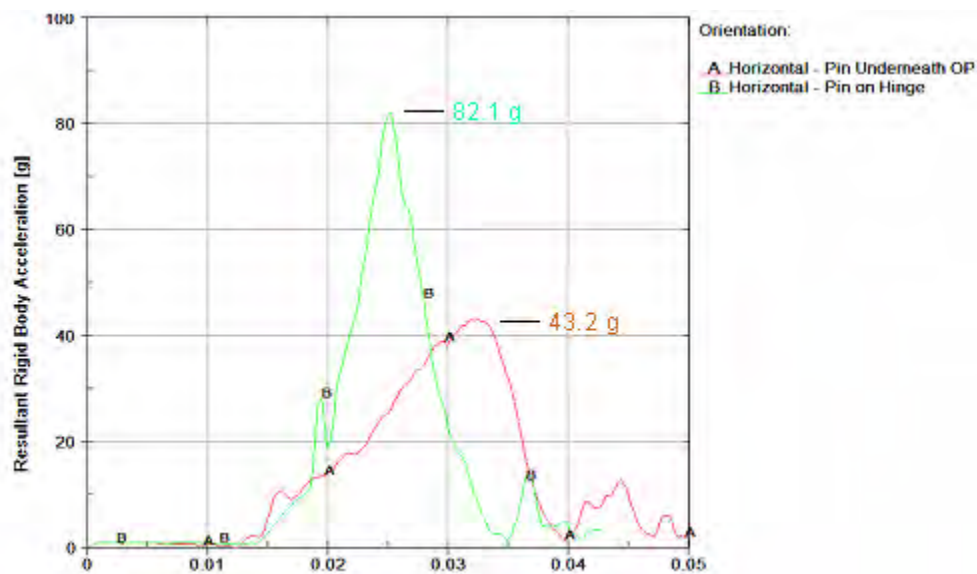


Figure 2-70 Predicted Fuel Assembly Accelerations (1m Drop onto 15mm Diameter Steel Pin)

Energy and Work Histories – Global energy and work for the 1 m pin puncture drops discussed above are shown in Figures 2-71, 2-72 and 2-73. These plots have an initial total energy (TE) of 22.3 kJ. This value correctly reflects the initial velocity (v) of 4.43 m/s applied to the 2,270 kg package mass (m) since our pin puncture simulations are initiated at the end of Outerpack free fall from 1 m; the total energy is comprised only of kinetic energy (KE), and $KE = \frac{1}{2}mv^2$. Total energy rises about 8% in these drop simulations. This reflects the work done by the package under gravity loading, i.e., the bending of the shipping package around the pin. Depending on drop orientation, the event was completed within 4 to 5 milliseconds as seen by the flattening of the kinetic energy and internal energies after that time. Moreover, acceptable levels of hourglass, sliding, and stonewall energies were obtained. This indicates a good overall numerical analysis was obtained in each simulation.

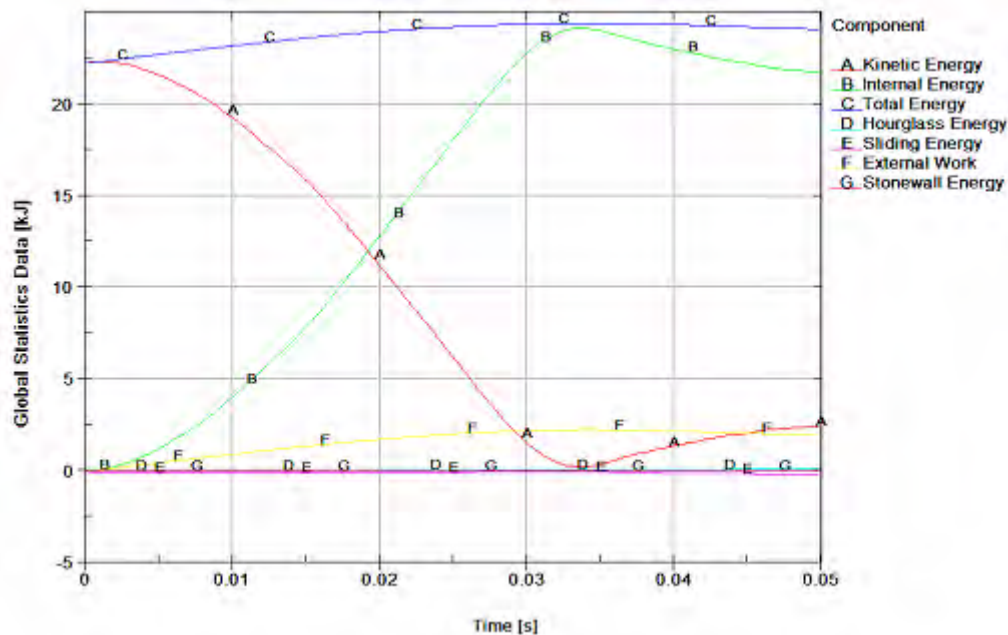


Figure 2-71 Predicted Energy and Work Histories for a 1 m Horizontal Pin Drop (Pin Underneath the Package CG)

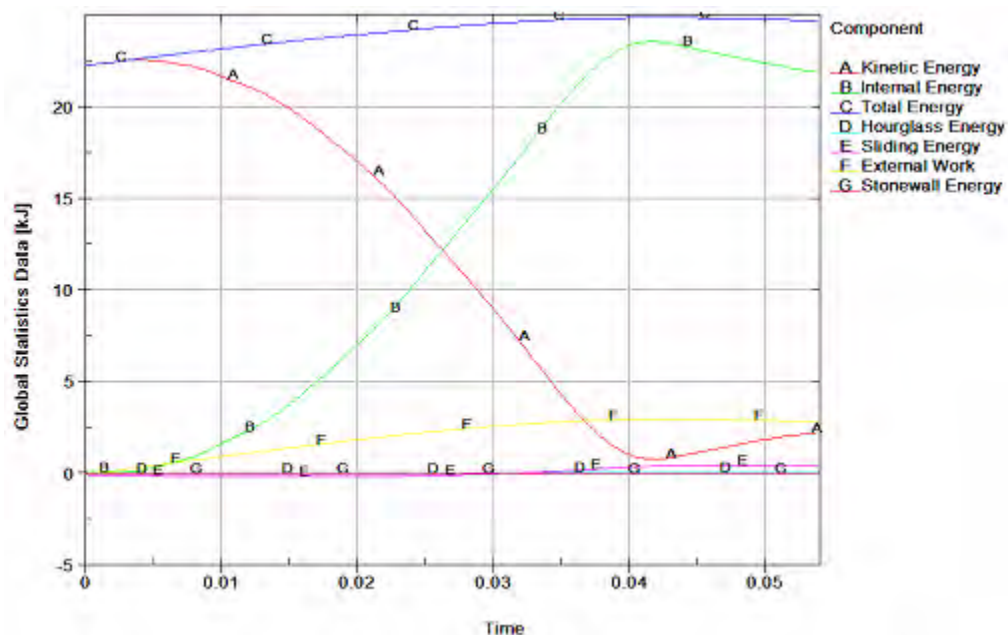


Figure 2-72 Predicted Energy and Work Histories for a 1 m Tilted Pin Drop (20° Tilt With TN End Down)

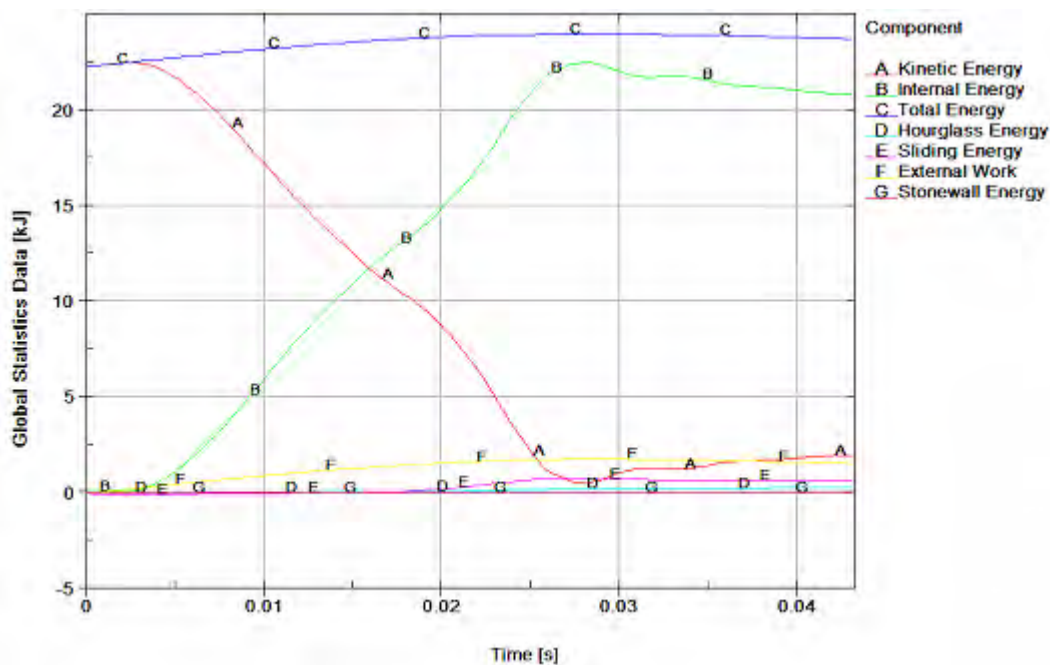


Figure 2-73 Predicted Energy and Work Histories for a 1 m Horizontal Pin Drop (Pin Hitting Hinge at Package CG)

Maximum Pin Indentation – Predicted maximum pin indentation for the horizontal underneath, inclined, Figure 2-65 and hinge pin puncture drops Figures 2-68 were, 67, 54 and 50 mm, respectively. This is shown in Figure 2-74.

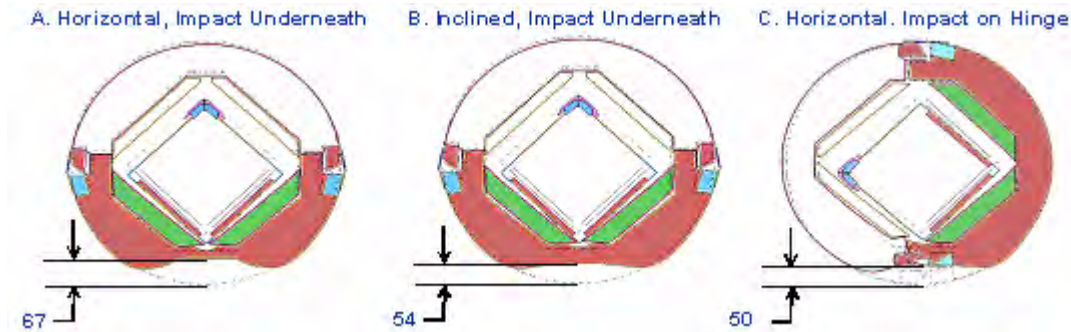


Figure 2-74 Comparison of Predicted Maximum Pin Indentations

Outer Steel Skin Damage – Predicted maximum plastic strains in the steel skin were only 12.6 and 15.7% for the horizontal and 20° tilted pin puncture simulations Figures 2-65A and 2-65B, respectively. These values are much less than the allowable 46.7% failure strain. Thus, it is unlikely the steel skin will be ruptured by the pin puncture test. Initial testing of the Traveller XL Prototype units were demonstrated that 11 gage (0.120" nominal thickness, 3.0 mm) 304 stainless steel had little difficulty passing the pin puncture tests. Those full-scale tests, in addition to the analytic work discussed previously, allowed designers the confidence to reduce the thickness of the Outerpak shells to 12 gage material (0.105" nominal thickness, 2.7 mm). Therefore, the QTU and CTU packages were all fabricated using 12 gage sheet material of the outer shells. Pin drop tests of QTU-1, QTU-2 and CTU packages confirmed that 12 gage material survived the pin puncture tests without failure.

Cumulative Damage – As previously stated, analysis of cumulative pin damage was based on the 9 m drop predicted to cause the most Outerpak damage. Indeed, this analysis placed the pin 1 m under, and normal to, the region of the top impact limiter which was (previously) predicted to flatten during the 9 meter CG-forward-of-corner drop onto the TN end of package with an 18° forward rotation Figures 2-64 and 2-25. The position of the pin was at the apex of the top impact limiter Figure 2-67. This location was chosen since it would most exacerbate the opening of the Outerpak seam predicted from the 9 m drop analysis.

Deformations, strains, and stresses from the previous 9 m analysis were used as the initial starting point for the cumulative pin puncture drop analysis. Inclusion of deformations was accomplished by use of the LSTC/LSPOST¹ capability to output deformations at the appropriate time (state) in LS-DYNA keyword format. The corresponding strains and stresses from the 9m analysis were written to a file (in LS-DYNA keyword format) via the LS-DYNA *INTERFACE_SPRINGBACK_DYNA3D command. A new master 1 m pin puncture analysis keyword file was created that defined all parts, materials, nodes (with deformed

1. LSPOST is the pre- and postprocessor by LSTC provided with LS-DYNA.

positions), element connectivity, loading, etc. Stresses and strains were then brought into the analysis by use of the LS-DYNA *INCLUDE and *STRESS_INITIALIZATION commands.

Maximum Loads – The Westinghouse analysis indicates the shipping package is subjected to higher loads when dropped on a previously damaged end than in any other orientation analyzed, including a drop onto a hinge. Indeed the maximum predicted Outerpack load was 734 kN for the 2nd hit Figure 2-75. This is 17% higher than the 627 kN predicted for a drop onto the Outerpack hinge Figure 2-69. The greater load is attributed to the lower cushioning available due to the foam in being highly compressed during the 9m drop. Even so, the maximum predicted fuel assembly acceleration was just 38.2 g's Figure 2-76.

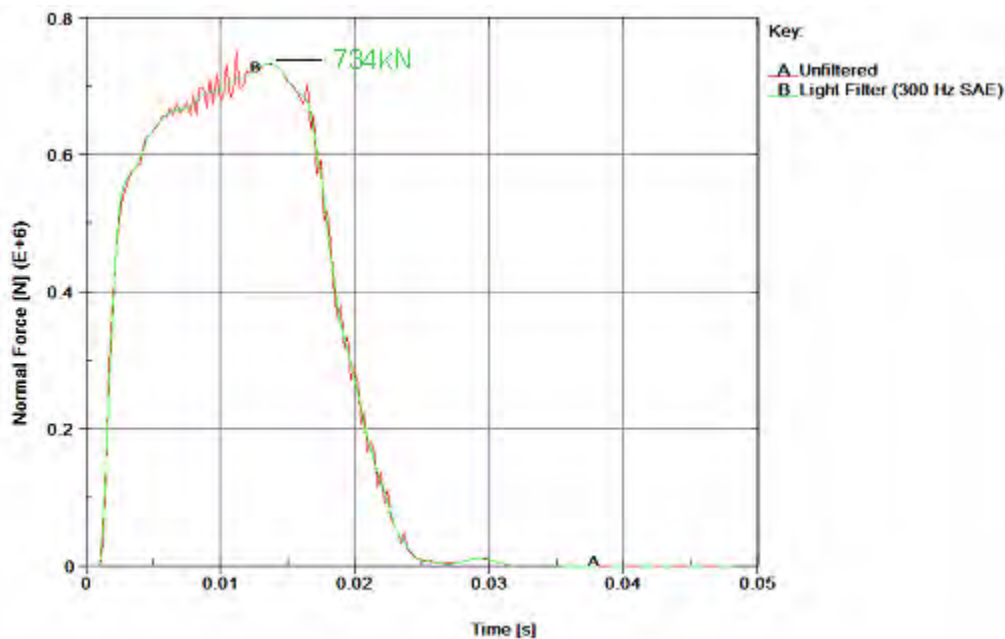


Figure 2-75 Predicted Outerpack/Pin Interface Forces (1 m Drop onto 15 mm Diameter Steel Pin After 9m Drop)

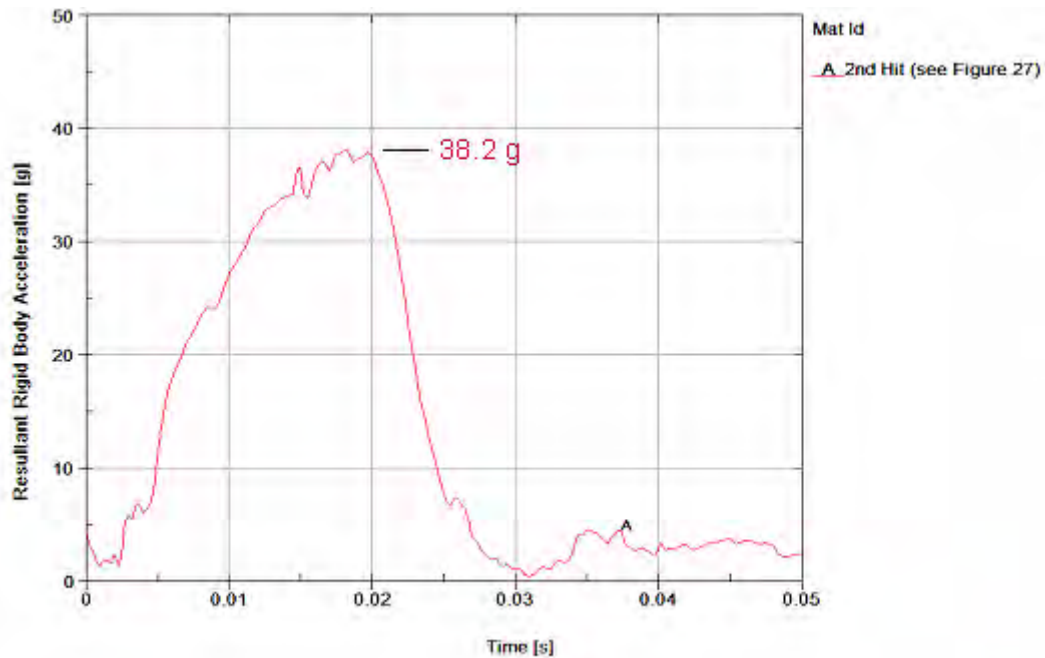


Figure 2-76 Predicted Fuel Assembly Accelerations (1 m Drop onto 15mm Diameter Steel Pin after 9 m Drop)

Additional Damage – As previously discussed, our primary concern for this sequence of drops (a 9 m CG-forward-of-corner drop onto the top nozzle end of the package followed by the 1 m pin puncture) was the extent of Outerpack seam opening Figure 2-28. Our measures of Outerpack seam opening, D1 and D2 (see Figure 2-48), would increase from 20 to 22.9 mm and from 20 to 22.2 mm, respectively.

Energy and Work Histories – Predicted global energy and work for the 1 m pin puncture drop following a 9 m CG-forward-of-corner drop onto the top nozzle end of the package is shown in Figure 2-77. The sliding energy in this plot is related to the initial penetration between the crushed impact limiter foam and outer steel skins. It is not necessarily an error. Moreover, the predicted increase in damage due to the pin puncture test simply does not warrant further investigation of this issue.

Pin Puncture Summary – Our analyses indicate the Traveller XL package is very capable of withstanding the 1 m pin puncture test. Indeed, it was determined that the likelihood of rupturing the outer steel skin is very low. Thus, the 1 m pin puncture test is a relatively benign test for the Traveller XL package. These conclusions were confirmed by the prototype test results as subsequently discussed.

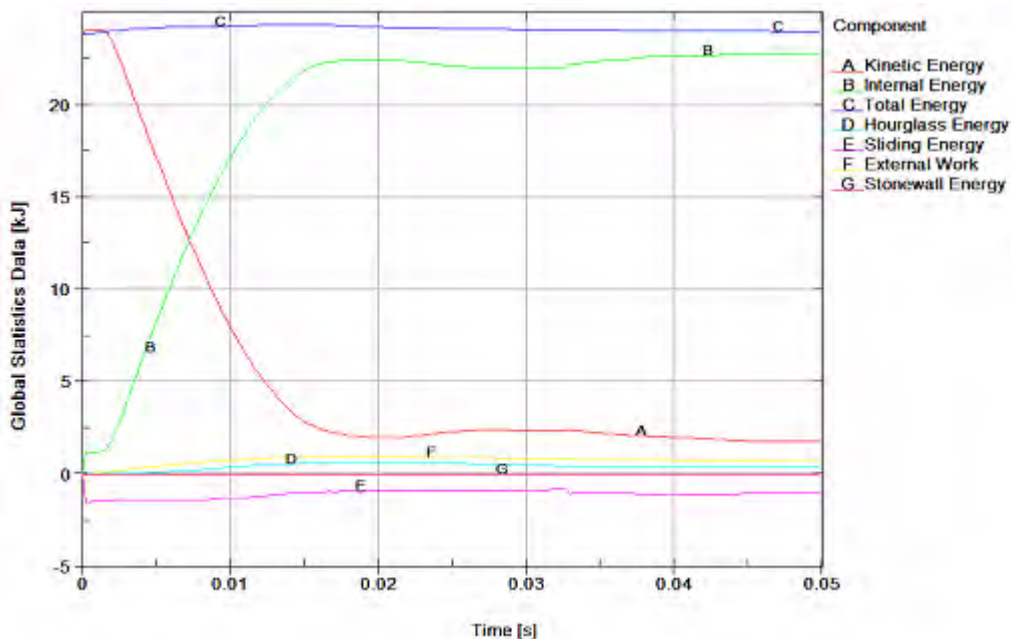


Figure 2-77 Predicted Energy and Work Histories (1 m Drop onto 15 mm Diameter Steel Pin after 9 m Drop)

2.12.4.3 Comparison of Test Results and Predictions

Two prototype Traveller XL packages were drop tested on January 28 and 29, 2003. Details of these tests are provided in Appendix 2.12.5, Traveller Drop Test Results.

Results from the extensive prototype tests in January, 2003 were reviewed to find the best ones for comparison with FEA predictions. Comparison cases were chosen to include tests with prototype units which did not have extensive previous test damage, those which represented a unique test configuration (i.e., the pin puncture) and those in which accelerometer data was obtained. The four selected cases are identified in Table 2-22 and Figure 2-78.

There was good overall agreement between predicted and actual drop performance of the prototype Traveller XL package. This is evident by comparisons of predicted and actual permanent deformations, failed parts and measured and predicted accelerations at specific positions on the Outerpack and Clamshell.

Table 2-22 Prototype Tests Used to Compare with Analysis					
Test ID (corresponds to [6])	Analysis ID	Drop Height [m]	\dot{E}_x	\dot{E}_z	Comment
1.1, 9 m Low Angle	C1-25	9.1	14.5°	180°	T/N primary impact on OP top
1.2, 9 m CG-over-corner	C1-31	9.1	-71°	90°	B/N primary impact on OP hinge
2.2, 1 m Pin-puncture	Punc2-2nh	1.04	20°	135°	CG (Axial) on OP topside, T/N end down
2.3, 9 m CG-over-corner	C1-29	9.1	108°	0°	T/N primary impact on OP top

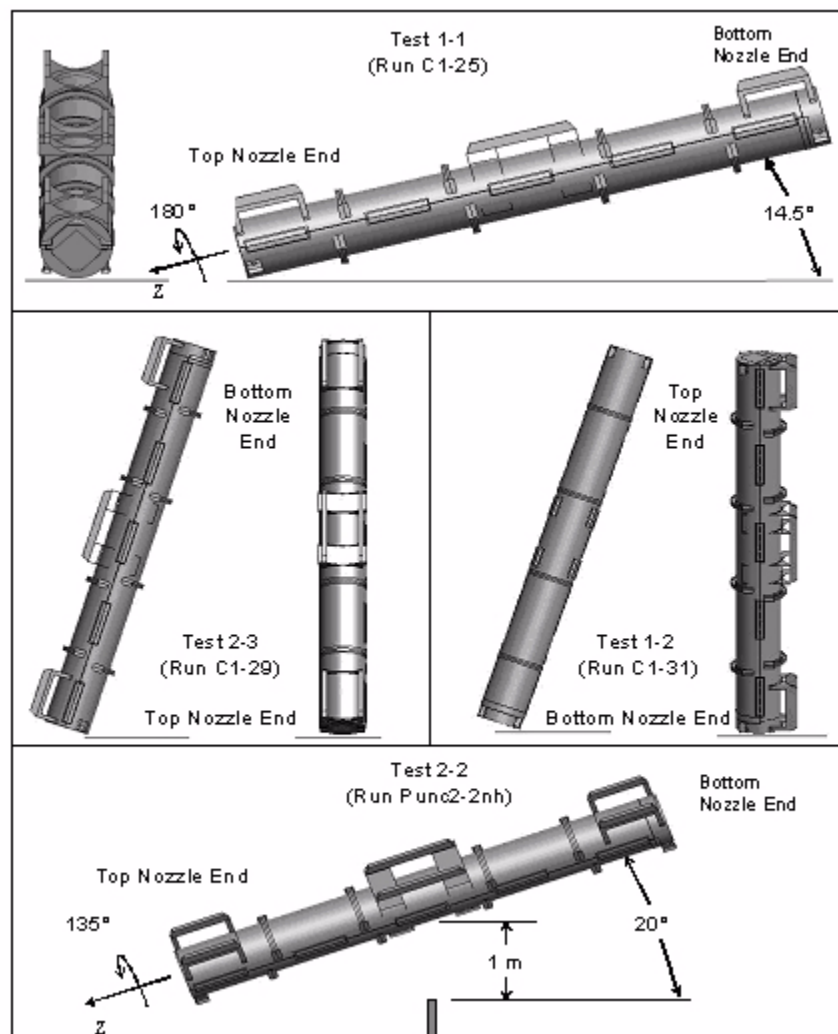


Figure 2-78 Prototype Drop Tests Used To Benchmark Analysis

2.12.4.3.1 Prototype Unit-1 Test 1.1

Prototype Unit-1, Test 1.1 was chosen for the first comparison. As indicated in Table 2-22 and Figure 2-78, this was an inclined drop from 9.1 meters onto the upper Outerpack (the unit was rotated 175° about its long axis and inclined 14.5° with the end of the package nearest the top of the fuel assembly hitting first.¹ Four frames taken from a video recording of test 1.1 are shown in Figure 2-79. These frames show the test sequence was comprised of the initial impact on the top nozzle end of the package (frame 1), rollover (frames 2 and 3), and a secondary impact to the bottom nozzle end of the package (frame 4).



Figure 2-79 Prototype Unit 1 Drop Test

Deformations – As reported in, test 1.1 produced noticeable permanent deformations in several locations of the Outerpack and no significant permanent deformations in the Clamshell. Outerpack permanent deformations were primarily at the ends of the package.

1. This will be referred to as the “top nozzle end” of the package. Likewise, the end of the package nearest the bottom of the fuel assembly will be called the “bottom nozzle end.”

An overall sense of the correspondence between predicted and actual Outerpack permanent deformations may be obtained by reviewing Figures 2-80 through 2-87. Quantitative comparison between predicted and documented measurements is given in Table 2-23.

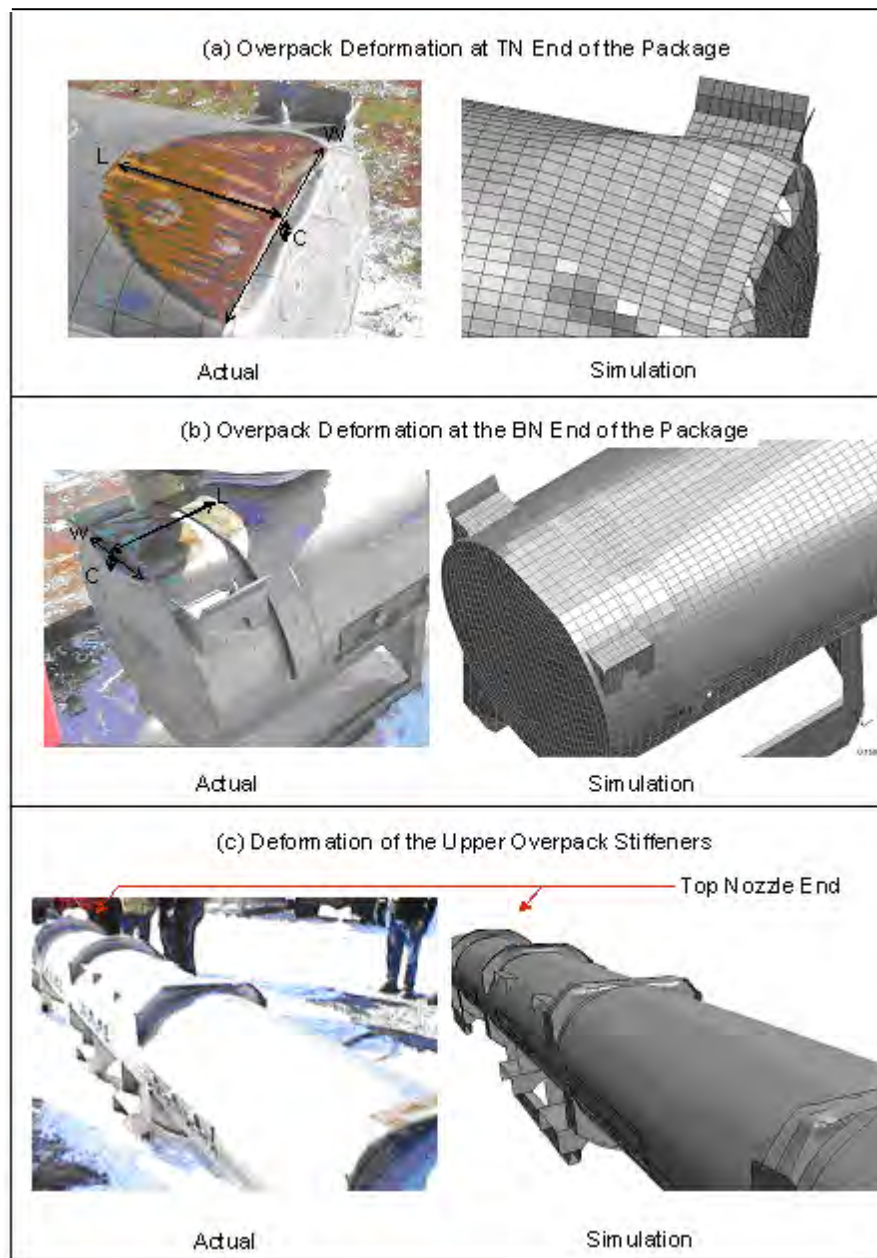


Figure 2-80 Comparison of Test 1.1 with Analytical Results

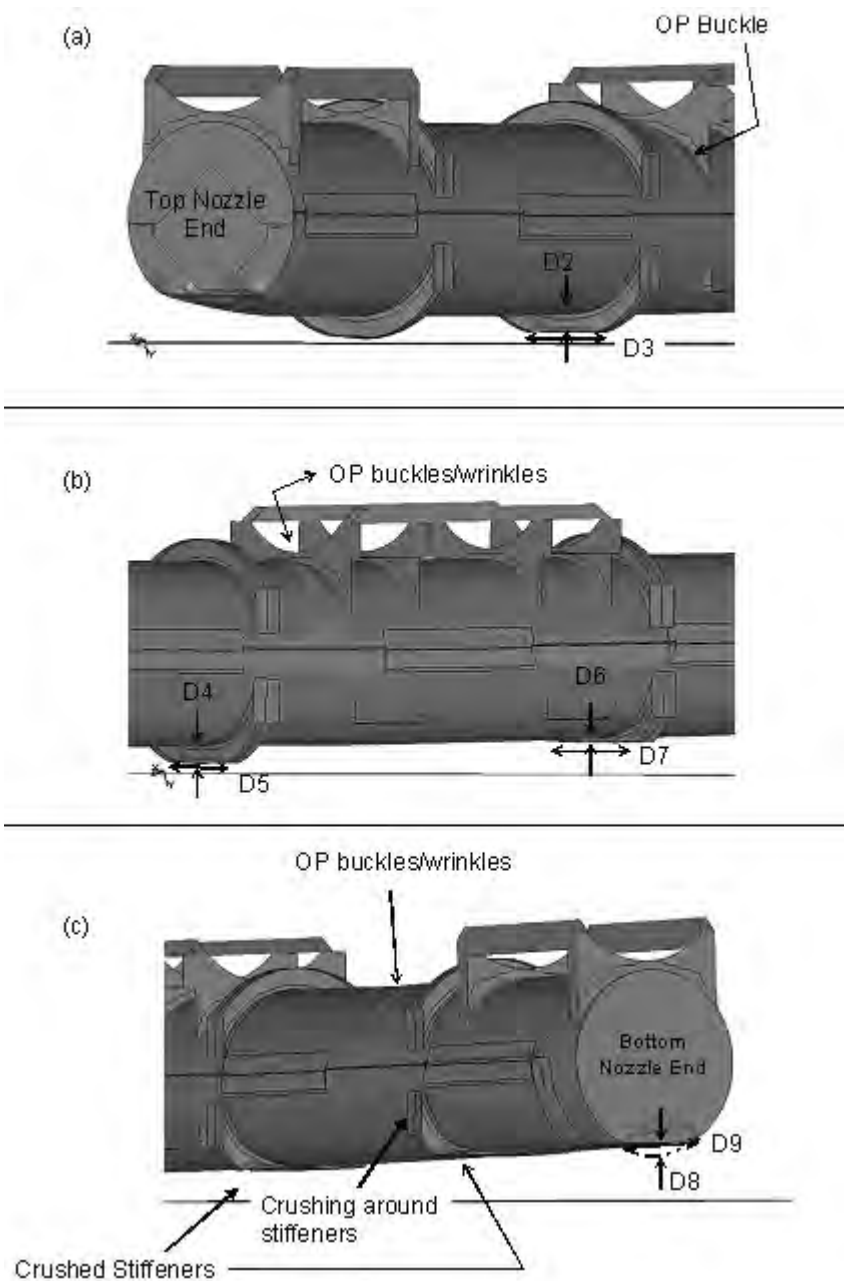


Figure 2-81 Comparison of Test 1.1 with Analytical Results

Table 2-23 Comparison of Predicted and Actual Deformations for Test 1-1									
Item	Location	Measured (Reference 6)		Predicted		Nodes used to make Prediction		Difference	Conservativ e
		(in)	(mm)	(in)	(mm)				
1	Top nozzle end								
	Dim L in Figure 2-80	9.0	229	11.9	302	192658	134223	32.2%	Yes
	Dim W in Figure 2-80	12.0	305	14.6	371	134052	134170	21.7%	Yes
	Dim C in Figure 2-80	1.5	38	1.65	42	134062	223918	10.0%	Yes
2	Bottom nozzle end								
	Dim W in Figure 2-80	11.5	292	11.9	302	214342	190946	3.5%	Yes
	Dim L in Figure 2-80	10.57	268	13.0	330	94120	213639	23.0%	Yes
	Dim C in Figure 2-80	0.75	19	1.5	38	93833	214433	100.0%	No
3	Upper Overpack Stiffeners								
	Dim D2 in Figure 2-81	0.8	19	0.7	17	115715	115853	-10.7%	Yes
	Dim D3 in Figure 2-81	N/A		11.9	303	115702	116484	-	
	Dim D4 in Figure 2-81	2.4	60	2.2	56	112621	112759	-6.4%	No
	Dim D5 in Figure 2-81	N/A			-			-	
	Dim D6 in Figure 2-81	N/A		1.0	26	109526	110131	-	
	Dim D7 in Figure 2-81	16.0	406	18.4	468			15.1%	Yes
	Dim D8 in Figure 2-81	N/A			-			-	
	Dim D9 in Figure 2-81	23	584	22.6	574			-1.7%	No
Average Difference:								22.4%	

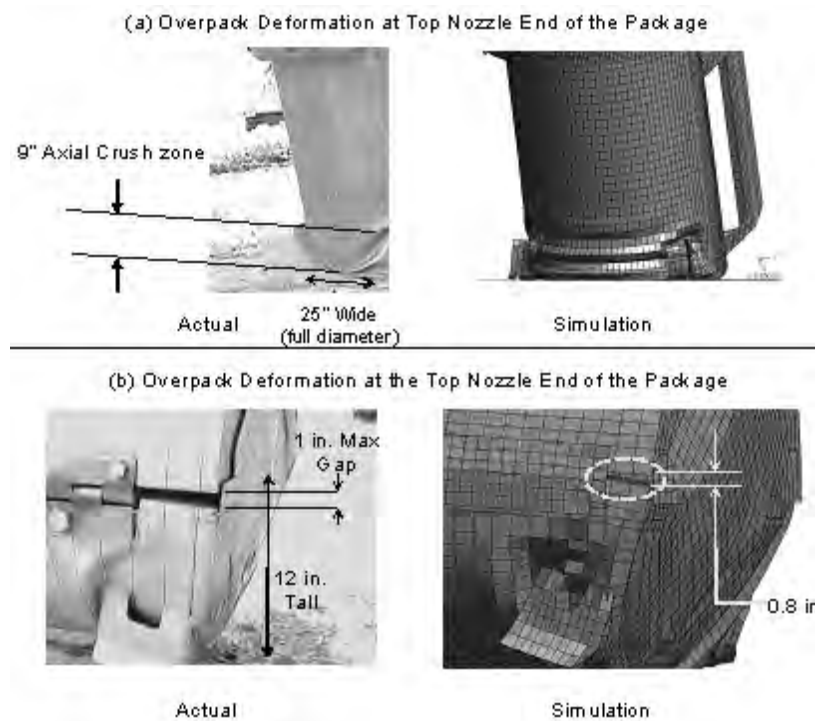
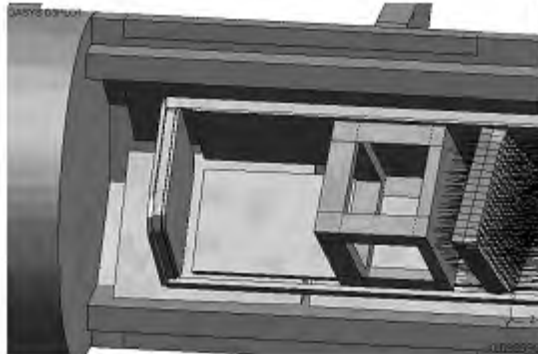


Figure 2-82 Deformations at End of Package

(a) FA Displacement at Bottom Nozzle End of the Package



Actual

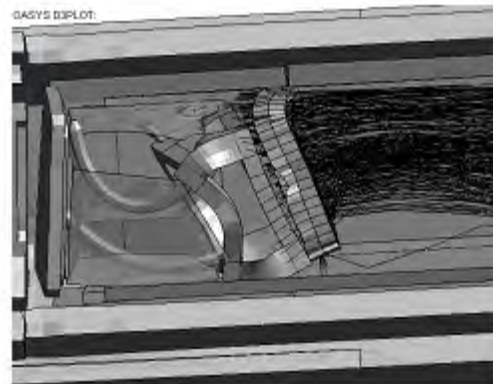


Simulation

(b) Deformation at the Top Nozzle End of the Package



Actual



Simulation

Figure 2-83 Internal Deformations at Inside Outerpak

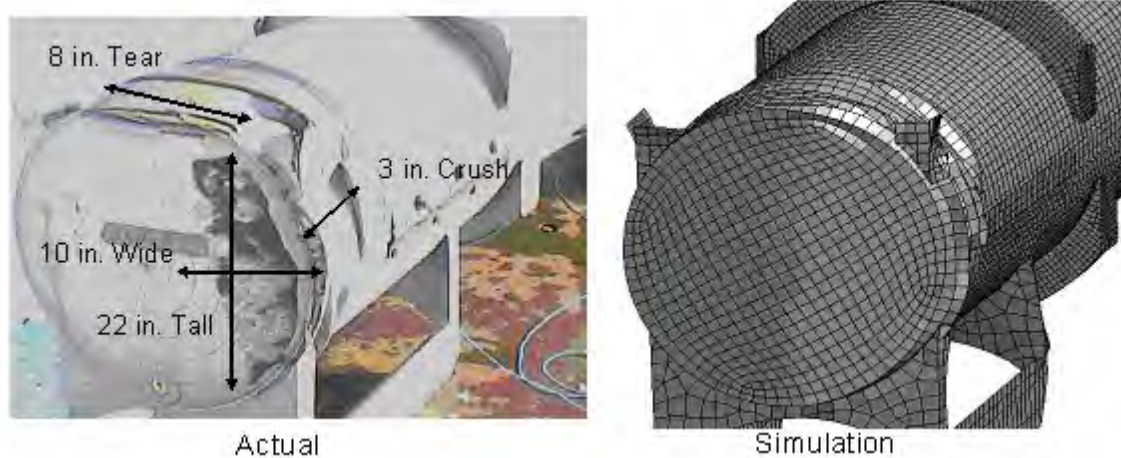


Figure 2-84 Outerpack Deformations at Bottom Nozzle End of Package

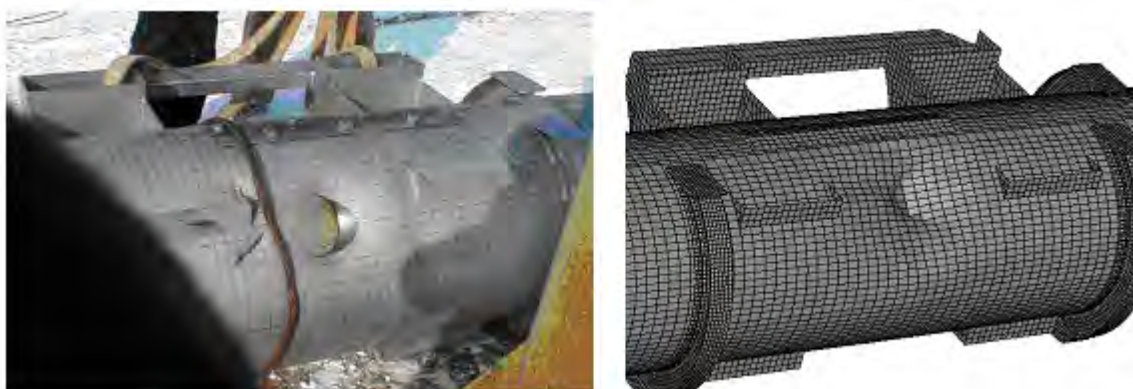


Figure 2-85 Pin Puncture Deformations

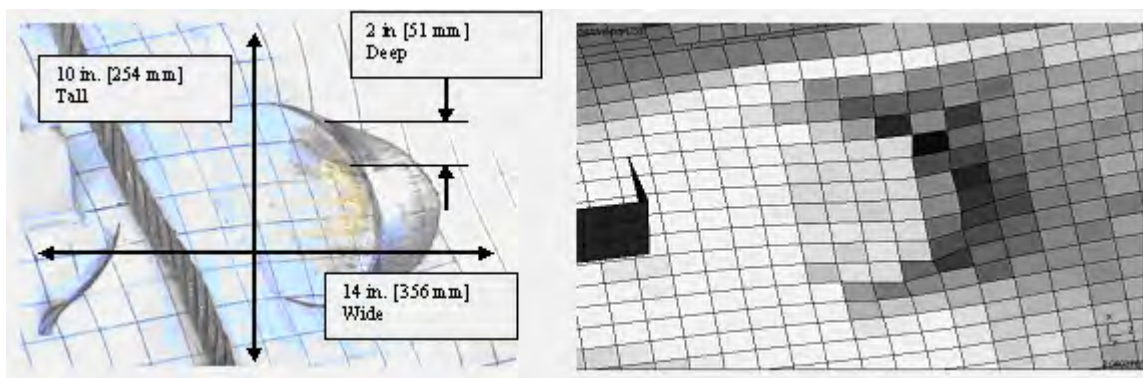


Figure 2-86 Dimensions of Pin Puncture Deformations

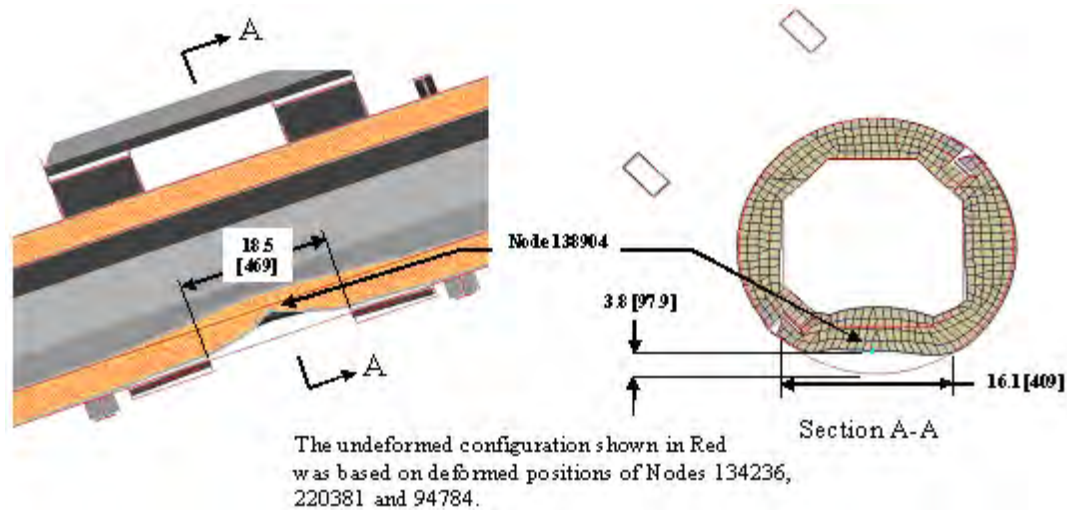


Figure 2-87 Outerpak Predicted Deformations of Pin Drop

2.12.4.3.2 Accelerations

Vertical accelerations (Y-direction) measured during test 1.1 are compared with the FE-based predictions in Figures 2-88 through 2-92. Agreement was good. Indeed, discrepancies between the two could easily be attributed to the inherent error associated with obtaining such data.

For the Outerpak, both measured and predicted traces contained two peaks, Figure 2-88. These corresponded to the two impacts associated with this test as illustrated in Figure 2-78. (Note: the larger acceleration with the secondary impact should not be interpreted as meaning larger forces were associated with the second impact. Rather, the larger magnitude simply reflects that the accelerometer was much nearer the secondary impact end.) While there were two visible peaks, the measured response was very small for the primary impact. For the secondary impact, the predicted acceleration was 1270 g's. This was in accordance with the measured peak acceleration which indicated accelerations were greater than 950 g's.

For unknown reasons, the accelerometers on both the Clamshell top and bottom plates gave erroneous readings late into the drop. This is clearly evident from accelerometer data in Appendix 2.12.5 that the accelerometers "saturate" for over 0.025 seconds and provide no meaningful response afterwards. Thus, only the first 0.05 seconds of the Clamshell data was compared in this report. For the accelerometer on the Clamshell top plate, measured and predicted accelerations corresponding to the first impact (at time 0.01 seconds in Figure 2-90) were 555 g's. This was also in accordance with measurements which indicated a peak acceleration greater than 525 g's was experienced. As shown in Figure 2-91, peak accelerations of 205 g's were measured on the Clamshell bottom plate. The corresponding predicted acceleration is also shown. Note the peak predicted acceleration was 155 g's.

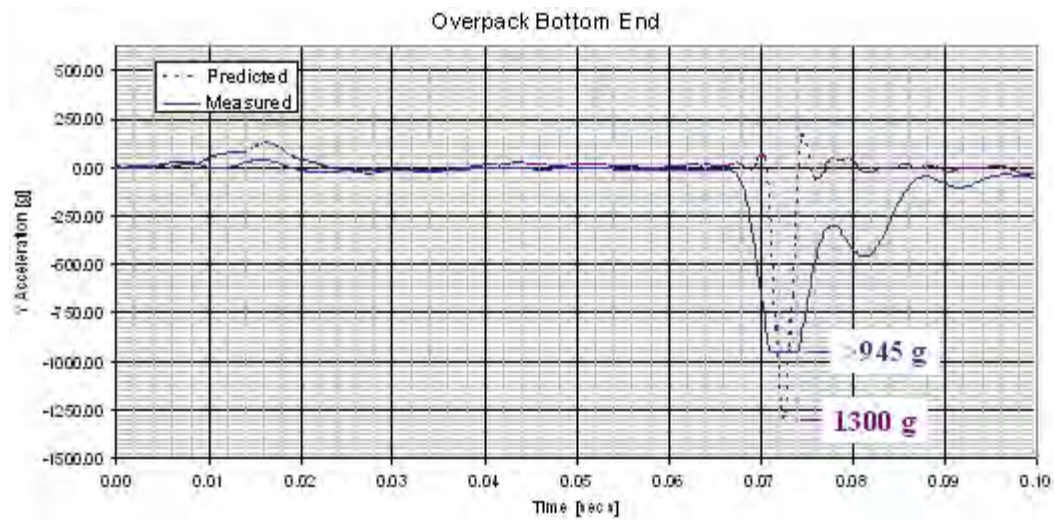


Figure 2-88 Predicted and Measured Y Accelerations

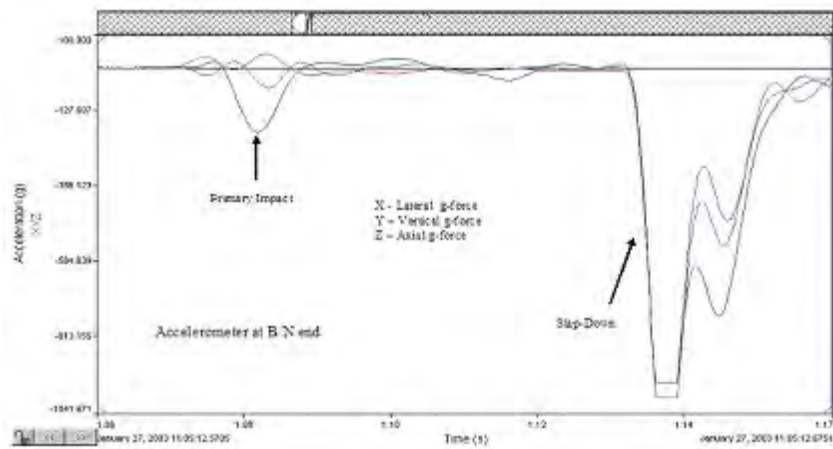


Figure 2-89 Three Axis Measured Accelerations

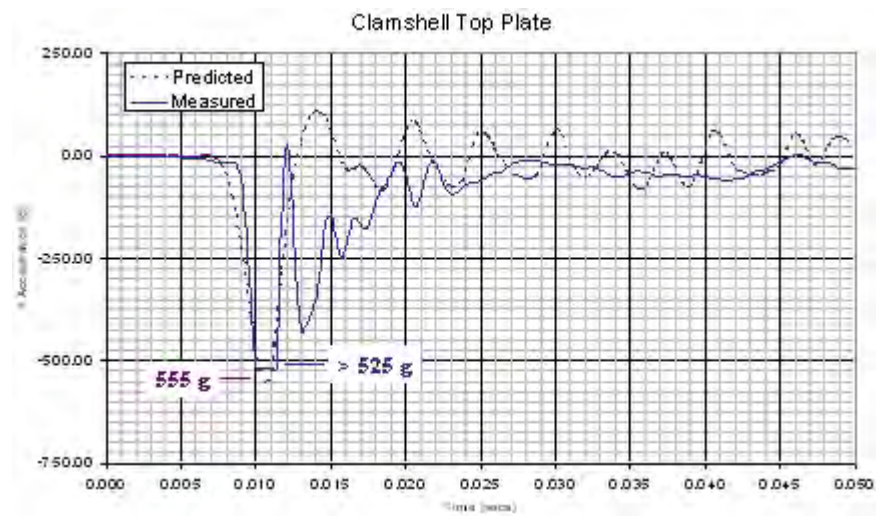


Figure 2-90 Predicted and Measured Y Accelerations

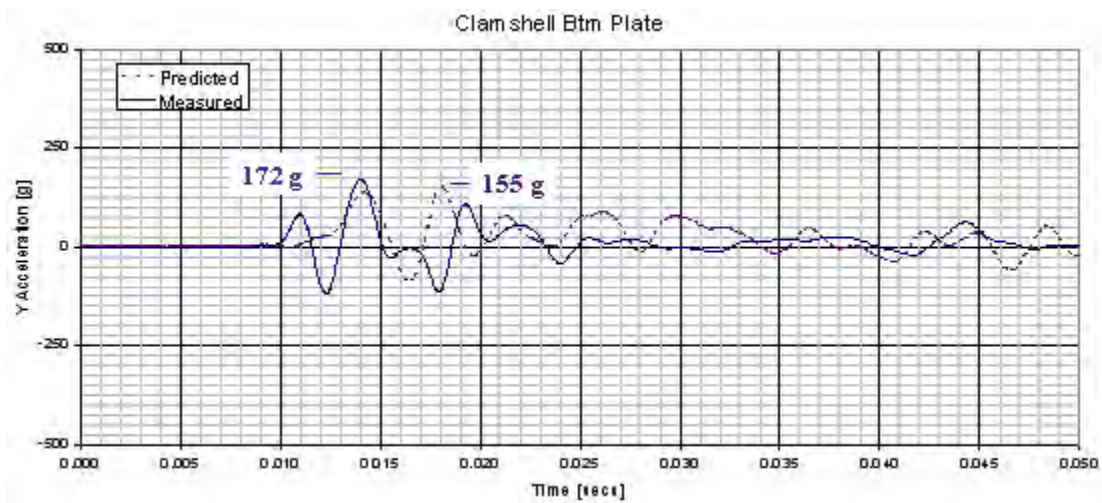


Figure 2-91 Predicted and Measured Y Accelerations

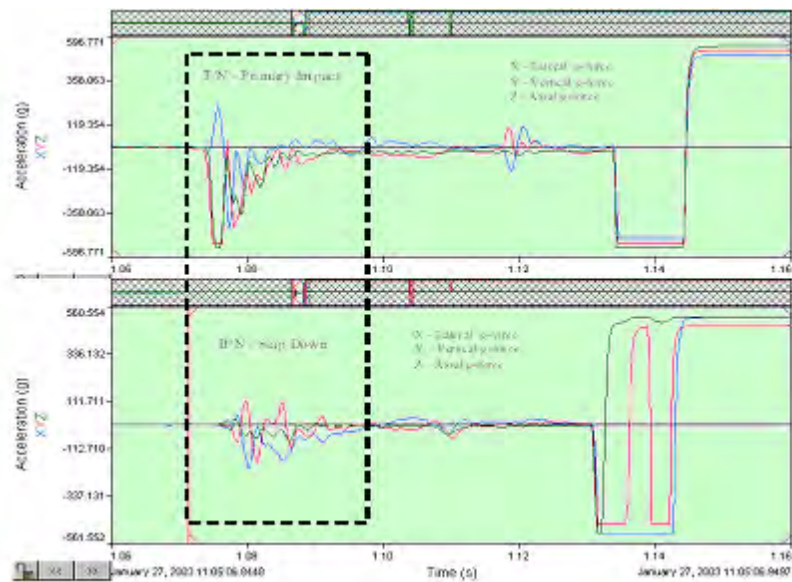


Figure 2-92 Measured Primary and Secondary Accelerations

2.12.4.4 Discussion of Major Assumptions

The many assumptions used to develop the LS-DYNA non-linear finite element stress code, including those needed to model the materials and impact, were found valid for simulating drop tests of the Traveller XL package. It is clearly evident from comparisons between prototype test results and predictions that the key physical phenomena governing shipping container impacts is captured within the LS-DYNA code.

The only major additional assumption was that bowing of the fuel assembly did not result in excessive additional loading of the Clamshell side walls, hinges and latches. Test results showed this was a valid assumption.

LS-DYNA 960 build no. 1647 (single precision, MPP) was used in these calculations because it has the very needed “no put-back” contact capability. However, the official quality tested and assured version is currently DYNA 960 build no. 1106 (single precision, MPP) which does not have the no put-back contact capability. ARUP is expecting to officially release LS-DYNA 970 (probably build no. 3858) in late October, 2004. This version, which does have the no put-back capability, must be installed and tested on the claxgen computers. Then a Traveller XL drop test case must be run to verify results in this calculation note correspond with results from the quality-assured version of LS-DYNA.

2.12.4.5 Calculations

2.12.4.5.1 Method Discussion

The finite element method was used to determine the loads, displacements, accelerations, strains, etc. of a Traveller XL shipping package containing an XL fuel assembly when dropped on a flat surface from 9 m and onto a 15 mm diameter pin from 1 m. The LS-DYNA explicit finite element code was used. This software was selected because it allowed the analysis to include the effects of large deformation, large strain, material non-linearity, contact, and failure of connections between parts and assemblies.

The goal of the analysis was to predict the deformation and damage that the Traveller XL shipping package and contained fuel will experience when subjected to the HAC impact tests. Although it would have been more conservative, it was not feasible to build a model which allowed failure of all joints and any deformation pattern. Such a model would have been unduly complex and calculation intensive and have required extraordinary development time. Rather, the Traveller XL prototype and qualification unit finite element models were constructed with consideration of all probable relative displacements, contact and failures. The premise in choosing this deliberately restrictive approach was that it would not affect accuracy because it would include provisions for the actual deformation and damage. Test results substantiated the accuracy of the prototype unit model, see Appendix 2.12.5.

The models described herein were primarily developed to aid in determining the drop orientations and number of drops needed to meet the HAC requirements. Thus, any point on the Outerpack outer periphery was a potential impact point and there was no one point in which a finer mesh could be afforded. Thus, the actual strains and stresses determined in the model can not be considered refined. Rather, the relative deformations, decelerations and energy absorption between drop orientations should be considered. This limitation applies to both models of the prototype unit and the qualification unit.

Model Descriptions – A basic description of the Traveller XL prototype and qualification units is discussed in section 1 above. All design details are available in and. Details of the finite element models are described in the following two sections.

In both models, units were tonnes (mass), millimeters (length), seconds (times) and Newtons (force).

2.12.4.5.2 Prototype Models

The Prototype models, Units 1 and 2, were constructed from many input files, Figure 2-94. These files defined various details of the model and were included with, or without, transformations of coordinates and renumbering of identities as the model was assembled.

The main file, Apr6.key, contains the control cards, specifies outputs, contact definitions, and many attributes common to more than one subassembly. The major subassemblies were the Outerpack, Clamshell, and fuel assembly. These were defined in the OP.key, CS.key, and XL_FAr.key files, respectively. These subassemblies are detailed in Figures 2-95 through 2-97. A total of 363,646 elements were used in the model (199128 shells, 150717 solids and 13801 beams).

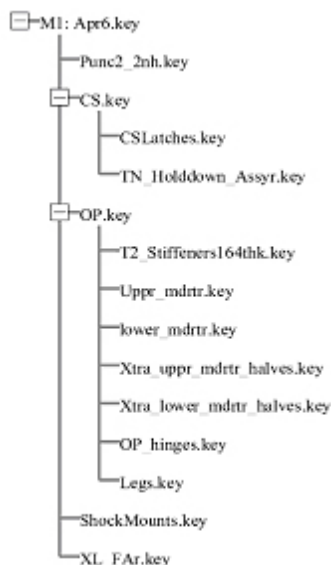


Figure 2-93 FEA Model Input Files

The orientation for each run was defined in individual load case files. Obviously, only one load case file and one material file was invoked per run.

The Clamshell Figure 2-96 is mounted to the Outerpack, Figure 2-94 with 22 rubber shock mounts. These shock mounts were modeled as discrete elements (springs). The stiffness of these elements was 92.7 N/mm in the global X direction, 135.4 N/mm in the global Y direction and 42.3 N/mm in the global Z direction. These values were obtained through tests. These details are included in the 'ShockMounts.key' file.

Predicted model weight for the Prototype units was 2.39 tonnes (5258 lbs). This matched the Prototype unit's 5065 lb. average weight within 3.8%.

Predicted model weight for the Qualification units was 2.27 tonnes (4994 lbs). This matched the Qualification unit's 4786 lb. average weight within 4.4%.

The Traveller program performed drop tests as input into the design process. As a result, there were changes in the design of the Traveller between the prototypes discussed on page 2-130 and the qualification test units described on page 2-133. The changes resulted in slightly different weights as noted in the descriptions.

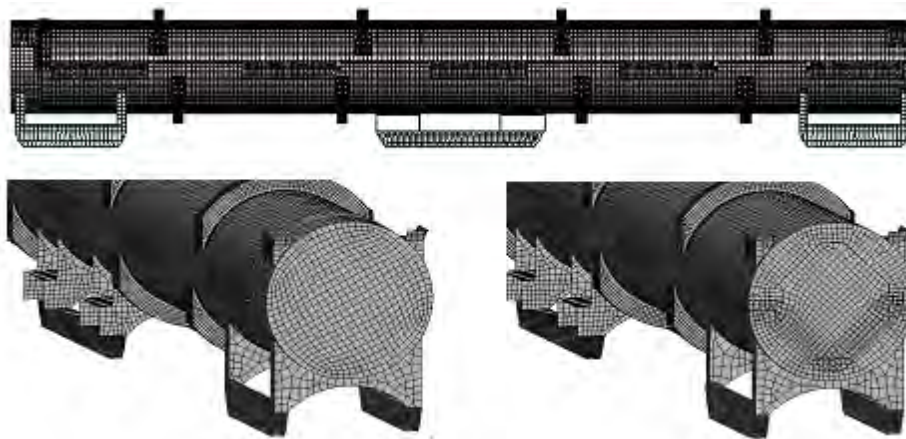


Figure 2-94 Outerpack Mesh in Prototype Model

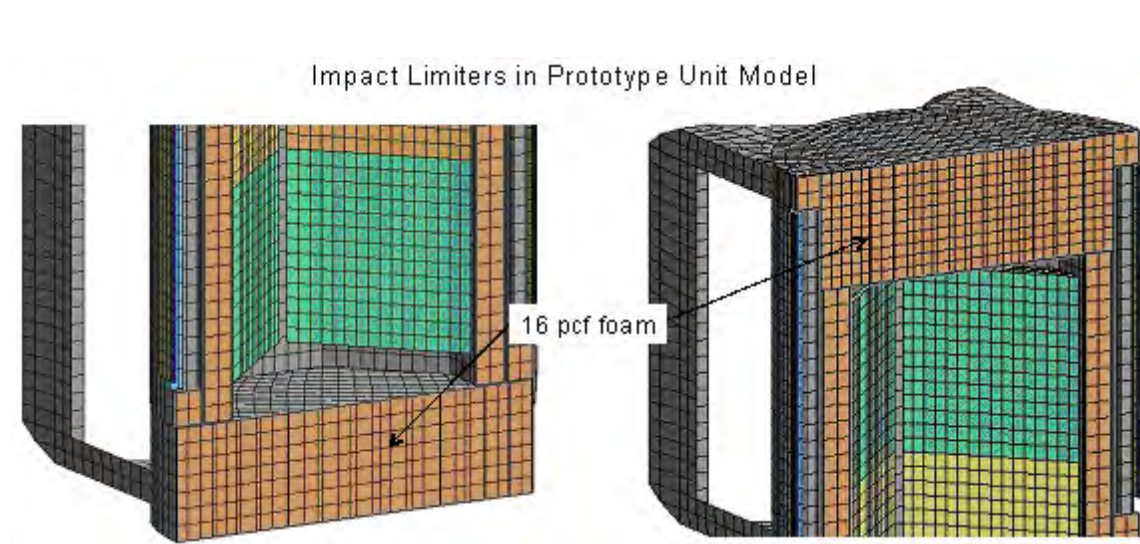


Figure 2-95 Impact Limiter in Prototype Unit Model

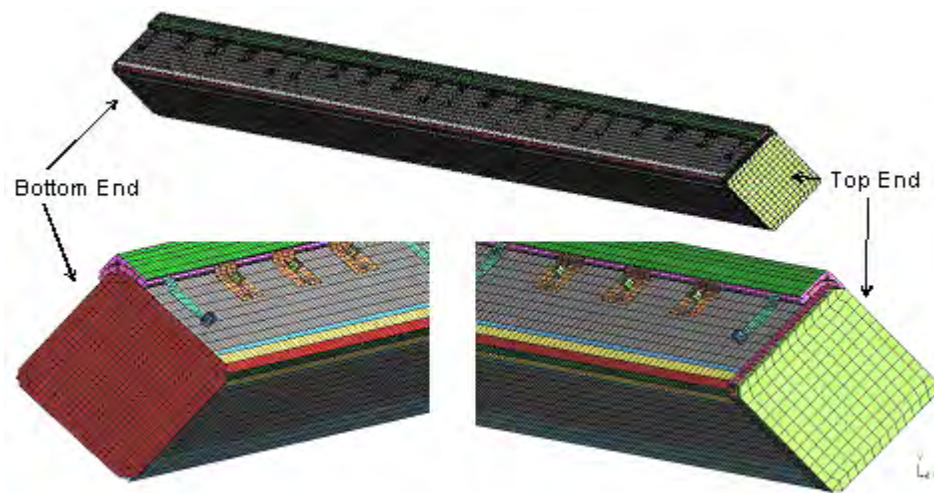


Figure 2-96 Clamshell Mesh in Qualification Unit Model



Figure 2-97 Fuel Assembly in Both Prototype and Qualification Unit Models

The Outerpack hinge details are shown in Figure 2-98. There were three bolts in the upper hinge plate in the Prototype models and only two for the Qualification unit models (shown). The bolts were modeled as spotweld beams. The spotweld beams and hinge plate shared nodes. The spotweld beam node at the hinge block was tied with LS-DYNA's NODAL_RIGID_BODIES. It should be noted that the manner of modeling the bolts allows for compression loading of the bolt, whereas in reality compression loads are not typically carried in bolted joints. However, in the horizontal side impact drops, the bolt heads themselves may impact the drop pad and compressive bolt loads are expected. Thus, our bolt model should be accurate in instances where compressive loads are developed and conservative elsewhere. The hinge pin was simulated using the LS-DYNA REVOLUTE_JOINT feature.

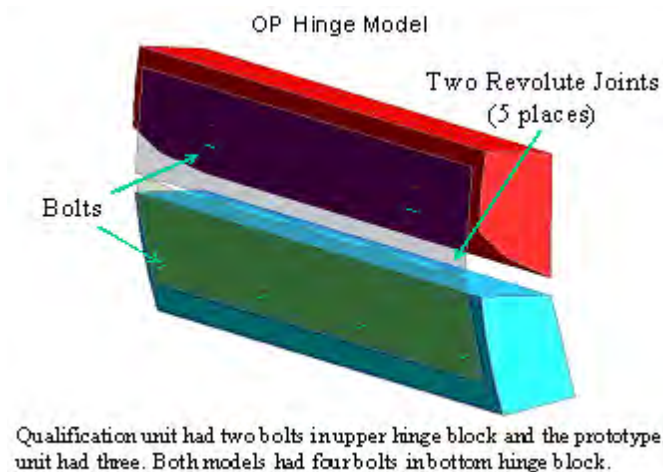


Figure 2-98 Outerpack Hinge Model

2.12.4.5.3 Qualification Unit Models (QTUs)

As with the Prototype units, the QTUs were constructed from many input files, see Figure 2-99. These files defined various details of the model and were included with, or without, transformations of coordinates and renumbering of identities as the model was assembled.

The main file, Aug19.key, contains the control cards, specifies outputs, contact definitions, and many attributes common to more than one subassembly. The major subassemblies were the Outerpack, Clamshell, and fuel assembly. These were defined in the OPs.key, CS_06_26sl6.key, and FA_remesh_FRslip.key files, respectively. The Outerpack and Clamshell subassemblies are detailed in Figures 2-101, 2-102 and 2-103 (The fuel assembly model was very similar to the one depicted previously in Figure 2-97. A total of 361,333 elements were used in the model (185985 shells, 157031 solids and 18317 beams).

The orientation for each run was defined in individual load case files. Likewise, the material property data was defined in three files which represented three different temperatures and foam densities. Obviously, only one load case file and one material file was invoked per run.

The Clamshell, Figure 2-102 is mounted to the Outerpack, Figure 2-100, with 14 rubber shock mounts. These shock mounts were modeled as discrete elements (springs). Outerpack hinge details were described in the previous section, see Figure 2-98.

Predicted model weight was 2.27 tonnes (4994 lbs). This matched the qualification unit's 4786 lb. average weight within 4.4%.

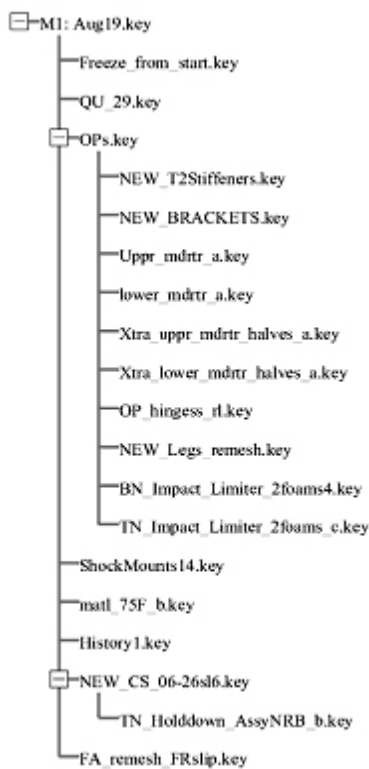


Figure 2-99 FEA Input Files

2.12.4.5.4 Qualification Unit – Outerpack Model Details

The FE model of the outerpack is shown in Figures 2-100 through 2-101A. Key features of the outerpack include the combination circumferential stiffeners/legs, the forklift pockets, the upper and lower outerpack halves, the hinges/latches on the sides, the stacking brackets, and the circumferential stiffeners on the upper outerpack. These features were included in the FE model as described below.

The circumferential stiffeners/legs and forklift pockets (Figure 2-100A) were modeled using 4-node Belytschko-Tsay shell elements (LS-DYNA elform = 2). These elements were integrated at three locations through the thickness using Gaussian quadrature. 1,008 of these elements were used to model the forklift pockets and 4,436 were used modeling the legs.

Both the circumferential stiffeners/legs and forklift pockets are welded to the lower outerpack outer casing. In the model, these parts were attached to one another using a penalty based tied contact algorithm (LS-DYNA's TIED_NODES_TO_SURFACE_OFFSET contact algorithm).

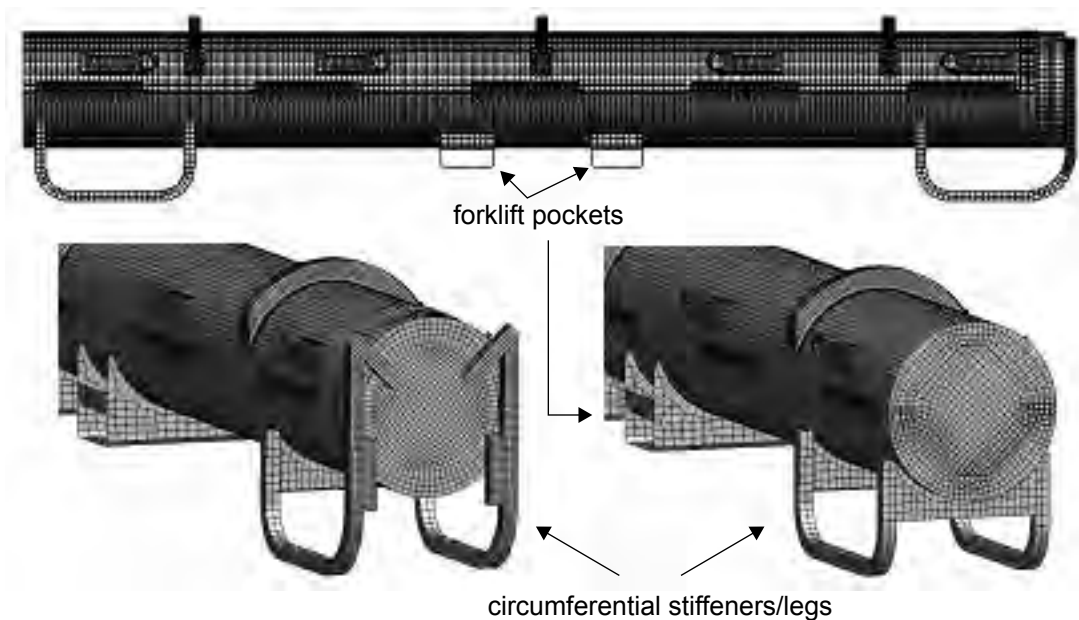


Figure 2-100 Outerpack Mesh in Qualification Unit Model

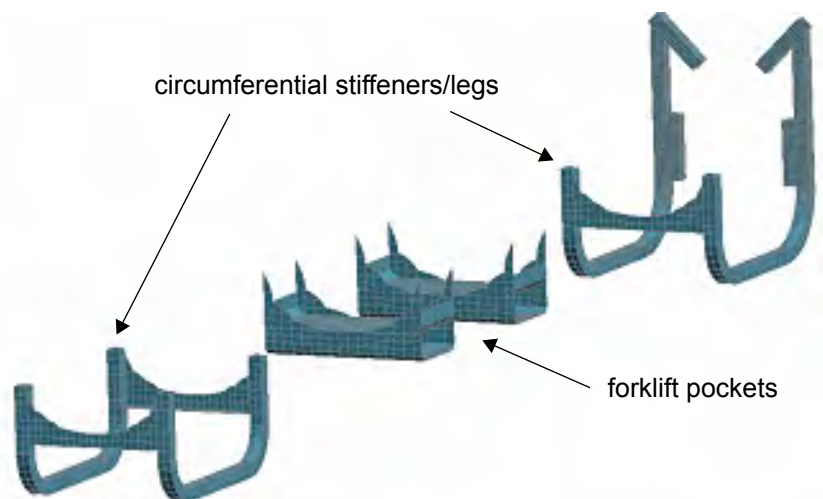


Figure 2-100A FE Meshes of Outerpack Legs and Forklift Pockets

The FE model of the QTU lower outerpack is depicted in Figures 2-100B and 2-100C. In addition to the previously mentioned circumferential stiffeners/legs, the lower outerpack is comprised of a long thick-walled “half-barrel” body and an impact limiter attached to one end (Figure 2-100A). The “half barrel” body is a sandwich construct of 10 pcf foam encased in 0.105 inch thick 304 stainless steel (Figure 2-100C). The outer steel casing was modeled using the same element formulation and integration scheme used for the

circumferential stiffeners/legs. 19,516 elements were required. The 10 pcf foam was modeled using 8 node selectively reduced fully integrated solid elements (LS-DYNA elform = 2) in conjunction with a material formulation developed especially for crushable foam (LS-DYNA material type = 63). Modeling the 10 pcf foam in the lower outpack required 36,617 elements. Since this foam was poured-in-place, it is adhered to the stainless steel casing. This was modeled by enforcing tied contact between the outer nodes of the foam and the casing. The moderator blocks in the lower outpack were modeled using 26,368 constant stress solid elements (LS-DYNA elform =1). Linear elastic material properties were used. The moderator blocks were attached to the lower outpack using four bolts each for the full length moderator sections and two bolts each for the half-length moderator sections at the ends. These bolts were modeled using beam elements (LS-DYNA elform = 9) with a “spot weld” material formulation (LS-DYNA material type = 100.) Contacts between the moderator blocks, the lower outpack, and the clamshell were defined using a penalty-based contact algorithm that accounts for shell thicknesses and for self contact as well as contact between different parts (LS-DYNA’s AUTOMATIC_SINGLE_SURFACE contact algorithm). Contact stiffness was found by dividing the nodal mass by the square of the time step size with a scale factor to ensure stability (LS-DYNA’s SOFT=1 contact option.) This approach was used because the foam has stiffness that is one or more orders of magnitude less than the metal parts. (Contact would possibly have broken down with other approaches that basically use the minimum stiffness of the two contact surfaces.)

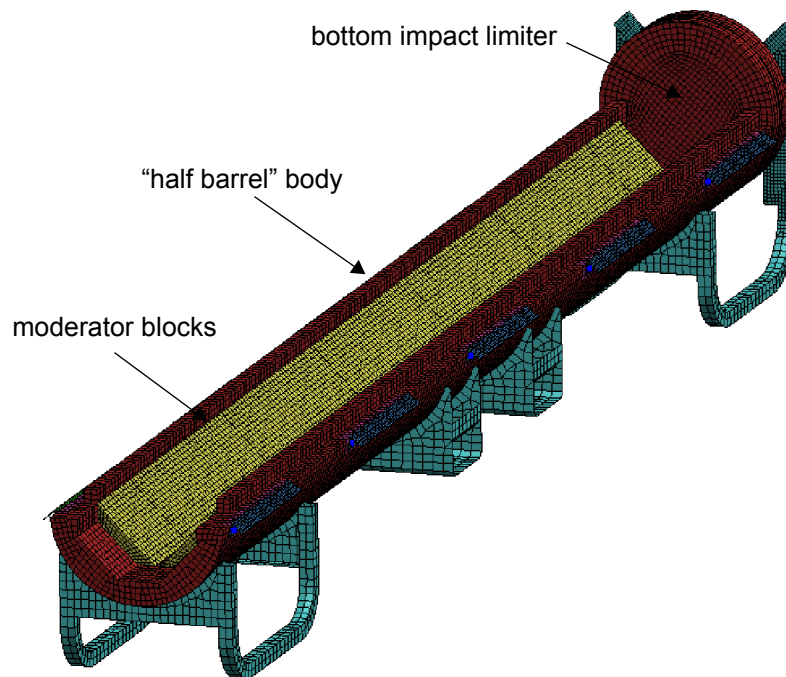


Figure 2-100B Lower Outpack Mesh for Qualification Unit Model

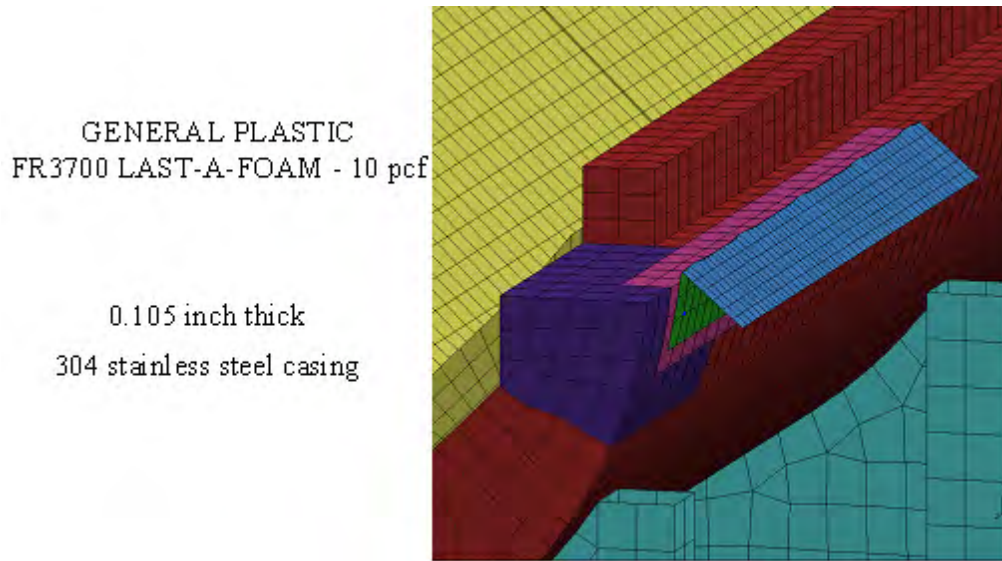


Figure 2-100C Qualification Unit Model Mesh Detail

The FE model of the QTU upper outpack is depicted in Figure 2-100D. It primarily consists of a long thick-walled “half-barrel” body and an impact limiter attached to one end (Figure 2-100D). The “half barrel” body is a sandwich construct of 10 pcf foam encased in 0.105 inch thick 304 stainless steel. The outer steel casing was modeled using the same element formulation and integration scheme used for the circumferential stiffeners/legs and lower outpack casing. 18,634 elements were required. The 10 pcf foam was modeled using 8 node selectively reduced fully integrated solid elements (LS-DYNA elform = 2) in conjunction with a material formulation developed especially for crushable foam (LS-DYNA material type = 63). Modeling the 10 pcf foam in the lower outpack required 36,094 elements. Since this foam was poured-in-place, it is adhered to the stainless steel casing. This was modeled by enforcing tied contact between the outer nodes of the foam and the casing. The moderator blocks in the upper outpack were modeled using 26,368 constant stress solid elements (LS-DYNA elform = 1). Linear elastic material properties were used. The moderator blocks were attached to the upper outpack using four bolts each for the full length moderator sections and two bolts each for the half-length moderator sections at the ends. These bolts were modeled using beam elements (LS-DYNA elform = 9) with a “spot weld” material formulation (LS-DYNA material type = 100). Contacts between the moderator blocks, the upper outpack, and the clamshell were defined using a penalty-based contact algorithm as described for the lower outpack.

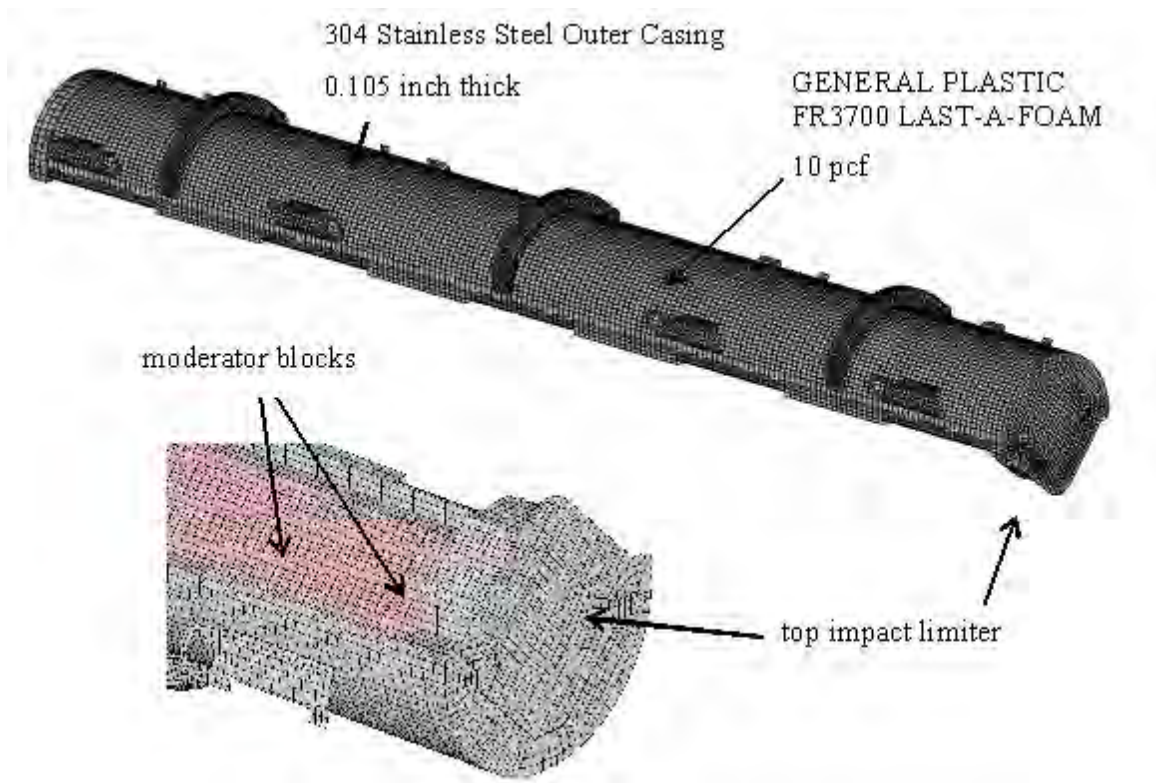


Figure 2-100D Upper Outerpack Mesh for Qualification Unit Model

Model details of the impact limiters are shown in Figure 2-101. Both consisted of two separate foam pieces: a 7 pcf foam block was placed inboard nearest the clamshell and 14 pcf foam covered both ends of the overpacks. These foam pieces were separated and covered by stainless steel. The foams were modeled using the same element formulation and material model as described for the 10 pcf foam in the overpack “barrels” except that each foam density had its own stress-strain curve. The 7 pcf foam in the bottom impact limiter was modeled with 2112 solid elements; the 14 pcf foam was modeled with 4480. The 7 pcf foam in the top impact limiter was modeled with 5248 elements; the 14 pcf foam was modeled with 1755 elements. Because these foams were “cut-to-fit,” they were not bonded to the steel cases. Thus, contact between the steel casings and the foam was defined using LS-DYNA’s AUTOMATIC_SINGLE_SURFACE contact algorithm as previously described (for contact between the lower outerpack, moderator blocks and clamshell).

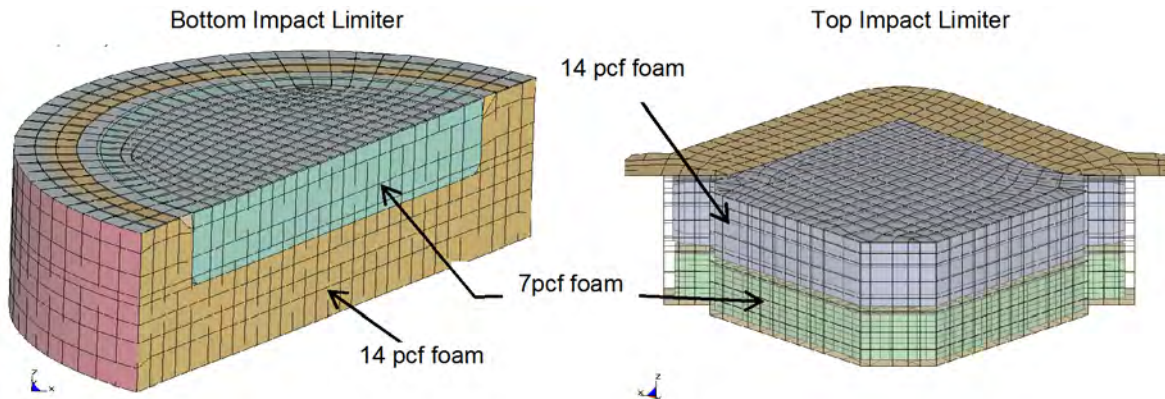


Figure 2-101 Impact Limiter Meshes in Qualification Unit Model

The stacking brackets and circumferential stiffeners on the upper overpack (Figure 2-100D) were modeled using the same element formulation and integration scheme used for the circumferential stiffeners/legs and outerpack casings. 4,404 of these elements were used to model the stiffeners and 1,376 were used modeling the stacking brackets. Both the stiffeners and brackets were secured to the upper outerpack casing using a tied contact algorithm as described for the circumferential stiffeners/forklift pockets and lower overpack casing.

The bolts which secure the outerpack hinges/latches are all that prevent the upper and lower outerpacks from separating upon impact. This was simulated in the model by replication of each physical part of the hinge/latch assemblies. In particular, hinge/latch assemblies including mounting blocks, hinge leaves, and the bolts were modeled (see Figure 2-98 and associated description in Section 2.12.3.5). These assemblies were attached to the upper and lower outerpacks via tied (penalty-based) constraints. This methodology permitted relative rotations between the upper and lower outerpacks along the axes of the hinges/latches while resisting any relative translations. Thus, the model forced the overpack latch bolts to prevent the displacement shown in Figure 2-101A. This allowed predicted deformations at the outerpack seam to be realistic (e.g., Figures 2-30B and 2-74.)

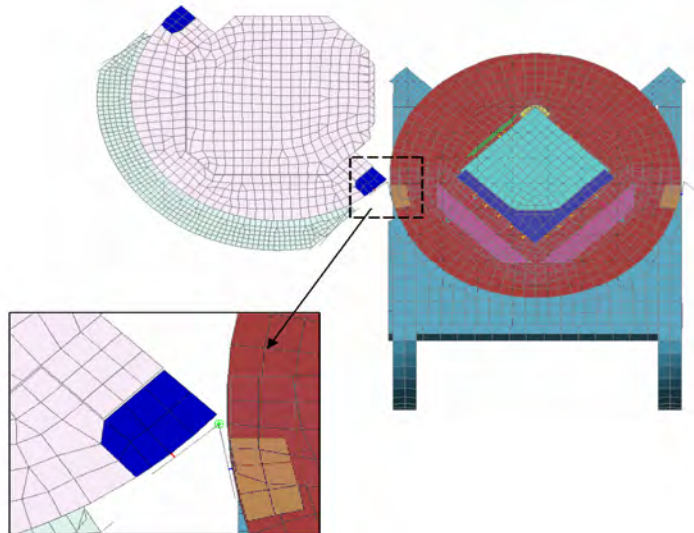


Figure 2-101A Hinge/Latch Feature in Qualification Unit Model

2.12.4.5.5 Qualification Unit – Clamshell Model Details

The FE model of the clamshell is shown in Figures 2-102 through 2-102C. Key features of the clamshell include: the clamshell top assembly, the V-shaped extrusion, the two doors including the hinges, middle latch and locks, and the bottom plate. These features were included in the FE model as described below.

The clamshell top assembly has two major features. First it can swivel from either side to allow access to the top portion of the fuel assembly. This is shown in Figure 2-102A where the CS head is swiveling about its right side. This feature was built into the FE model using the LS-DYNA revolute joint elements. (This is very similar to what was done for the overpack hinges/latches.)

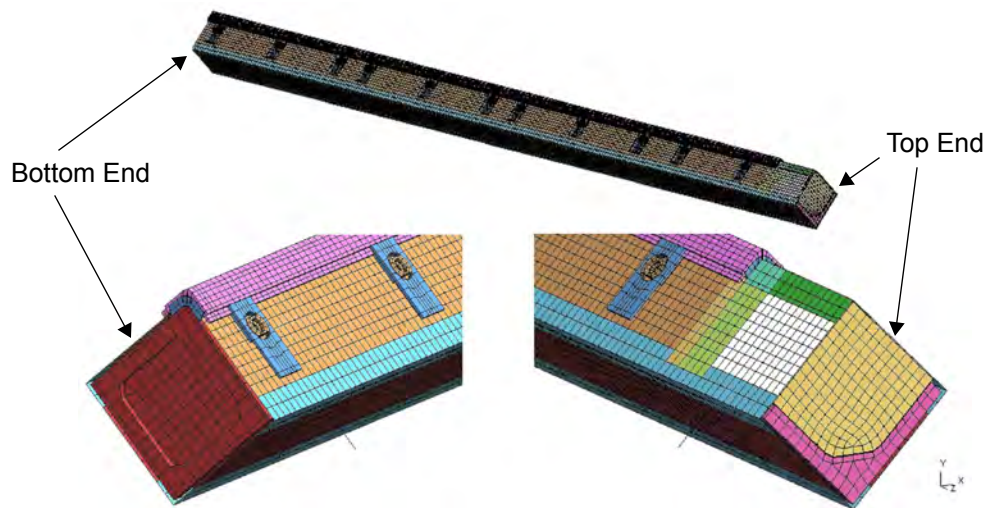


Figure 2-102 Clamshell Mesh in Qualification Unit Model

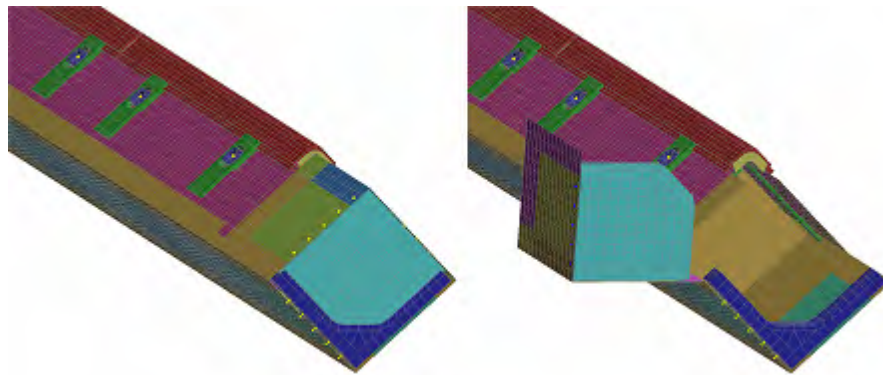


Figure 2-102A Clamshell Top Head in Qualification Unit Model

The second major feature was the top nozzle hold-down bars as shown in Figure 2-102B. Although this hardware has length adjustments to accommodate different fuel assembly heights, the hold-down bar was modeled for the height of an XL fuel assembly. If other fuels were to be modeled, the hold-down bars would need to be scaled in the z-direction. The hold-down bars were modeled with 8 node solid elements and contact between the top nozzle and other fuel and clamshell parts in the near vicinity was defined using LS-DYNA's AUTOMATIC_SINGLE_SURFACE contact algorithm.

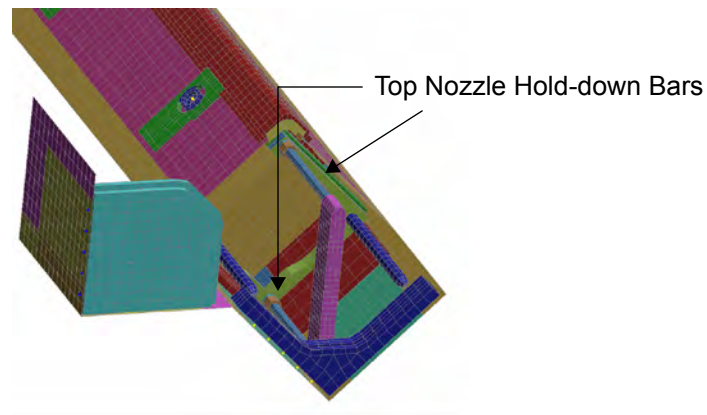


Figure 2-102B Clamshell Top Nozzle Hold-down Bars in Qualification Unit Model

The model of the clamshell latch and hinges allow the doors to rotate about the hinge centerlines as depicted in Figure 2-102C. These features were added using the LS-DYNA revolute joint element as already described.

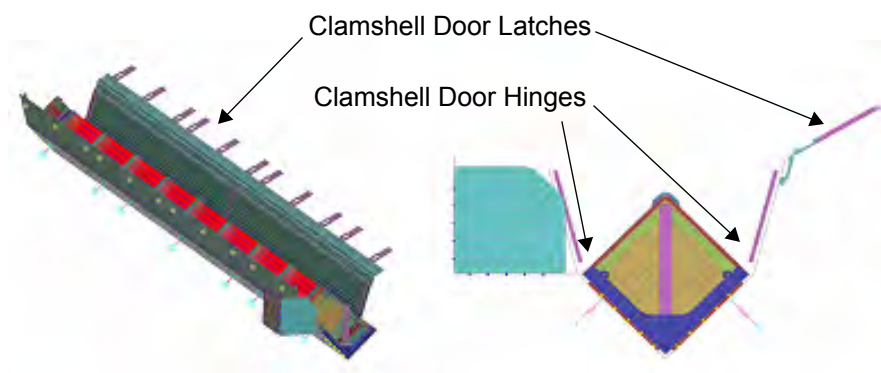


Figure 2-102C Clamshell Hinges and Latches in Qualification Unit Model

2.12.4.6 Model Input

Information needed to construct finite element models of the prototype and qualification units included load and boundary condition details, the stiffness and density of the comprising materials, the shipping package geometry, and the interconnections between the various shipping container subassemblies.

Drop Orientation and Initial Conditions – For modeling convenience, different drop orientations were modeled by changing the velocity and gravitational fields instead of rotating the model relative to the

This page intentionally left blank.

|

model global axes. Loadings were therefore specific to each drop orientation. Further, each analysis was initiated just prior to impact with the shipping package positioned just above the impact surface, having an initial velocity based on drop height (9.14 m for the free drops and 1 m for the pin puncture), and undergoing earth's gravitational pull. This analysis approach minimized computation effort since only minimal calculations of the shipping package during free-fall were needed. The required calculations were as follows.

2.12.4.6.1 Initial Velocity Magnitude (Speed)

The velocity, V , of any object having fallen for a drop height, h , in a constant gravitational field, g , is:

$$V = \sqrt{2gh}$$

Thus, using 9810 mm/s as the value of g , the calculated magnitude of the initial velocities (speed) for the 9 meter free drop and 1 meter pin puncture tests were as shown in Table 2-24.

Table 2-24 Initial Velocities 9 Meter Drop and 1 Meter Pin Puncture Analyses		
Test	Drop Height [m]	Initial Velocity (Speed) [mm/s]
9 m drop		
Prototype model	9.0	13288
Qualification model	9.14 (30 ft)	13389
Pin Puncture		
Prototype & Qualification models	1.0	4429

Velocity and Gravitational Fields – In general, a complete description of the position and orientation of an object in 3-dimensional space requires three coordinates and three direction cosines. However, for these drop tests, specification of only two direction cosines is sufficient. This is because both the drop pad and impact pin may be modeled as two-dimensional rigid walls or surfaces. In other words, these items have no distinct feature with respect to the shipping package that requires specification of the angle θ_y in Figure 2-103. Thus, only the angles θ_x and θ_z are needed to define the velocity and gravitational fields.

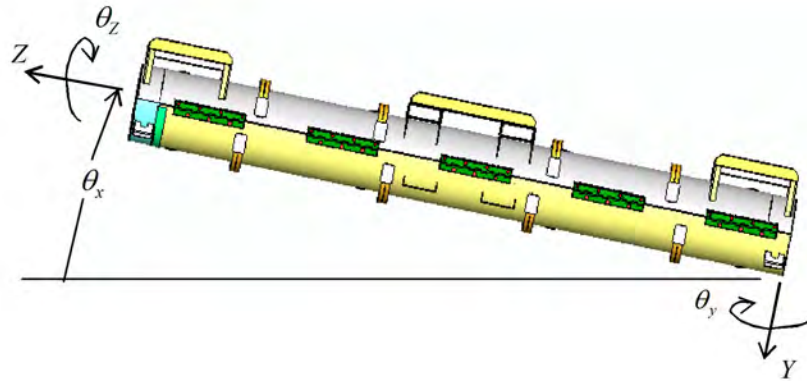


Figure 2-103 Package Drop Angle

Using the angles θ_x and θ_z shown in Figure 2-69, the velocity and gravitational fields are, respectively,

$$v = A^T \begin{Bmatrix} 0 \\ -V \\ 0 \end{Bmatrix}$$

and

$$a = A^T \begin{Bmatrix} 0 \\ g \\ 0 \end{Bmatrix}$$

where

$$A = \begin{bmatrix} \cos \theta_z & \sin \theta_z & 0 \\ \cos \theta_x \cdot \sin \theta_z & \cos \theta_z \cdot \cos \theta_x & -\sin \theta_x \\ \sin \theta_x \cdot \sin \theta_z & \sin \theta_x \cdot \cos \theta_z & \cos \theta_x \end{bmatrix}$$

The normal to the plane of impact (drop pad surface or pin face) is given by

$$n = A^T \begin{Bmatrix} 0 \\ -1 \\ 0 \end{Bmatrix}$$

The initial velocity field was implemented into the finite element model with the *INITIAL_VELOCITY command in LS-DYNA. The gravity field was applied using the *LOAD_BODY_GENERALIZED command. Finally, the impact plane was defined using the *RIGIDWALL_PLANAR or *RIGIDWALL_GEOMETRIC_CYLINDER commands. This approach allowed the drop orientation to be changed without altering the model coordinates. It should be noted that the gravity load was applied as a ramped load as shown in Figure 2-70. This was done as a precaution to minimize any numerical oscillations. However, this was probably unnecessary – applying the full gravity load at time zero would most likely produced equivalent results.

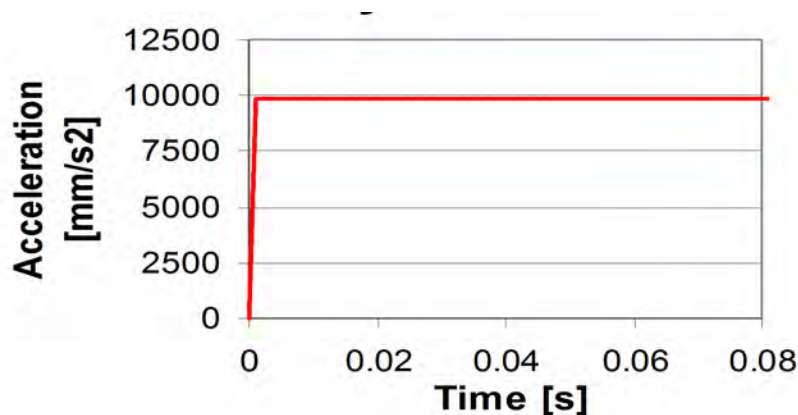


Figure 2-104 Gravity Load Profile

2.12.4.6.2 Material Properties

The crush strength of the polyurethane foam used in the Traveller XL package (LAST-A-FOAM® from General Plastics Manufacturing Company) is strongly influenced by temperature. For example, the perpendicular-to-rise dynamic crush strength of 10 pcf foam at 40% strain is approximately 940 psi at -40°F, 550 psi at 75°F, and just 338 psi at 160°F. Furthermore, foam crush strength is also directly related to foam density. Per the foam procurement specification, density is held within ± 1 pcf for the 7 and 10 pcf foam and $\pm 10\%$ for the 14 pcf foam. Both effects were included in our analyses. This was accomplished by specifying the foam crush strength at highest temperature (160°F) and lowest density (nominal density minus 1 pcf or 10%) and at lowest temperature (-40°F) and highest density (nominal density plus 1 pcf or 10%). Foam stress-strain curves used in the qualification unit analysis are shown in Figure 2-105. These were obtained from General Plastics data except that; 1) the curves were extended past General Plastics' recommend maximum strain limit to fully compressed (100% strain) using linear regressions of the last three known points, and 2) the two most crushable foams (6 pcf @160°F and 7 pcf @75°F) were made to follow the 8 pcf @ -40°F curves at strains above 50%, Figure 2-105). The latter adjustment was needed to prevent the foam elements from inverting under the high strains (i.e., this prevented “negative volumes”).

Stress-Strain Characteristics of General Plastics FR-3700 LAST-A-FOAM

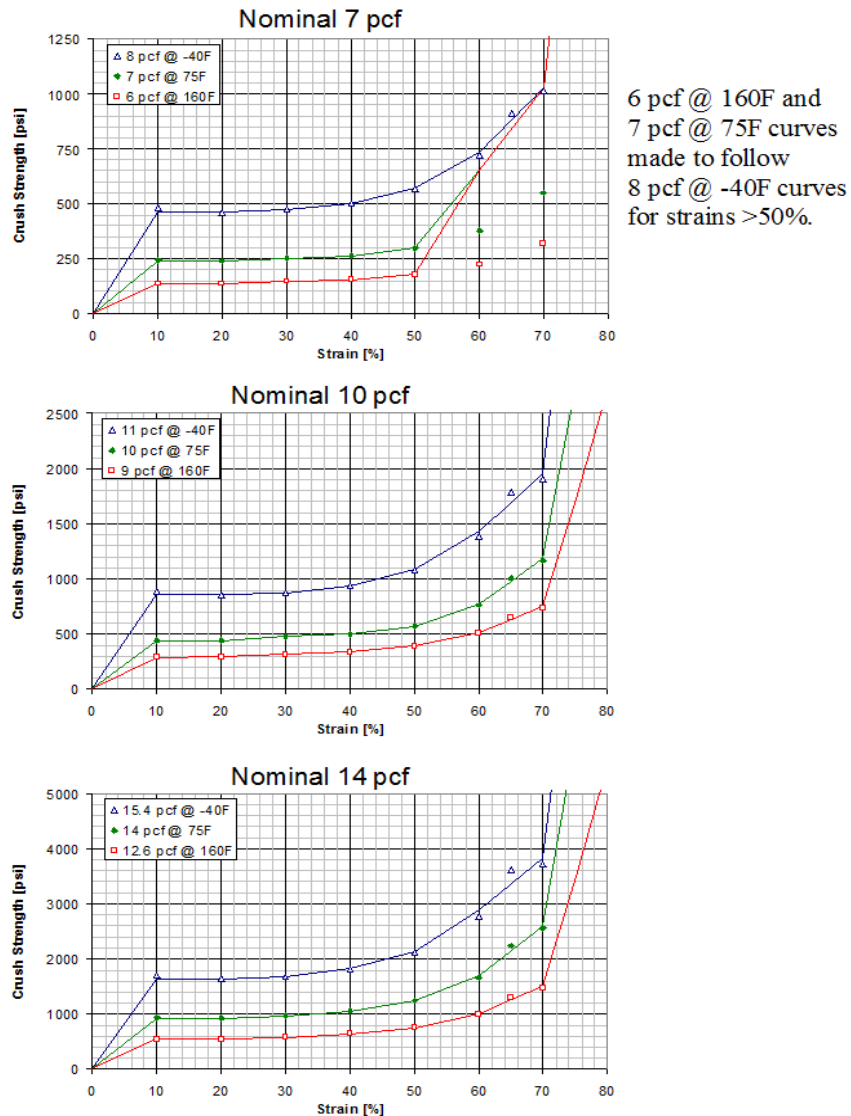


Figure 2-105 Stress Strain Data for LAST-A_FOAM

The use of a linear elastic material model from 0-10% strain was selected to evaluate the effects of temperature and foam density on drop test reaction forces. From Section 2.12.3.2.6, foam linear data demonstrated that temperature and foam density have a minor effect on the drop test response of the Traveller. The use of true stress-strain data ranging from 0-10% would not impact the conclusions of the comparative analysis.

A typical comparison of foam stress-strain behavior demonstrates that the available strain energy of a linear model is less than that observed with true stress-strain data. The use of true stress-strain data is expected to result in greater foam deflection when compared to linear modeling. Since greater crushing would absorb more kinetic energy, the predicted reaction force of the outerpack using true stress-strain data is expected to be less compared to linear data. It is concluded that the use of linear stress-strain data in the 0-10% range adds additional conservatism to the model.

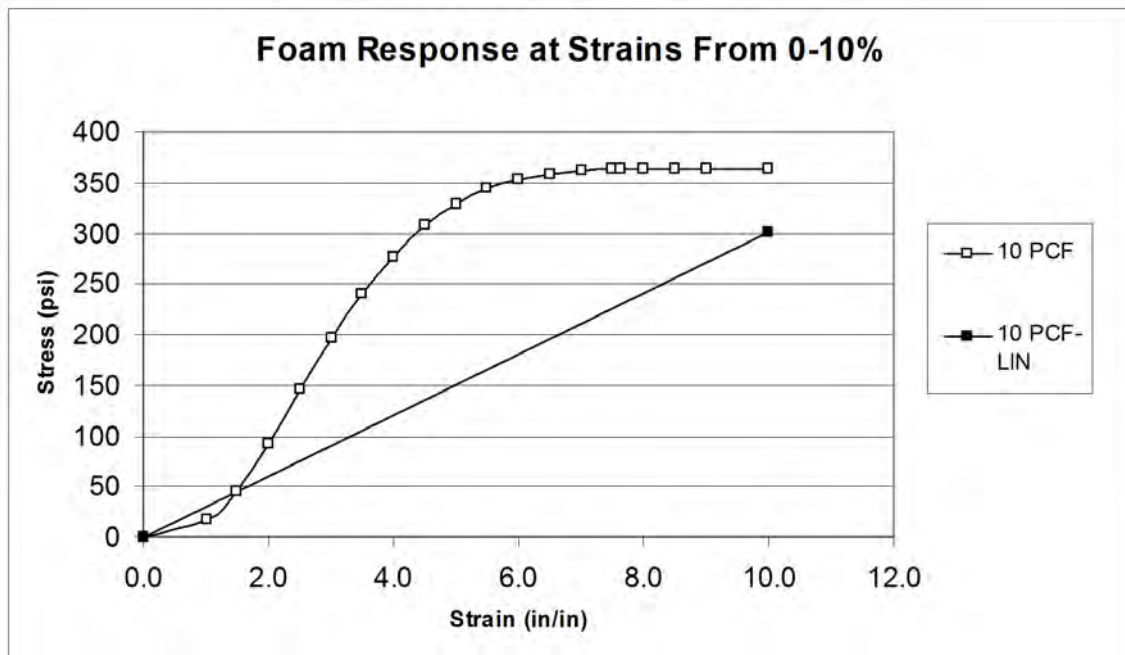


Figure 2-105A Foam Response at Strains from 0-10%

Stress strain characteristics for the 304 stainless steel used in these analyses are shown in Figure 2-106. The 75°F characteristics were obtained from pull tests of samples used in the prototype unit. Based on MIL_HDBK-5H "Metallic Materials and Elements for Aerospace Vehicle Structures," see Figure 2-107, performance at 160°F was estimated by lowering both yield and ultimate strengths to 90% of their values at 75°F. Similarly, the performance at minus 40°F was estimated by raising yield and ultimate strengths to, respectively, 112 and 132% of their values at 75°F, Figure 2-107.

This page intentionally left blank.

|

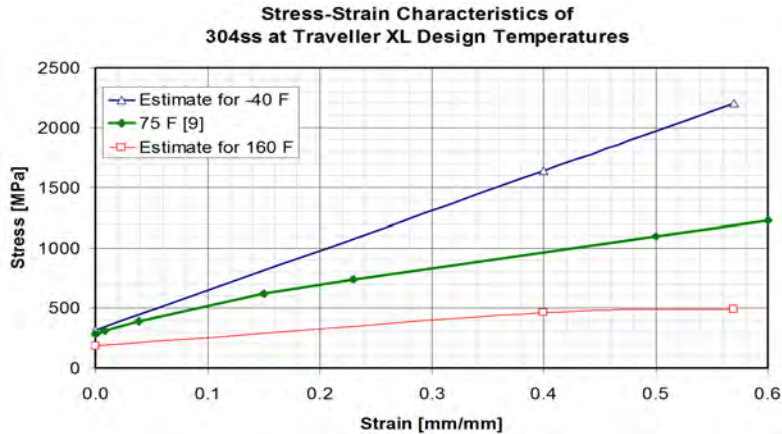


Figure 2-106 Stress-Strain Curves for 304 Stainless Steel

Temperature Effects on Tensile Properties of Annealed Stainless Steel

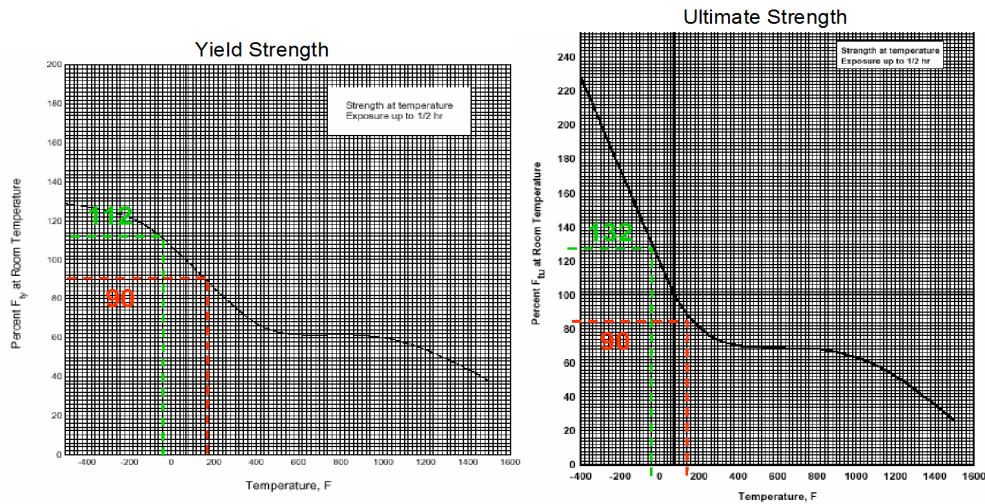


FIGURE 2.7.1.1.1(a) Effect of temperature on the tensile yield strength (F_y) of AISI 301, 302, 304, 304L, 321, and 347 annealed stainless steel. [16]

FIGURE 2.7.1.1.1(b) Effect of temperature on the tensile ultimate strength (F_u) of AISI 301, 302, 304, 304L, 321, and 347 annealed stainless steel. [16]

Figure 2-107 Temperature Effects on Tensile Properties of Annealed Stainless Steel

Estimated stress strain characteristics for the 6005-T5 aluminum used in these analyses are shown in Figure 2-108. The 75°F characteristics are typical of those for 6061-T6 used in the aerospace and automotive industries.¹ The 6005-T5 properties are similar based on their similar yield and ultimate strength and elongation. Because there was no available temperature dependent data, the curves for -40°F and 160°F were estimated based on the temperature dependence of aluminum alloy 6061T6. This was judged acceptable because alloy 6061-T6 is very similar to 6005-T5. However, for conservatism, we doubled

1. This data is not published. However, a similar curve is available from ALCAN

the impact that temperature had on 6061-T6 when estimating the temperature dependence of 6005-T5. For example, yield and ultimate strengths of 6061-T6 at 160°F is expected to be 6 and 4% less than at 75°F, Figure 2-109. However, we estimated these quantities for 6005-T5 by lowering the 75°F values by 12 and 8%. Likewise, when estimating the performance of 6006-T5 at -40°F, we increased the yield and ultimate strengths at 75°F by 8 and 12%, respectively. This is twice the reported impact this temperature reduction has on 6061-T6, Figures 2-109.

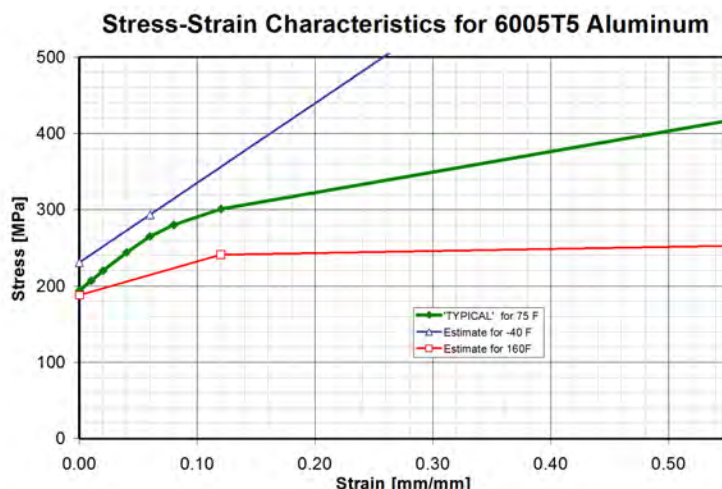


Figure 2-108 Stress-Strain Characteristics of Aluminum in Clamshell

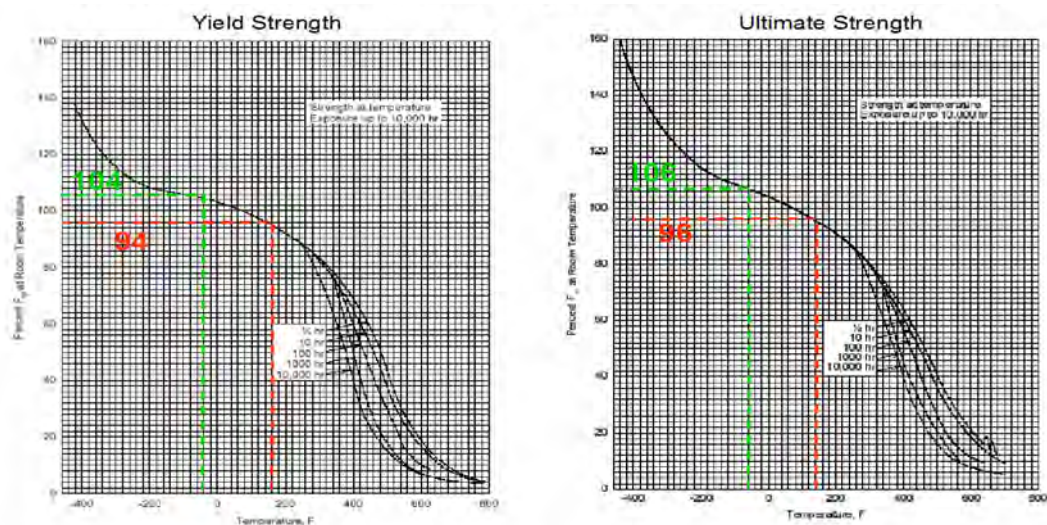


Figure 3-6-2-2 1(b). Effect of temperature on the tensile yield strength (F_y) of 6061-T6 aluminum alloy (all products). [16]

Figure 3-6-2-2 1(a). Effect of temperature on the tensile ultimate strength (F_u) of 6061-T6 aluminum alloy (all products). [16]

Figure 2-109 Temperature Effects on Tensile Properties of Aluminum in Clamshell

Finally, modulus of elasticity and Poisson's ratio are also influenced by temperature. However, this effect is minimal and was neglected in this highly inelastic analysis. Thus, elastic properties determined at 75°F were used in the model. These are shown in Table 2-25.

Table 2-25 Summary of Elastic Properties		
Material	Modulus of Elasticity [GPa]	Poisson's Ratio
304 stainless steel	206.7 ^a	0.32 ^a
6005T5 aluminum	70 [10]	0.3 [10]
Foam	0.37 ^b	N/A
Notes:		
a. This value of modulus is approximately 8% higher than the 192.0 GPa recommended at Westinghouse. This Poisson's ratio is approximately 23% higher than the 0.26 recommendation. However, these elastic values were consistently used and these differences likely had little effect in this highly non-elastic analysis.		
b. Determined by using stress value at 10% strain instead of offset yield point.		

2.12.4.7 Evaluations, Analysis and Detailed Calculations

Many billions of calculations required in these analyses were performed on the HPJ6000 workstation cluster (claxgen1, 2, 3 and 4). However, three additional sets of calculations were required. These were; 1) the calculations of the gravity and velocity fields and the orientation for the rigid wall surface or pin, 2) calculations of bolt factors of safety, and 3) calculations of accelerations from differentiated velocities. Example Calculations of Impact Plane Normal, Gravity Field, and Velocity Field

Horizontal Drop onto Outerpack Latches – A horizontal drop onto the Outerpack latches is shown in Figure 2-26. Using the coordinate system shown in Figure 2-103, this orientation is obtained when $\theta_x = 0$ and $\theta_z = 90^\circ$. Further, $V = 13,389 \text{ mm/s}$ for a 9.14 m drop, Table 2-24, and $g = 9810 \text{ mm/s}^2$. Thus,

$$A = \begin{bmatrix} 0.0 & 1.0 & 0.0 \\ 1.0 & 0.0 & 0.0 \\ 0.0 & 0.0 & 1.0 \end{bmatrix},$$

$$n = \begin{bmatrix} 0.0 & 1.0 & 0.0 \\ 1.0 & 0.0 & 0.0 \\ 0.0 & 0.0 & 1.0 \end{bmatrix}^T \cdot \begin{bmatrix} 0 \\ -1 \\ 0 \end{bmatrix} = \begin{bmatrix} 1 \\ 0 \\ 0 \end{bmatrix},$$

$$v = \begin{bmatrix} 0.0 & 1.0 & 0.0 \\ 1.0 & 0.0 & 0.0 \\ 0.0 & 0.0 & 1.0 \end{bmatrix}^T \cdot \begin{bmatrix} 0 \\ -13,389 \\ 0 \end{bmatrix} = \begin{bmatrix} -13,389 \\ 0 \\ 0 \end{bmatrix},$$

and

$$g = \begin{bmatrix} 0.0 & 1.0 & 0.0 \\ 1.0 & 0.0 & 0.0 \\ 0.0 & 0.0 & 1.0 \end{bmatrix}^T \cdot \begin{Bmatrix} 0 \\ 9,810 \\ 0 \end{Bmatrix} = \begin{Bmatrix} 9,810 \\ 0 \\ 0 \end{Bmatrix}$$

Example Calculation of Bolt Factor of Safety – The equation below is utilized to calculate bolt factor of safety. For example, suppose a Clamshell bolt is subjected to an axial force of 5,134 lb_f and shear forces of 925 and 3380 lb_f. A factor of safety is calculated by first calculating the “Actual” (load) using these values of load, Table 2-26.

$$\begin{aligned} Actual &= \left(\frac{F_{axial}}{FN_{ult}} \right)^2 + \left(\frac{F_{yshear}}{FS_{ult}} \right)^2 + \left(\frac{F_{zshear}}{FS_{ult}} \right)^2 \\ &= \left(\frac{5,134}{12,070} \right)^2 + \left(\frac{925}{6,040} \right)^2 + \left(\frac{3,380}{6,040} \right)^2 \\ &= 0.5175 \end{aligned}$$

This value must be divided into the “Allowable” which is 1.0. Thus, the factor of safety for the bolt in this example is 1.93. (These loads correspond to those predicted for the Clamshell keeper bolt which is third down from the top end of the Clamshell during a horizontal side drop onto the latches at time 0.0072s. The calculated value for factor of safety corresponds to that shown in Table 2-11.

Description of Acceleration Calculations – Predicted accelerations, as shown in Figures 2-88 through 2-92, were obtained by differentiating predicted nodal velocities sampled at a frequency of 4 KHz and applying a “light” (SAE 180 Hz) filter. This technique was used because the finite-difference technique used in LS-DYNA yields very noisy accelerations. These nodal accelerations are indeed accurate in an average sense, but not in an absolute value. The differentiated velocity technique allowed the true trend in accelerations to be discerned. The calculations were accomplished with the LS-POST program.

2.12.4.8 Accelerometer Test Setup

Prior to testing, piezoelectric accelerometers were mounted on the Outerpack and Clamshells of both test prototypes. The intent was to measure the accelerations at a few critical points so that the forces involved in the drops would be better known and so that the FEA results could be validated.

Three accelerometers were positioned on the Prototype Unit-1 Test series 1, Figure 2-110. One accelerometer was on the Clamshell top plate and thus was near the initial impact end. The other two were positioned on the secondary impact end at the Clamshell bottom plate and bottom impact limiter. Further details of this instrumentation are available in Appendix 2.12.5.

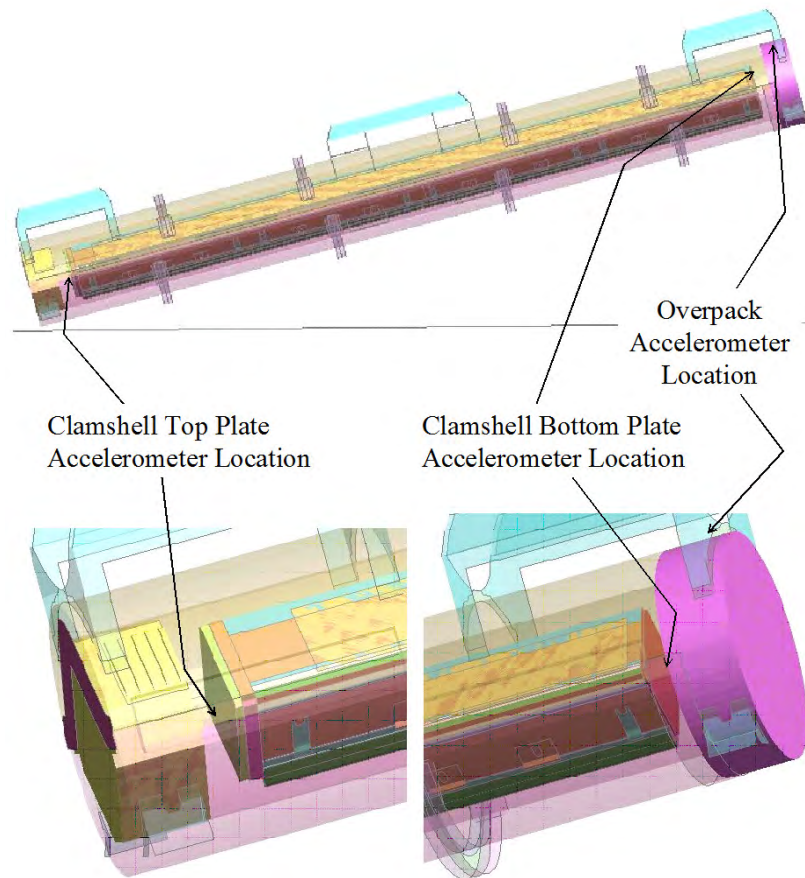


Figure 2-110 Accelerometer Locations on Prototype Unit 1

2.12.4.9 Bolt Factor of Safety Calculation

Bolt factors of safety (FS)

$$F.S. = \frac{\text{Allowable}}{\text{Actual}} \quad (H-1)$$

were based on the failure criteria

$$\left(\frac{F_{\text{axial}}}{F_{N_ult}} \right)^2 + \left(\frac{F_{\text{yshear}}}{F_{S_ult}} \right)^2 + \left(\frac{F_{\text{zshear}}}{F_{S_ult}} \right)^2 \geq 1. \quad (H-2)$$

This commonly-used criterion was chosen because it accounts for the effects of both axial and shear forces. (Note: the left side of equation H-2 is the “Actual” in equation H-1 and the “Allowable” is unity.)

The loads in equation H-2 were determined from the finite element analysis; the tensile and shear strengths are shown in Table 2-26. Initially, the tensile strengths were estimated from the tensile to proof strength ratios for Grade 2 bolts, Tables 2-27 and 2-28, obtained from. Use of the ratios obtained for Grade 2 bolts was justified because the proof strengths of these bolts should be just above Grade 2 levels based on their minimum strength of 70 ksi. However, bolt strengths estimated in this manner did not result in adequate factors of safety for each Outerpac bolt when the Traveller XL package was dropped horizontally, Figure 2-26. However, the specification for the Outerpac bolts was changed in the design of the CTU unit. The new bolt specification for CTU and production packages is ASTM A193 Class 1 B8 which has an ultimate tensile strength minimum of 75 ksi. Additionally, the number of Outerpac hinge bolts has increased to 12 bolts per side on the top leaf and bottom hinge leaf for both the XL and STD packages. This increase in the number of bolts, and the increase in strength results in a factor of safety of 1.12 for the bounding Traveller XL's worst bolt, in the worst case bolt failure orientation (the side drop).

Table 2-26 Bolt Strength Summary							
Location	Size	Thread Area [in ²] [13]	Minimum Yield Strength [ksi]	Estimated Minimum Proof Strength [lbf] ⁽¹⁾	Ratio of Tensile to Proof Strength ⁽²⁾	FN_ult [lbf]	NS_ult [lbs] ⁽⁵⁾
CS bolts	1/2"-13	0.142	70 [14]	8,940	1.35	12,070 ⁽³⁾	6,040
Bottom OP hinge bolts	5/8"-11	0.226	70 [14]	14,240	1.35	19,200 ⁽³⁾	9,600
Top OP hinge bolts	3/4"-10	0.334	70 [14]	21,040	1.34	28,200 ⁽³⁾	14,100
			100 [18]	30,060	N/A	41,750 ⁽⁴⁾	20,900
Notes:							
(1) 0.9 * thread area * min yield strength							
(2) Based on estimated proof strength and Table 2-28							
(3) Estimated min proof strength * ratio of Tensile to proof strength							
(4) Minimum Ultimate Tensile Strength of 125 ksi * thread area							
(5) 0.5 *FN_ult							

Table 2-27 Strengths of Various Classifications of Bolts [14]															
Nominal Dia of Product and Threads per in	Stress Area, in ²	Grade 1		Grade 2		Grade 4		Grades 5 and 5.2		Grade 5.1		Grade 7		Grades 8, 8.1, and 8.2	
		Proof Load, lb	Tensile Strength min, lb	Proof Load, lb	Tensile Strength min, lb	Proof Load, lb	Tensile Strength min, lb	Proof Load, lb	Tensile Strength min, lb	Proof Load, lb	Tensile Strength min, lb	Proof Load, lb	Tensile Strength min, lb	Proof Load, lb	Tensile Strength min, lb
Coarse-Thread Series – UNC															
No. 6-32	0.00909	–	–	–	–	–	–	–	–	750	1,100	–	–	–	–
8-32	0.0140	–	–	–	–	–	–	–	–	1,200	1,700	–	–	–	–
10-24	0.0175	–	–	–	–	–	–	–	–	1,500	2,100	–	–	–	–
12-24	0.0242	–	–	–	–	–	–	–	–	2,050	2,900	–	–	–	–
1/4-20	0.0318	1,050	1,900	1,750	2,350	2,050	3,650	2,700	3,800	2,700	3,800	3,350	4,250	3,800	4,750
5/16-18	0.0524	1,750	3,150	2,900	3,900	3,400	6,000	4,450	6,300	4,450	6,300	5,500	6,950	6,300	7,850
3/8-16	0.0775	2,550	4,650	4,250	5,750	5,050	8,400	6,600	9,300	6,600	9,300	8,150	10,300	9,300	11,600
7/16-14	0.1063	3,500	6,400	5,850	7,850	6,900	12,200	9,050	12,800	9,050	12,800	11,200	14,100	12,800	15,900
1/2-13	0.1419	4,700	8,500	7,800	10,500	9,200	16,300	12,100	17,000	12,100	17,000	14,900	18,900	17,000	21,300
9/16-12	0.182	6,000	10,900	10,000	13,500	11,800	20,900	15,500	21,800	15,500	21,800	19,100	24,200	21,800	27,300
5/8-11	0.226	7,450	13,600	12,400	16,700	14,700	25,400	19,200	27,100	19,200	27,100	23,700	30,100	27,100	33,900
3/4-10	0.334	11,000	20,000	18,400	24,700	21,700	38,400	28,400	40,100	–	–	35,100	44,400	40,100	50,100
7/8-9	0.462	15,200	27,700	15,200	27,700	30,000	53,100	39,300	55,400	–	–	48,500	61,400	55,400	69,300
1-8	0.606	20,000	36,400	20,000	36,400	39,400	69,700	51,500	72,700	–	–	63,600	80,600	72,700	90,900
1-1/8 - 7	0.763	25,200	45,800	25,200	45,800	49,600	87,700	56,500	80,100	–	–	80,100	101,500	91,600	114,400
1-1/4 - 7	0.969	32,000	58,100	32,000	58,100	63,000	111,400	71,700	101,700	–	–	101,700	127,700	116,300	145,400
1-3/8 - 6	1.155	38,100	69,300	38,100	69,300	75,100	132,800	85,500	121,300	–	–	121,300	153,600	138,600	173,200
1-1/2 - 6	1.405	46,400	84,300	46,400	84,300	91,300	161,600	104,000	147,500	–	–	147,500	186,900	168,600	210,800

Table 2-28 Bolt Strength Ratio						
Size	Tensile to Proof Strength Ratio					
	Grade 1	Grade 2	Grade 4	Grades 5, 5.1 and 5.2	Grade 7	Grades 8, 8.1 and 8.2
½-13	1.81	1.35	1.77	1.40	1.27	1.25
5/8-11	1.83	1.35	1.73	1.41	1.27	1.25
¾-10	1.82	1.34	1.77	1.41	1.26	1.25

2.12.5 TRAVELLER DROP TESTS RESULTS

Three series of full scale drop tests have been performed on the Traveller package to evaluate the performance of the design. This appendix will summarize structural performance of the Traveller during these tests. The objectives, test articles, results and lessons learned will be described. The three series were:

- Prototype Tests
- Qualification Tests
- Certification Tests

2.12.5.1 Prototype Test Unit Drop Tests

Testing was conducted at Columbiana High Tech Company (CHT) in Columbiana, Ohio during the week of January 27-30, 2003 (Ref. 3).

An as-built Traveller package prototype is shown in Figures 2-111 and 2-112. Figure 2-111 shows the internal packaging including the 17x17 XL fuel assembly, Clamshell, and moderator blocks. Figure 2-112 shows the closed Outerpack. The prototype packages employed 11 pcf foam along the axial section of the package and 16 pcf foam in the endcaps. Furthermore, the Outerpack consisted of 11 gage inner and outer skin. Each package also contained 22 shock mounts to connect the Clamshell to the Outerpack.

Test Series 1 – Test series 1 was conducted on January 27th through 28th and included two 9 meter drop tests plus a pin-puncture test. The package's test weight was 5072 pounds. Drop orientations are shown in Figure 2-113 and Table 2-29.

The Outerpack retained its basic circular pre-test shape except for localized plastic deformation from the 9 meter drop tests and the pin-puncture test. One bolt on the lower Outerpack hinge failed after completion of the last 9 meter drop test. The Outerpack did not separate after any impacts, and the pin did not perforate the inner or outer shell. The internal damage was minimal. The fuel assembly's envelope decreased from 8.418" nominal to 8.25" maximum after the first 9 meter drop test, and reduced further to 8.13" maximum after second 9 meter drop test. Fuel rod gaps globally decreased (the fuel envelope decreased), but local expansion was noted between a few rods with a maximum measured gap of .188" for the first 9 meter drop test and .625" maximum measured gap for second 9 meter drop test (compared to the nominal gap of .122"). The polyethylene moderator blocks and aluminum neutron "poison plates" maintained position. The Clamshell doors remained closed, but the top and bottom heads were separated from the Clamshell. The separation was caused by the fuel assembly deceleration forces reacting against the clamshell end plate. The bearing force of the bolts (a shear effect on the top head plate) from impact was sufficient to fail the material in the bolt slots for both head pieces. The fuel inspection indicated that no fuel rods had ruptured, and that the axial position of fuel rods maintained location between bottom and top nozzle. The failure the clamshell endplates was due to the bolt slots being modified as a result of warping of the clamshell during fabrication.

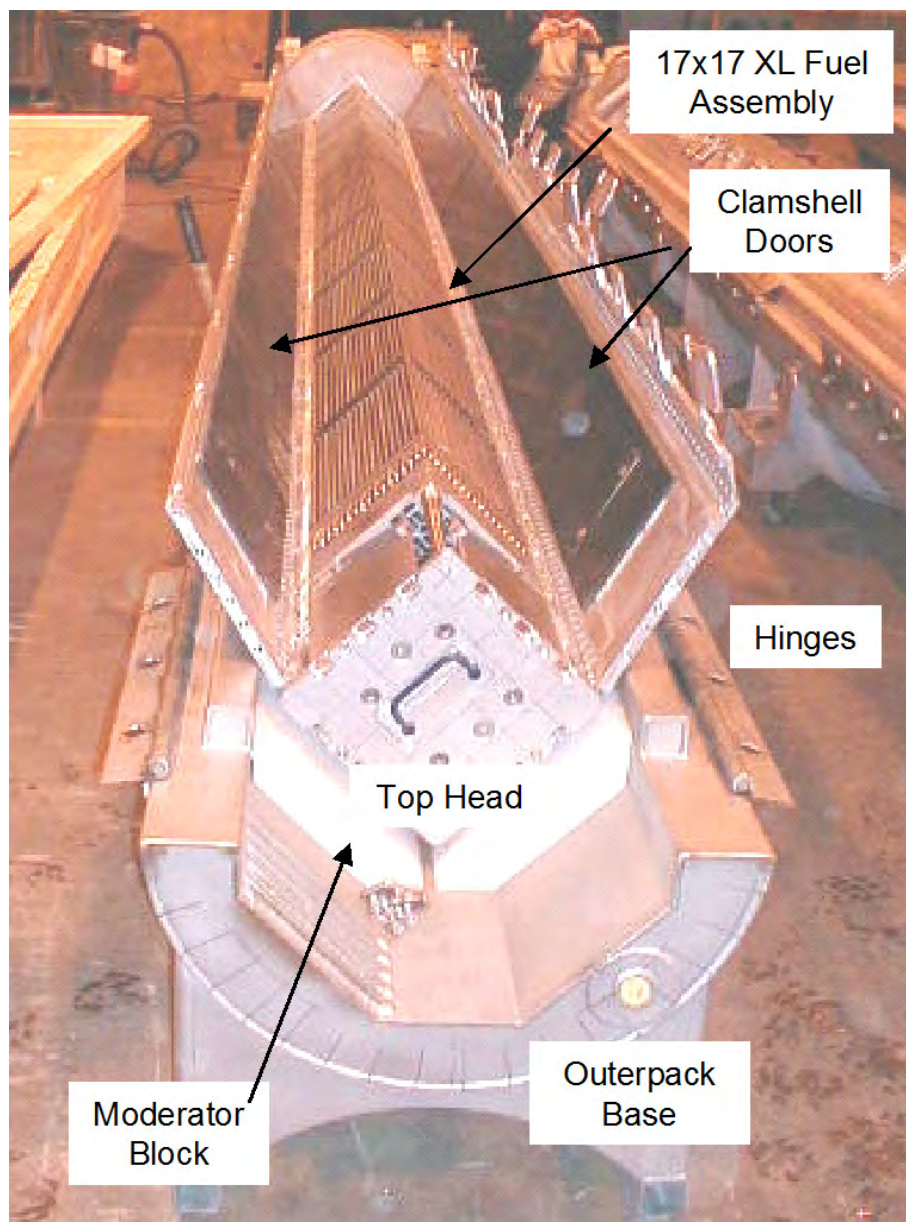


Figure 2-111 Traveller Prototype Internal View

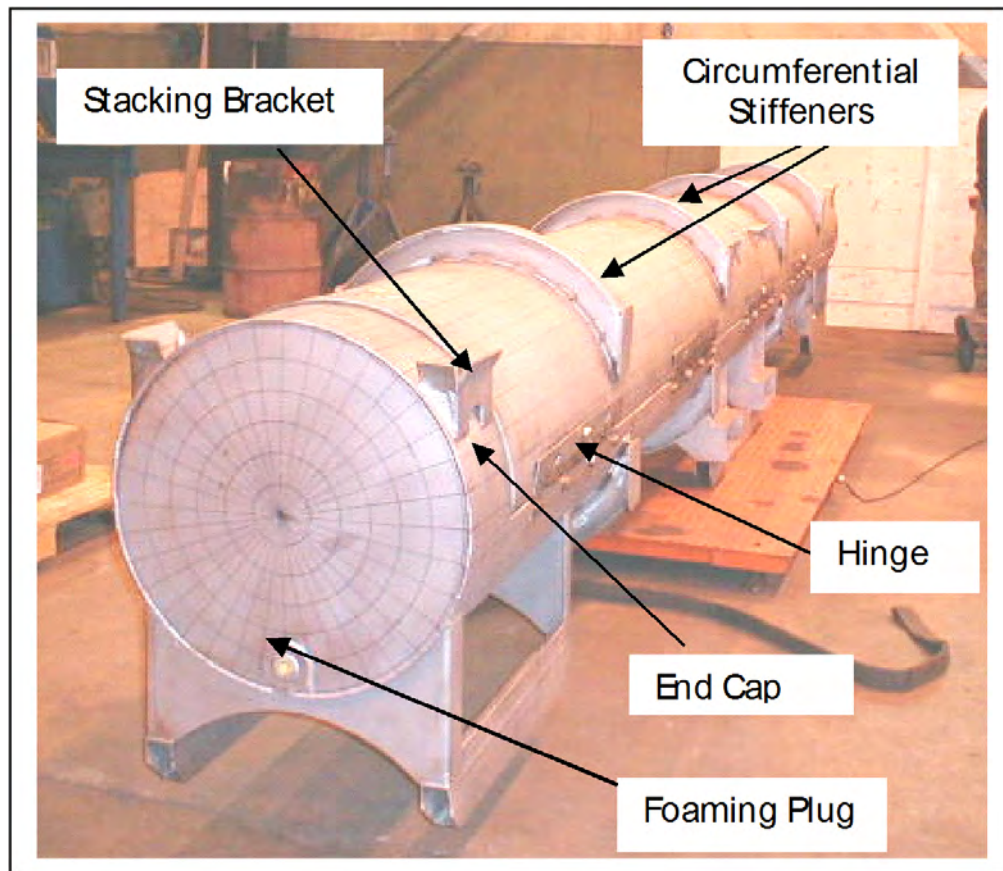


Figure 2-112 Traveller Prototype External View

Table 2-29 Series 1 As-Tested Drop Conditions			
Test Sequence	Test Pitch Attitude	Test Roll Attitude	Impact Location
1.1) 9 m Low Angle	14.5°	180°	T/N primary impact on OP top
1.2) 9 m CG-over-corner	71°	90°	B/N primary impact on OP hinge
1.3) 1 m Pin-puncture	20°	180°	Center of Gravity (Axial) on OP top, T/N end down

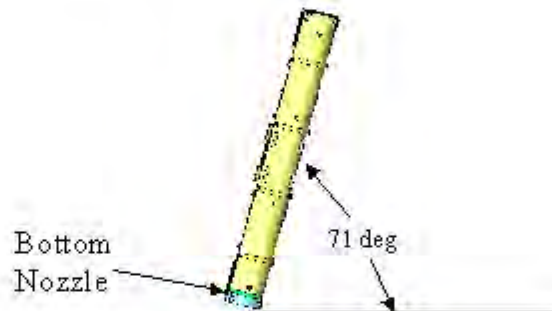
Test 1.1 – The Outerpack retained its basic circular pre-test shape except for localized plastic deformation from the 9 meter drop test. Impact zones from the drop test were localized at the nozzle impact locations on the package ends. The Outerpack did not separate after the impact, and no bolt failures on the Outerpack hinge were noted. The top nozzle damage zone consisted of local crush approximately 12" wide, 9" axially and a maximum crush of approximately 1.5". The circumferential stiffeners were crushed (Figure 2-114) and inhibited global crushing on the Outerpack. The bottom nozzle damage zone consisted of local crush approximately 11.5" wide, a maximum crush of approximately 3/4", and axially from the package end to

the edge of the stiffening ring. The internal damage was minimal as shown in Figures 2-113 and 2-114. The polyethylene moderator blocks and aluminum neutron “poison plates” maintained position. The Clamshell doors remained closed, but the Clamshell bulged outwardly approximately 0.25" locally at the grid locations in a section 54" long at the bottom nozzle end. The fuel inspection indicated that no fuel rods had ruptured, and that the axial position of fuel rods maintained location between bottom and top nozzle. The average measured fuel envelope decreased from 8.418" nominally to 8.25" maximum, and the maximum measured fuel rod gap was found to be 0.188" locally (observed at one or two rods along the envelope) compared to the nominal gap of 0.122". Figures 2-114 and 2-115 summarize the results of this drop test.

Test 1.1
9 m Low Angle
Slap Down



Test 1.2
9 m CG over corner
on Hinge



Test 1.3
1m Pin Puncture

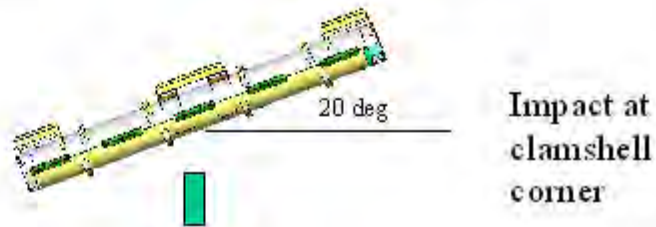
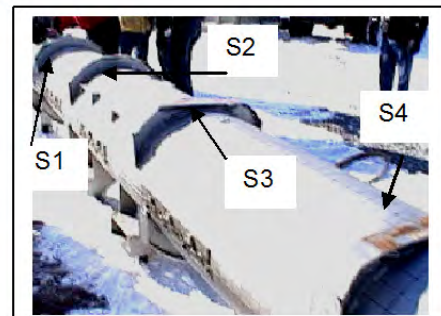
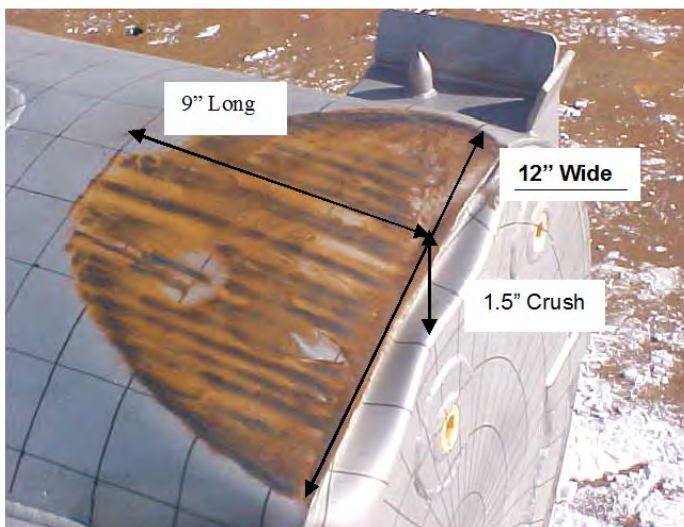
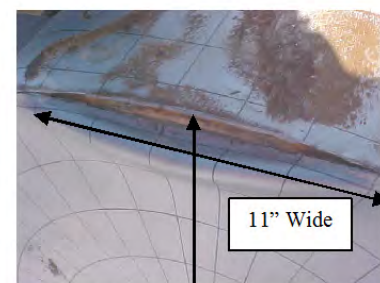
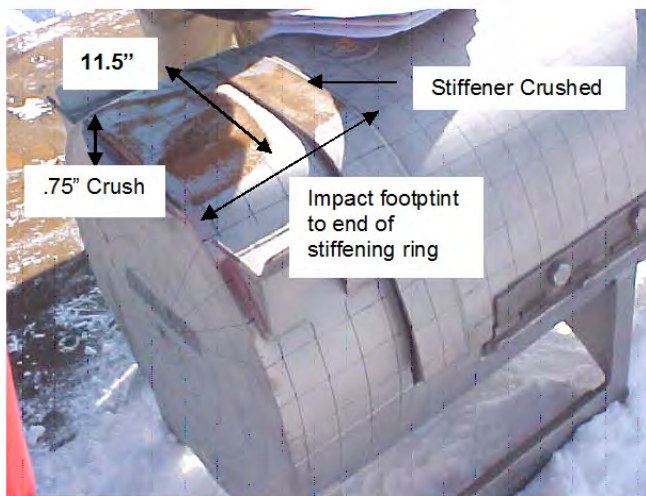


Figure 2-113 Drop Orientations for Prototype Test Series 1



Stiffening rings show
progressive damage from T/N



Small tear at Bottom End
cap/Plate Seam

Figure 2-114 Traveller Prototype Exterior After Test 1.1

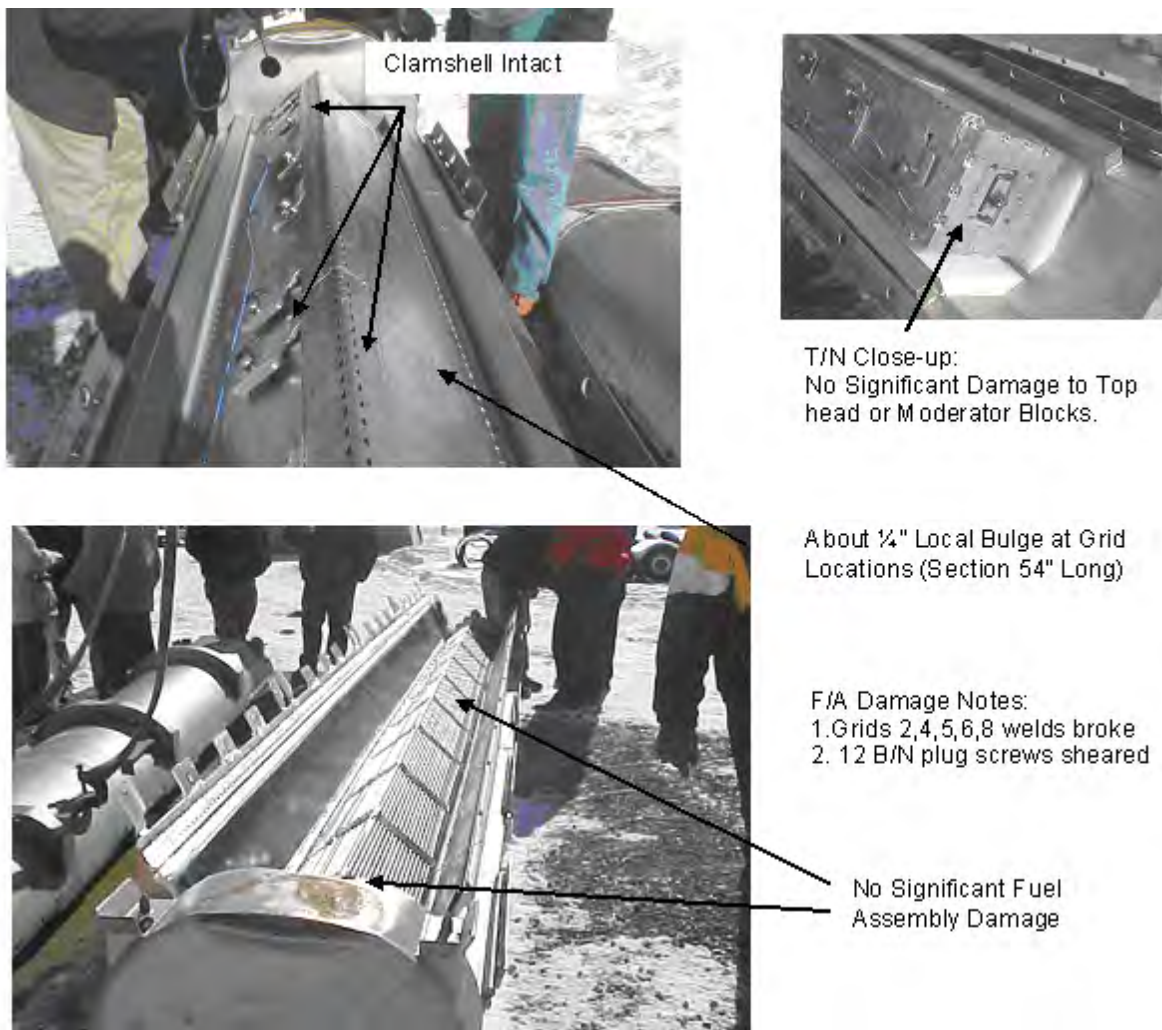


Figure 2-115 Traveller Prototype Interior After Test 1.1

Test 1.2 – The Outerpack retained its basic circular pre-test shape except for localized plastic deformation from the 9 meter drop test. Impact zones from the drop test were localized at the nozzle impact locations on the package ends. The Outerpack did not separate after the impact. One bolt failure on the Outerpack lower hinge, top nozzle end was noted. The bottom nozzle damage zone consisted of local crush approximately 10" wide, 22" tall and a maximum crush of approximately 3". The impact encompassed the stacking bracket which caused local buckling at the top/bottom Outerpack joint. A small ripple occurred in the Outerpack at this location. In addition, a tear in the Outerpack end cap measuring 8" wide resulted from the impact. The top nozzle damage zone consisted of local crush approximately 6" wide, 13" long and a maximum crush of approximately 1/4". The relatively small amount of crushing is attributed the stacking bracket impacting the Outerpack in a normal direction and spreading the load more uniformly along the Outerpack length. The internal damage was more substantial than the previous drop test. The polyethylene moderator blocks and aluminum neutron "poison plates" maintained position. The Clamshell doors remained closed, but the top

and bottom head pieces separated from the Clamshell. The separation was caused by material shear-out as the top head connector bolts beared against the bolt slots. The bearing force of the bolts (a shear effect on the top head plate) from impact was of sufficient load to fail the material in the bolt slots for both head pieces. The fuel inspection indicated that no fuel rods had ruptured, and that the position of fuel rods maintained axial location between bottom and top nozzle. The maximum measured fuel envelope compressed from 8.25" after test 1.1 to 8.13", and the maximum measured fuel rod gap increased from 0.188" to 0.625" locally (observed at one or two rods along the envelope). The fuel rod gap expansion was also localized to Grids P, 1, 2, 3, and 4. In addition, Grid 2 failed by means of the weld joint tearing on the grid corner. External and internal results are summarized in Figures 2-116 and 2-117.

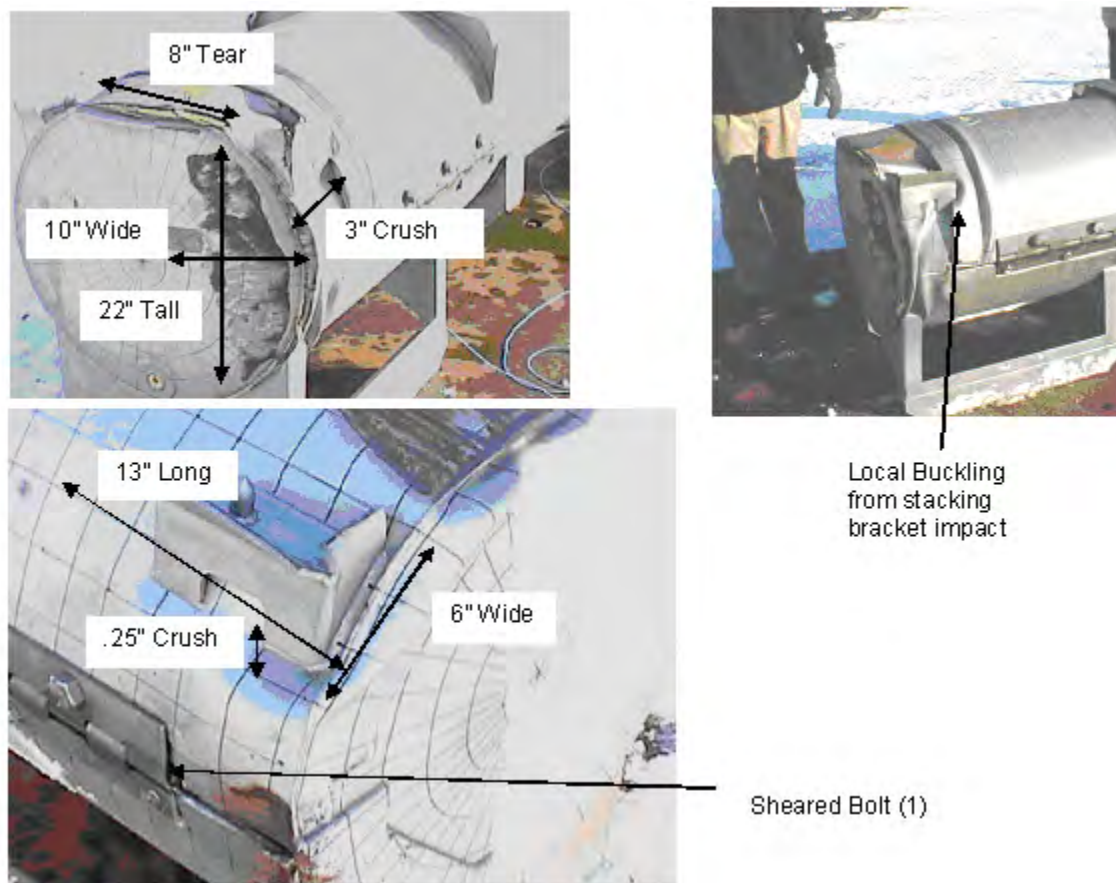


Figure 2-116 Traveller Prototype Exterior After Test 1.2

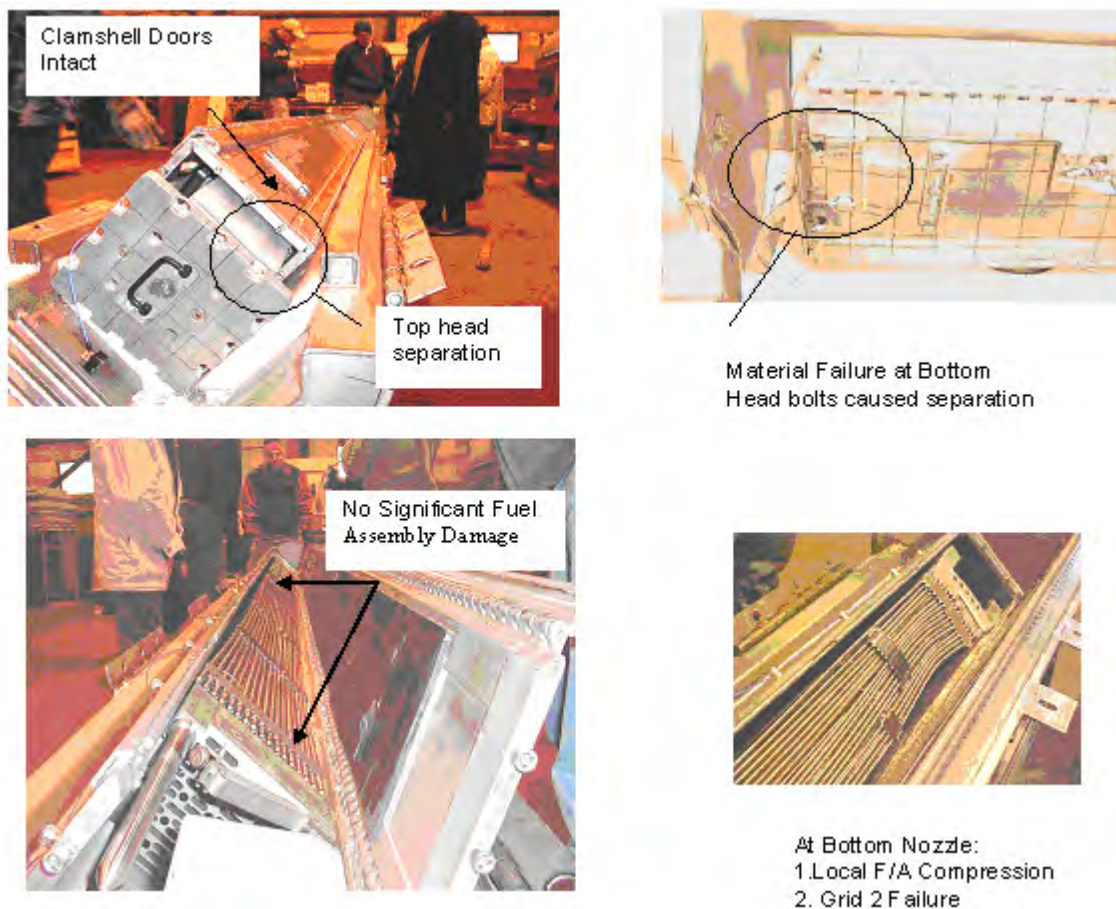


Figure 2-117 Traveller Prototype Interior After Test 1.2

Piezoelectric accelerometers were mounted on the Clamshell and Outerpack for drop tests 1.1 and 1.2. On the Clamshell, one 0-500 g accelerometer was mounted on the top head, and the other 0-500 g accelerometer on the bottom head. On the Outerpack, one 0-1000 g accelerometer was mounted on the underside of the bottom nozzle end (secondary impact location for test 1.1). After test 1.1, the accelerometer on the top head was replaced. The locations of these accelerometers are shown in Figure 2-117A. Figure 2-118 shows the accelerometer traces for the Clamshell from test 1.1. On the primary impact end (top nozzle), the accelerometer saturated in the vertical and axial directions, and the peak lateral deceleration was 453 g. The peak deceleration was 203 g and the resultant vector deceleration sum was 247 g at the secondary impact end (bottom nozzle).

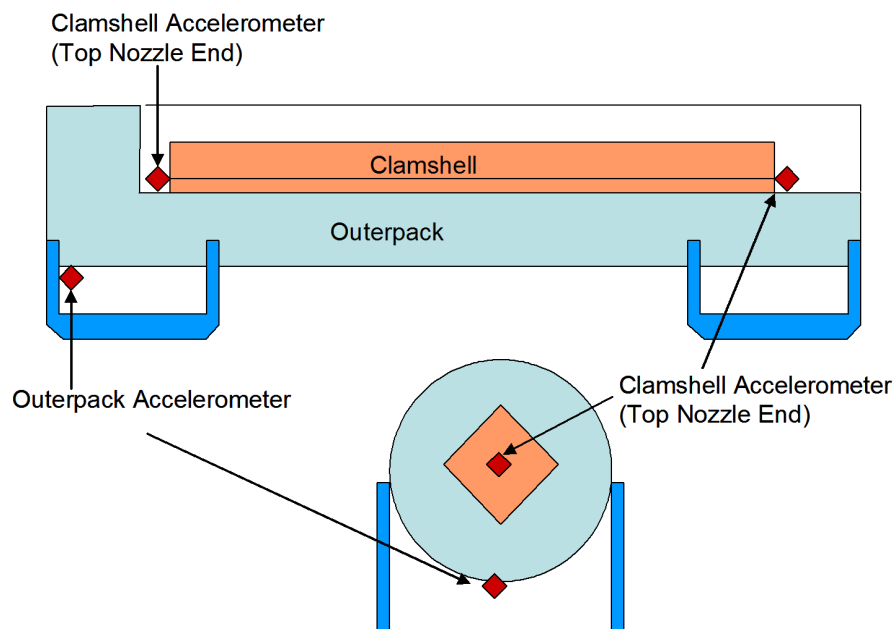


Figure 2-117A Accelerometer Locations on Prototype Drop Test

The 0-1000 g accelerometer trace for the Outerpack is shown in Figure 2-119. The Outerpack vector deceleration sum for the primary impact measured 204 g, and the peak deceleration force measured 191 g in the vertical direction. The slap-down (secondary impact) resulted in decelerations which saturated each directional accelerometer.

The deceleration data for test 1.1 is summarized in Table 2-30.

This page intentionally left blank.

|

Table 2-30 Measured Decelerations in Prototype Test 1.1				
Accelerometer Position	Measured Deceleration Force, g			
	Vertical	Lateral	Axial	Vector Sum
Clamshell T/N end	>500	435	>500	N/A
Clamshell B/N end	205	118	78	247
Outerpack – Primary Impact	191	59	42	204
Outerpack – Slap Down	>1000	>1000	>1000	N/A

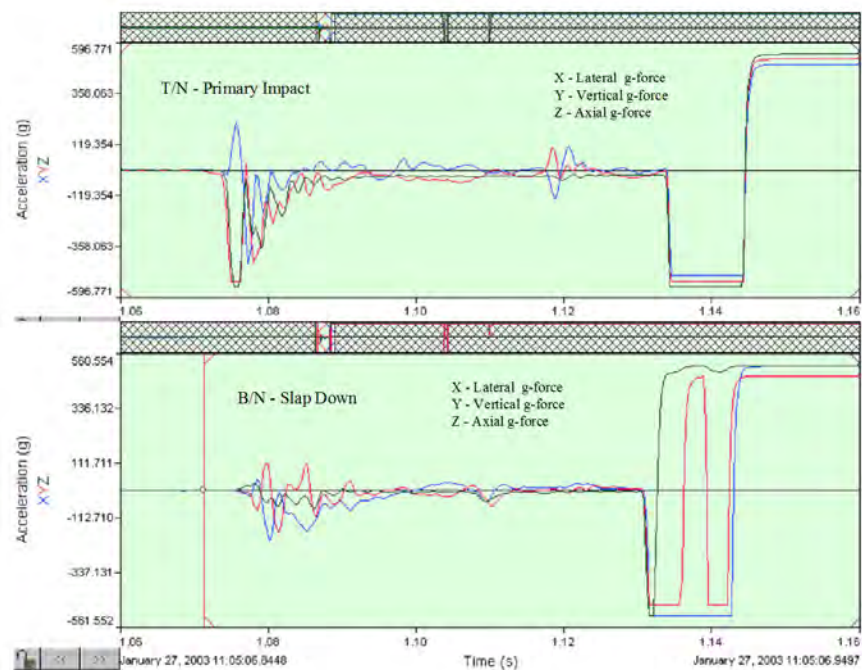


Figure 2-118 Clamshell Accelerometer Trace for Prototype Test 1.1

The top head accelerometer was replaced prior to test 1.2. Due to damaged instrumentation, no data was recorded for the bottom head or the Outerpack. The primary impact occurred on the bottom nozzle end. The top head accelerometer measured the deceleration trace of the primary impact as shown in Figure 2-119. The vector deceleration sum of the primary impact measured 417 g, and the peak deceleration force measured 260 g in the axial direction. The deceleration data for test 1.2 is summarized in Table 2-31.

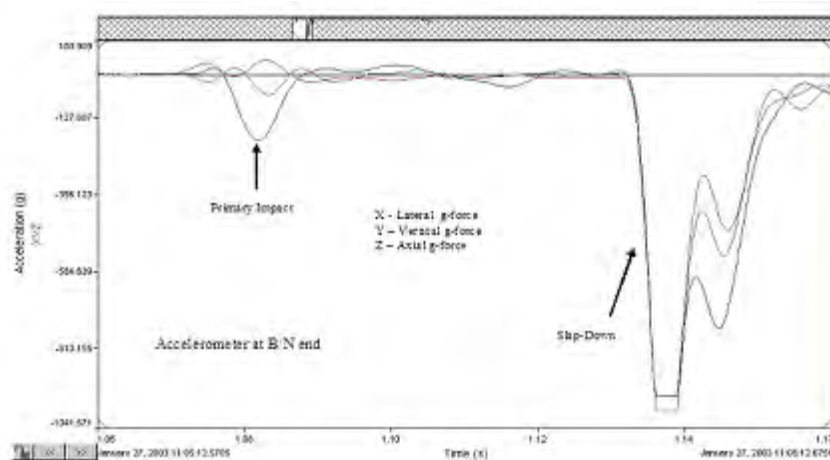


Figure 2-119 Outerpack Accelerometer Trace for Prototype Test 1.1

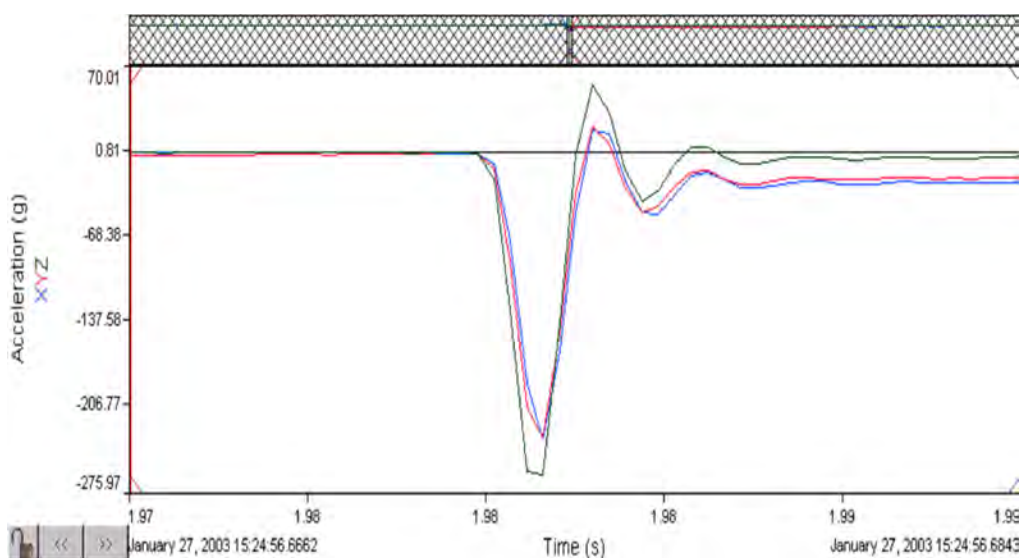


Figure 2-120 Clamshell Accelerometer Trace for Prototype Test 1.2

Table 2-31 Measured Accelerations in Test 1.2				
Accelerometer Position	Measured Deceleration Force, g			
	Vertical	Lateral	Axial	Vector Sum
Clamshell T/N end	230	232	260	417
Clamshell B/N end	No data	No data	No data	N/A
Outerpack – Primary Impact	No data	No data	No data	N/A
Outerpack – Slap Down	No data	No data	No data	N/A

Test 1.3 – The 1-meter pin puncture test resulted in little damage to the package. The outer skin of the Outerpack was locally punched approximately 1.63" and the width of the impact was approximately 10.5" as shown in Figure 2-121. The impact did not perforate the outer skin. The subsequent inspection of the inner side of the Outerpack top indicated that a small dent approximately 7/16" to 1/2" and 15" wide resulted from the pin puncture test. The moderator blocks were not impacted by the pin test.

Test Series 2 – Test series 2 was conducted on January 30th (Table 2-32) and included a 1.2-meter Normal accident condition free drop, a 1-meter pin-puncture test, and a 9-meter free drop test. The package's test weight was 5057 pounds.

The cumulative external damage from the regulatory drop test sequence was localized to plastic deformation at the impact zones. There was no significant changes in the Outerpack geometry, and no bolt failures were noted. Upon an internal inspection, the pin did not perforate the inner or outer shell. The internal damage was minimal. The fuel assembly's envelope decreased from 8.418" nominal to 8.25" maximum. Fuel rod gaps globally decreased (the fuel envelope decreased), but local expansion was noted between a few rods with a maximum measured gap of .188" compared to the nominal gap of .122". The polyethylene moderator blocks and aluminum neutron "poison plates" maintained position. The Clamshell doors remained closed, and the modified top head and bottom heads maintained position. A subsequent fuel inspection indicated that no fuel rods had ruptured, and that the axial position of fuel rods maintained location between bottom and top nozzle.

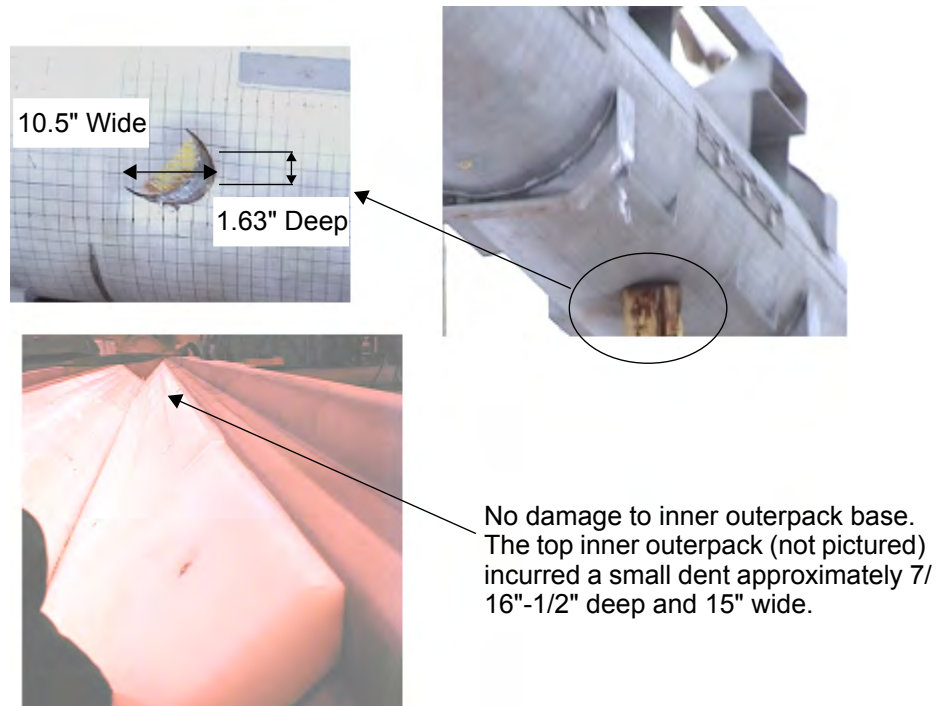
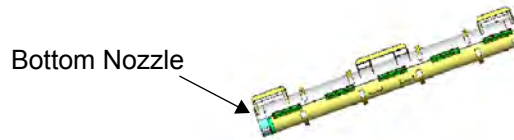


Figure 2-121 Traveller Prototype After Test 1.3

Table 2-32 Prototype Test Series 2			
Test Sequence	Test Pitch Attitude	Test Roll Attitude	Impact Location
2.1) 1.2-m NAC drop	20°	180°	B/N primary impact on OP top
2.2) 1-m Pin-puncture	20°	135°	CG (Axial) on OP topside, T/N end down
2.3) 9-m CG-over-corner	72°	180°	T/N primary impact on OP top

Test 2.1
1.2 m Low Angle
Step Down



Test 2.2
1 m Pin Puncture



Test 2.3
9 m CG over Corner
on Top

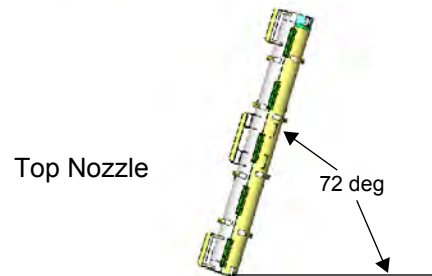


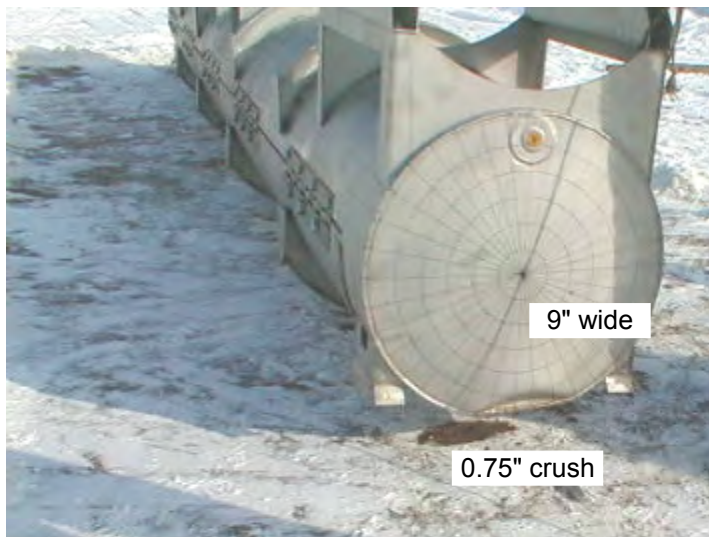
Figure 2-122 Drop Orientations for Traveller Prototype Test Series 2

Test 2.1 – The 1.2 meter normal condition drop test resulted in minimal damage to the Outerpack. The impact created an impact zone at the bottom end 9" wide, 2.5" in axial length, and crushed the Outerpack .75" as shown in Figure 2-123. Two stiffeners near the Outerpack center crushed approximately .75" over a width of 6". The energy absorption of the circumferential stiffeners precluded damage to the secondary impact end (top nozzle).

Test 2.2 – The second test of this drop sequence was a 1-meter pin drop on the package side, Figure 2-122. The 1-meter pin puncture test resulted in little damage to the package. The outer skin of the Outerpack was locally punched in approximately 2" as shown in Figure 2-124. The impact punch zone was 10" tall and the width of the impact was approximately 14". The impact did not perforate the outer skin.

Test 2.3 – The 9-meter drop test resulted in local damage to the primary impact region (top nozzle end). The secondary impact region was in the vicinity of the impact region of the 1.2-meter free drop and did not result in additional damage. From Figure 2-125, the damage zone was approximately 25" wide, 12" tall, and produced a crush zone approximately 9" axially. Due to the impact attitude, the Outerpack top tended to shear relative to the Outerpack bottom. A gap approximately 1" resulted from the impact, but did not comprise the Outerpack closure. No bolt failures were noted.

In general, the test sequence resulted in minimal Clamshell and fuel damage. The top nozzle end of the Clamshell was slightly bowed in a localized region at the top nozzle end (Figure 2-126), but did not result in fuel expansion. The modified top and bottom head pieces remained intact, and no shock mount failures were noted. The fuel inspection indicated that the assembly had moved axially toward the top nozzle 3-3/8" as a result of the spacer movement. There was no significant fuel damage at the bottom nozzle. Also the top nozzle region of the fuel assembly incurred some local damage. The guide pins buckled. Four (4) fuel rods moved axially (maximum of 1"), but did not extend beyond the neutron poison plates. The fuel inspection also indicated that no fuel rods had ruptured. The fuel rod gap measurements indicated the maximum measured fuel rod gap increased from 0.122" nominally to 0.188" locally (observed at one or two rods along the envelope). The measured fuel envelope compressed from 8.418" nominally to 8.25" maximum. The moderator blocks did not move from their original position even though two studs were sheared off. The pin-puncture test produced a 24" long by 5/8" deep dent on the inner Outerpack surface.



The axial damage zone is approximately 2.5".

No damage at T/N end.



Stiffeners crushed about .75" and also dented OP about .75". Crush width 6".

Figure 2-123 Traveller Prototype After Test 2.1

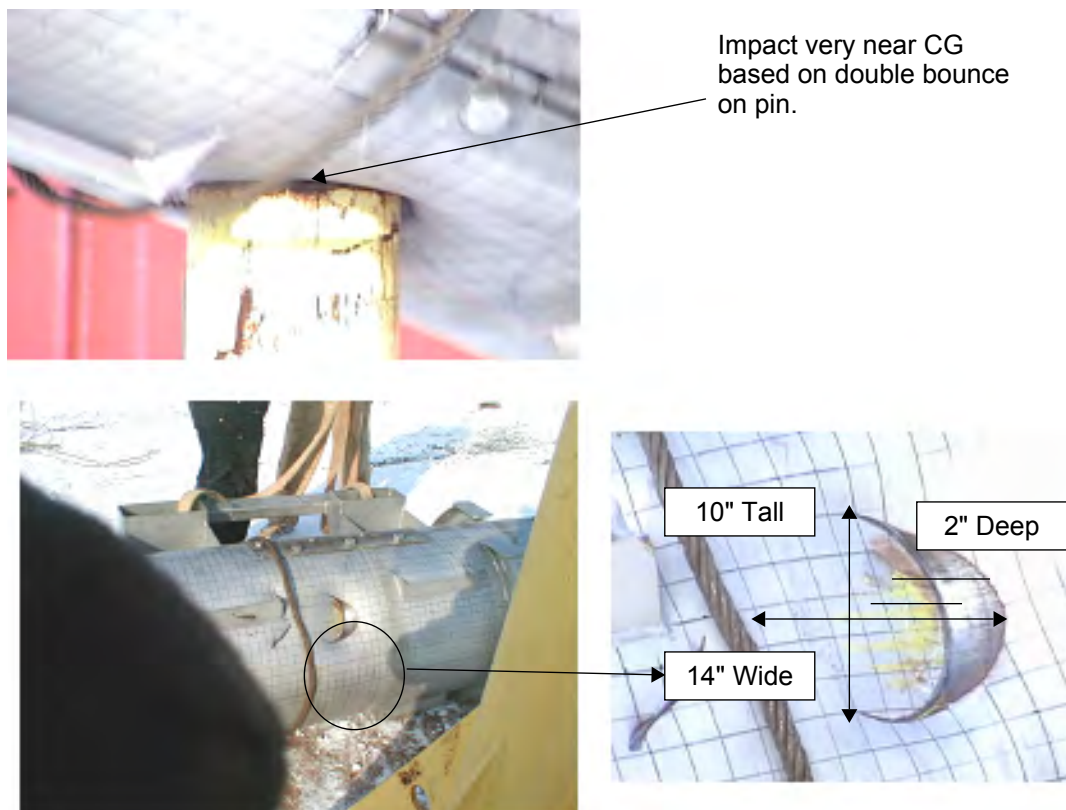


Figure 2-124 Traveller Prototype After Test 2.2

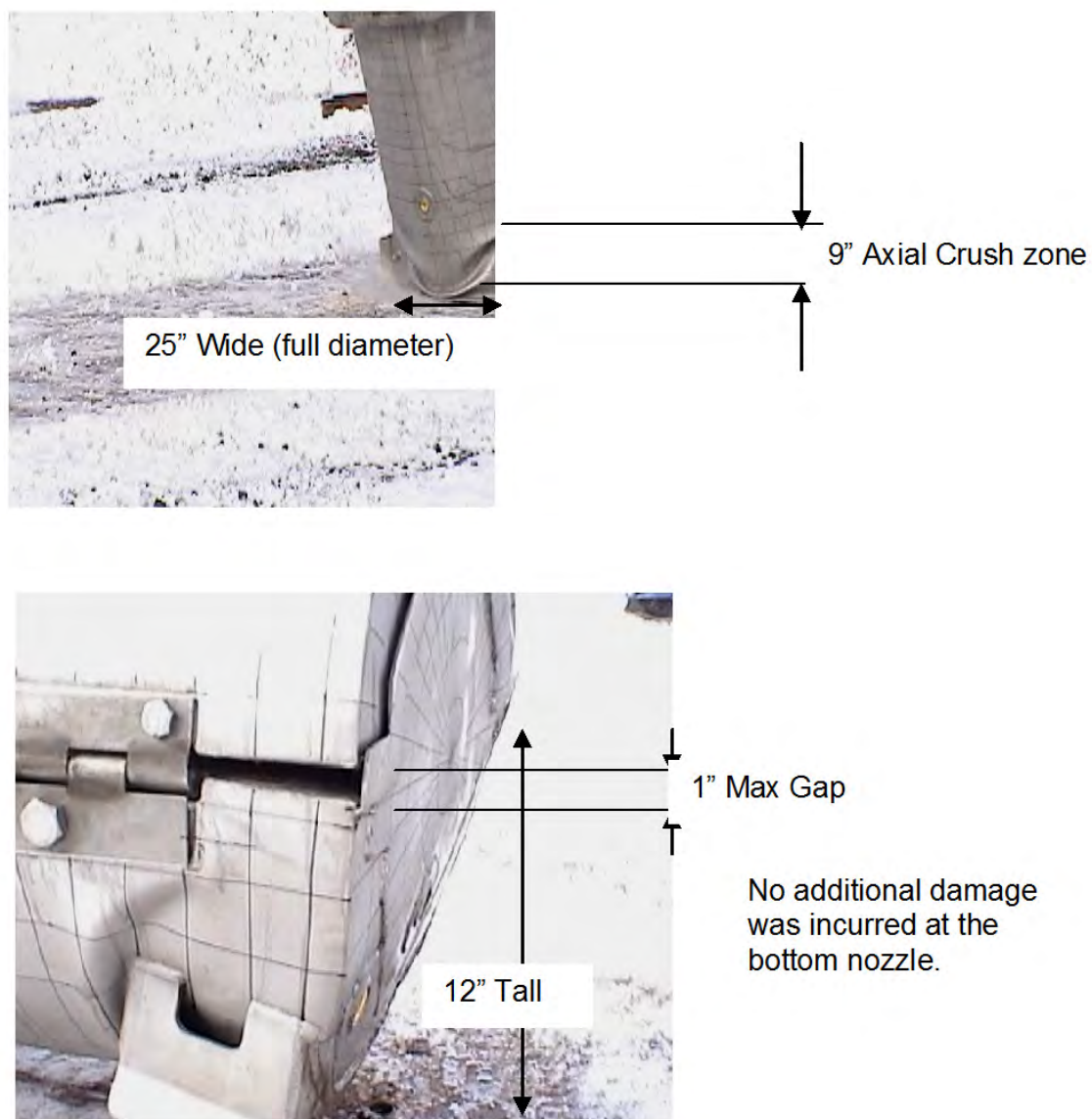


Figure 2-125 Traveller Prototype After Test 2.3

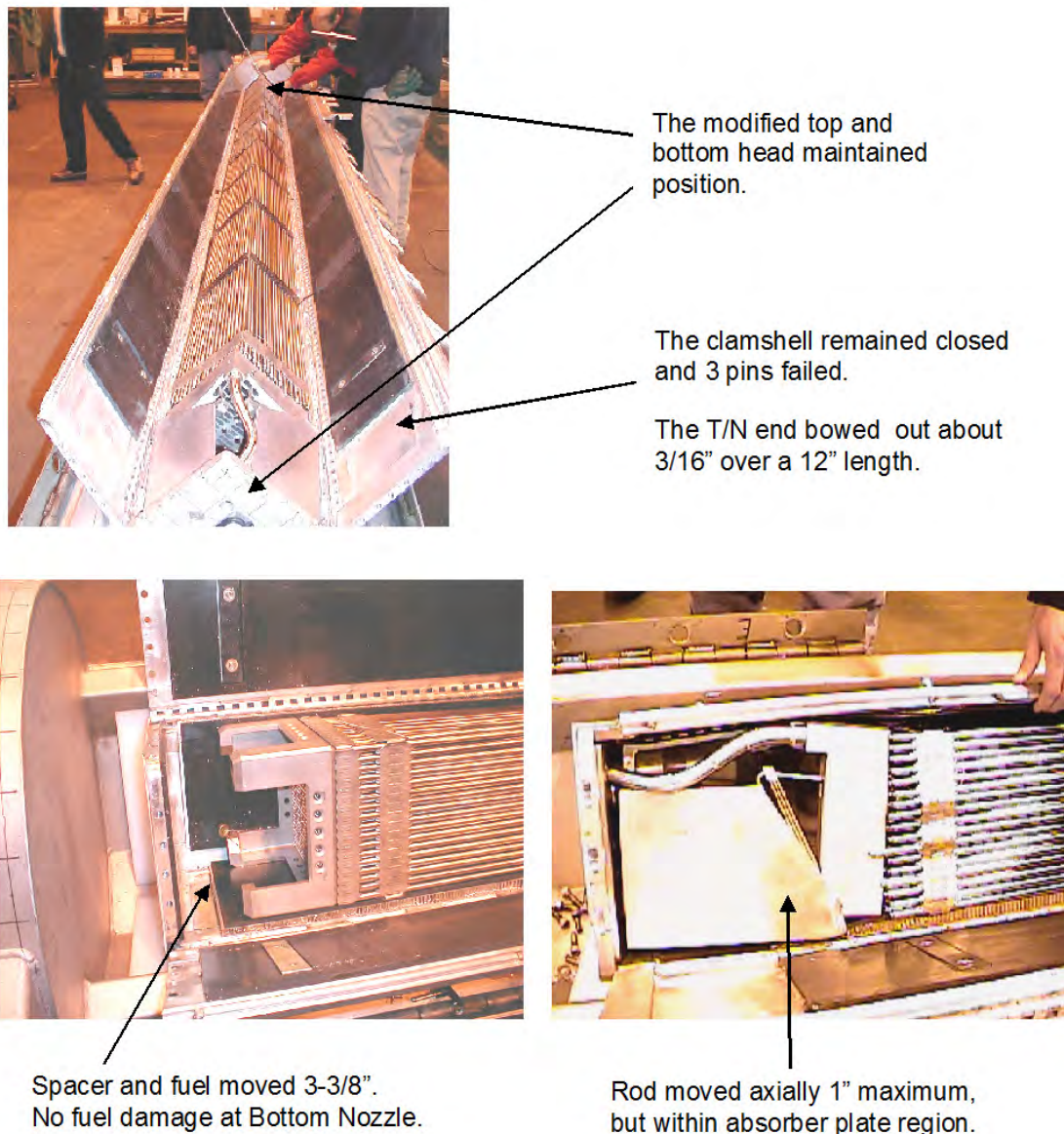


Figure 2-126 Traveller Prototype Interior After Test Series 2

Test Series 3 – Test Series 3 consisted of three 9-meter drop tests conducted to evaluate design features of the Outerpack after modifications to the Clamshell and Outerpack. The test sequence and measured drop attitudes are summarized in Table 2-33. The test series employed was Prototype 2 that had been used for test Series 2. The purpose of this test series was to evaluate design features and evaluate design margin. External damage assessments were performed following each supplementary drop test, and a general internal assessment was conducted after the completion of test 3.3. However, the inspections for this test series were

not intended for use in nuclear criticality safety analysis. Prior to test 3.1, the following modifications were made to the package:

- Removed 1 bolt from each of the 5 top Outerpack hinges (reduced bolt count by 33%).
- Removed sheet metal from endcap inner surface
- Removed 2 of the 5 pins that secure each Clamshell clip

Table 2-33 Traveller Prototype Drop Tests Performed in Test Series 3			
Test Sequence	Test Pitch Attitude	Test Roll Attitude	Impact Location
3.1) 9-m Axial End drop	90°	0°	B/N impact
3.2) 9-m Flat drop	0.5°	0°	Impact on OP feet
3.3) 9-m Side drop	0°	270°(90°CCW)	Impact on OP hinges

Figure 2-127 shows that the Outerpack sustained minimal damage. The Outerpack remained closed and no bolts failed after the completion of drop test series 3. The first drop test of this series resulted in slight crushing (approximately 1-5/8" deep) at the bottom nozzle end. The crushed circumferential stiffeners precluded excessive Outerpack damage as the package slapped down after the axial drop. Drop test 3.2 crushed the feet and forklift supports completely, but otherwise did not comprise the Outerpack structural integrity. The direct hinge impact (test 3.3) did not fail any hinges or result in any substantial damage to the Outerpack.

The cumulative overall damage to the Clamshell was also minimal as shown in Figure 2-127. The Clamshell retained its geometry, no Clamshell clip pins failed, and no shock mount failures were noted. The notable Clamshell damage was located at the bottom head, which was separated from the Clamshell by the impacting fuel, Figure 2-128. It is presumed that the 3-3/8" gap from the Clamshell bottom plate to the base of the fuel assembly bottom nozzle provided sufficient distance for the fuel assembly to attain enough kinetic energy to separate the Clamshell bottom head upon impact.

The fuel was in good condition. No measurements were taken since this test series was qualitative in nature.



Figure 2-127 Traveller Prototype Clamshell and Bottom Impact Limiter After Test Series 3

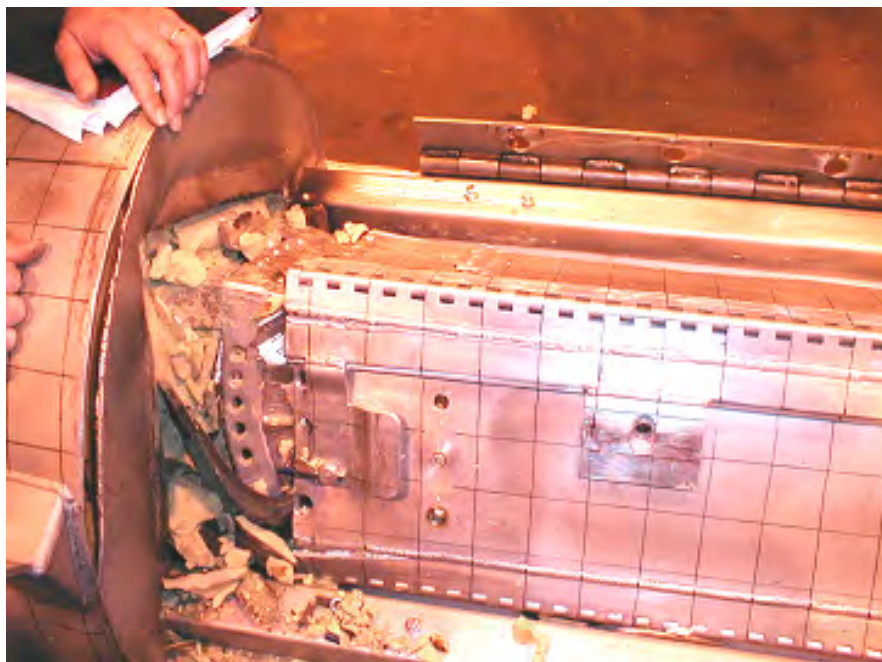


Figure 2-128 Traveller Prototype Clamshell and Bottom Impact Limiter After Test Series 3

Minor design modifications were recommended for the Traveller package based on this testing. The top and bottom heads required additional bolting to preclude Clamshell separation. The number of Clamshell clip retaining pins (and clips) could be reduced. It was found that sufficient design margin against material failure existed allowing the Outerpack gage metal can be reduced slightly in thickness. In addition, the number of Outerpack bolts can be reduced on the top hinge by at least 1/3.

2.12.5.2 Qualification Test Unit Drop Tests

The following section delineates the second of three (3) full-scale testing campaigns of the Traveller development program. This campaign utilized two units called Quality Test Units, or QTU-1 and 2. A total of two (2) QTUs were built and tested, with minor changes to improve burn performance incorporated into the second QTU article.

2.12.5.2.1 QTU Test Series 1

Test series 1 was conducted on the afternoon of September 11 and included a 50 inch (1.27 m) slap down, a 33.3 feet (10.15 m) center of gravity-over-corner free drop test, and a 42 inch (1.07 m) pin-puncture test. The package's test weight was 4793 pounds (Table 2-34). The internal inspection of the fuel assembly was conducted after completion of the fire test on September 16, 2003.

Table 2-34 QTU-1 Measured Weight		
Test Weights	Nominal	Actual
Weight of Outerpack (Empty):	3033 lb	3032 lb
Weight of Clamshell (Empty):	425 lb	400 lb
Weight of package (Empty):	3477 lb	3432 lb
Total package test weight:	5422 lb	4793 lb

Test series 1 was conducted on the afternoon of September 11 and included a 50.75 inch (1.29 m) slap down, a 33.3 feet (10.15 m) free drop test, and a 42 inch (1.07 m) pin-puncture test. QTU1 pre-test data and observations are shown in Form 1A. The test sequence and measured drop attitudes are summarized in Table 2-35 and shown in Figure 2-129. A pitch angle of 72 degrees was measured along the outerpack surface for Test 1.2. The angle of 108 degrees should be located as shown in Figure 2-129. The reference to "hinge side" in Test 1.3 indicates the package side that pivots, rather than the actual hinge. The impact point of Test 1.3 (Figure 2-132) was on the top nozzle end and on the pivot (left) side of the package. A fuel damage assessment was conducted after the completion of the hypothetical fire condition test conducted on September 16, 2003 at the South Carolina Fire Academy near Columbia, SC.

The Outerpack retained its basic circular pre-test shape except for localized plastic deformation at the top nozzle end accumulated from the drop test series. No bolts failed on the Outerpack after completion of the drop test series. The Outerpack did not separate after any impacts, and the pin did not perforate the inner or outer shell. The most notable Outerpack damage was the resulting joint tear of approximately 1-1/8" at the Outerpack corner located at the top, left hinge side. The fuel assembly damage was minimal. At the top nozzle portion, the fuel assembly locally expanded from 8.375" nominal to 8.625" maximum over a length of approximately 2-3". The fuel rod gaps were globally unchanged but local expansion was noted between one rod near Grid 10 with a maximum measured gap of 0.250". The resulting measured maximum local pitch was 0.625 inches. Three rods were found to be in contact with each other while the remaining rods

were nominally positioned. Intermediate grids 2-7 were buckled locally, but the fuel rod envelope was unchanged. The bottom nozzle portion of the fuel assembly was slightly compressed from 8.375" nominally to 8.250" measured. Based on the condition of the fuel assembly, the Clamshell was concluded to have performed successfully. The fuel inspection also indicated that no fuel rods had visibly ruptured, and that the axial position of fuel rods maintained location between bottom and top nozzle.

Table 2-35 QTU-1 Drop Test Orientations					
Test Article ID	F/A Type	Test Sequence	Test Pitch Attitude	Test Roll Attitude	Design Feature Tested
QTU1	17x17 XL	P1.1)1.2 m, NAC, Low angle ¹	10°	180°	Operations of hinges/doors
		P1.2)9 m CG-over-Corner ¹	108°	90°	OP hinge shear, CS latches
		P1.3)1 m Pin-puncture ¹	83°	90°	Joint Integrity – Fire test

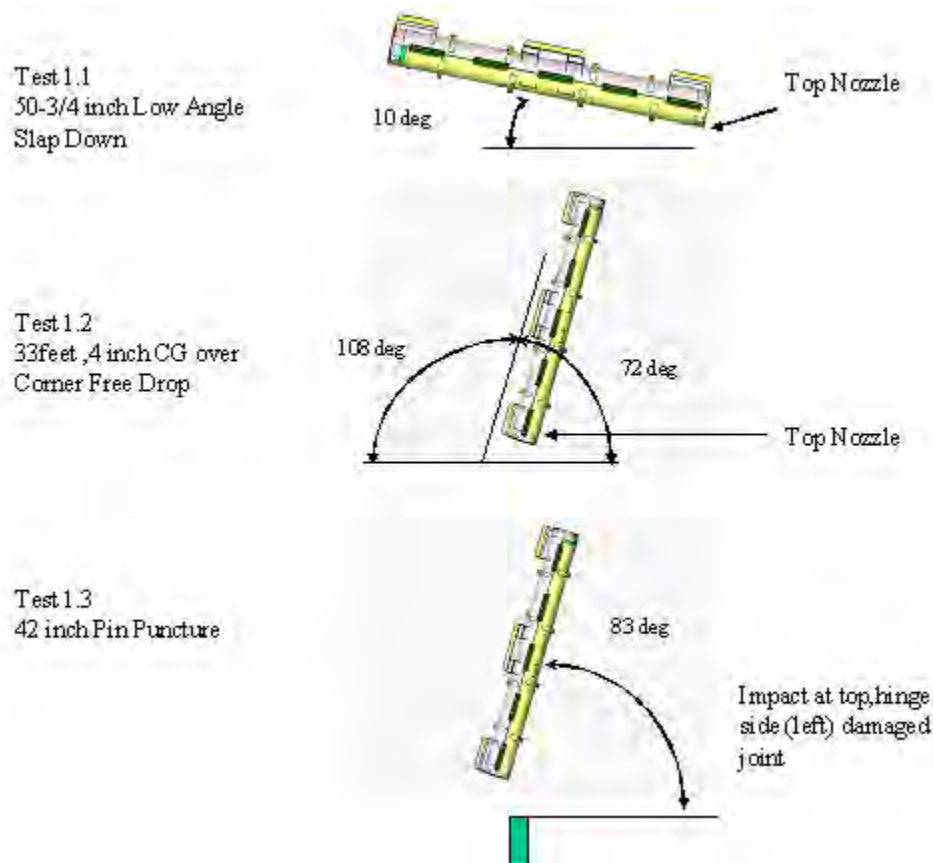


Figure 2-129 Drop Orientation for QTU Test Series 1

Test 1.1 – The 50.75 inches (1.29 m) drop onto the Outerpack lid was performed first. As shown in Figure 2-130, this drop resulted in a small indentation in the outer skin of the Outerpack.

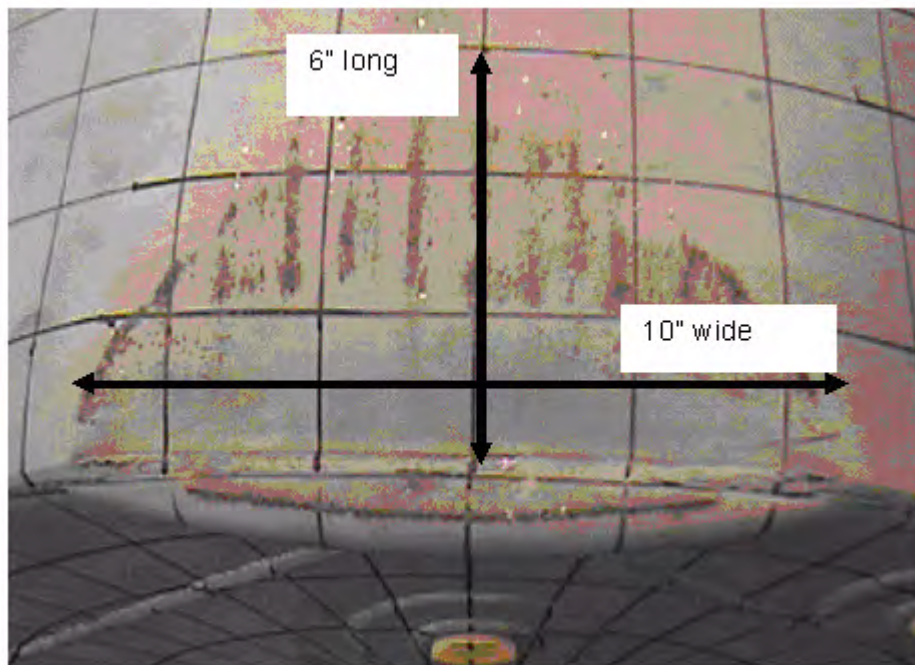


Figure 2-130 QUTU-1 Outerpack After Test 1.1

Test 1.2 – The 33.3-foot free drop resulted in localized damage to the top nozzle end region. One of the hoist rings was sheared off as a result of the impact, Figure 2-131. The impact opened a small tear at the top and bottom Outerpack seam (also in circled region). The entire 25" diameter face of the top nozzle end was dented approximately 3-1/2". The stiffeners were also dented across their tops, but were intact. Two welds located at the bottom nozzle end stiffener were broken, but this did not compromise the stiffener position.

Test 1.3 – The pin puncture test was located in the top left (hinge) side of the Outerpack top nozzle end. The objective of the test was attempt to increase the Outerpack separation incurred by the previous 33.3-ft drop. Additional tearing of the joint was noted which resulted in measured tear of approximately 1-1/8". The indentation resulting from the pin puncture was approximately 1-1/2" deep (Figure 2-132).

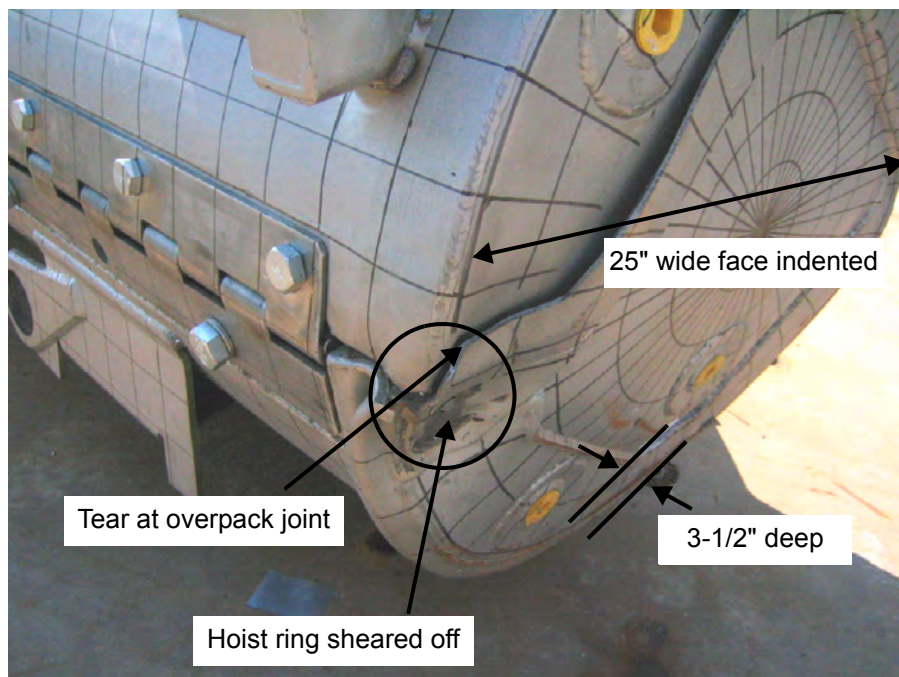


Figure 2-131 QTU-1 Outerpack After Test 1.2

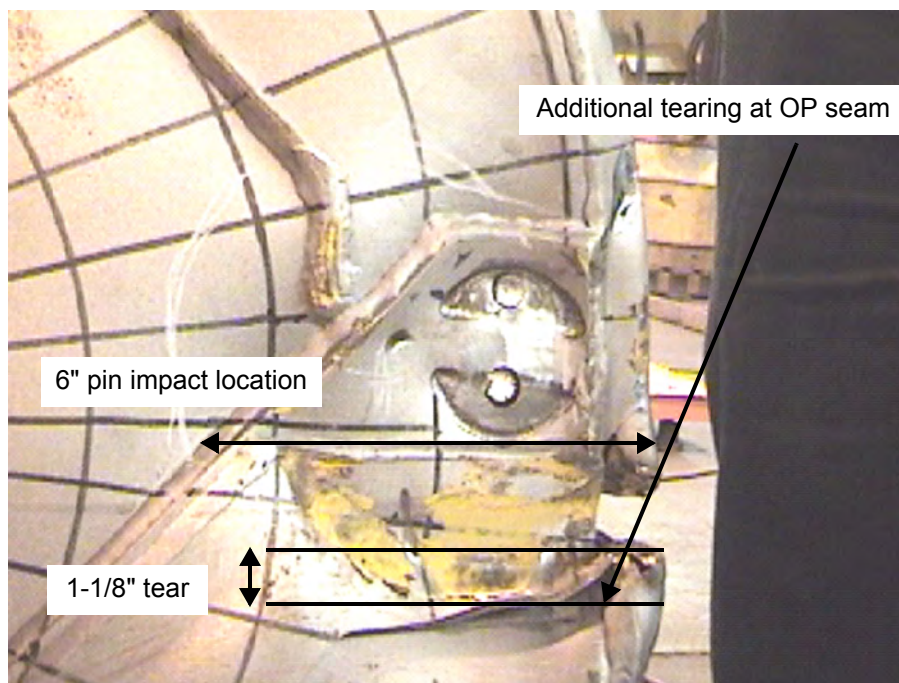


Figure 2-132 QTU-1 Outerpack After Test 1.3

QTU-1 was not opened until after the fire test. The Clamshell and fuel assembly were examined for damage at that time. The fuel assembly of QTU-1 was essentially undamaged, Figure 2-133. The most damage occurred at the top nozzle section where an area of approximately 2-3" in length increased from 8.375" nominal to 8.625". Grid 10 was torn, and all other grids were buckled but intact. The nozzles were essentially undamaged. The impact resulted in buckling of the core line-up pins attached to the top nozzle. The fuel rods appeared visibly undamaged.

The fuel assembly in QTU-1 was measured before the test and after the burn test at locations shown in Figure 2-134. Table 2-36 provides the pretest dimensions. Tables 2-37 and 2-38 provide the post test dimensions.

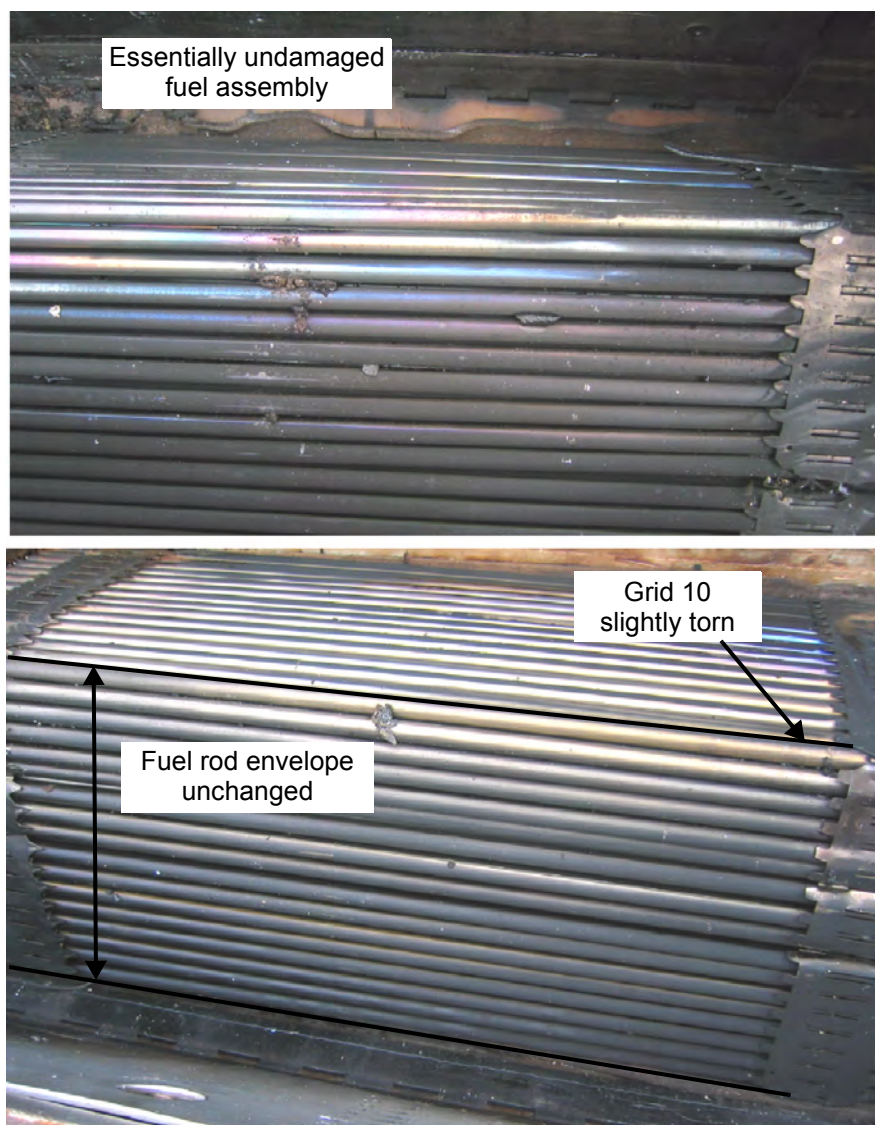


Figure 2-133 QTU-1 Fuel Assembly After Drop and Burn Tests

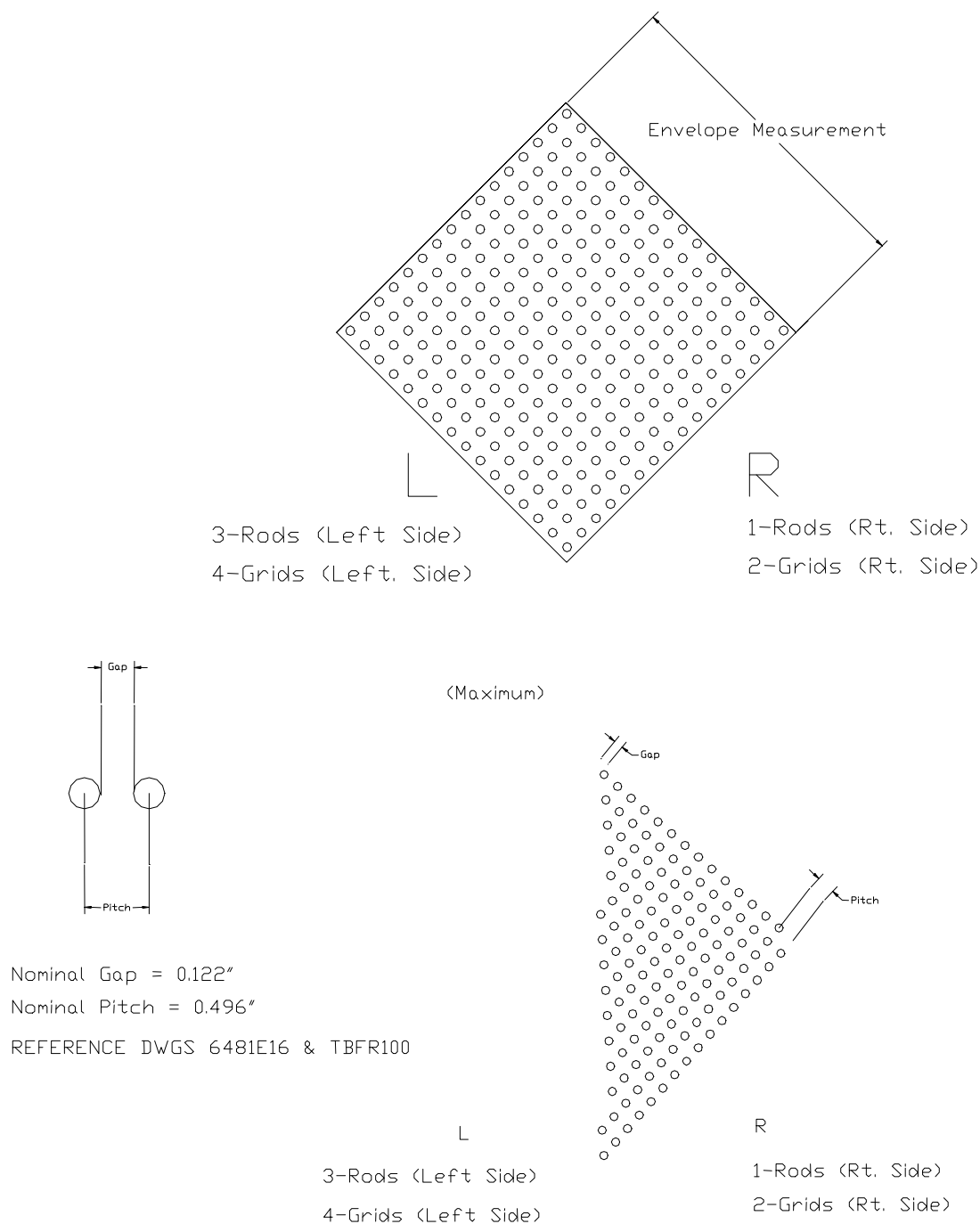


Figure 2-134 Measurements Made on QTU-1 Fuel Assemblies Before and After Drop Tests

Table 2-36 Key Dimensions of QTU-1 Fuel Assembly Before Testing			
Fuel Assembly ID: <u>503007, B/N # 02-6703</u>			
F/A Location	Fuel Envelope (inches)	Gap (inches)	Pitch (inches)
B/N – Grid 1	1 – 8.330 2 – 8.455 3 – 8.250 4 – 8.446 8.375 Meas. Nominal*	L – 0.122 R – 0.123 0.125 Meas. Nominal*	L – 0.497 R – 0.498 0.500 Meas. Nominal*
Grid 1 – Grid 2	1 – 8.338 2 – 8.418 3 – 8.326 4 – 8.415 8.375 Meas. Nominal*	L – 0.124 R – 0.124 0.125 Meas. Nominal*	L – 0.499 R – 0.499 0.500 Meas. Nominal*
Grid 2 – Grid 3	8.375 Meas. Nominal*	L – 0.123 R – 0.120 0.125 Meas. Nominal*	L – 0.498 R – 0.495 0.500 Meas. Nominal*
Grid 3 – Grid 4	8.375 Meas. Nominal*	0.125 Meas. Nominal*	0.500 Meas. Nominal*
Grid 4 – Grid 5	8.375 Meas. Nominal*	0.125 Meas. Nominal*	0.500 Meas. Nominal*
Grid 5 – Grid 6	8.375 Meas. Nominal*	0.125 Meas. Nominal*	0.500 Meas. Nominal*
Grid 6 – Grid 7	8.375 Meas. Nominal*	0.125 Meas. Nominal*	0.500 Meas. Nominal*
Grid 8 – Grid 9	8.375 Meas. Nominal*	0.125 Meas. Nominal*	0.500 Meas. Nominal*
Grid 9 – Grid 10	8.375 Meas. Nominal*	0.125 Meas. Nominal*	0.500 Meas. Nominal*
Grid 10 – T/N	8.375 Meas. Nominal*	0.125 Meas. Nominal*	0.500 Meas. Nominal*
Note: * Measured nominal values were measured to nearest 1/8".			

Table 2-37 QTU-1 Fuel Assembly Grid Envelope After Testing			
Fuel Assembly Envelope Inspection Table			
Location	Envelope Dimension, Inches		Maximum Fuel Rod Gap from Form 1F (Nominal Gap = 0.122")
	Left Side, LS	Right Side, RS	
Between B/N and Grid 1	8.125	8.250	0.250
Between Grids 1 and 2	8.125	8.000	0.250
Between Grids 2 and 3	8.000	8.250	0.188
Between Grids 3 and 4	8.375	8.375	0.125
Between Grids 4 and 5	8.375	8.375	0.125
Between Grids 5 and 6	8.375	8.375	0.188
Between Grids 6 and 7	8.375	8.375	0.188
Between Grids 7 and 8	8.375	8.375	0.188
Between Grids 8 and 9	8.375	8.375	0.188
Between Grids 9 and 10	8.375	8.500	0.250
Between Grid 10 and T/N	8.500	8.625	0.250
MAXIMUM VALUE	8.500	8.625	0.250

Table 2-38 QTU-1 Fuel Rod Pitch Data After Testing			
Fuel Rod Pitch Inspection Table			
Location	Maximum Gap, inches		Maximum Pitch
	Left Side, LS	Right Side, RS	
Between B/N Grid 1	0.250	0.188	0.625
Between Grids 1 and 2	0.250	0.250	0.625
Between Grids 2 and 3	0.188	0.188	0.563
Between Grids 3 and 4	0.125	0.125	0.500
Between Grids 4 and 5	0.125	0.125	0.500
Between Grids 5 and 6	0.125	0.188	0.563
Between Grids 6 and 7	0.125	0.188	0.563
Between Grids 7 and 8	0.188	0.188	0.563
Between Grids 8 and 9	0.188	0.188	0.563
Between Grids 9 and 10	0.125	0.250	0.625
Between Grid 10 and T/N	0.125	0.250	0.625
MAXIMUM VALUE	0.250	0.250	0.625

2.12.5.2.2 QTU Test Series 2

Test series 2 was conducted on the afternoon of September 11 and included a 50 inch (1.27 m) slap down, a 33.4 feet (10.18 m) free drop test, and a 42 inch (1.07 m) pin-puncture test. The test sequence and measured drop attitudes are summarized in Table 2-39 and shown in Figure 2-135. Weights for QTU-2 are recorded on Table 2-40.

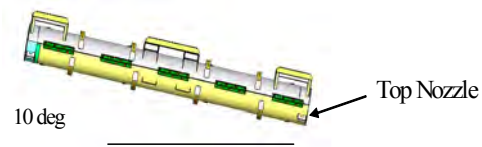
Table 2-39 QTU Series 2 As-Tested Drop Conditions					
Test Article ID	F/A Type	Test Sequence	Test Pitch Attitude	Test Roll Attitude	Design Feature Tested
QTU2	17x17 XL	P2.1) 1.2-m, NAC, Low angle ⁽¹⁾	10°	180°	Operations of hinges/doors
		P2.2) 9-m End (B/N) ⁽¹⁾	90°	0°	Lattice exp., FR axial position
		P2.3) 1-m Pin-puncture ⁽¹⁾	22°	0°	OP stiffness
Note: (1) Actual test heights are reported in Figure 163 and post-test forms.					

Table 2-40 QTU-2 Weights		
Test Weights	Nominal	Actual
Weight of Outerpack (Empty):	3033 lb	2611 lb
Weight of Clamshell (Empty):	425 lb	400 lb
Weight of package (Empty) :	3477 lb	3011 lb
Total package test weight:	5422 lb	4778 lb

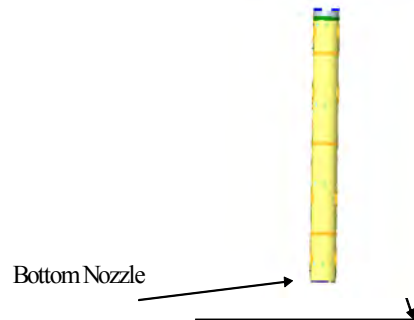
The Outerpack retained its basic circular pre-test shape except for localized plastic deformation accumulated from the 1.2 meter and 33.4 foot (10.18m) drop test. Damage zones from the drop test were localized to impact locations on the package end. The Outerpack did not separate after the impact, and no bolt failures on the Outerpack hinges were noted. From Figure 2-136, the 1.2 meter free drop resulted in a local crush zone at the top nozzle end measuring approximately 9-1/2" wide, 6" long axially and 7/8" deep. The Outerpack damage from the 33.4 foot drop, Figure 2-136 consisted of local crumple zone approximately 7" long maximum as demonstrated by the buckled Outerpack at the bottom nozzle end. A small weld tear was noted on each side of the Outerpack where the leg stand is connected to the end cap. The pin puncture damage was isolated to the impact point located at the package center-of-gravity. From As shown in Figure 2-138, pin puncture damage zone was an indented oval of measured dimensions 9" long by 6" wide and 2-7/8" deep.

The Clamshell was essentially undamaged from the drop test series, Figure 2-138. No change in the Clamshell grid markings were noted indicating that the Clamshell had not bulged outward (nor compressed). The polyethylene moderator blocks and aluminum neutron "poison plates" maintained position. The fuel assembly was found to be within the confines of the Clamshell and intact. The impact resulted in a slight ovalizing of the fuel assembly at the bottom nozzle region. Figure 2-139 shows the approximate angle of ovality is 118° at Grid 1 location. Localized expansion from 8.375" nominal to 8.625" was measured over a length of approximately 12" (30.48cm). The maximum fuel rod gap measured was 0.722 inches resulting in a maximum measured fuel rod pitch of 1.097 inches. The top nozzle portion of the tested fuel assembly was essentially undamaged. The axial position of fuel rods maintained location between bottom and top nozzles.

Test 2.1
50 inch Low Angle
Slap Down



Test 2.2
33 feet, 5 inch End
on Bottom Nozzle



Test 2.3
42-1/2 inch Pin Puncture



Figure 2-135 QTU Test Series 2 Drop Orientations

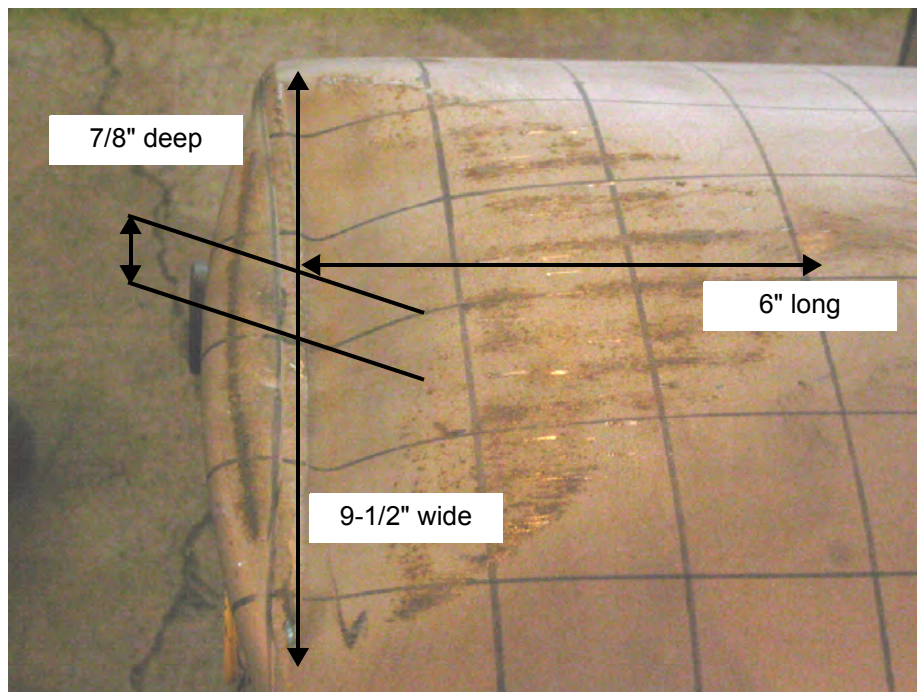


Figure 2-136 QTU Outerpack After Test 2.1

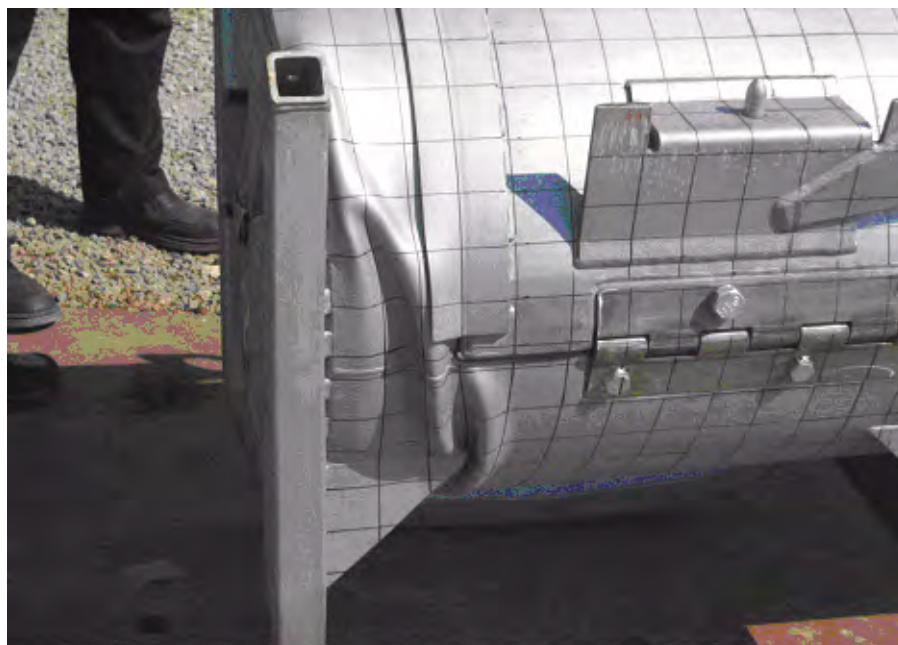


Figure 2-137 QTU Outerpack After Test 2.2

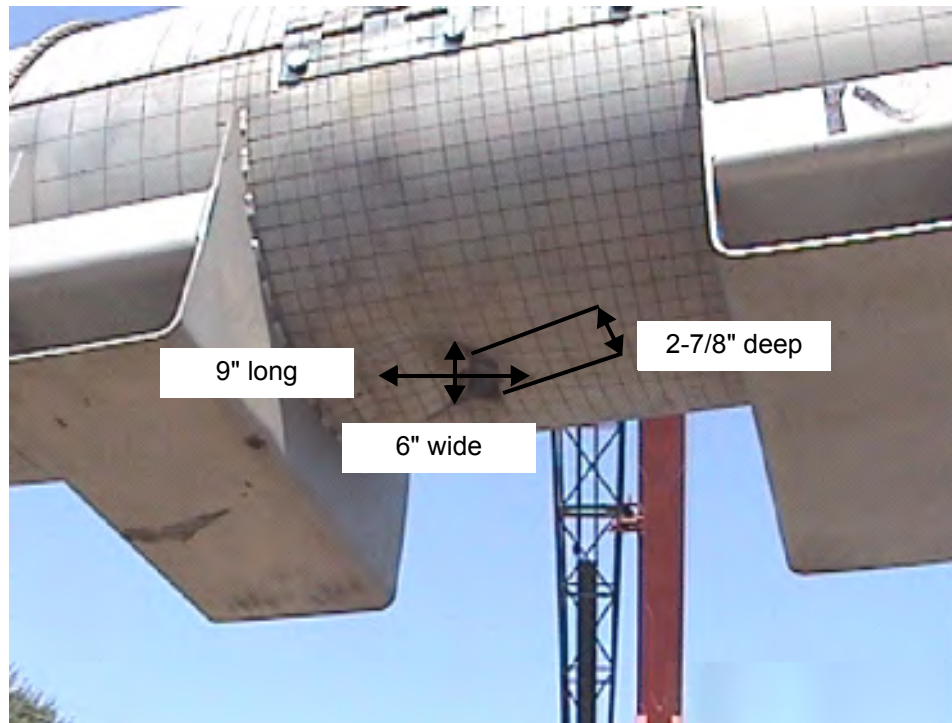


Figure 2-138 QTU Outerpack After Test 2.3

The fuel assembly in QTU-1 was measured before the test and after the burn test at locations shown in Figure 2-134 above. Table 2-41 provides the pretest dimensions. Tables 2-42 and 2-43 provide the post test dimensions.

The post-test inspections concluded that the tested configuration of the Traveller Outerpacks and Clamshells were acceptable. Furthermore, the tests concluded that Test Series 1 imparted the most damage to the Outerpack, and Test Series 2 imparted the most damage to the fuel assembly. Also, testing demonstrated that the Traveller Outerpack is suitable for transport with two top Outerpack bolts per hinge. The post-test geometry of the fuel assemblies for both test series was also acceptable.

In summary, testing demonstrated the Traveller package is suitable for compliance to normal and hypothetical mechanical drop test conditions described in 10 CFR 71 and TS-R-1.

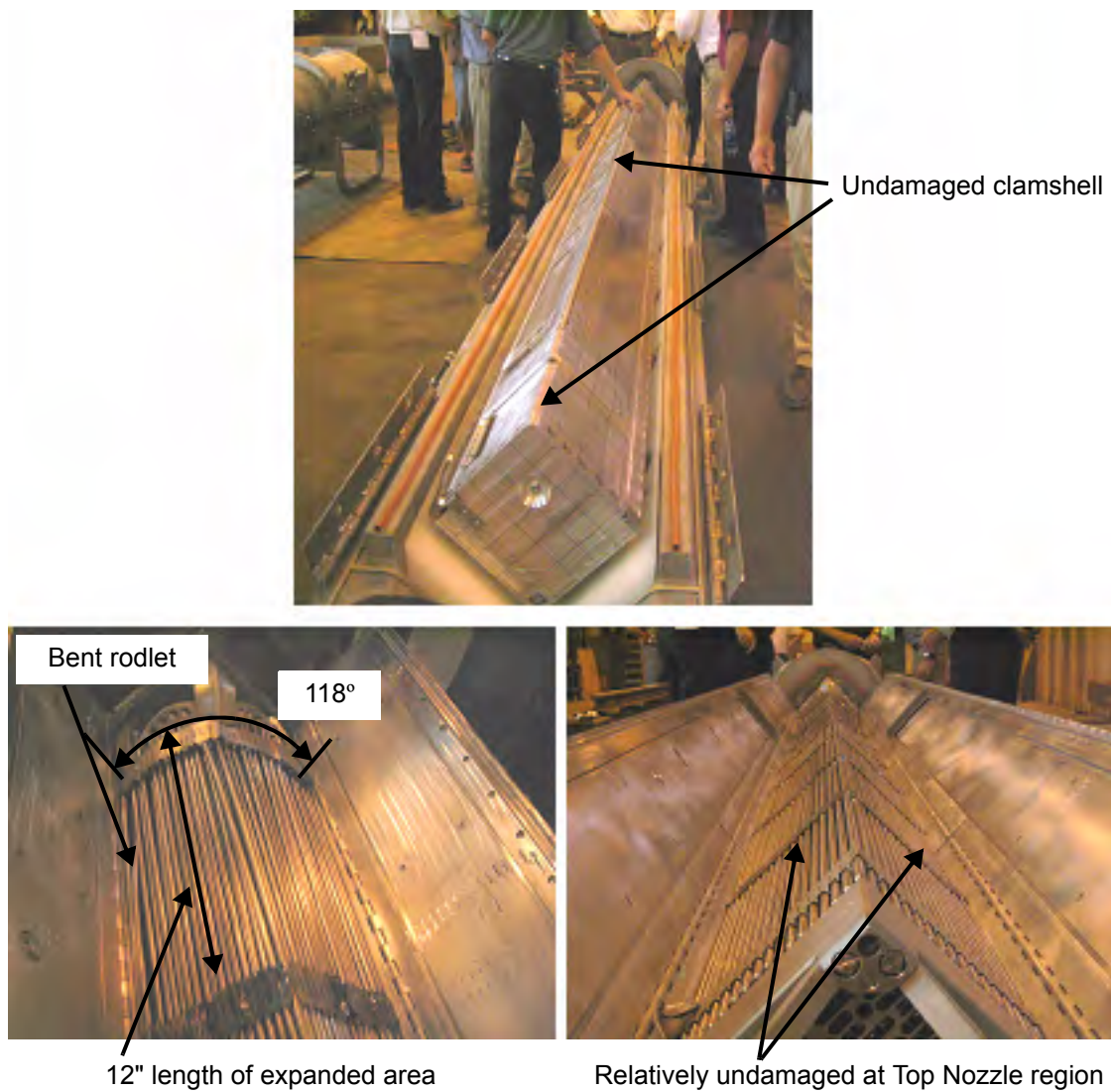


Figure 2-139 QTU-2 Clamshell and Fuel Assembly After Drop Tests

Table 2-41 Key Dimensions of QTU-2 Fuel Assembly Before Testing			
Fuel Assembly ID: 503005, B/N # 97-2480Y			
F/A Location	Fuel Envelope (inches)	Gap (inches)	Pitch (inches)
B/N – Grid 1	1 – 8.356 2 – 8.463 3 – 8.329 4 – 8.430 8.375 Meas. Nominal*	L – 0.124 R – 0.123 0.125 Meas. Nominal*	L – 0.499 R – 0.498 0.500 Meas. Nominal*
Grid 1 – Grid 2	1 – 8.325 2 – 8.415 3 – 8.319 4 – 8.420 8.375 Meas. Nominal*	L – 0.121 R – 0.123 0.125 Meas. Nominal*	L – 0.496 R – 0.498 0.500 Meas. Nominal*
Grid 2 – Grid 3	1 – 8.333 2 – 8.410 3 – 8.329 4 – 8.411 8.375 Meas. Nominal*	L – 0.121 R – 0.123 0.125 Meas. Nominal*	L – 0.496 R – 0.498 0.500 Meas. Nominal*
Grid 3 – Grid 4	1 – 8.311 2 – 8.435 3 – 8.310 4 – 8.24 8.375 Meas. Nominal*	L – 0.124 R – 0.123 0.125 Meas. Nominal*	L – 0.499 R – 0.498 0.500 Meas. Nominal*
Grid 4 – Grid 5	8.375 Meas. Nominal*	0.125 Meas. Nominal*	0.500 Meas. Nominal*
Grid 5 – Grid 6	8.375 Meas. Nominal*	0.125 Meas. Nominal*	0.500 Meas. Nominal*
Grid 6 – Grid 7	8.375 Meas. Nominal*	0.125 Meas. Nominal*	0.500 Meas. Nominal*
Grid 8 – Grid 9	8.375 Meas. Nominal*	0.125 Meas. Nominal*	0.500 Meas. Nominal*
Grid 9 – Grid 10	8.375 Meas. Nominal*	0.125 Meas. Nominal*	0.500 Meas. Nominal*
Grid 10 – T/N	8.375 Meas. Nominal*	0.125 Meas. Nominal*	0.500 Meas. Nominal*
Note: * Measured nominal values were measured to nearest 1/8".			

Table 2-42 QTU-2 Fuel Assembly Grid Envelope After Testing			
Fuel Assembly Envelope Inspection Table			
Location	Envelope Dimension, Inches		Maximum Fuel Rod Gap from Form 2F (Nominal Gap = 0.122")
	Left Side, LS	Right Side, RS	
Between B/N and Grid 1	8.625	8.500	0.722
Between Grids 1 and 2	8.000	7.938	0.539
Between Grids 2 and 3	7.938	7.688	0.316
Between Grids 3 and 4	7.813	7.625	0.137
Between Grids 4 and 5	8.063	7.875	0.153
Between Grids 5 and 6	8.250	8.250	0.143
Between Grids 6 and 7	8.375	8.375	0.146
Between Grids 7 and 8	8.375	8.375	0.141
Between Grids 8 and 9	8.375	8.375	0.162
Between Grids 9 and 10	8.375	8.375	0.141
Between Grid 10 and T/N	8.438	8.438	0.127
MAXIMUM VALUE	8.625	8.500	0.722

Table 2-43 QTU-2 Fuel Rod Pitch Data After Testing			
Fuel Rod Pitch Inspection Table			
Location	Maximum Gap, inches		Maximum Pitch, inches
	Left Side, LS	Right Side, RS	
Between B/N and Grid 1	0.722	0.501	1.097
Between Grids 1 and 2	0.539	0.501	0.914
Between Grids 2 and 3	0.250	0.316	0.691
Between Grids 3 and 4	0.137	0.125	0.512
Between Grids 4 and 5	0.153	0.132	0.528
Between Grids 5 and 6	0.142	0.143	0.518
Between Grids 6 and 7	0.145	0.146	0.521
Between Grids 7 and 8	0.141	0.138	0.516
Between Grids 8 and 9	0.162	0.122	0.537
Between Grids 9 and 10	0.139	0.141	0.516
Between Grid 10 and T/N	0.127	0.123	0.502
MAXIMUM VALUE	0.722	0.501	1.097

2.12.5.3 Certification Test Unit Drop Tests

A Traveller XL package was fabricated by Columbiana High Tech to serve as the certification test unit (CTU), Figures 2-140 and 2-141 and Table 2-44. This unit was subjected to a regulatory drop test performed February 5, 2004 in Columbiana, Ohio. The test included a 50 inch (1.27 m) slap down, a 32.8 feet (10.0 m) free drop test impacting the bottom nozzle, and a 42 inch (1.07 m) pin-puncture test, Figure 2-142 and Table 2-45. The CTU package was thermally saturated for approximately 15 hours prior to testing at a temperature of about 17°F (-8.3°C). At the time of testing the temperature was approximately 24°F (-4.4°C). The package's test weight was 4863 pounds.

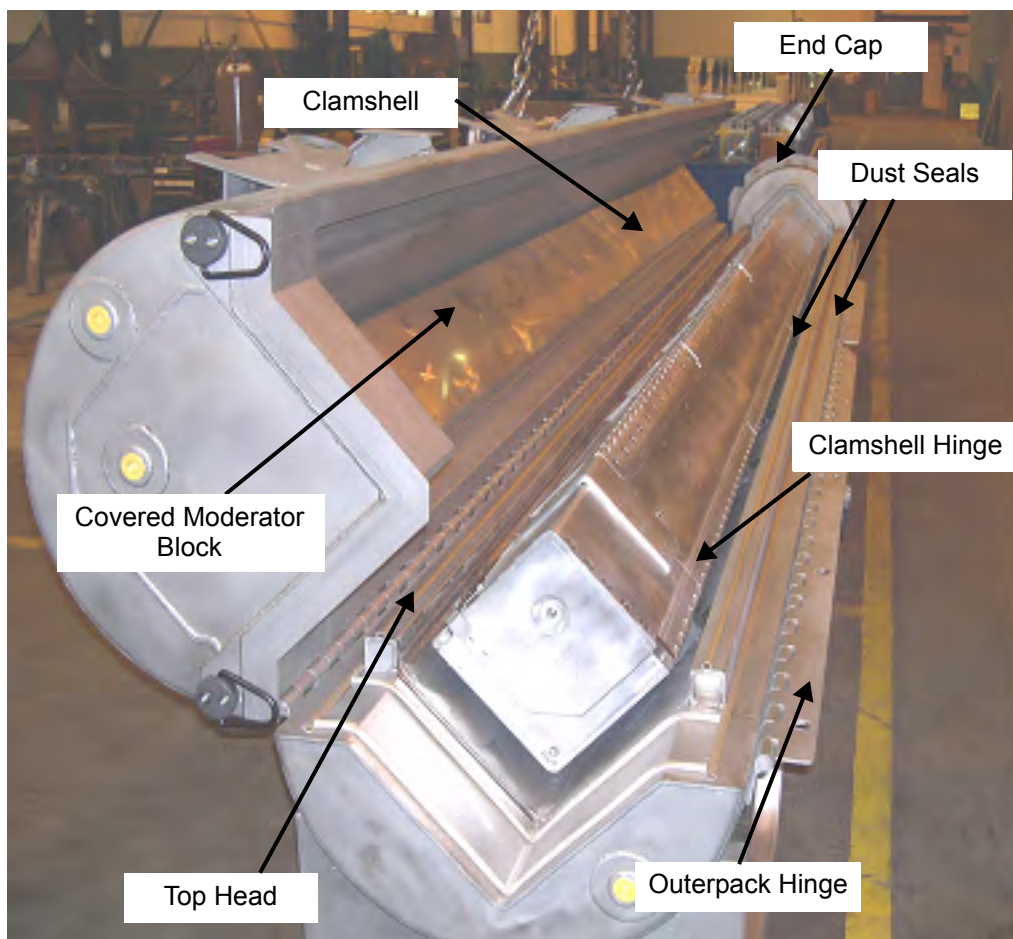


Figure 2-140 Traveller CTU Test Article Internal View

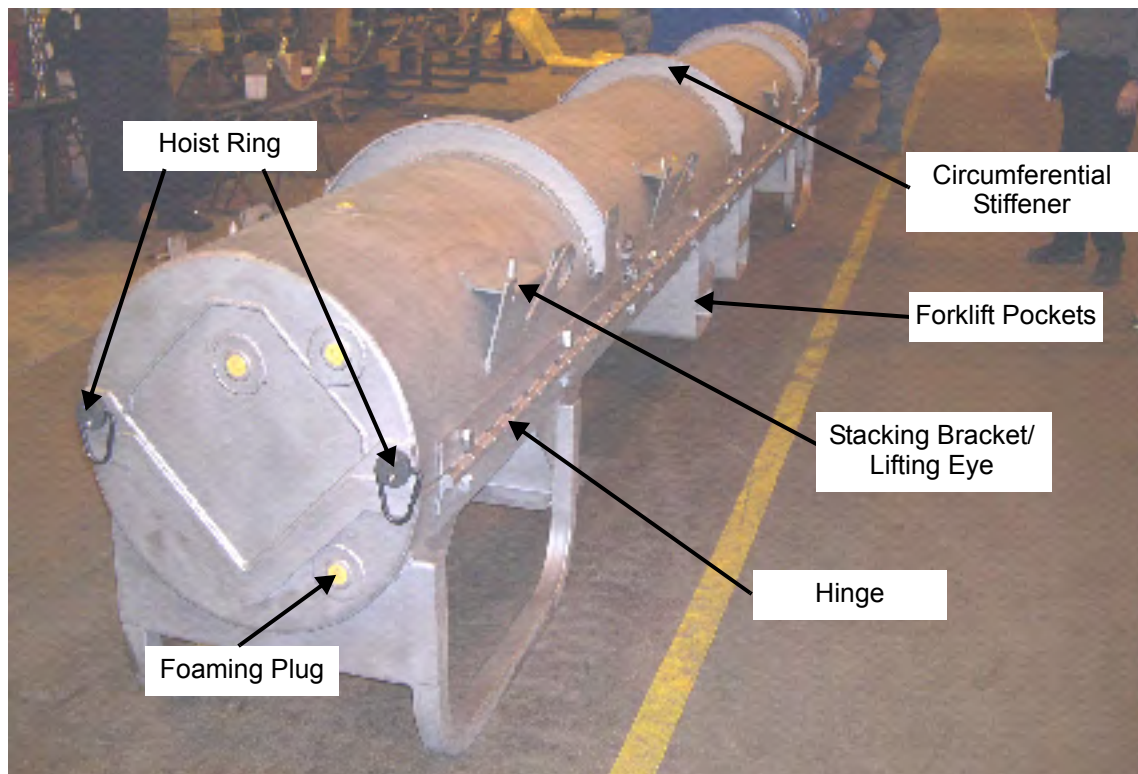


Figure 2-141 Traveller CTU External View

Table 2-44 Test Weights		
	Nominal* Wt	Actual Wt
Weight of Outerpack (Empty):	2633 lb	2671 lb
Weight of Clamshell (Empty):	425 lb	440 lb
Weight of package (Empty) :	3058 lb	3111 lb
Total package test weight:	4810 lb	4863 lb
Note: * Nominal total weight includes only Fuel Assembly since drop test was conducted without RCCA. Maximum expected design weight is estimated to be 5071 pounds (Ref. 3). The top Outerpack section weight is 1063 pounds empty and the bottom Outerpack section weight is 1608 pounds empty.		

Exterior Inspections After Drop Tests – The exterior of the package was examined after each drop. The inspections found that the Outerpack retained its circular pre-test shape except for localized plastic deformation at the ends. No hinge bolts failed on the Outerpack, the Outerpack did not separate, and neither the inner nor outer shell were perforated in the pin drop test.

Test 1.1

50 inch Low Angle
Slap Down



Test 1.2

32 feet, 10 inch End
Drop on B/N



Test 1.3

42 inch Pin Puncture

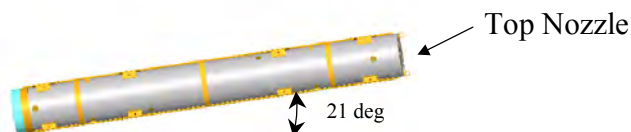


Figure 2-142 CTU Drop Test Orientations

Table 2-45 CTU Drop Test Orientations					
Test Article ID	F/A Type	Test Sequence	Test Pitch Attitude	Test Roll Attitude	Design Feature Tested
CTU	17x17 XL	P1.1) 1.2-m, NCT, Low angle ¹	9°	180°	Operations of hinges/doors
		P1.2) 9-m End Drop ¹	90°	0°	Lattice exp., FR axial position
		P1.3) 1-m Pin-puncture ¹	21°	90°	Hinge structural integrity

Test 1 – The 1.2 meter drop test resulted in a localized dent at the top nozzle end, and near the bottom nozzle end, the stiffener was dented over a length of about 8". Figures 2-143 and 2-144 shows the damage observed. The normal condition drop produced only local damage to the impact area. The depth of the crush was minimal.

Test 2 – The 9m (32.8-foot) free drop resulted in localized damage to the bottom nozzle end region. The two bottom nozzle stiffener keeper pins were detached as a result of the impact. The impact created a circumferential ripple located at 9" (bottom Outpack) and 12" (top Outpack) from the package bottom

end. The ripple resulted in a 1/2" crumple impact, which effectively shortened that section of the package slightly. Two stitch welds located inside the bottom nozzle end stiffener were broken, but this did not compromise the stiffener position. The bottom nozzle end cap stiffener separated to form a 1-3/16" gap, and the gap between the hinge and the cover lip was measured to be approximately 7/16". The hinge at the bottom nozzle end was separated about 1/16" from the Outerpack skin surface after the drop test. Figures 2-145 – 2-147 shows the damage observed.

Test 3 – The pin puncture test was located on the hinge of the Outerpack at approximately the axial center of gravity. The impact zone locally dented 6" of hinge length to a maximum measured depth of approximately 1-3/8", Figure 2-148. The hinge knuckles were not compromised as a result of the test. Hinge separation of 1/2" was noted about 7-1/2" from the impact point towards the top nozzle end.

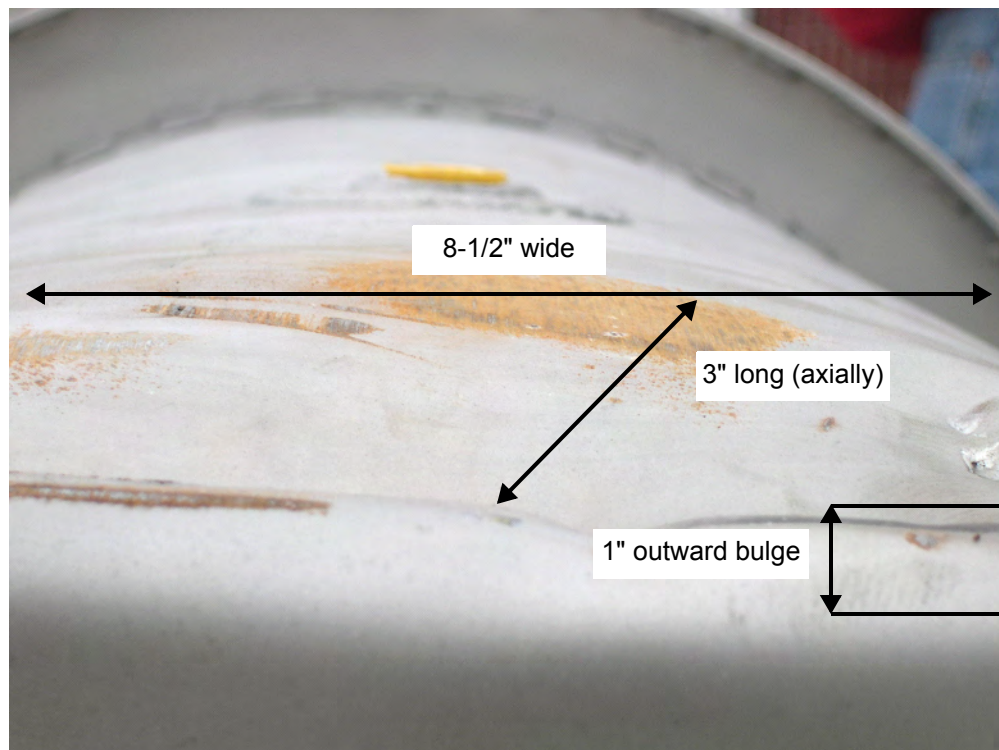


Figure 2-143 Top Nozzle End Outerpack Impact Damage

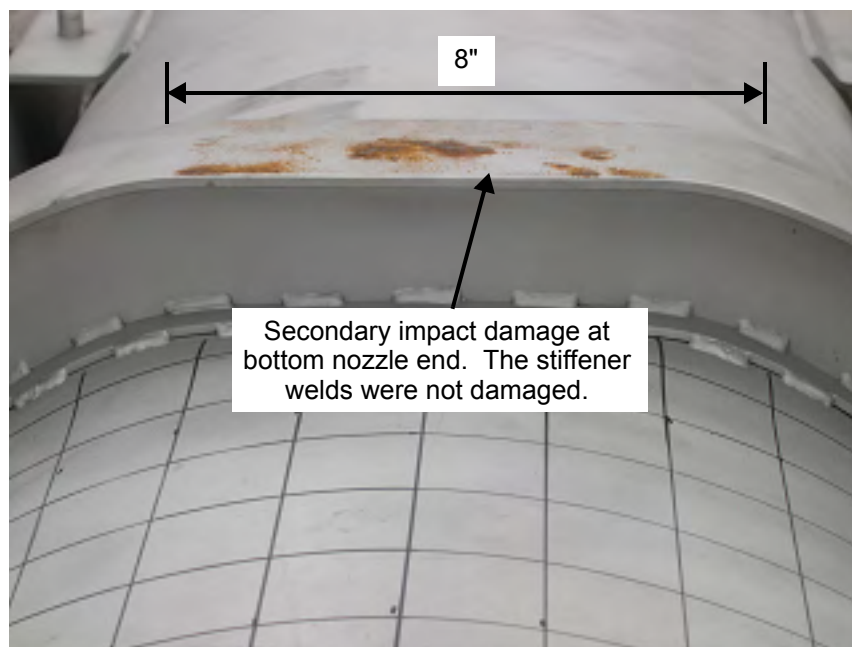


Figure 2-144 CTU Outerpack Stiffener After Test 1

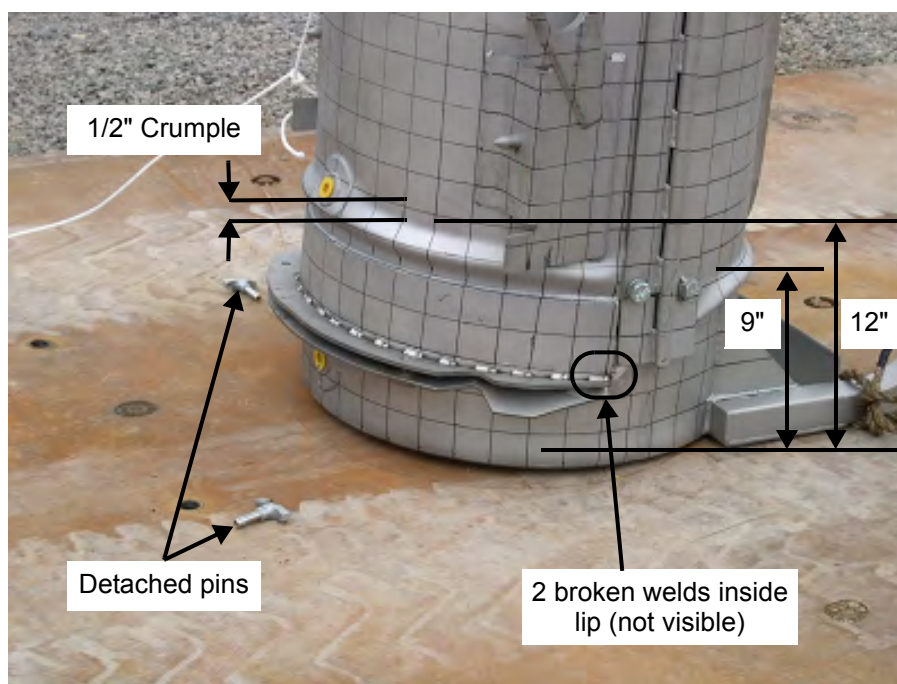


Figure 2-145 CTU Outerpack After Test 2

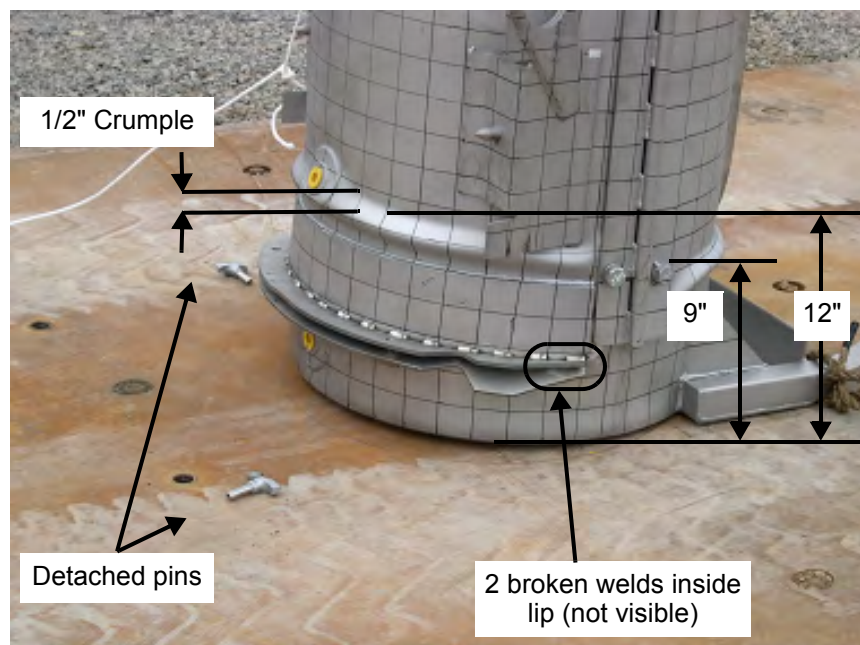


Figure 2-146 CTU Outerpack After Test 2

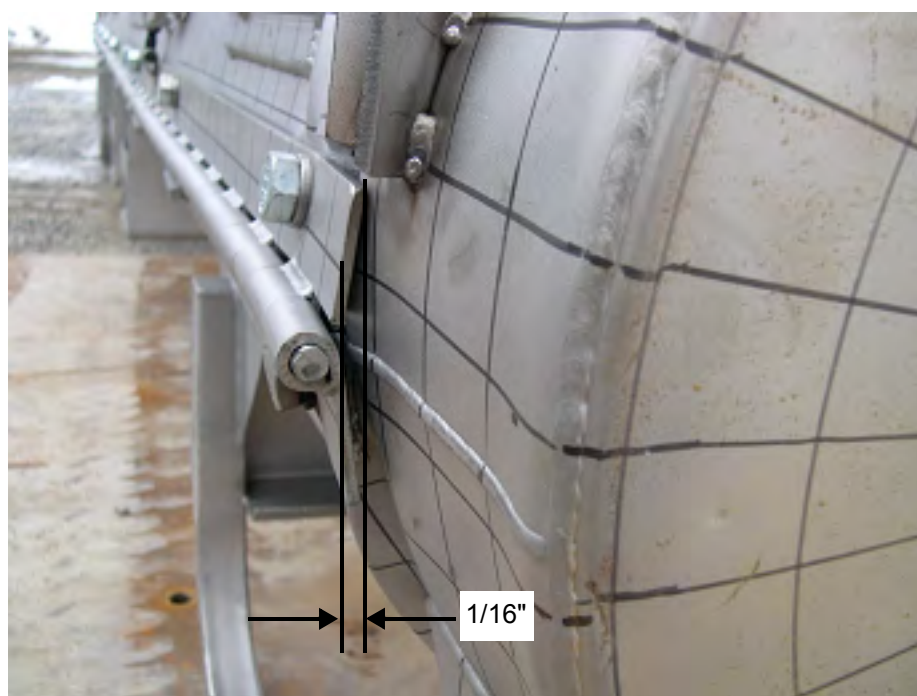


Figure 2-147 Hinge Separation at Bottom Nozzle End From Test 2

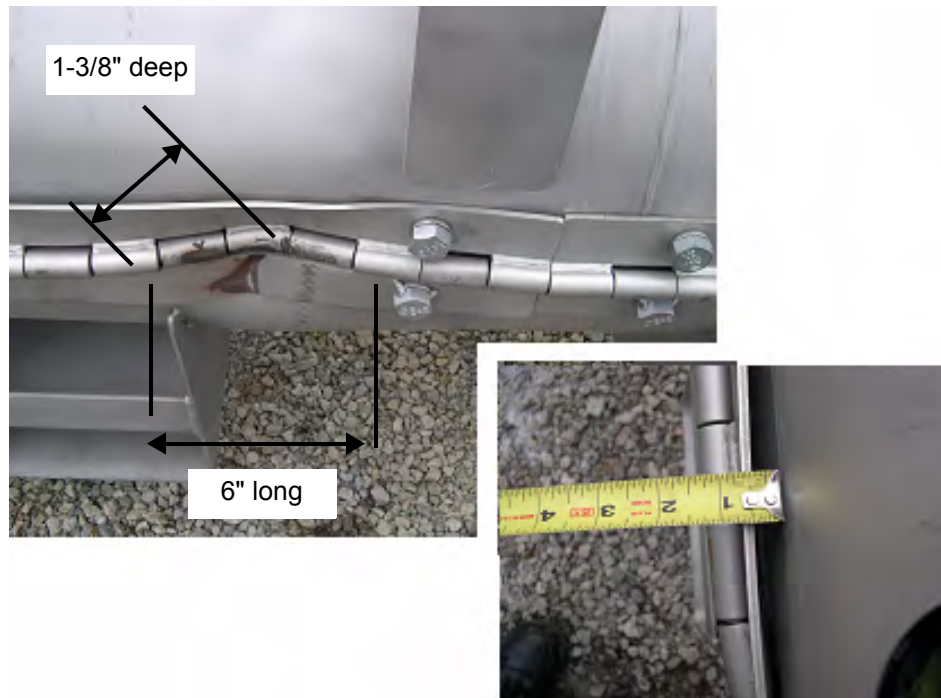


Figure 2-148 CTU Outerpack After Test 3

Interior Inspection Results – The CTU was sent to the South Carolina Fire Academy for the burn test immediately after the drop tests were completed. The package was not opened until the following week, approximately five hours after the fire test was completed. In general, the drop test and fire test resulted in minor damage to the Traveller internal structural components. The Clamshell was found intact and closed, Figure 2-149, and the simulated poison plates maintained position. All shock mounts were found to be visibly intact. At the bottom Clamshell plate, a 2-1/2" and a 2-3/4" piece of end lip sheared off. The measured gap was less than 1/16" and in the axial direction. The axial location of the fuel rods maintained position between the bottom and top nozzle. Finally, the moderator blocks were found to be intact and essentially undamaged after the completion of the drop and fire test. The moderator stud bolts on the top Outerpack were found sheared off, but the moderator cover maintained the moderator position. The stainless steel moderator cover was removed and the polyethylene moderator was examined. As shown in Figure 2-150, the moderator was intact and essentially undamaged.

Figure 2-151 provides the damage sketch overlaying the pre-tested fuel assembly for comparative purposes. For the 20" span from the bottom nozzle to Grid 2 of the fuel assembly, the fuel rod envelope expanded from 8-3/8" average nominal to 9-3/16". The grid envelope expanded from 8-7/16" nominal to 8-5/8" over the same 20" axial distance. The maximum measured fuel rod pitch in this region increased from 0.496" nominal to 0.990". This was caused by a single bent rod which was bent outward approximately 1/2". Otherwise, the typical pitch pattern consisted of 2 rod rows touching and the remaining 14 rows at nominal pitch, Figure 2-152.



Figure 2-149 CTU Clamshell After Drop and Fire Tests

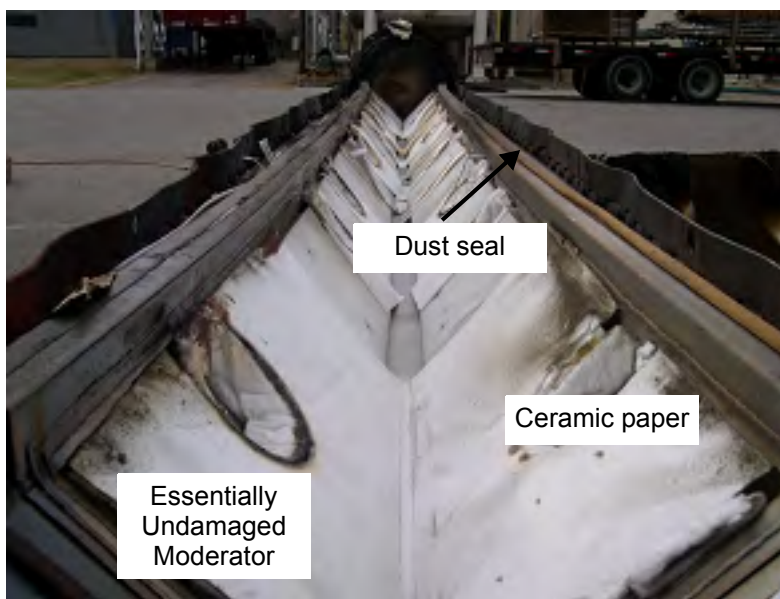


Figure 2-150 Outerpack Lid Moderator After Testing

For a length of 10" above Grid 2, the fuel rod envelope compressed from 8-3/8" nominal to 8-1/4". This slight compression is due to the single top rod slightly compressed inward. Above this 10" region, the single rod bent outward about 1/2" for a length of approximately 25".

For the 25" length from between Grids 2 and 3 and up to Grid 4, the single rod resulted in a measured envelope of 8-7/8", but the remaining envelope of 16 rows was slightly compressed (about 1/16"). The maximum pitch caused by the single rod was 0.740" compared to 0.496" nominal. Otherwise, the average pitch was nominal.

For the remainder of the fuel assembly from Grid 4 to the top nozzle, the fuel rod envelope compressed about 0.15" and the grid envelope compressed about 1/4". The average pitch decreased from 0.496" to 0.459" in this region.

Grid 1 was severely buckled, and the ovality was measured to be 120° for a length of about 20", Figure 2-153. Grids 2 and 3 were broken at the top corner, but otherwise intact. Grids 4-10 were relatively undamaged. The fuel inspection also indicated that 7.5% (20 of 265 rods) were cracked at the end plug locations (Figure 2-154). The average crack width measured was approximately 0.030" (30 mils) and the average length was 50% of the rod diameter. The cracked rods were located at the four corners, indicating the vertical impact created symmetrical impact forces to be transmitted through the bottom nozzle and fuel rods (Figure 2-155).

The fuel assembly in QTU-1 was measured before the test and after the burn test at locations shown in Figure 2-134 above. Table 2-46 provides the pretest dimensions. Tables 2-47 through 2-50 provide the post test dimensions.

2.12.5.4 Application to Higher Contents Weights

As discussed in section 2.12.3.2, the vertical drops on the bottom nozzle end of the package were determined to be the most damaging to the fuel assembly. Therefore, vertical drops were performed in the last two drop tests series, QTU-2 and CTU. This provided the maximum challenge to the fuel assembly and the clamshell heads. The tests were performed with lead filled fuel assemblies that did not incorporate rod cluster control assemblies (RCCA) or other internals. This was done because the RCCA, although adding weight, would increase the rigidity of the fuel assembly. This increased rigidity would decrease the forces on the clamshell walls. Additionally, when the fuel assembly is shipped with an RCCA, an additional axial restraint is provided to secure the total payload.

The two vertical drop tests are summarized below:

QTU-2 – 9 m drop test

Outerpack wt.	2611 lbs
Clamshell wt.	400 lbs
FA wt.	1767 lbs

Total wt. 4778 lbs
Drop ht 33.4 ft (10.2 m)

CTU – 9 m drop test

Outerpack wt. 2671 lbs
Clamshell wt. 440 lbs
FA wt. 1752 lbs
Total wt. 4863 lb
Drop ht 32.8 ft (10.0 m)

Drop heights greater than 9 m were used to bound maximum possible weights and other uncertainties. Because potential energy is directly proportional to drop height the bounding weights for each test result as:

QTU-2 at 9 meters

FA wt. 2000 lb
FA & Clamshell wt. 2453 lb
Total package wt. 5409 lb

CTU at 9 m

FA wt. 1947 lb
FA & Clamshell wt. 2433 lb
Total package wt. 5398 lb

During the vertical drop, the fuel assembly remains stationary with respect to the clamshell until the clamshell hits the outerpack impact limiter and begins to decelerate. When the outerpack hits the ground, it quickly decelerates as the foam and outerpack metal skin absorb the outerpack kinetic energy. As shown Figures 2-136 and 2-137, the amount of deformation to the outerpack was very small with a total crush of the outside of the bottom impact limiter < 0.5 inches (averaged).

The dynamic characteristics of the actual test performed with QTU-2 from 10.2 m are slightly different than a 9.0 m drop of a heavier package (and heavier fuel assembly), as described below. The terminal velocity of the test was approximately 14.2 m/s instead of the 13.3 m/s from a 9.0 meter drop. This will result in slightly different impact times between the clamshell and outerpack. The magnitude of this difference can be estimated with the following assumptions:

- Although the outerpack impact limiter has a total crush of approximately 0.5 inches (0.013 m) before the clamshell impact, the interior dimensions of the outerpack remain essentially the same as before impact.
- Initial separation distance between the clamshell and outerpack interior of 4.0 inches (0.102 m)
- There are no interaction between the clamshell/fuel assembly and the outerpack occurs until the clamshell hits the inside of the outerpack.

The actual QTU-2 drop was performed with a gross weight of 4778 lbs (2167 kg) from a 10.2 meter height. This is compared with a second theoretical Traveller drop test with a gross weight of 5409 lbs (2452 kg) from a 9.0 meter height. The outerpack cavity on QTU-2 was approximately eight inches longer than clamshell inside that cavity.

In the actual QTU-2 drop, the Traveller was falling at 14.2 m/s when the outerpack hits the ground. Assuming the clamshell was in its nominal position, it would continue to fall over a distance of four inches (0.102 m) before it hits the inside of the outerpack impact limiter. It takes the clamshell approximately 7.2 milliseconds for the clamshell to hit the inside of the outerpack after the outerpack comes to rest. This is calculated by:

$$0.102 = 14.15 t + 0.5 \cdot 9.81 t^2$$

In the theoretical Traveller drop, the clamshell package velocity at the time of outerpack impact is 13.2 m/s. If the clamshell is in the nominal position within the outerpack cavity, it will take approximately 7.7 milliseconds for the clamshell to hit the inside of the outerpack after the outerpack comes to rest. This is calculated by:

$$0.102 = 13.29 t + 0.5 \times 9.81 t^2$$

This results in a time difference between the two scenarios of 0.5 milliseconds. If the clamshell is located the maximum distance from the bottom impact limiter (8 inches or 0.204 m) the time to hit the impact limiter increases to 14.5 milliseconds and 15.3 milliseconds for the actual and theoretical drops respectively. In this case, there is a time difference of 0.8 milliseconds.

This simplified analysis does not include the deformation of the outerpack and the resulting deceleration profile which is not instantaneous. The FEA model provides a reasonable estimation of these deformations and predicts that the clamshell will hit the interior of the outerpack 15 milliseconds after the outerpack touches the ground (section 2.12.3.2.5). Because a small portion of the outerpack deformation is elastic, the outerpack probably rebounds slightly. The rebound was not observed in the tests but the FEA model does predict it to occur approximately 25 milliseconds after the outerpack impact.

The analysis above does show, however, the relative magnitude of the two different situations. The time difference between the actual drop and theoretical drop described above is only 0.5 to 0.8 milliseconds. This difference will not cause the clamshell to hit during the outerpack rebound (approximately 10 milliseconds

after clamshell contact) and the actual positions and velocities of the Traveller components will not be significantly different between the two drop scenarios.

The comparison above was made for the QTU-2 test. The general observations are applicable to the CTU tests however. As a result, the QTU-2 and CTU test drops justify payload weights significantly higher than the 1767 and 1752 lb fuel assemblies actually used in the testing.

2.12.5.5 Conclusions

Three series of drop tests were performed during the development and certification of the Traveller shipping package. This included two prototype units, two qualification test units and one certification test unit. Design improvements were made at each step based on the results of the drop tests and subsequent fire tests. The drop test series included a regulatory normal free drop of 1.2 meters, a 9-meter end drop onto the bottom nozzle, and a 1-meter pin-puncture test on the hinge. Minor structural Outerpack damage indicated that the Traveller Outerpack design satisfied the hypothetical accident condition defined in 10 CFR 71 and TS-R-1. Furthermore, the Clamshell was found to meet the acceptance criteria of the test by maintaining closure and its pre-test shape. The post-test geometry of the fuel assembly was determined to meet the acceptance criteria since only local expansion was noted in the lower 20" of the bottom nozzle region and the cracked rod gaps were all measured less than a pellet diameter.

In summary, testing demonstrated the Traveller package is suitable for compliance to normal and hypothetical mechanical drop test conditions described in 10 CFR 71 and TS-R-1.

This page intentionally blank.

|

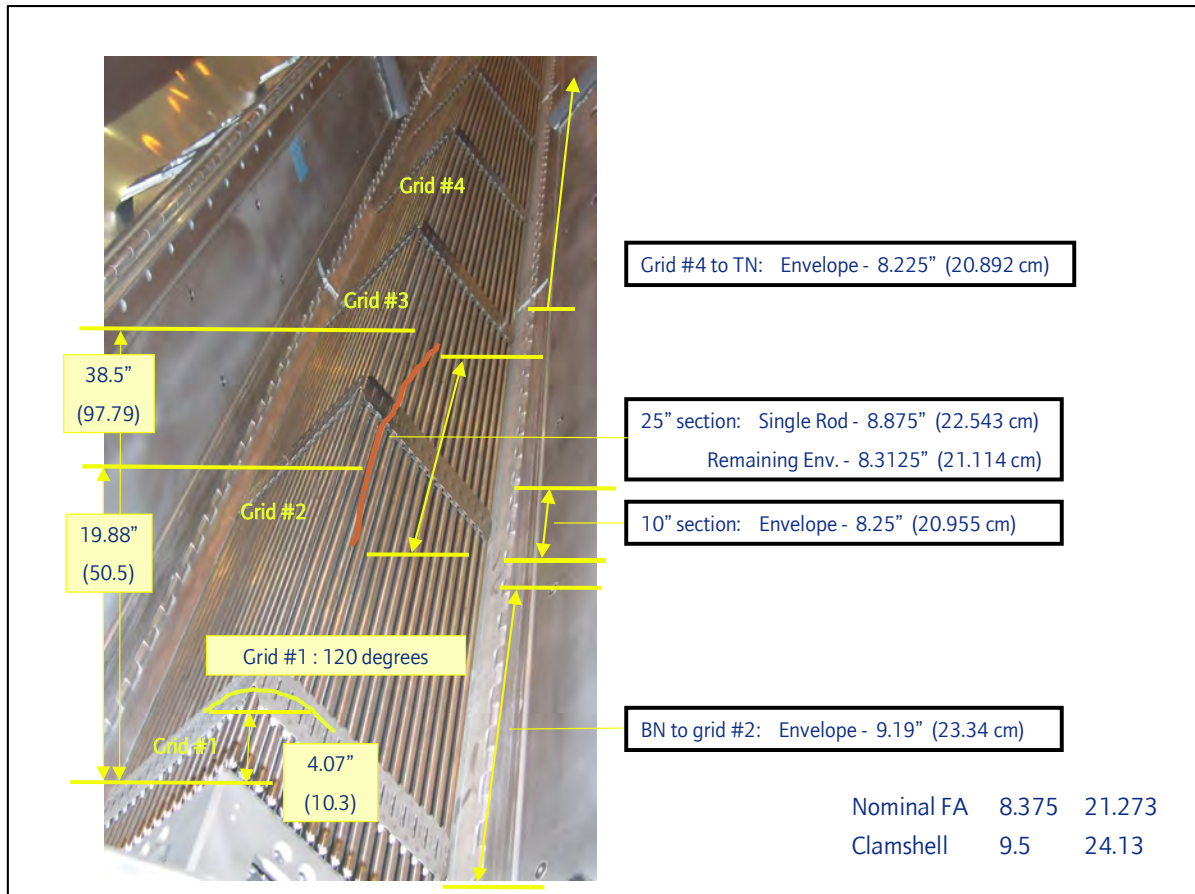


Figure 2-151 Fuel Assembly Damage Sketch and Pre-test Assembly

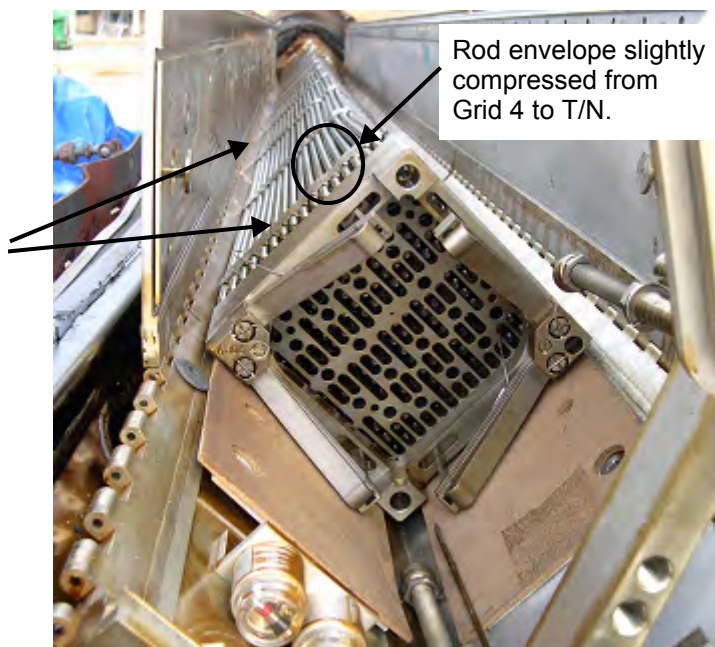


Figure 2-152 CTU Fuel Assembly After Testing

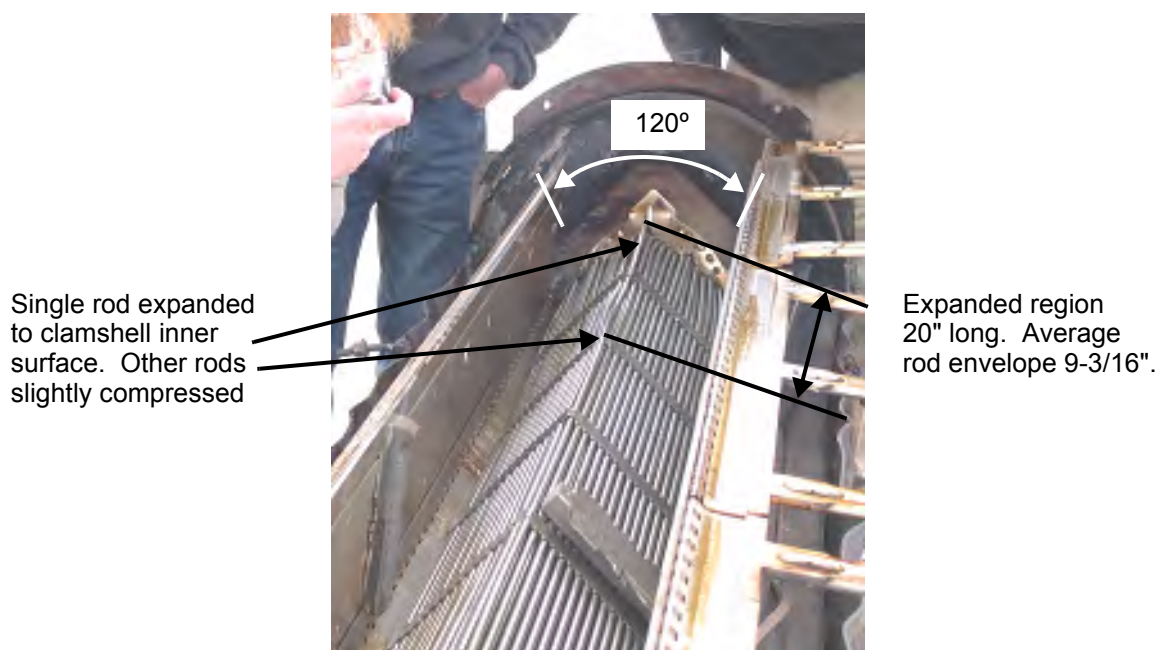


Figure 2-153 CTU Fuel Assembly Top End After Testing

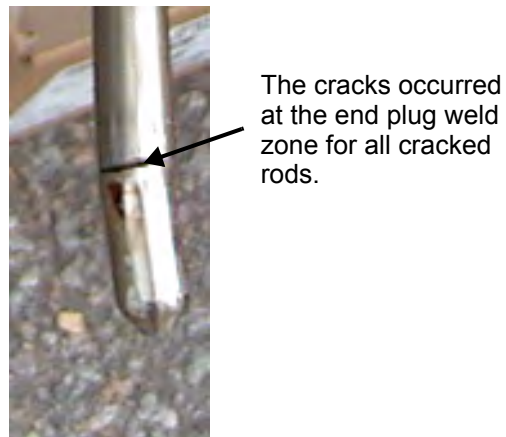


Figure 2-154 Cracked Rod From CTU Fuel Assembly

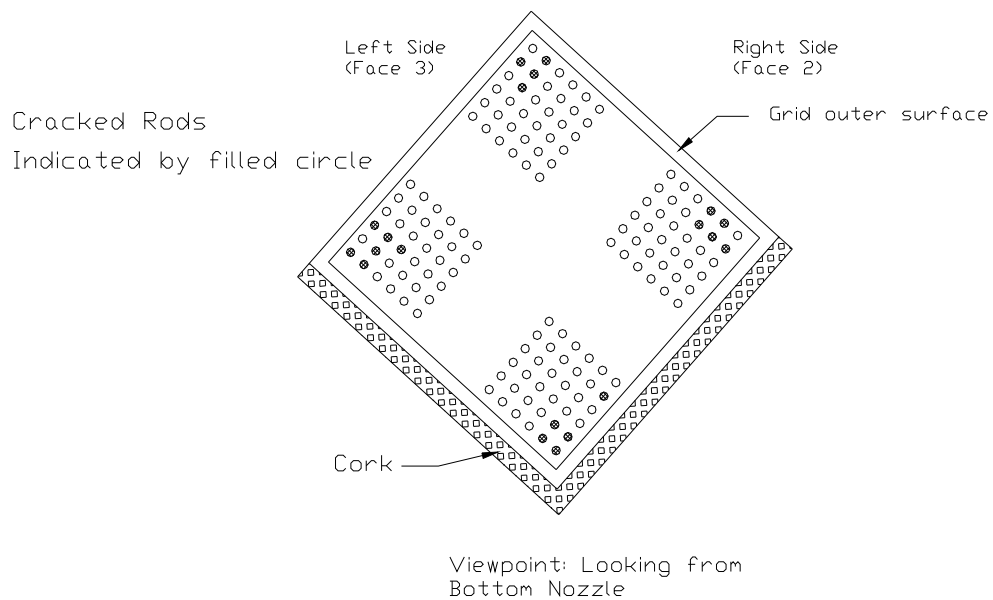


Figure 2-155 Cracked Rod Locations on CTU Fuel Assembly

Table 2-46 Fuel Assembly Key Dimension Before Drop Test			
Fuel Assembly ID: T/N # LM1F2N			
F/A Location	Fuel Envelope (inches)	Gap (inches)	Pitch (inches)
B/N – Grid 1	1: 8-3/8 2: 8-7/16 3: 8-3/8 4: 8-7/16	L – 0.123 R – 0.121	L – 0.498 R – 0.495
Grid 1- Grid 2	1: 8-3/8 2: 8-7/16 3: 8-3/8 4: 8-7/16	L – 0.123 R – 0.124	L – 0.497 R – 0.499
Grid 2- Grid 3	1: 8-3/8 2: 8-7/16 3: 8-3/8 4: 8-7/16	L – 0.121 R – 0.121	L – 0.495 R – 0.495
Grid 3- Grid 4	1: 8-3/8 2: 8-7/16 3: 8-3/8 4: 8-7/16	L – 0.123 R – 0.123	L – 0.497 R – 0.498
Grid 4- Grid 5	Rods: 8-3/8 Grids: 8-7/16	0.121	0.495
Grid 5- Grid 6	Rods: 8-3/8 Grids: 8-7/16	0.123	0.498
Grid 6- Grid 7	Rods: 8-3/8 Grids: 8-7/16	0.122	0.497
Grid 7- Grid 8	Rods: 8-3/8 Grids: 8-7/16	0.123	0.497
Grid 8- Grid 9	Rods: 8-3/8 Grids: 8-7/16	0.123	0.498
Grid 9- Grid 10	Rods: 8-3/8 Grids: 8-7/16	0.121	0.495
Grid 10 – T/N	Rods: 8-3/8 Grids: 8-7/16	0.122	0.497
AVERAGE	Rods: 8-3/8 Grids: 8-7/16:	0.122	0.497
Note: * Measured fractional values were measured to nearest 1/16". Measured decimal values were measured to the nearest 0.001".			

Table 2-47 CTU Fuel Assembly Grid Envelop Dimensions After Testing		
Location	Measured Grid Envelope Dimension, Inches	
	Left Side, LS	Right Side, RS
Grid 1	9-0	8-3/4
Grid 2	8-7/16	8-3/8
Grid 3	9-1/2	9-1/2
Grid 4	8-1/8	8-1/4
Grid 5	8-1/8	8-1/4
Grid 6	8-1/4	8-1/4
Grid 7	8-1/8	8-3/16
Grid 8	8-5/16	8-3/16
Grid 9	8-5/16	7-7/8
Grid 10	8-3/8	8-1/2
MAXIMUM VALUE	9-1/2	9-1/2

Table 2-48 CTU Fuel Assembly Rod Envelope Data After Testing			
Fuel Assembly Rod Envelope Inspection Table			
Location	Measured Envelope Dimension, In.		Calculated Maximum Fuel Rod Pitch from Form 1G (Nominal Pitch = 0.496")
	Left Side, LS	Right Side, RS	
Between B/N and Grid 1	9-0	8-3/4	0.566
Between Grids 1 and 2	8-5/16 ⁽¹⁾	8-5/16 ⁽¹⁾	0.990
Between Grids 2 and 3	8-1/2	8.-0	0.740
Between Grids 3 and 4	8-7/16	8-1/2	0.715
Between Grids 4 and 5	8-3/16	8-3/16	0.472
Between Grids 5 and 6	8-3/16	8-3/8	0.578
Between Grids 6 and 7	8-1/16	8-1/16	0.550
Between Grids 7 and 8	8-3/8	8-3/16	0.541
Between Grids 8 and 9	8-0	7-13/16	0.483
Between Grids 9 and 10	8-3/8	8-1/2	0.498
Between Grid 10 and T/N	8-3/8	8-0	0.497
MAXIMUM VALUE	9-0	8-3/4	0.990
Note: (1) A single rod was measured to the inner Clamshell surface (9-1/2"). See Figure 2-153.			

Table 2-49 CTU Fuel Assembly Rod Envelope After Testing			
Fuel Assembly Rod Envelope Inspection Table			
Location	Measured Envelope Dimension, In.		Calculated Maximum Fuel Rod Pitch from Form 1G (Nominal Pitch = 0.496")
	Left Side, LS	Right Side, RS	
Between B/N and Grid 1	9-0	8-3/4	0.566
Between Grids 1 and 2	8-5/16 ⁽¹⁾	8-5/16 ⁽¹⁾	0.990
Between Grids 2 and 3	8-1/2	8.-0	0.740
Between Grids 3 and 4	8-7/16	8-1/2	0.715
Between Grids 4 and 5	8-3/16	8-3/16	0.472
Between Grids 5 and 6	8-3/16	8-3/8	0.578
Between Grids 6 and 7	8-1/16	8-1/16	0.550
Between Grids 7 and 8	8-3/8	8-3/16	0.541
Between Grids 8 and 9	8-0	7-13/16	0.483
Between Grids 9 and 10	8-3/8	8-1/2	0.498
Between Grid 10 and T/N	8-3/8	8-0	0.497
MAXIMUM VALUE	9-0	8-3/4	0.990
Note:			
(1) A single rod was measured to the inner Clamshell surface (9-1/2"). See Figure 2-153.			

Table 2-50 CTU Fuel Rod Gap and Pitch Inspection After Testing			
Fuel Rod Gap and Pitch Inspection Table			
Location	Measured Maximum Gap, Inches		Calculated Maximum Pitch, Inches
	Left Side, LS	Right Side, RS	
Between B/N Grid 1	0.093 (between rows 9 & 10)	0.193 (between rows 6 & 7)	0.566
Between Grids 1 and 2	0.616 (out-lying rod only)	0.563 (out-lying rod only)	0.990
Between Grids 2 and 3	0.207 (one rod) Others touching	0.366 (one rod) Others touching	0.740
Between Grids 3 and 4	0.336	0.340	0.715
Between Grids 4 and 5	0.099	0.050	0.472
Between Grids 5 and 6	0.204	0.084	0.578
Between Grids 6 and 7	0.173 (between rows 2 & 3) Others Nominal	0.176 (between rows 6 & 7) Others Nominal	0.550
Between Grids 7 and 8	0.166	0.064	0.541
Between Grids 8 and 9	0.109	0.060	0.483
Between Grids 9 and 10	0.124	0.090	0.498
Between Grid 10 and T/N	0.123	0.074	0.497
MAXIMUM VALUE	0.616	0.563	0.990
Note: The pitch is calculated by adding the measured gap to the fuel rod diameter.			

2.12.6 SUPPLEMENT TO DROP ANALYSIS FOR THE TRAVELLER XL SHIPPING PACKAGE –CLAMSHELL AXIAL SPACER STRUCTURAL EVALUATION

2.12.6.1 Background

The XL Clamshell may be configured to include an aluminum spacer assembly to ship fuel types that normally would ship inside a Traveller STD package as shown in Figure 2-158. The structural performance of the spacer assembly in a bottom-down 9m hypothetical drop is evaluated to determine if there is any buckling of the spacer, a 6-inch Schedule 40 aluminum pipe, that could then damage or deform the Clamshell.

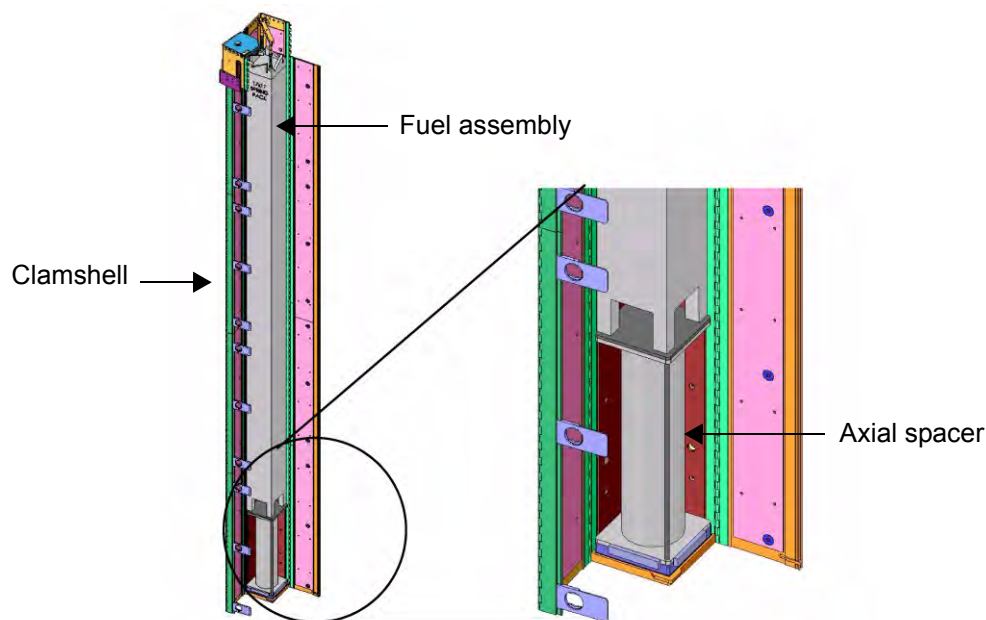


Figure 2-156 Axial Spacer below Fuel Assembly in Traveller XL Clamshell

The fuel assembly is assumed to be restrained in the clamshell to prevent any secondary impact within the clamshell. The spacer below the fuel assembly, when needed, and a top axial restraint restrain the contents to the clamshell, and as such the clamshell and contents decelerate as a coupled mass. The top axial restraint, fuel assembly structure, or spacer may absorb kinetic energy during the deceleration that results from an end drop impact.

Any structural deformation of the spacer assembly shall not change the shape of the clamshell or compromise the ability of the clamshell to confine the fuel assembly. The clamshell panel doors shall remain securely closed, end plates shall remain securely in place, hinges attaching the panel doors and multi-point cammed latch shall remain intact, and dimensions of the clamshell shall not be altered.

The primary impact with the unyielding surface occurs on the Outerpack end impact limiter. The Outerpack decelerates quickly within a few milliseconds of the primary impact because the contact area of the end surface is large and stiff, and there is no significant rebound. The Outerpack is completely decelerated by the time a secondary impact occurs inside the package as the Clamshell, suspended in the lower Outerpack on rubber mounts, continues to fall and contact the inside surface of the end impact limiter.

A crushable foam “pillow” is integrated into the end impact limiter to absorb kinetic energy from the secondary impact between the Clamshell and inside surface of the lower Outerpack end impact limiter. This pillow is a solid disk made from 6 pcf polyurethane foam. It has a nominal diameter of 12.00 inches (305 mm) and a nominal height of 3.60 inches (91 mm). The stiffer foam in the Outerpack end impact limiter, 20 lb/cu. ft. (0.32 g/cc) density, is located below and around the soft pillow. This stiffer component end impact limiter functions to decelerate the Outerpack at all high drop angle orientations.

2.12.6.2 Conclusions

Results of the simulated bottom-down 10m impact predict that there is no significant risk of damage to the Clamshell due to buckling of the spacer assembly. The 28.94 inch (735.1mm) long spacer assembly is too short to fail in a classic Euler buckling manner. Instead, the spacer pipe locally may crumple near its bottom and top ends during the impact. This local crumpling does not result in large column bowing displacements that could impart forces on the Clamshell panel doors or base.

2.12.6.3 Detailed Calculations and Evaluations

A Traveller TX finite element (FE) model of the entire package was originally used to simulate the impact testing. A new LS-DYNA Traveller model was created to simulate features of the TX package affected by the end impact orientation. The new model is more efficient and was used to evaluate the structural performance of the axial spacer in the vertical end impact.

Assumptions

Specific assumptions used in the FEA simulation are as follows:

1. The assumed mass of the 17STD FA (1,496 lbs, 678 kg) includes the heaviest core component, a Rod Control Cluster Assembly (RCCA) (180 lbs, 82 kg), Reference 5. The total FA mass was therefore, 1,676 lbs (760 kg) (RCCA dwg: 1554E27).
2. The FA is modeled with distributed point-element masses and is therefore not elastic. This is very conservative since actual drop testing revealed the weak axial stiffness of a FA (it vibrates and bows during end impacts).
3. The drop height was conservatively increased from 9m to 10m.
4. The FA bottom nozzle and spacer assembly were modeled without any restraints and they are therefore free to rotate/tilt. In actuality, the FA itself would keep the bottom nozzle relatively horizontal and the Clamshell walls will further restrain both items.

5. The majority of the mass of the Outerpak has not been included in this analysis because it does not significantly affect the Clamshell impact. More specifically, the Outerpak impact event is finished within only a few milliseconds, therefore the bottom limiter is simply waiting for the Clamshell impact into it. This assumption has been validated in a separate run which did include the remaining Outerpak mass.
6. The foam crush characteristics include extrapolation from 80% crush to 100% crush for model stability purposes. As mentioned earlier, actual pillow crushing was measured to be only about 50%. This is because the FA is not a rigid “hammer” that has no axial elasticity. This effect has been proven to be quite significant. However, in these simulations, the severe impact of the rigid-mass modeling of the fuel assembly was used. In some cases, this forces the crush curves to be extrapolated to 100%.
7. The longest spacer assembly is considered the bounding FA/Spacer combination.
8. LS-DYNA incorporates strain capability into the plastic regions of metallic material properties, therefore the “strain hardening” effects for aluminum were included in the model. These values are difficult to obtain, and therefore engineering judgement was used to assume the modulus after the yield. This was assumed to be a very low, linear value, of 268 MPa. This is almost no strain hardening from yield to failure.

Method

The Lawrence Livermore, LS-DYNA[®] finite element code was used to determine the loads, displacements, accelerations, strains, etc. of a Traveller XL shipping package containing a 17x17STD fuel assembly with RCCA when dropped onto a flat unyielding surface from a height of 10m. LS-DYNA 970, Revision 5434a, is a general purpose finite element code for analyzing the large deformation dynamic response of structures. This software was selected because it allows the analysis to include the effects of large deformation, large strain, material non-linearity, contact, and failure of materials.

Only the bottom end of the FA is modeled, the remainder of the assembly mass is simulated through point-mass elements. The weight of the remainder of the Clamshell is also modeled with point-mass elements. The Clamshell is an aluminum box with a solid 1 inch thick bottom plate. The spacer assembly is modeled with the 1.25 inch (31.8 mm) thick bottom rubber pad included, however, the 3/8 inch (9.5 mm) thick rubber pad on the top surface was not modeled.

Figure 2-157 shows components, materials, and meshing for the FEA simulation. The material properties assumed for the aluminum, stainless steel, and the crushable foams, and rubber pad are summarized in Tables 1 through 5. The compressive strength difference between the crushable foams is shown in Figure 2-158. Figure 2-159 shows the stress-strain curve of the 304 Stainless Steel properties used in the LS-Dyna simulation.

The appropriate properties of neoprene rubber for this simulation are difficult to determine exactly. Further, neoprene rubber does not obey Hook's law because it exhibits non-linear behavior. For this simulation, a value of 6.21 MPa was used for the shear modulus (G) of the 30 mm thick lower rubber pad.

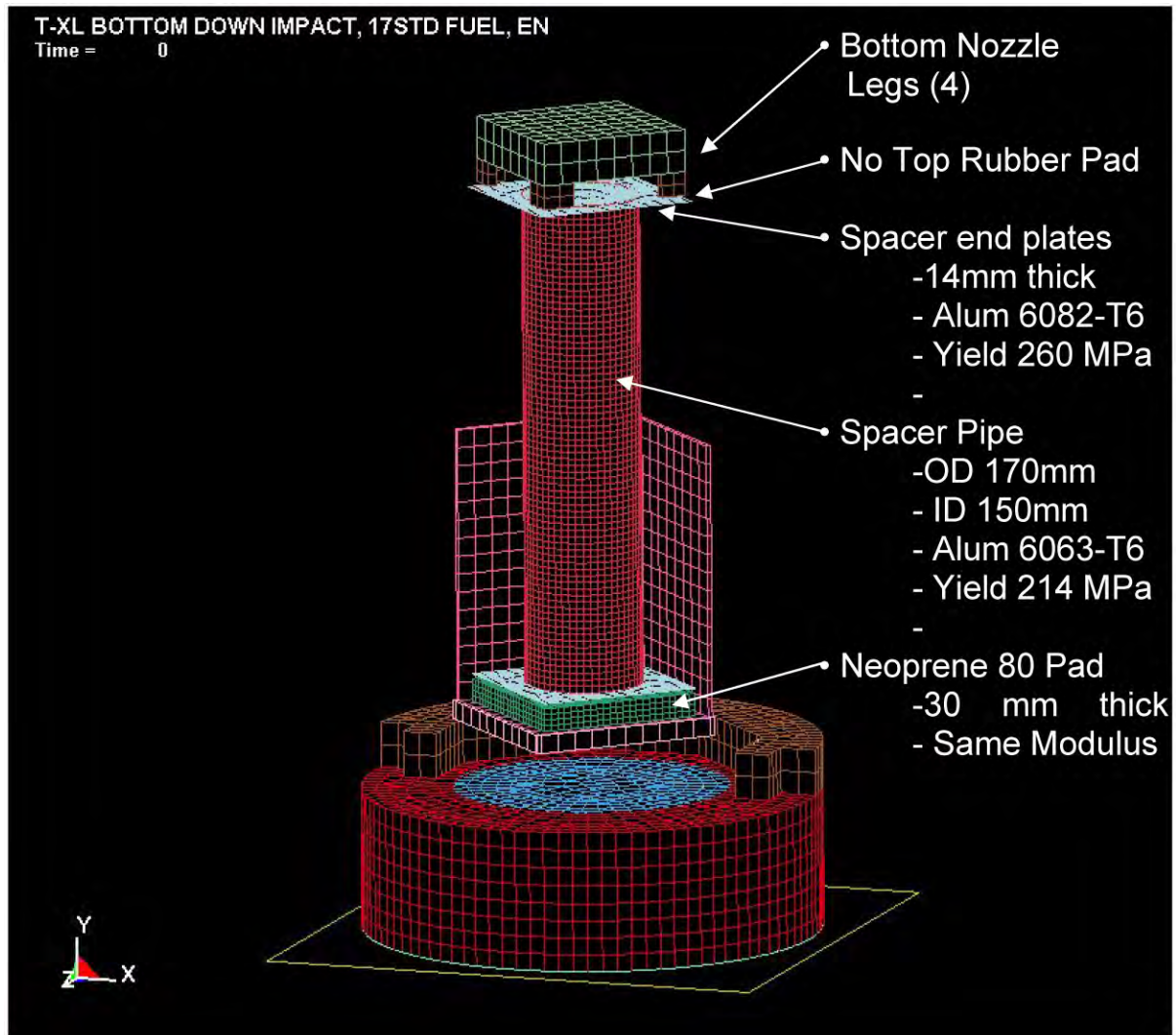


Figure 2-157 FEA Model – Axial Spacer

Table 2-51 Dimension and Material Properties of Axial Spacer	
Support Pipe:	
Exterior Diameter - mm (in):	170 (6.69)
Interior Diameter - mm (in):	150 (5.91)
Length - mm (in):	671.1 (26.42)
Wall Thickness - mm (in):	10 (0.39)
Material	6063-T6
Yield Strength - MPa (Ksi)	214 (31.0)*
Base Plates:	
Thickness - mm (in)	14 (.55)
Length - mm (in):	228.6 (9.00)
Material	6082-T6
Yield Strength - MPa (Ksi)	262 (38.0)*
Top Rubber Pad:	
Length - mm (in):	228.6 (9.00)
Thickness - mm (in)	10 (0.39)
Material	Neoprene 80
Bottom Rubber Pad:	
Length - mm (in):	228.6 (9.00)
Thickness - mm (in)	30 (1.18)
Material	Neoprene 80
Rod Handle:	No
Side Rubber Pad:	No
Total Assembly Length - mm (in):	735.1 (28.94)

Table 2-52 Aluminum Properties			
Aluminum Properties			
6005-T5 and 6061-T6 Aluminum at 75 degrees F			
Property	Symbol	Value	Units
Density	RO	2.71E-09	Mg/mm ³
Modulus	E	70	kN/mm ² (GPa)
Poisson's Ratio	PR	0.30	dimensionless
Yield Strength	SIGY	0.241	kN/mm ² (GPa)
Hardening Modulus	ETAN	0.25	kN/mm ²
Failure Strain	FAIL	0.35	In compression

Table 2-53 Annealed 304 Stainless Steel Properties			
Annealed 304 SS Properties			
Property	Symbol	Value	Units
Density	RO	8.00E-09	Mg/mm ³
Modulus	E	203	kN/mm ² (GPa)
Poisson's Ratio	PR	0.30	dimensionless

Table 2-54 Crushable Foam Properties			
Crushable Foam Properties			
	Density	Modulus	Poisson's Ratio
	Mg/mm ³	(MPa)	(dimensionless)
6 pcf Last-A-Foam	9.61E-11	30.14	0
10 pcf Last-A-Foam	1.60E-10	66.23	0
20 pcf Last-A-Foam	2.24E-10	192.76	0

Table 2-55 Neoprene (60 durometer) Properties			
Neoprene (Rubber) at 75 degrees F			
Property	Symbol	Value	Units
Density	RO	9.13E-10	Mg/mm ³
Shear Modulus	G	6.21E+00	MPa

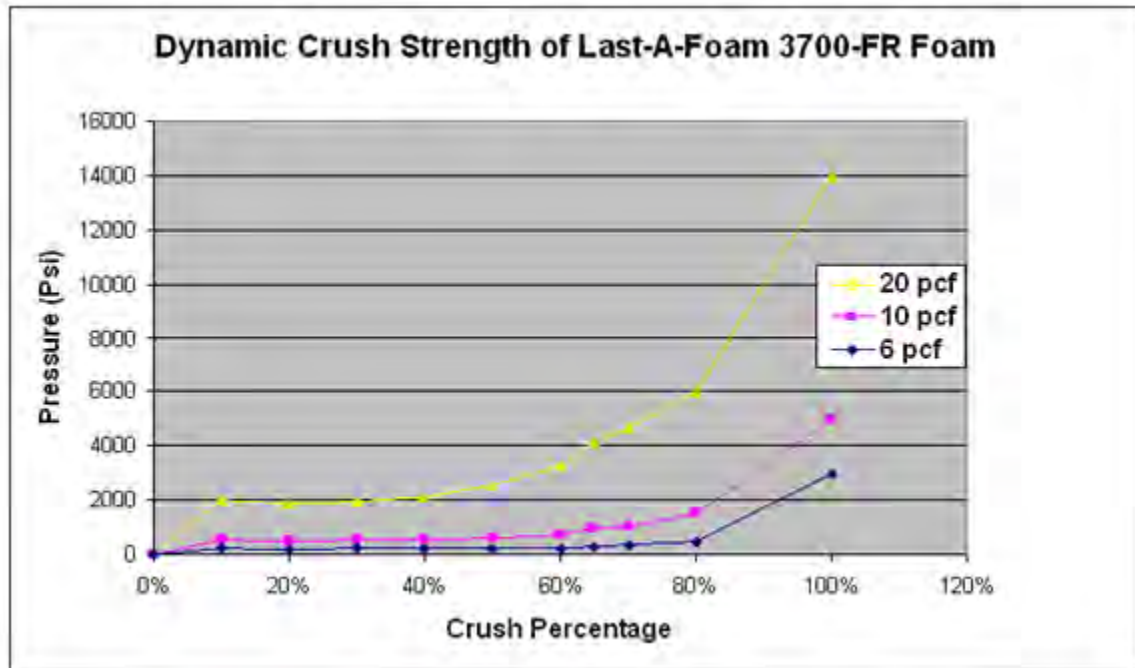


Figure 2-158 Dynamic Crush Strengths for Foam Materials Utilized in the Traveller

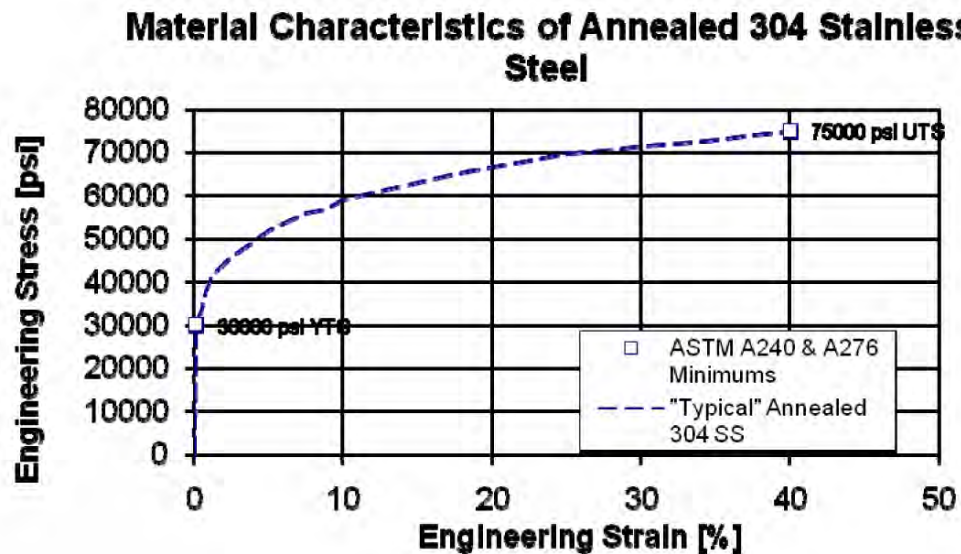


Figure 2-159 Annealed 304 Stainless Steel Stress-Strain Characteristics

Calculation Results

The 10m initial drop height of the Traveller simulation yields an impact velocity of 45.93 ft/sec (14.00 m/s). The FEA simulation shown in Figure 2-160 predicts deformation of the top spacer end plate, but no buckling or plastic deformation of the spacer pipe. From the displacement history of the top surface of the pillow shown in Figure 2-161, the total crush distance into the end impact limiter is approximately 94 mm (3.70 in). Figure 2-162 shows the kinetic energy history (mJ) of the axial spacer model.

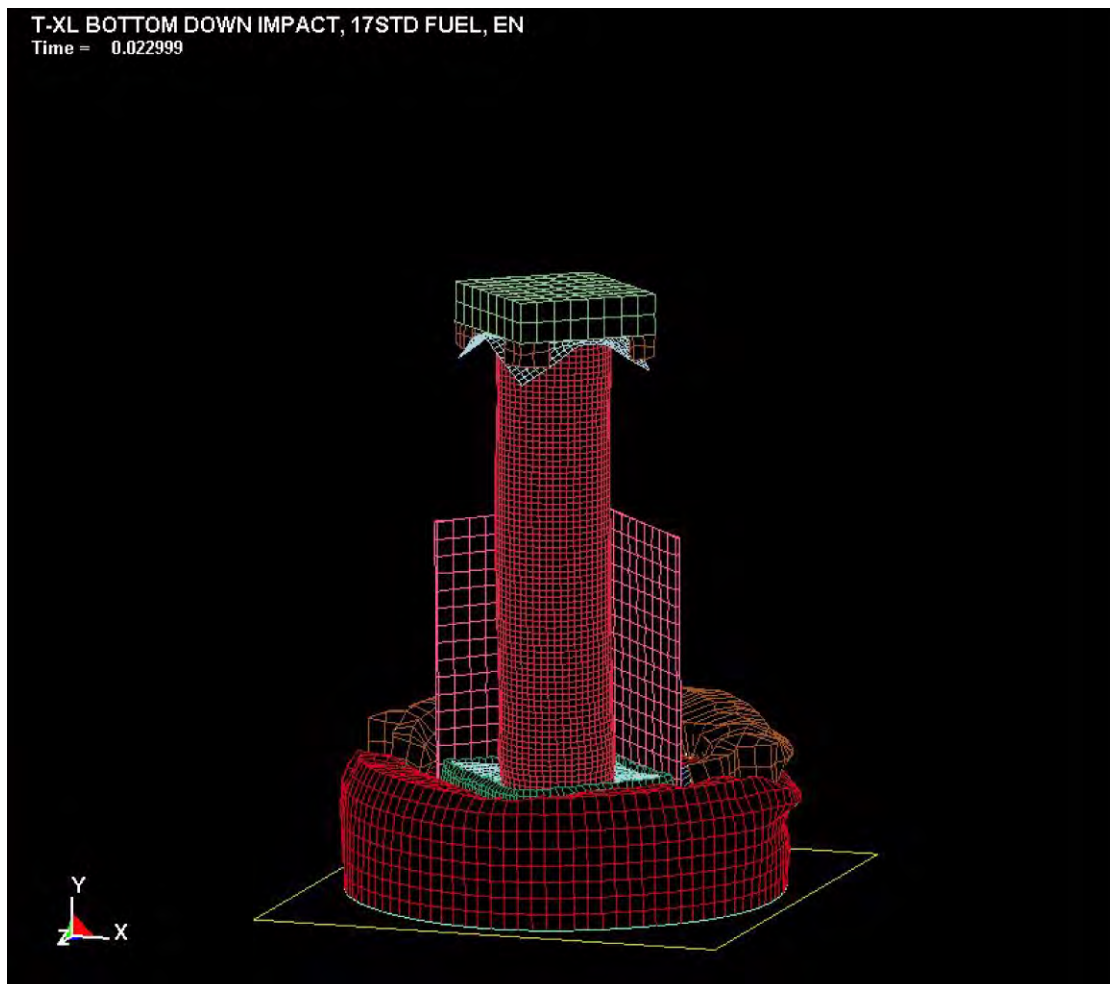


Figure 2-160 Deformed Model with Axial Spacer at 23 ms (the end of the impact)

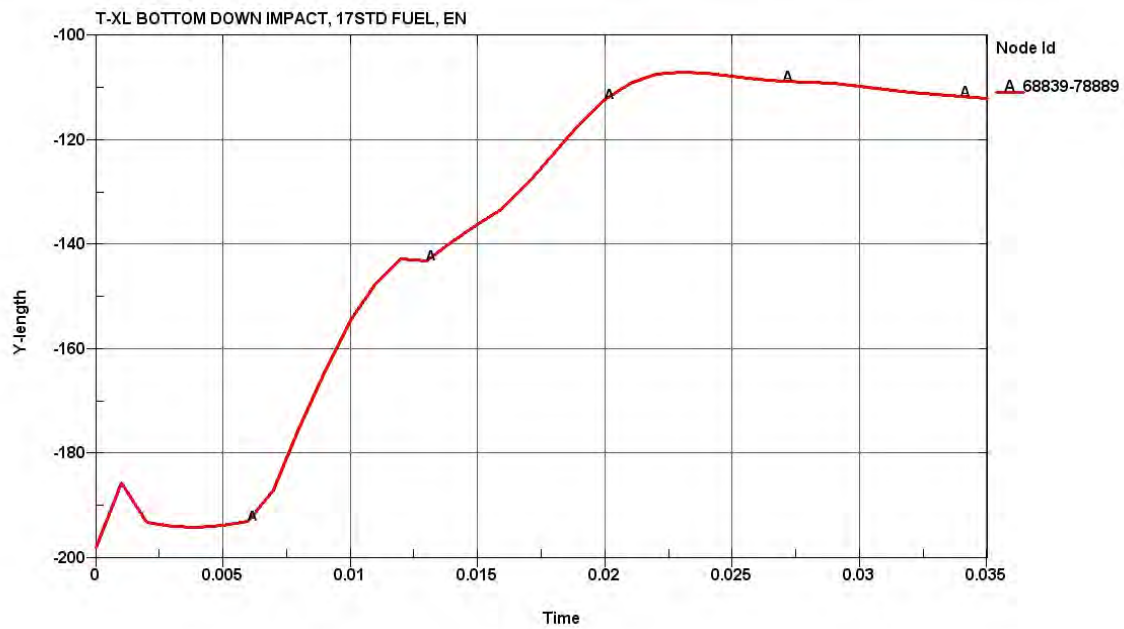


Figure 2-161 Predicted Total End Crushing (mm) with Axial Spacer

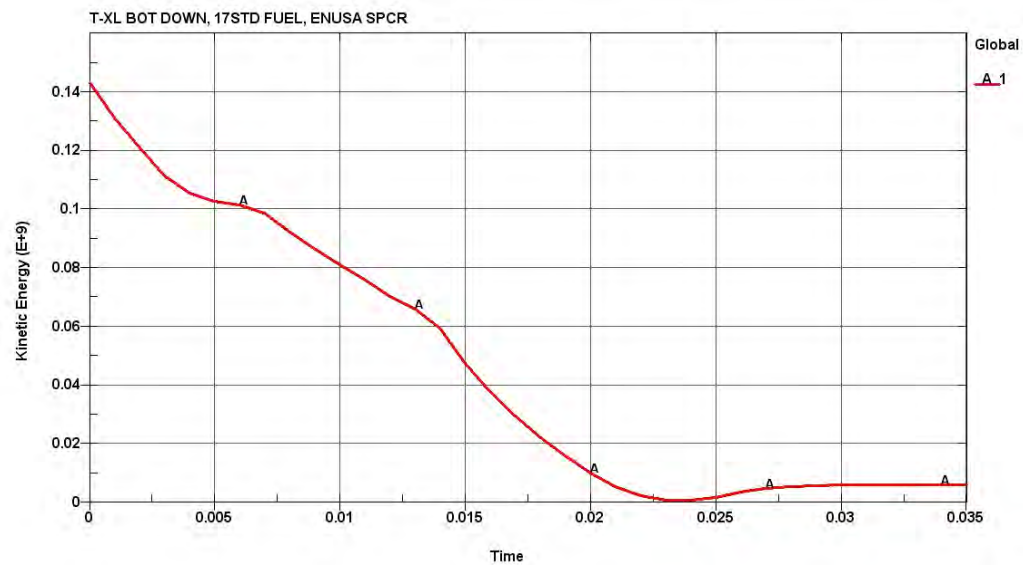


Figure 2-162 Kinetic Energy History (mJ) of the Axial Spacer Model

Validation

The many assumptions used to develop the LS-DYNA non-linear finite element stress code, including those needed to model the materials and impact, are validated by comparing the simulation results to the actual drop tests for the Traveller XL. Comparisons between certification test unit results and FEA simulation demonstrates that physical phenomenon governing shipping package impacts are simulated with adequate fidelity using the LS-DYNA model.

The pillow from a 10.0 m free drop impacting the bottom end of the package, CTU Test 1.2, was observed to crush approximately 1.8 inches. The simulation with axial spacer predicted the end limiter assembly (Pillow and high density end limiter) is crushed 92 mm (3.62 inches). The simulation predicts more absorption of the kinetic energy in the end impact limiter than observed in the actual drop test. This is due primarily to the assumption in the simulation that the fuel assembly is a rigid mass while for the actual drop test there was a significant energy absorbed in the deformation of the fuel assembly bottom nozzle and fuel rods during the deceleration.

In addition to the comparison energy absorbed by the end impact limiter, the axial force required to cause buckling of the spacer pipe, P_{cr} , can be estimated using the Euler buckling equation assuming that neither end is fixed (Reference: Shigley, "Mechanical Engineering Design", 3rd Edition, page 115):

$$P_{cr} = \pi^2 \times E \times I / L^2, \text{ where}$$

E = Modulus of elasticity, 1.00E+07 psi

I = Moment of inertia, $\pi/64 \times (D^4 - d^4)$, D =Outer diameter, d =Inner diameter

L = Length of the column

Using the dimensions from Table 1 the critical axial force is calculated as follows:

$$I = \pi/64 \times (6.69^4 - 5.91^4) = 38.44$$

$$P_{cr} = \pi^2 \times 1.00E+07 \text{ psi} \times 38.44 / 26.42^2 = 5.44E+06 = \text{lbf}$$

Assuming a conservative fuel assembly gross weight of 2,000 lbs and a deceleration of 200 g, the maximum load on the spacer would be approximately 400,000 lbs. This is significantly lower critical Euler values calculated for the axial spacer pipe. This result is consistent FEA simulation that predicted no buckling of the axial spacer.

Computer Code Input Files

CTUWSPCR.K Bottom-down end drop from 10m, with 17STD fuel and ENUSA Spacer Assy (dwg: CECT100, rev 1). This is Traveller XL pkg, production type, with 6pcf pillow. Temp = 75 F, Nominal foam densities

References

1. SFAD-10-72, Revision 2 (July 6, 2010), "Analysis of a Traveller XL Package in a Hypothetical Bottom-Down Impact With 17x17 STD Fuel and Spacer Assembly."

2.12.7 SUPPLEMENT TO DROP ANALYSIS FOR THE TRAVELLER XL SHIPPING PACKAGE – CLAMSHELL REMOVABLE TOP PLATE STRUCTURAL EVALUATION

2.12.7.1 Background

The fuel assembly is assumed to be restrained in the clamshell to prevent any secondary impact within the clamshell. The spacer below the fuel assembly, when needed, and an axial restraint restrain the contents to the clamshell, and as such the clamshell and contents decelerate as a coupled mass. The top end axial restraint, fuel assembly structure, or spacer may absorb kinetic energy during the deceleration that results from an end drop impact.

Operational experience with Traveller package revealed that some fuel types could not be loaded or unloaded vertically with existing customer handling tools. In particular, the 17x17 XL fuel with guide pins could not be vertically loaded/unloaded into the Traveller due to an interference between the handling tool and the Clamshell Shear Lip. Figure 2-163 shows the 17x17 XL top nozzle with the handling tool attached and fully seated. Figure 2-165 shows the potential interference. The tool cannot be installed or removed without tilting the fuel handling tool and potentially damaging the fuel assembly.

Additional evaluation revealed similar interference issues when handling fuel assemblies which include Core Component Assemblies (CCA). A new Clamshell top head configuration was designed to eliminate the interference from the Shear Lip. Both the original Fixed Top Plate (FTP) configuration and an alternate configuration called the Removable Top Plate (RTP) are described in Section 1 of the Safety Analysis Report (SAR).

The primary impact with the unyielding surface occurs on the Outerpack end impact limiter. The Outerpack decelerates quickly within a few milliseconds of the primary impact because contact area of the end surface is large and stiff, and there is no significant rebound. The Outerpack is completely decelerated by the time a secondary impact occurs inside the package as the Clamshell, suspended on rubber mounts, continues to fall and contact the inside surface of the end impact limiter.

A crushable foam “pillow” is integrated into the end impact limiter to absorb kinetic energy from the secondary impact between the Clamshell and inside surface of the Outerpack end impact limiter. This pillow is a solid disk made from 6 pcf polyurethane foam. It has a diameter of 12.00 inches (305 mm) and a height of 3.60 inches (91 mm). The stiffer foam in the Outerpack end impact limiter, 20 lb/cu. ft. (0.32 g/cc) density, is located below and around the soft pillow. This stiffer component end impact limiter functions to decelerate the Outerpack at all high drop angle orientations.

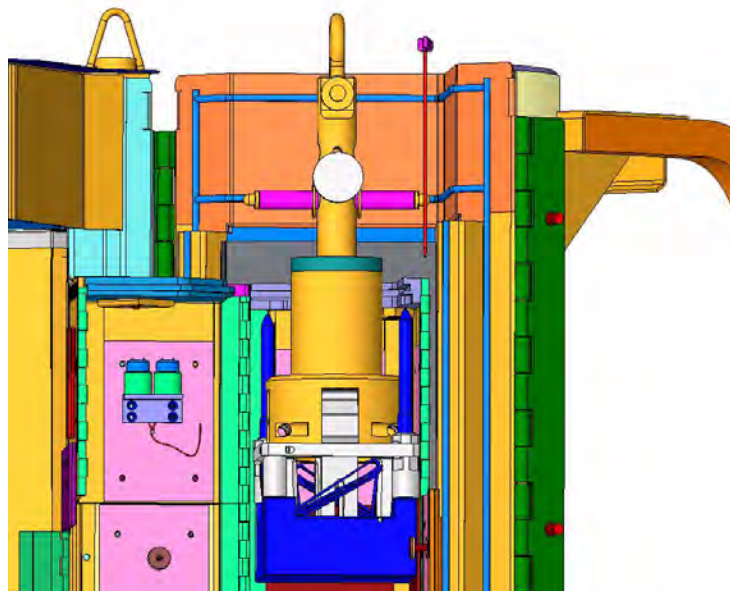


Figure 2-163 Fuel Handling Tool Grappled to a 17x17 Top Nozzle (in blue) within the Opened Outerpack and Clamshell

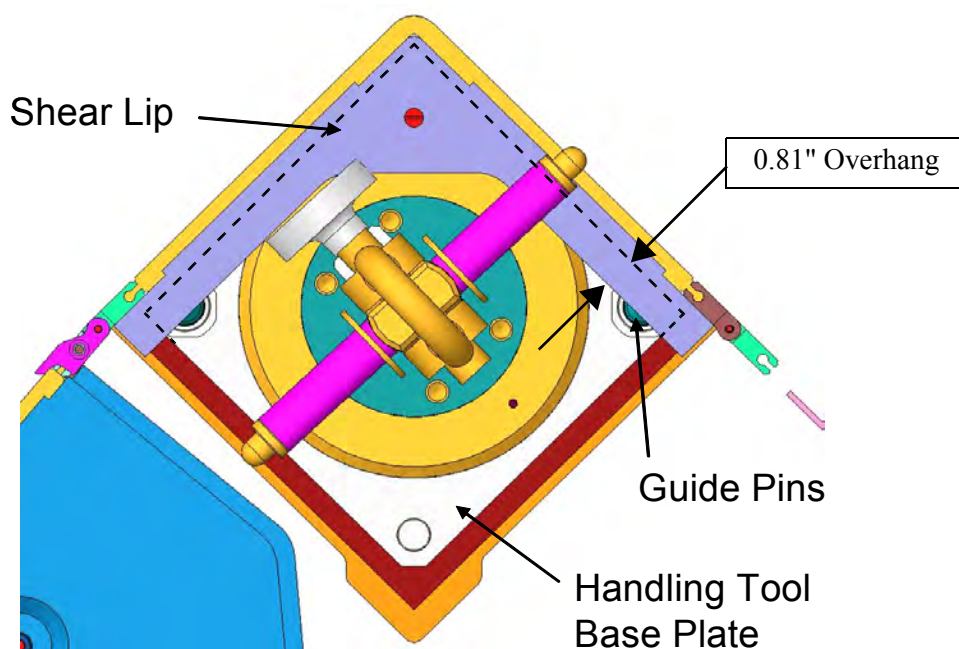


Figure 2-164 Fuel Handling Tool Shown Attached to a 17x17 XL Fuel Assembly and Behind the Overhanging Shear Lip

2.12.7.2 Conclusions

One of the most damaging orientations for the Clamshell and contents during impact is the end over center of gravity. The top-down impact challenges the integrity of the Clamshell's top end plate. End over center of gravity drop testing was performed using a certification test unit (CTU) and simulated using a finite element (FE) model. Both the actual drop tests and the FE model showed that the FTP design was acceptable. Simulation of the drop test with the RTP shows that this alternate end top plate design is also acceptable.

The screw fasteners that secure the top end plate components to the top access door and clamshell base are the weakest structure in either the FTP or RTP. These screws resist shear forces resulting from the secondary impact of the fuel assembly or fuel rod box on the top end plate during an end drop. Each screw is a stainless steel flat head cap screw, ½ inch diameter -13 threads per inch (1/2-13). These screw fasteners are not subject to large shear forces because the fuel assembly or fuel rod box is restrained in the Clamshell to prevent secondary impact on the end plate.

2.12.7.3 Detailed Calculations and Evaluations

A Traveller XL finite element (FE) model of the entire package was originally used to simulate the impact testing. A new LS-DYNA Traveller model was created to simulate features of the XL package affected by the end impact orientation. The new model is more efficient and was used to evaluate the structural performance of the axial space in the vertical end impact.

Method

The Lawrence Livermore, LS-DYNA[®] finite element code was used to determine the loads, displacements, accelerations, strains, etc. of a Traveller XL shipping package containing a 17x17 XL fuel assembly with RCCA when dropped onto a flat unyielding surface from a height of 10m. LS-DYNA 970, Revision 5434a, is a general purpose finite element code for analyzing the large deformation dynamic response of structures. This software was selected because it allows the analysis to include the effects of large deformation, large strain, material non-linearity, contact, and failure of materials.

Only the top end of the FA is modeled, the remainder of the assembly mass is simulated through point-mass elements. The weight of the remainder of the Clamshell is also modeled with point-mass elements. The Clamshell is an aluminum box with a solid 1 inch thick top plate. Figure 2-165 shows components and meshing for the FEA simulation.

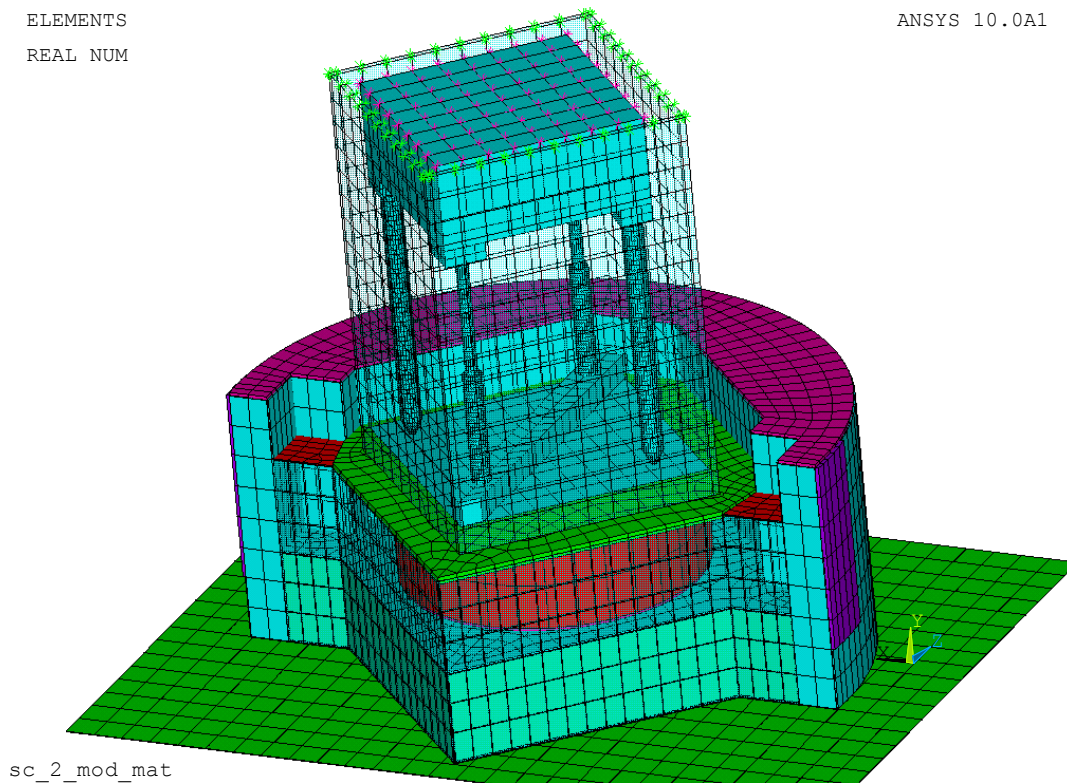


Figure 2-165 Traveller Top End Plate FEA Model

Calculation Results

The LS-Dyna model was also used to evaluate the maximum shear forces in the shear bar screws (simulated as the shear forces at the interfaces between the top plate and the extrusion walls). The peak shear force of the worst wall (i.e. across 5 screws) still showed a factor of safety of approximately 2.02 using conservative assumptions (i.e. ignoring friction between the wall and the plate for example).

The complete impact event for the RTP design without guide pins is shown in Figure 2-166 at various times. Figure 2-167 shows the rigid wall impact force history of RTP model and Figure 2-168 shows the kinetic energy history (mJ) of the axial spacer model.

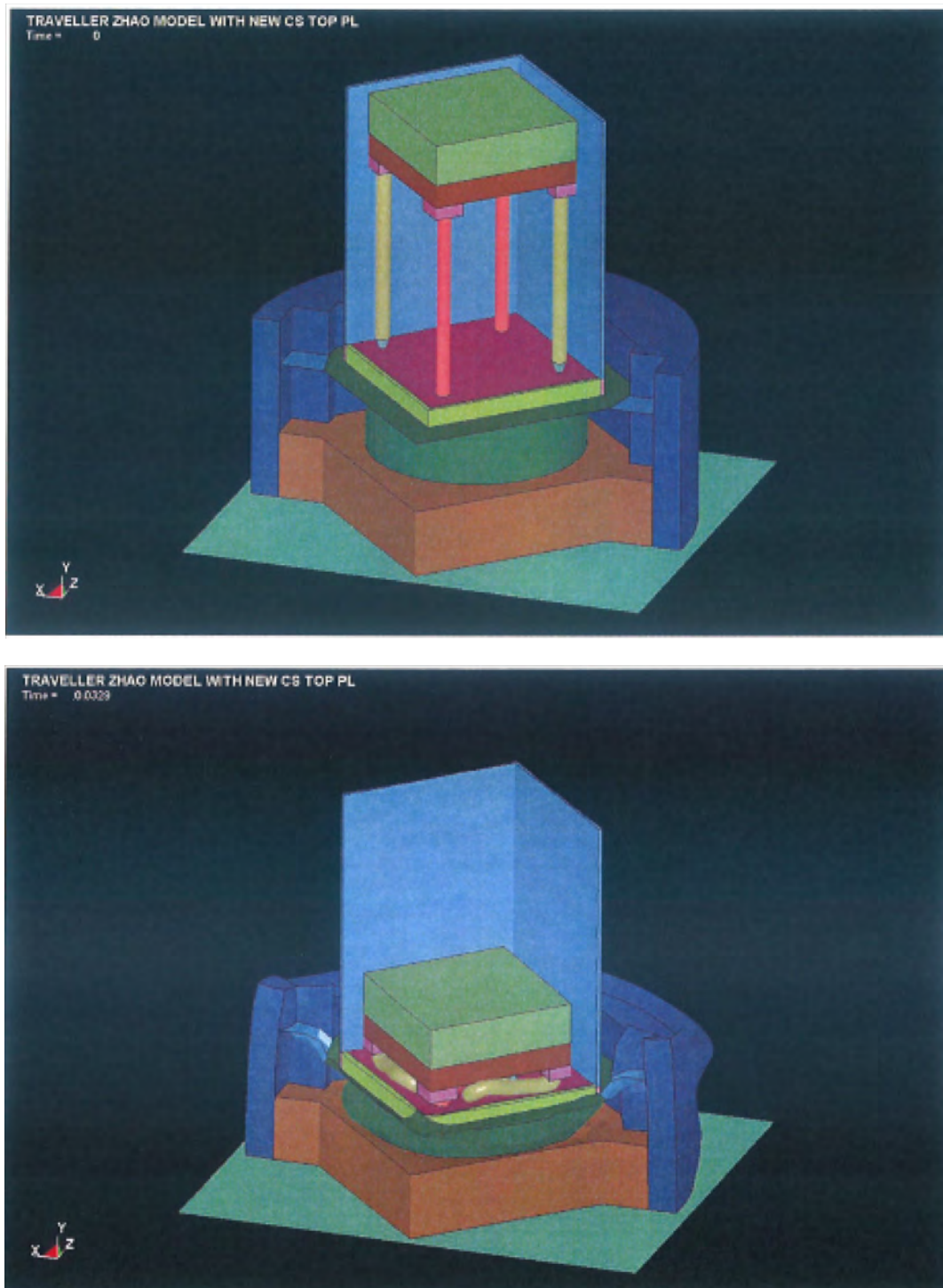


Figure 2-166 RTP Model at Beginning of Impact (0 ms) and End of Impact (33 ms)

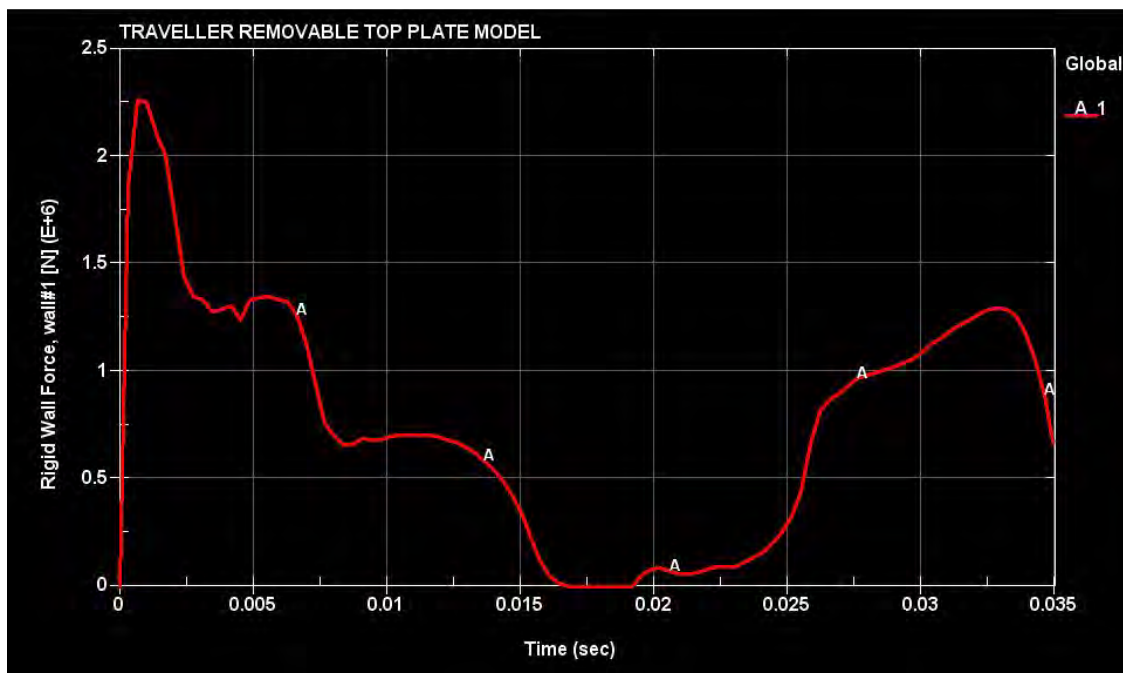


Figure 2-167 Rigid Wall Impact Force History of RTP Model

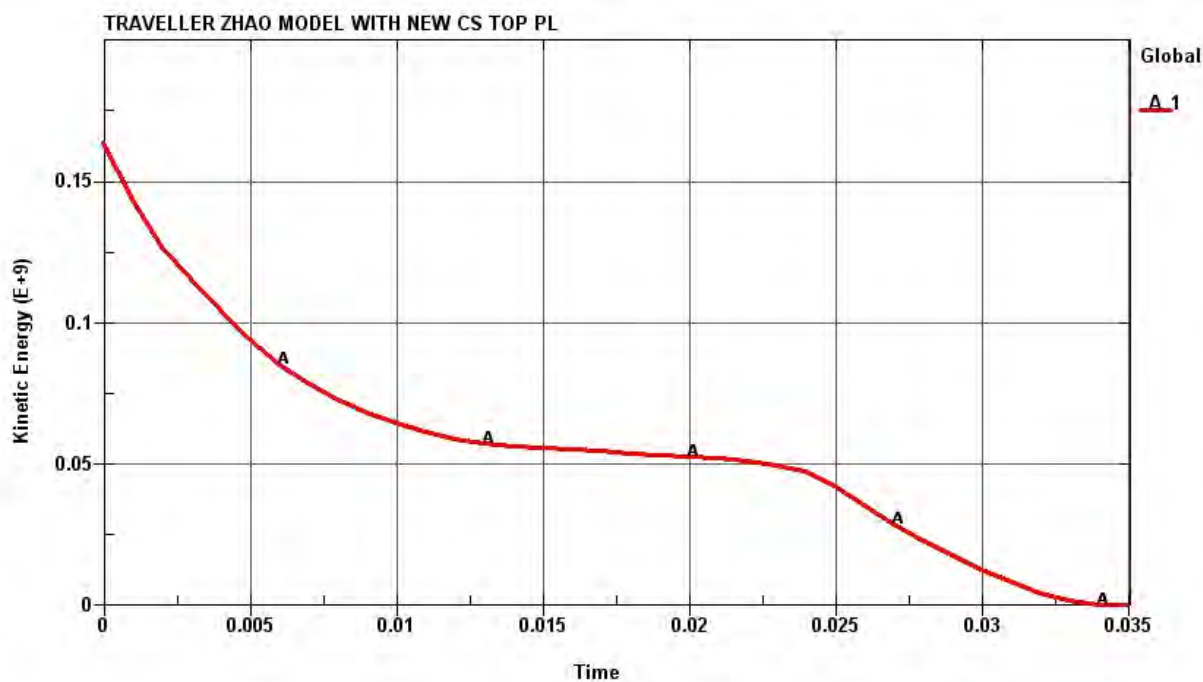


Figure 2-168 Kinetic Energy History of RTP Model (mJ vs s)

Validation

The many assumptions used to develop the LS-DYNA non-linear finite element stress code, including those needed to model the materials and impact, are validate by comparing the simulation results to the actual drop tests for the Traveller XL. Comparisons between certification test unit results and FEA simulation demonstrates that physical phenomenon governing shipping package impacts is simulated with adequate fidelity using the LS-DYNA model.

The buckling of the axial clamp studs and the Pillow are very similar to the previous the drop tests done with the qualification test unit (QTU). Figure 2-169 shows prediction of the post drop deformed shape of the top nozzle compared to the actual dropped onzzle.

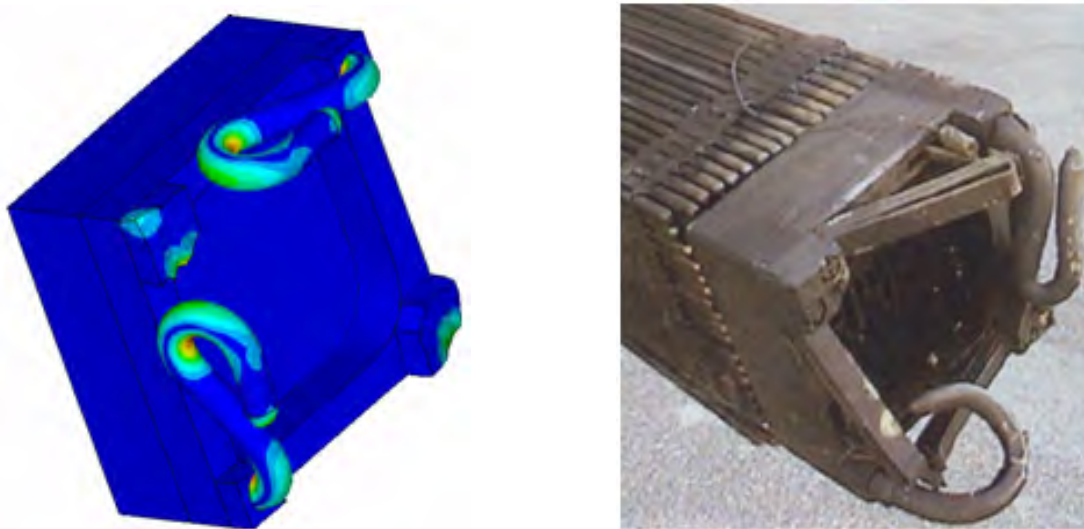


Figure 2-169 Comparison of Simulated Top Nozzle Damage (left) to Drop Test (right)

Computer Code Input Files

QTU1_9 w big axial studs 3.k

Traveller Top Nozzle Impact Study, New Top Plate Model

References

1. SFAD-09-184, Revision 1 (May 24, 2010) “ER 09-6 – Engineering Review Data Package for Revised Traveller Shear Lip”

2.12.8 Supplement to Drop Analysis for the Traveller XL Shipping Package - Structural Analysis of the Traveller VVER Shipping Package

2.12.8.1 Purpose and Background

Purpose

The purpose of this analysis is to evaluate the Traveller VVER shipping package for structural adequacy. Since the top-down impact represented one of the worst-case orientations for the Traveller XL Clamshell, it is therefore being used as a worst case study. Another “worst case” orientation is the low angle drop, or “slap-down.” A second finite element model was created to evaluate the VVER Clamshell in a 10 degree slap-down.

The Traveller VVER Clamshell will be shown to be as robust as the existing, and bounding, Traveller XL Clamshell. Evaluation of the Traveller VVER package’s Clamshell structural adequacy is presented by both by finite element modeling and standard engineering hand calculations.

Background

The Traveller VVER package is designed to carry one (1) hexagonal fuel assembly. The packaging is comprised of two basic components: 1) an Outerpak, and 2) a Clamshell. These are connected together with a suspension system that reduces the forces and shock loads to the fuel assembly during transport. Figure 2-170 shows an exploded view of the VVER shipping package. The fuel assembly is secured inside the Clamshell during transport using laterally with foam pads, and axially with a screw-activated top plate. Figure 2-171 shows the VVER Clamshell top detail view with the top plate and a closure latch identified.

The Traveller VVER package will be the third Traveller version; currently manufactured Traveller versions include the shorter Traveller STD and the slightly heavier Traveller XL package. The Traveller VVER Outerpak is identical to the Traveller XL Outerpak except that the shock mounts on the VVER are slightly smaller and stiffer and are attached to the lower Outerpak with a bracket. This change was needed because the sway space inside the VVER package is less than the XL package.

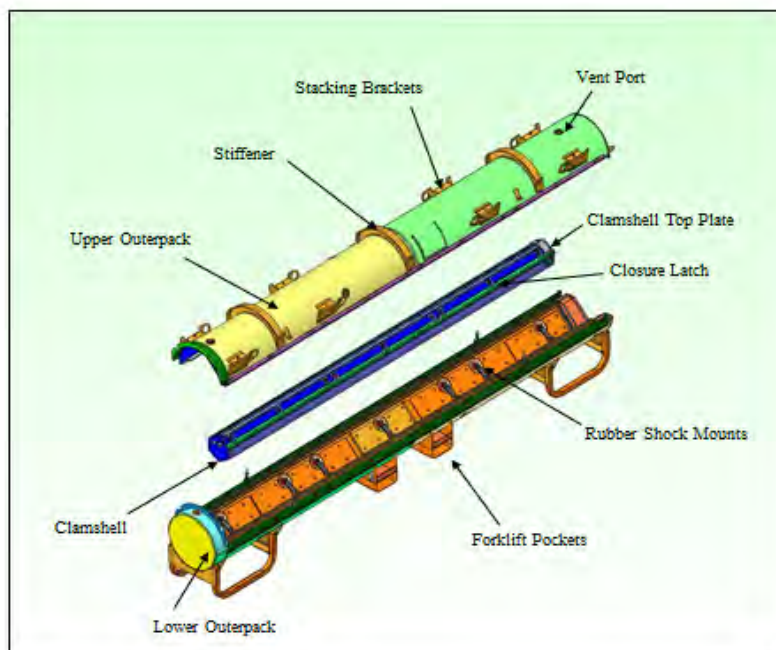


Figure 2-170 Traveller VVER Exploded View

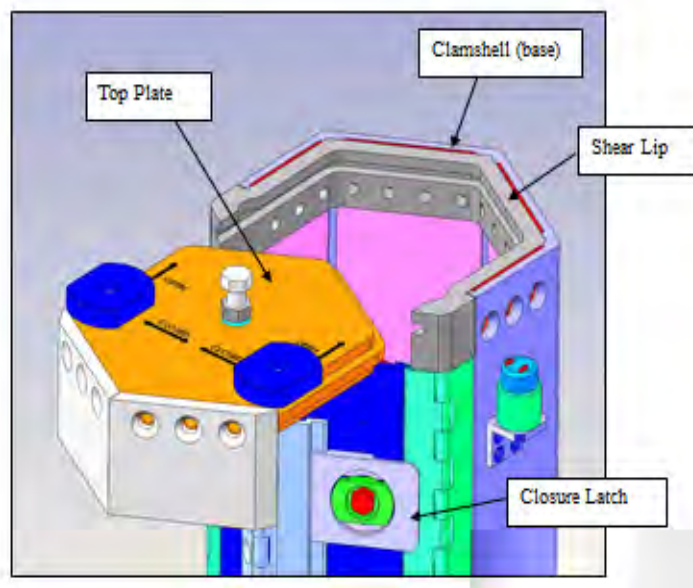


Figure 2-171 Traveller VVER Clamshell Top Detail

While the identical Traveller XL Outerpack will be used for VVER packages (albeit with different shock mounts), the Clamshell will be replaced with a hexagonal cross-section Clamshell. A cross-section comparison between the existing Traveller XL package and the VVER package is shown in Figure 2-172. As can be seen in Figure 2-172, the hexagonally-shaped Clamshell does fit within the Traveller XL Outerpack envelope. However, the Traveller VVER sway space is slightly less when compared to a Traveller XL package. The Traveller XL sway space is approximately 0.86 inches (21.8 mm) with no gravity effects to compress the shock mounts. This occurs at the upper faces of the Clamshell. The minimum sway space for the VVER Clamshell is 0.64 inches (16.3 mm) with no gravity effects. Actual sway space on the upper half of the VVER Clamshell will be higher due to the weight of the fuel which compresses the rubber shock mounts slightly. The shock mounts themselves behave as non-linear springs so impact with the bottom halves is not likely since they stiffen considerably as they are compressed.

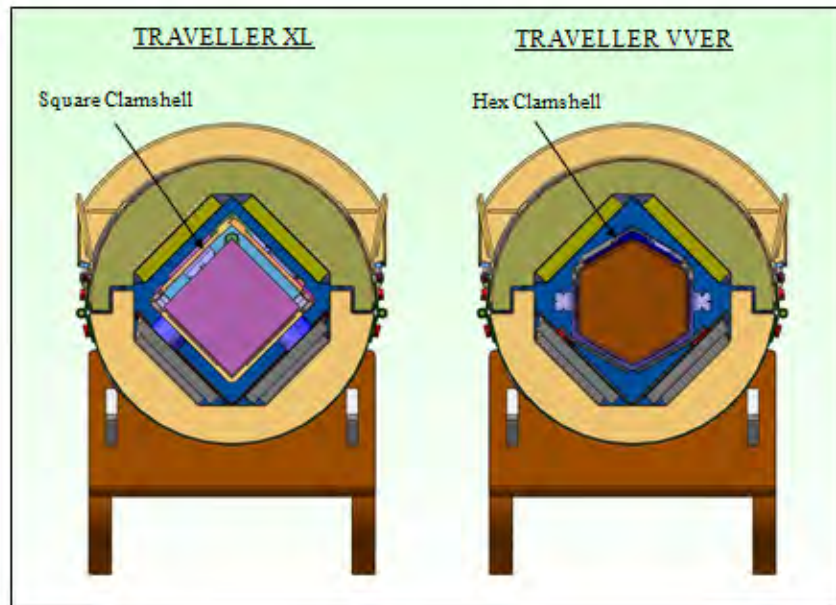


Figure 2-172 Cross-Section Views of Traveller XL and Traveller VVER Shipping Packages

The VVER type fuel is shorter than the bounding 17x17XL fuel carried by the XL package; 180.4 inches [4582.2 mm] vs. 199.2 inches [5059.7 mm], respectively. This allows a much shorter, therefore lighter, VVER Clamshell to be designed. Figure 2-173 provides a comparison of the Traveller VVER and Traveller XL Clamshells within the Outerpack.

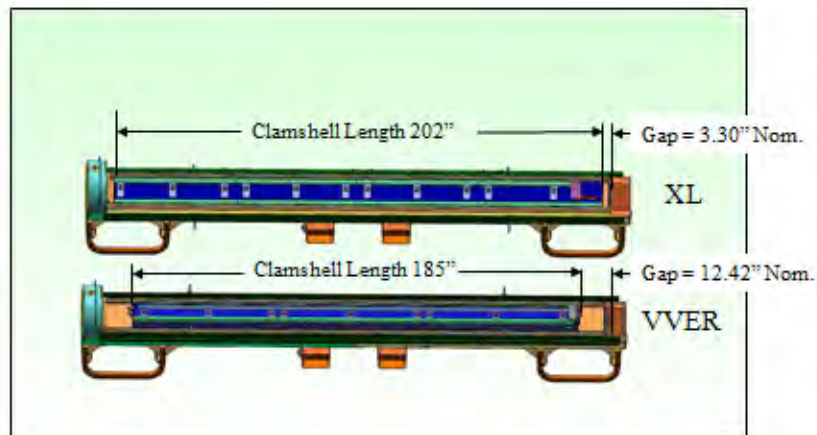


Figure 2-173 XL and VVER Clamshell Lengths Shown with the Outerpack Lid Removed

The structural design development and licensing strategy for the Traveller VVER package incorporates the existing Traveller XL Outerpack, so only the Traveller VVER Clamshell and suspension system needed to be developed and integrated with the Outerpack. As such, every effort was made to design the VVER Clamshell with the same, or greater, strength, as the Traveller XL Clamshell. The bounding fuel assembly for the Traveller XL package (17x17XL) is heavier than the fuel carried by the Traveller VVER package. A 17x17XL fuel assembly weighs 1971 lbs, including RCCA. The VVER type fuel weighs 1850 lbs maximum, including RCCA. Design basis weights of all Traveller models, including major components and maximum fuel assembly masses are shown in Table 2-6.

The Traveller VVER Clamshell design process began with the aluminum extrusion design. These were designed with the same wall thicknesses as the Traveller XL Clamshell, as shown in Figure 2-174. The wall thicknesses of all extrusions are the same, the door hinges are identical, the door "tongue and groove" joint is the same, and the latch extrusions are nearly identical. The nominal wall thicknesses are 0.438 inches near the corners and 0.313" at the thinner "pockets." The thinner sections along the faces are to accommodate 1/8" thick poison plates (for neutron absorption).

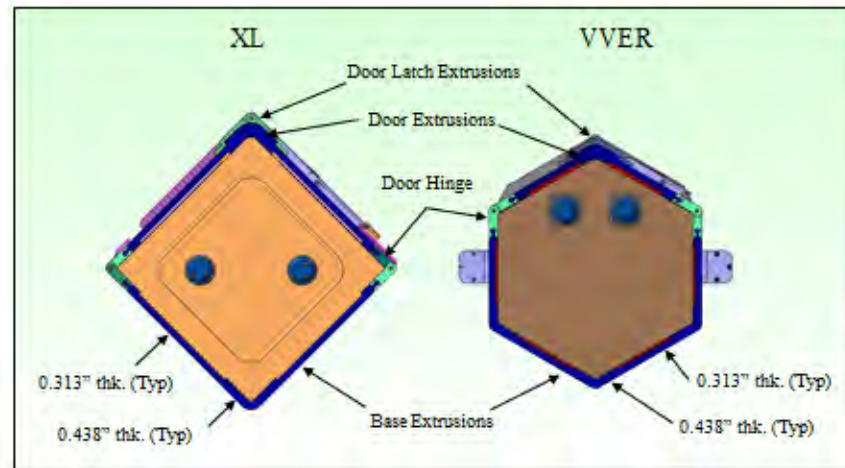
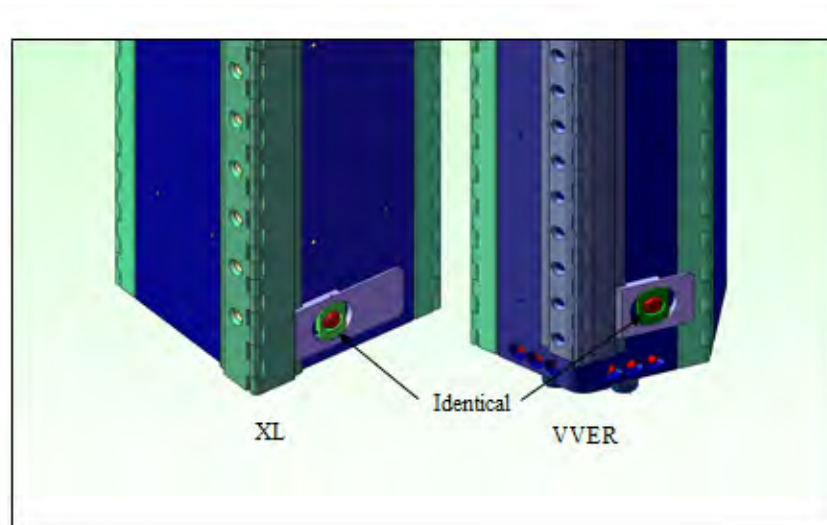


Figure 2-174 Similarity of XL and VVER Clamshell Extrusions

The Traveller VVER Clamshell main doors operate in the same manner as the Traveller XL package and are secured with identical hinge extrusions and door locking mechanisms as shown in Figure 2-175. The door latch for the Traveller VVER is shorter than the Traveller XL, but its function is the same. As with the Traveller XL, the Traveller VVER hinge extrusions are welded to the doors and the base extrusions.



**Figure 2-175 Identical hardware for XL and VVER Clamshell Quarter-turn Latches
(Shown in Locked Orientation)**

The fuel assembly top plate axial restraint was shown in Figure 2-171 as it fits into the Clamshell shear lip. Figure 2-176 provides the Traveller VVER top plate detail (underside isometric view); specifically the retractable top clamp plate is shown. Once the fuel is loaded into the Clamshell and the main doors are closed, the top plate assembly is slid into position with the clamp plate retracted. After locking the top plate to the shear lip, using the quarter-turn locking knobs, the center clamp plate actuating stud (Figure 2-176) is turned. This lowers the round clamp plate until the rubber pad contacts the fuel. A jam nut is used to keep the stud from turning during shipment.

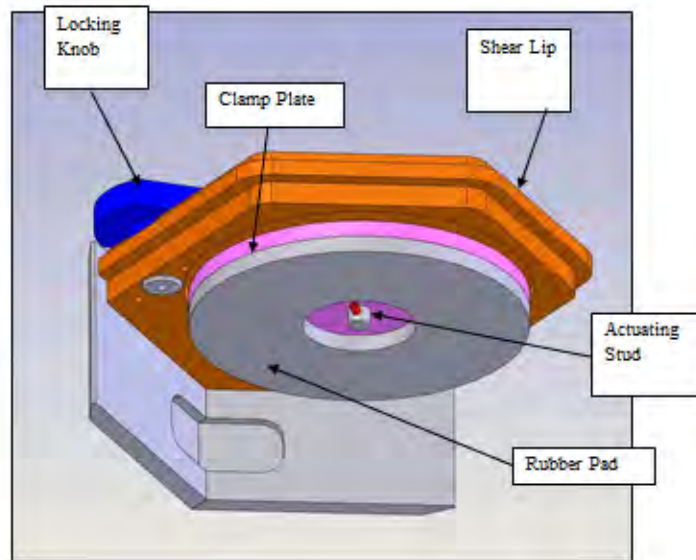


Figure 2-176 Traveller VVER Clamshell Top Plate Assembly

The VVER type fuel assembly is positioned into the Traveller VVER in the same manner as fuel of square cross-section design (for Traveller STD and XL). Figure 2-177 shows an open upper Outerpack; the top plate assembly installed and the round axial clamp extended into the clamped position contacting the VVER fuel assembly (model). Note that the main Clamshell doors are open in the figure for visual purposes only. They would be closed and locked during transport. One side of the top plate assembly covers (gray in color) is also hidden in the figure for visualization purposes. Figure 2-178 shows a VVER type fuel assembly (model) inside the Clamshell and seated against the bottom plate.

The Traveller VVER top and bottom end plates were designed thicker than their respective Traveller XL counterparts. The Traveller VVER top plate thickness is 1.25" (31.8 mm) and the bottom plate thickness is 1.50" (38.1 mm) thick as compared to 1.00" (25.4 mm) thick plates for both the Traveller XL (and STD) Clamshell end plates.

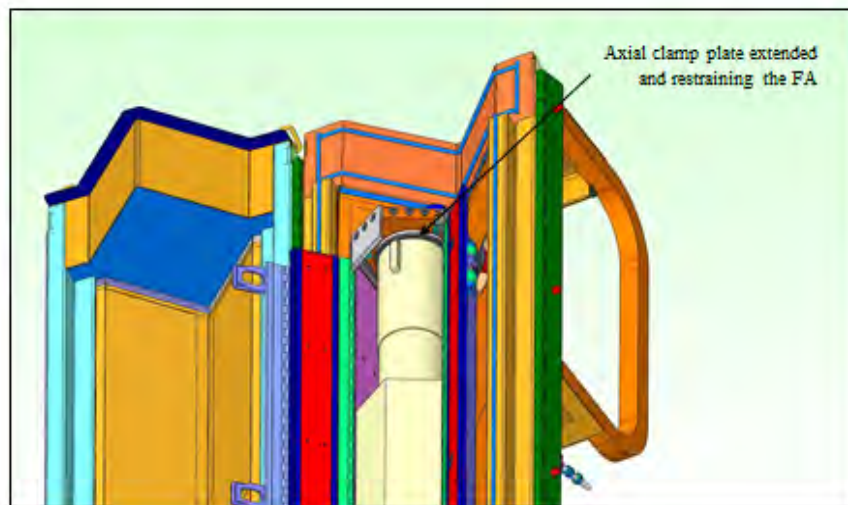


Figure 2-177 VVER Fuel Assembly Installed - Top Nozzle Region

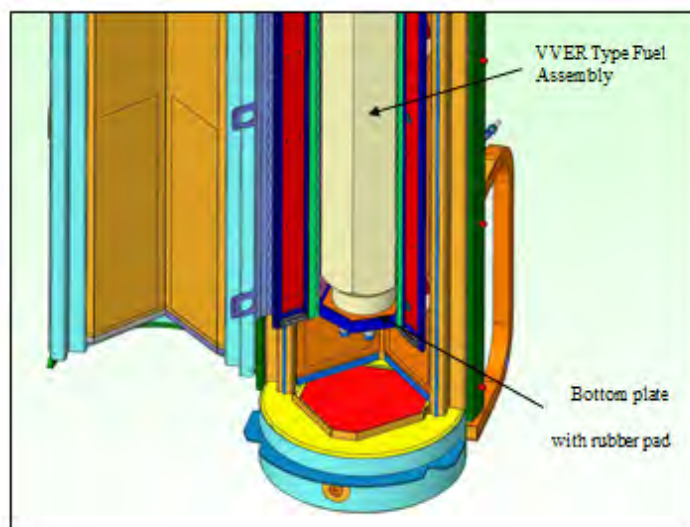


Figure 2-178 VVER Fuel Assembly Installed - Bottom Nozzle Region

Since the Hypothetical Accident Condition (HAC) top-down impact represented one of the most structurally challenging orientations for the Traveller XL Clamshell, it was also used for the Traveller VVER evaluation. During the top-down impact, most of the fuel assembly impact load path force is directed through the top plate. Hence, calculations were performed to demonstrate the robust structural design of the top plate shear lip by accommodating the entire shear load from the fuel assembly deceleration. Another structurally challenging orientation is the low angle drop, or "slap-down." A second finite element model was created to evaluate the VVER Clamshell in a 10 degree slap-down. The model simulated the fuel assembly as a solid rubber mass so as to minimize the bending stiffness of the fuel assembly itself. This assumption forced the Clamshell to resist all fuel assembly forces and accelerations.

2.12.8.2 Results and Conclusions

Results of the VVER top-down impact analysis indicate robust performance. The calculated deceleration of the VVER Clamshell was 72.5 g's, and, as expected, is less than the calculated Traveller XL top-down impact of 102 g's. This relatively low deceleration ensures that the retaining top plate bolts are stressed to a lesser degree than the XL Clamshell in the same orientation. Additionally, the strength and stability of the Clamshell walls, top plate assembly and other components are structurally adequate. Subsequent shear lip joint hand calculations demonstrate the structure has adequate strength to absorb the maximum impact load without significant damage.

The results of the low angle impact also indicated robust performance. No significant Clamshell damage at the first or second impact end was noted by virtue of the calculated 0.12% plastic strain at peak bending, in the bottom edge, near the mid-span. The Clamshell provided excellent structural performance in the slap-down event.

It is concluded that the VVER Clamshell survives the most damaging 9m drop orientations, a top-down end drop and a low angle slap-down. The walls of the Clamshell do not significantly deform and thus they keep the fuel envelope confined. The top plate assembly also exhibits a low degree of plastic deformation, which only occurs locally.

2.12.8.3 Detailed Calculations and Evaluations

Finite Element Modeling

Computer analysis of the Traveller VVER shipping package was performed using a large-strain capable, nonlinear, finite element code to verify Traveller VVER package performance. No actual drop testing was performed due to the similarity of the design with the Traveller XL. The finite element code used for this work was LS-Dyna, which is commercially available through Livermore Software Technology Corporation.

The bounding Traveller XL was also analyzed with this software. At that time, the analysis was only used for worst case drop orientation parametric studies. For example, how the package would behave for different drop angles. These were compared against each other and not for actual performance verification. Other factors such as skin thickness changes, foam density effects, and temperature effects were compared. The "sensitivity study" nature of the finite element modeling was to compare relative hypothetical drop

orientations. As a result, the primary basis for package compliance was through execution of actual drop testing. Agreement between computer modeling and actual drop testing was remarkably good. The original finite element model was extremely detailed and could accommodate all drop orientations. Subsequent to the Traveller licensing, a new, simplified LS-Dyna model was created to explore other changes and parametric studies. This new model was benchmarked against the original model and used to demonstrate structural adequacy of the Removable Top Plate (Section 2.12.7). In this analysis, the simple model was modified for the VVER design.

The computer model was created to simulate a 30 ft free-drop onto an unyielding surface. The entire model except the unyielding "ground" was initially set with a velocity of 13,380 mm/s (43.91 ft/s). This corresponds to free drop height of 9.13 m (30.0 ft). In the model coordinate system the velocity vector is pointed in the Y direction (see coordinate triad in Figure 2-182, in the lower left corner).

Using the results of the large-strain dynamic finite element analysis, the average deceleration of the Clamshell can be calculated and compared to the bench-marked Traveller XL analysis. The deceleration is based upon the total crushing Y-distance of the components below the Clamshell top plate. This includes the Pillow and the end limiter foam. At the top of the Pillow is a relatively thick stainless steel "puncture plate." It is the green plate shown in Figures 2-181 and 2-182. The displacement of this plate represents the total displacement of the Clamshell. LS-Dyna was queried for the time dependent displacement (Y-direction in model axis) for a node (node #120) in the center of the puncture plate. A plot is shown in Figure 2-179 below.

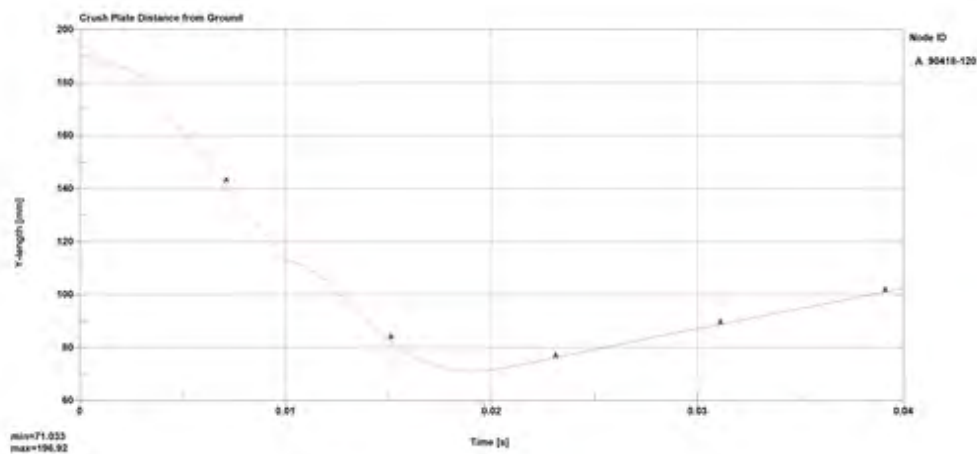


Figure 2-179 Puncture Plate Distance from Ground During Impact

The Traveller Clamshell is a long aluminum structure (hexagonal cross-section box) which is attached to the Outerpack with rubber shock mounts. While these shock mounts were not explicitly modeled in this analysis, their contribution to Clamshell stability and restraint was incorporated by applying a non-rotation boundary condition on the Clamshell "cut" face (at the upper face in Figure 2-181). With this boundary condition, the Clamshell cut face was not allowed to move or rotate about the X and Z axes. Similarly, the fuel assembly mass (see Figure 2-182) is also restrained from rotation because an actual fuel assembly is a long and fully supported mass. The fuel assembly mass was not allowed to rotate around the X and Z axes.



Figure 2-180 Traveller VVER Clamshell Model Showing Key Components

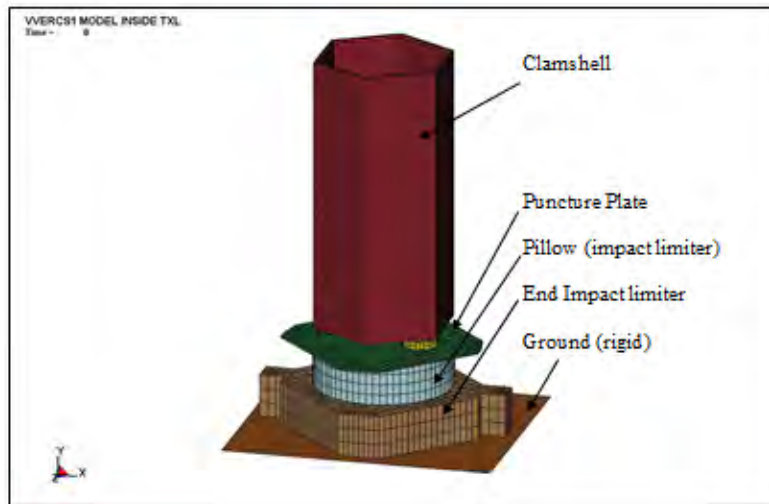


Figure 2-181 Traveller VVER Finite Element Model

Previous Traveller XL drop test analyses were revised based upon increased measured Outerpack weights. The remainder of the upper Outerpack was not discretely modeled because it does not affect performance of the Clamshell. The impact of the upper and lower Outerpack halves does not affect the performance of the Clamshell in a significant way. To bound the as-measured condition, 122 pounds was added to the SAR weights, and subsequent analysis used this weight increase for the Clamshell. This condition was applied to the Traveller VVER finite element analysis. Although the nominal Clamshell weight is 463 pounds (210 kg), the analyzed weight is 585 pounds (265 kg). The VVER fuel assembly weight used for the analysis is 1850 pounds (839 kg). This mass is simulated with very high density material within the hexagonal FA component as shown in Figure 2-181.

Figure 2-183 shows the underside of the top plate assembly and the axial clamp plate and stud. The plate is 0.5" thick 6061-T6 aluminum and the rubber is neoprene, 60 durometer. The center stud is 5/8"-11 bolt with a jam nut on the outside of the top plate to keep it from rotating during shipment.

For this analysis, the structural integrity of Clamshell is of key interest. To obtain this information, the initial material parameters were set, which included the initial impact velocity of 13,380 mm/s (43.91 ft/s). This corresponds to free drop height of 9.13 m (30.0 ft), see Section 2.12.8.2. All part configurations were obtained from the SolidWorks® CAD models and transferred into LS-Dyna using IGES files. Material properties for the various materials can be found in the Assumptions section below.

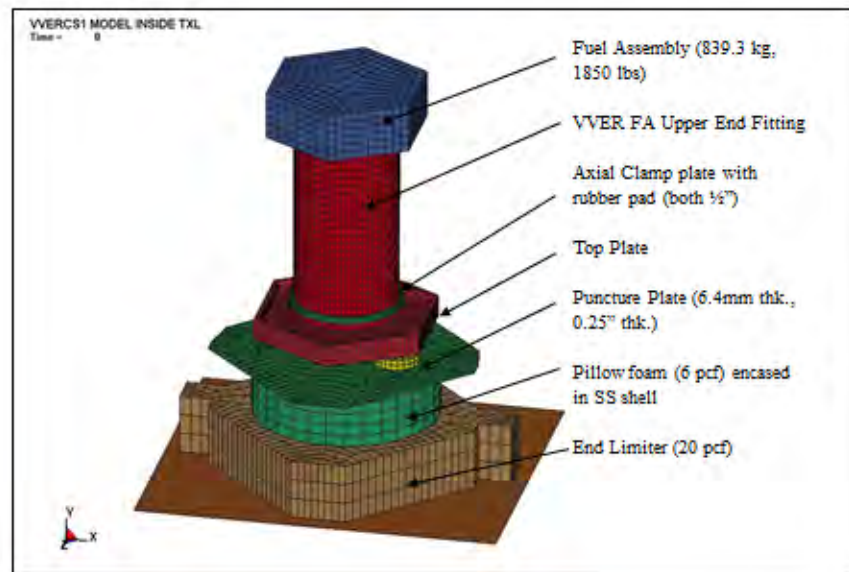


Figure 2-182 Traveller VVER Model with Clamshell Walls and End Limiter Cover Plate Hidden

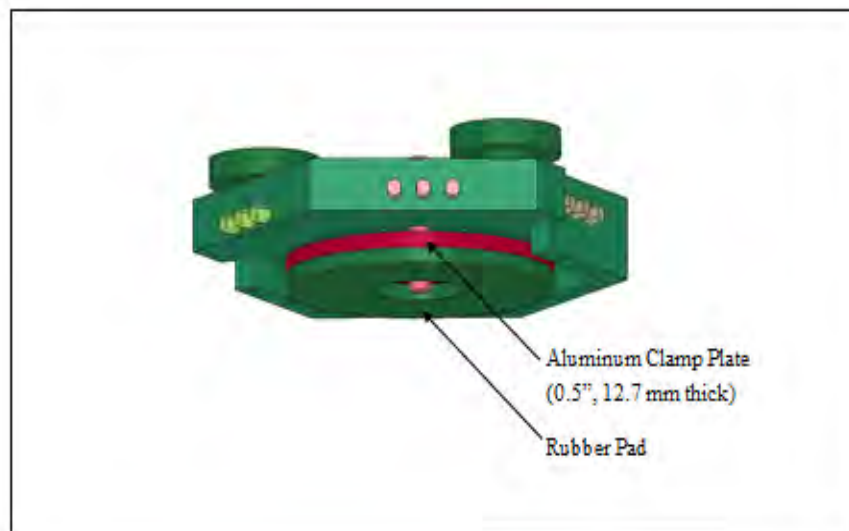


Figure 2-183 Traveller VVER Top Plate Assembly Showing Integral Axial Clamp and Rubber Pad

Assumptions

Many assumptions are used to develop a model for the LS-DYNA non-linear finite element stress code, including those needed for material properties and boundary conditions. These assumptions were found valid for simulating drop tests of the Traveller XL package through comparison with actual drop tests. It is clearly evident from comparisons between prototype test results and predictions that the key physical phenomena governing shipping package impacts is captured within the LS-DYNA code.

This simulation was performed using conservative assumptions which include the following:

- 1) The assumed mass of the VVER FA in the model was 1,850 lbs (839 kg).
- 2) The FA is modeled as an upper end fitting (pipe) and a hexagonal lump of steel with a higher than normal density. It is therefore essentially rigid. This is very conservative since actual drop testing revealed the weak axial stiffness of a fuel assembly (it vibrates and bows during end impacts). Fuel rod "slip" also tends to reduce the stiffness of the fuel.
- 3) The drop height corresponds to 9.13m (30 ft), slightly greater than the 10CFR71.73, 9 m drop height requirement.
- 4) The majority of the mass of the Outerpack has not been included in this analysis (i.e. the lower Outerpack) because it does not significantly affect the Clamshell impact. More specifically, the Outerpack impact event is finished within only a few milliseconds, therefore the bottom limiter (the Pillow) is simply waiting for the Clamshell impact into it.
- 5) The foam crush characteristics shown in Figure 2-184 include extrapolation from 80% crush to 100% crush for model stability purposes. As mentioned earlier, actual pillow crushing during actual testing was measured to be only about 50%. This is because the fuel assembly is not a rigid "hammer" that have no axial elasticity. This effect has been proven to be quite significant. However, in these simulations, the severe impact of inelastic modeling of the fuel assembly was used. In some cases, this forces the crush curves to be extrapolated to 100%.
- 6) In the slap-down model, the FA was modeled as rubber so that the Clamshell had to stabilize it. A stiff fuel assembly would have prevented the Clamshell from large scale deformations and plastic strain.

Axial Free Space Between the Clamshell and the Impact Limiter

The Traveller VVER design has an additional 9.12 inches of free space between the end of its Clamshell and the contact surface of the Outerpack impact limiter compared to the Traveller XL (12.42 inches versus 3.30 inches; Figure 2-173). The Traveller XL finite element models simulate a 30 foot free-drop onto an unyielding surface and the start of the simulation places the Outerpack just above the ground plane. The Outerpack impacts the unyielding surface and comes to rest before the Clamshell impacts it.

The gap for the Traveller XL finite element analysis was set at 0.048 inches. The Clamshell is positioned near the Outerpack so as to minimize the "free fall" of the Clamshell to optimize the model. However, a sufficient gap exists to allow the Outerpack to essentially come to rest first, before the Clamshell impacts it. This occurs over an approximate 2 millisecond duration. Because the Outerpack does not have time to bounce in these few milliseconds, it is essentially at rest awaiting the Clamshell impact. The Clamshell then impacts the Outerpack with the same initial velocity as it had at the start of the simulation. Even though the Traveller XL actual 3.30 inch gap was not explicitly modeled, the finite element analysis results were in a good agreement with the physical drop testing. The same finite element analysis techniques were employed for the Traveller VVER. In both cases, the Outerpack and the Clamshell have an initial velocity of approximately 43.9 feet/second to simulate the 30 foot free-fall impact forces.

Material Properties

The material properties assumed for the aluminum, stainless steel, and the crushable foams can be seen in Tables 2-56, 2-57, and 2-58, respectively.

Table 2-56 Aluminum Properties for Traveller VVER Analysis			
6005-T5 and 6061-T6 Aluminum at 75 Degrees F			
Property	Symbol	Value	Units
Density	RO	2.71E-09	Mg/mm ³
Modulus	E	69	kN/mm ² (GPa)
Poisson's Ratio	PR	0.33	Dimensionless
Yield Strength	SIGY	0.241	kN/mm ² (GPa)

Table 2-57 Annealed 304 Stainless Steel Properties for Traveller VVER Analysis			
Property	Symbol	Value	Units
Density	RO	7.85E-09	Mg/mm ³
Modulus	E	207	kN/mm ² (GPa)
Poisson's Ratio	PR	0.30	Dimensionless

Table 2-58 Crushable Foam Properties for Traveller VVER Analysis

Property	Density Mg/mm ³	Modulus kN/mm ² (GPa)	Poisson's Ratio Dimensionless
6 pcf Last-A-Foam	9.61E-11	30.14	0
10 pcf Last-A-Foam	1.60E-10	66.23	0
20 pcf Last-A-Foam	3.20E-10	192.76	0

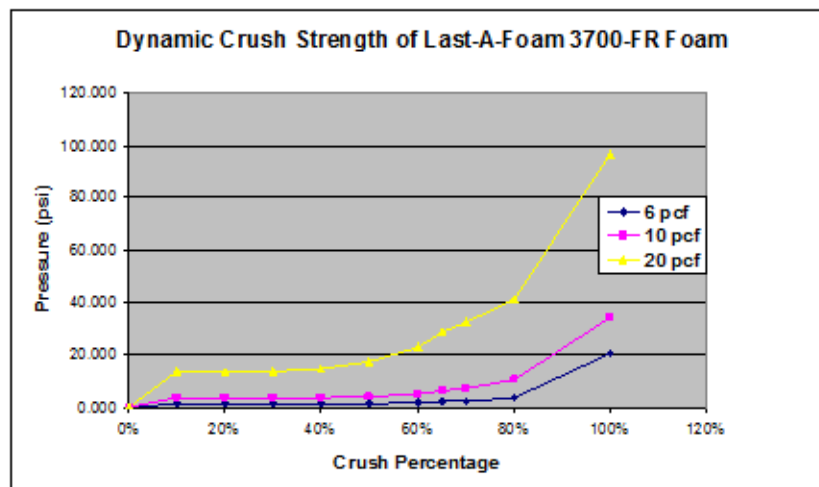


Figure 2-184 Comparison of Dynamic Crush Strengths of the Foams Components

Figure 2-185 shows the stress-strain curve of the stainless steel properties used in the LS-Dyna simulations.

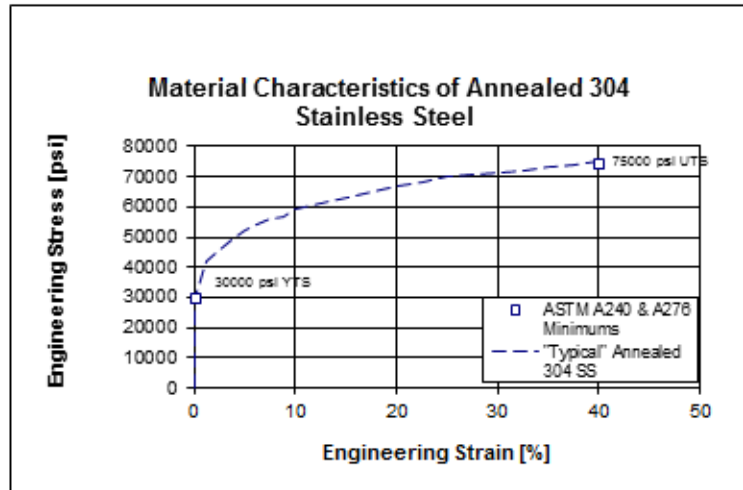


Figure 2-185 Annealed 304 Stainless Steel Stress-strain Characteristics

Top-down Evaluation and Results

Results of the VVER top-down impact analysis (see Figure 2-186, below) with VVER fuel indicate robust performance. The calculated deceleration of the Clamshell was 72.5 g's compared to the calculated XL top-down impact of 102 g's. The Traveller XL Clamshell demonstrated robust structural integrity for the applied 102g deceleration load. The strength and stability of the Clamshell walls, top plate assembly and other components are adequate. As with all Traveller variants, in high-angle drops, the soft "Pillow" foam provides a crushable cushion for the Clamshell (and fuel) to impact.

The analysis conservatively models the fuel as a solid mass with a simulated top end fitting. This is very conservative because the fuel is not a rigid mass; it is very susceptible to fuel rod bowing, buckling, and vibrations, as well as fuel rod slippage within the skeleton. All of these factors lessen the impact energy and subsequent forces through the Clamshell.

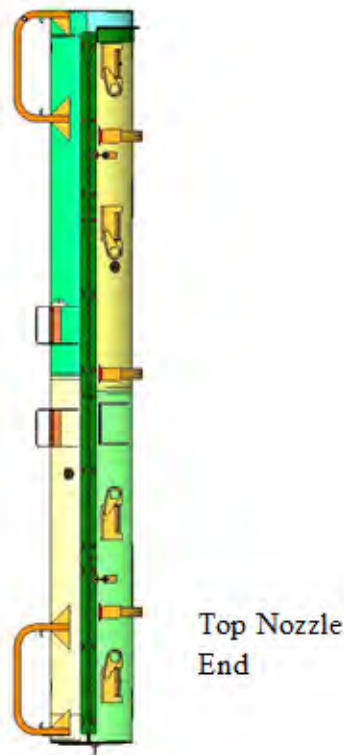


Figure 2-186 Traveller XL Shown in a Top-down Impact Orientation

The axial load path in the top-down end drop is primarily from the fuel through the top plate and into the Pillow foam, however, any axial differential shearing loads (Clamshell walls and top plate) are reacted by the ½ inch diameter screws which fix the top plate and shear lip to the Clamshell walls. In the case of the Traveller XL, 20 screws are used to make this attachment. Despite the reduced weight of the VVER fuel, the VVER Clamshell also utilizes 20 screws to affix the top plate and shear lip to the walls and doors.

The model results are shown in Figure 2-187, in 5 ms increments. The VVER Clamshell walls and bottom limiter cover plate have been hidden for viewing of the fuel assembly and Pillow. The end foam components crushed a total of 125.9 mm (4.96 inches) during the 20ms impact. A plot of the kinetic energy of the model is also shown in Figure 2-188. Note that the impact event is over by 20 milliseconds (i.e., kinetic energy is near zero). Note that a small amount of energy is retained due to rotation of the Clamshell within the Outerpack. This moment will be balanced by the Outerpack walls.

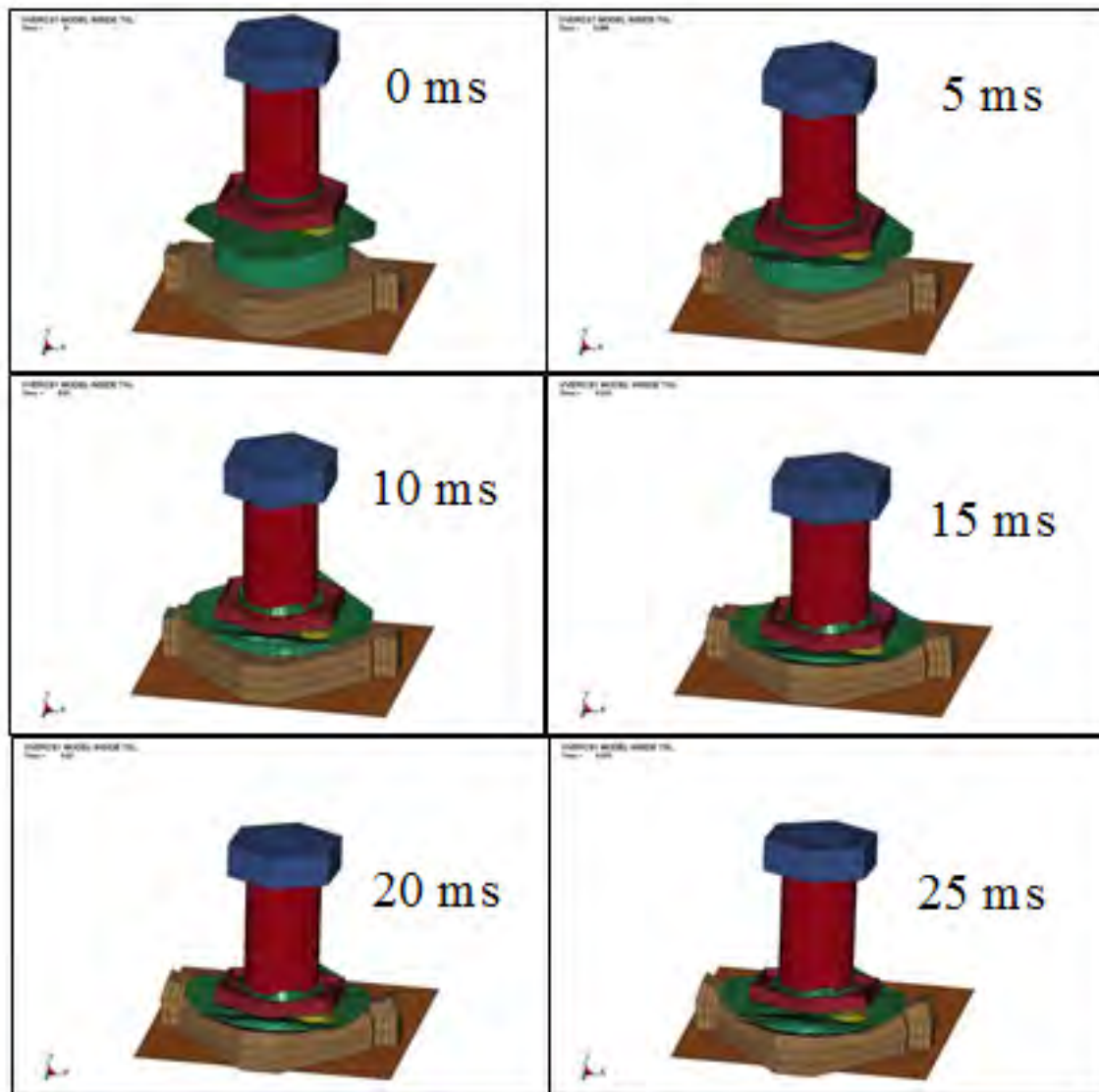


Figure 2-187 Top Down 9m Impact of Traveller VVER Package in 5 ms Increments

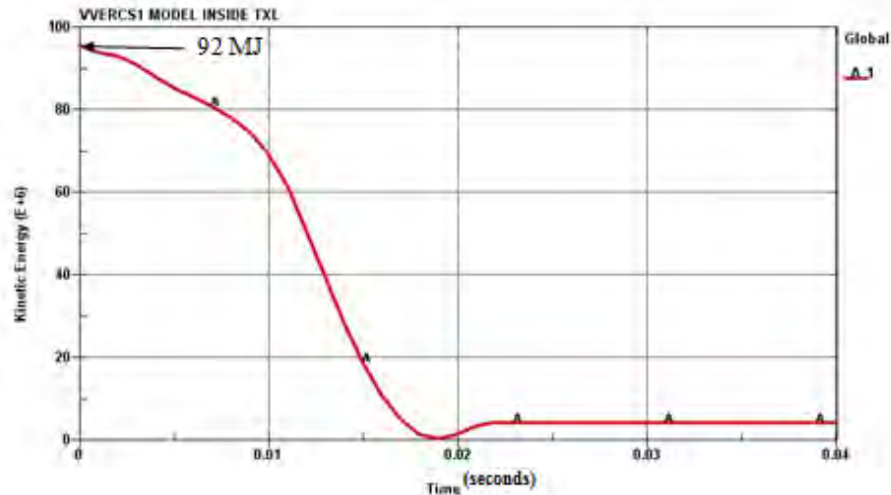


Figure 2-188 Kinetic Energy Plot for VVER Model (Time in Seconds, Energy in J)

The model predicts no crumpling of either the Clamshell walls or the VVER fuel assembly top nozzle (upper end fitting). Both components remain geometrically stable throughout the impact event.

Figure 2-189 shows the final shape of the VVER Clamshell and Outerpack at the end of the impact, 20 ms. As expected the aluminum axial clamp plate and the rubber pad are considerably deformed during a top-down impact. This energy absorption provides a positive effect on the overall structural performance of the Clamshell by reducing its absorbed energy. The locking knobs on the outside of the top plate do not significantly absorb impact energy due to their geometry and location on the top plate. There is very low plastic strain in the VVER Clamshell structural walls which includes the main doors and base extrusions. See Figure 2-190. The general state of the plastic strain in the results demonstrate a very robust structural design.

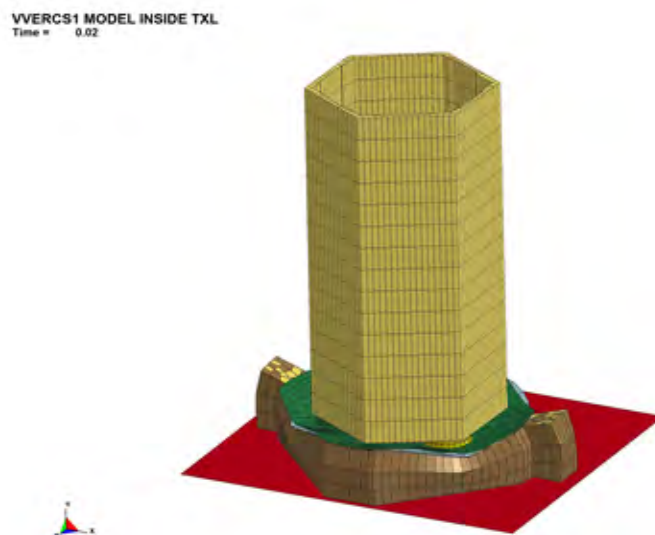


Figure 2-189 Deformed Shape of Model at 20ms

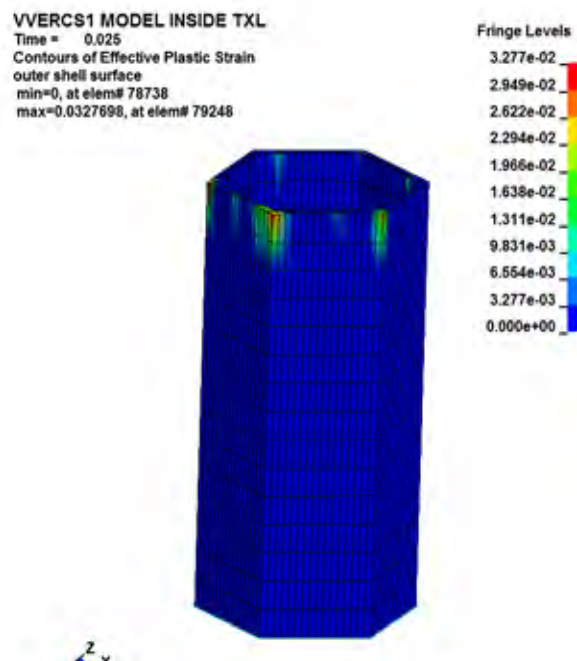


Figure 2-190 Max. Plastic Strain in the Clamshell Main Walls

Using the finite element results, the average deceleration of the Clamshell can be calculated. The deceleration is based on the total crushing Y-distance of the components below the Clamshell top plate. This includes the Pillow and the end limiter foam. At the top of the Pillow is a thick stainless steel "puncture plate." It is the 0.25 inch green plate shown in Figure 2-182. The displacement of this plate represents the total displacement of the Clamshell.

The total displacement of the crush plate is approximately 196.92 mm - 71.03 mm = 125.9 mm (4.96 inches).

The initial velocity of the package when dropped from 9.13 meters is:

$$V_f^2 = V_i^2 + 2 \times g \times d$$

Where: V_f is the velocity immediately at impact (mm/s)

V_i is the initial velocity when dropped (= 0)

g is the acceleration due to gravity, 9,810 mm/s²

d is the drop height, 9,130 mm (9.13 m)

Solving for V_f gives:

$$V_f = (2 \times 9810 \times 9130)^{0.5}$$

$$V_f = 13,380 \text{ mm/s (43.91 ft/s)}$$

During the impact, the Clamshell is decelerated to zero velocity after crushing 196.92 mm (4.96 inches). Using the same formula as above, the average Clamshell deceleration is:

$$V_f^2 = V_i^2 + 2 \times a_{ave} \times d$$

Where: V_f is 0

V_i is 13,380 mm/s (43.91 ft/s)

d is 125.9 mm (4.96 in)

a_{ave} is the average deceleration of the Clamshell structure

Then: $a_{ave} = - (13,380\text{mm/s})^2 / (2 \times 125.9 \text{ mm})$

$$a_{ave} = - 7.11\text{e}5 \text{ mm/s}^2$$

And dividing by the acceleration due to gravity (9810 mm/sec^2) gives:

$$g_{ave} = 72.5 \text{ g's (decelerating)}$$

This relatively low deceleration ensures that the retaining top plate bolts are stressed to a lesser degree than the Traveller XL Clamshell in the same orientation.

Slap-down Model Evaluation and Results

While the end drop represents the orientation which is the most structurally challenging to the fuel assemblies and Clamshell end features, a low-angle slap-down orientation is also very stressful for the Outerpack and Clamshell. Therefore, a second LS-Dyna model was created to analyze a low angle drop of 10 degrees. This model is shown in Figure 2-191. All material properties and initial conditions were applied to the slap-down model in a similar fashion to the top-down model. The initial velocity corresponded to the 9.13 m drop height. The impact angle was set to 10 degrees. The VVER Clamshell was also modeled using the wall thickness set to 0.436 inches which is a reasonable approximation of the composite wall thickness since the poison plate completely fills in the thinner sections of the extrusions, and the latch hinge and door hinges add even more material to the cross sectional strength. Most of the extraneous components such as the legs, lifting eyes, stiffeners, etc. associated with the Traveller were not modeled for the sake of simplicity, conservatism since they all add strength and reduce Clamshell forces by absorbing energy. Figure 2-192 shows the slap-down model with the upper Outerpack removed.

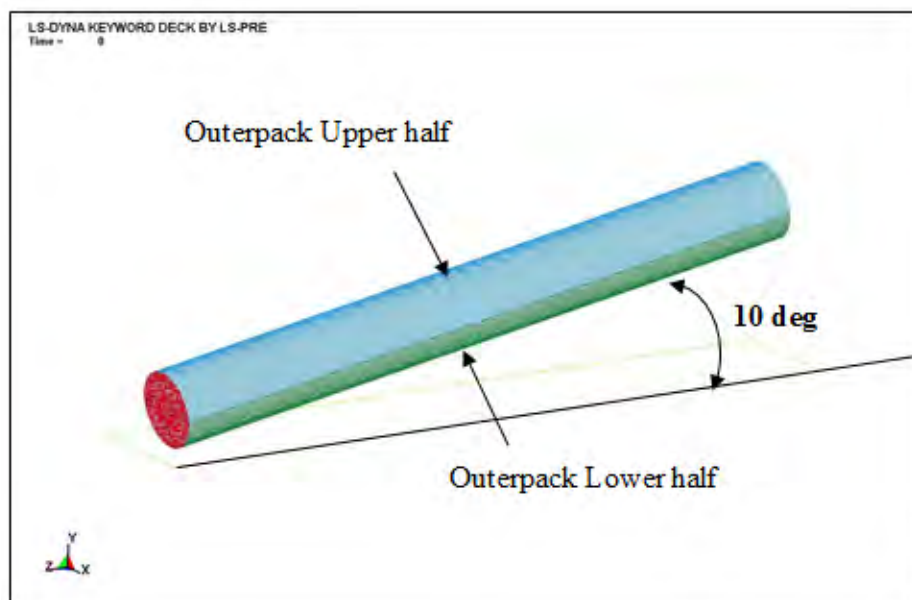


Figure 2-191 Slap-down Model

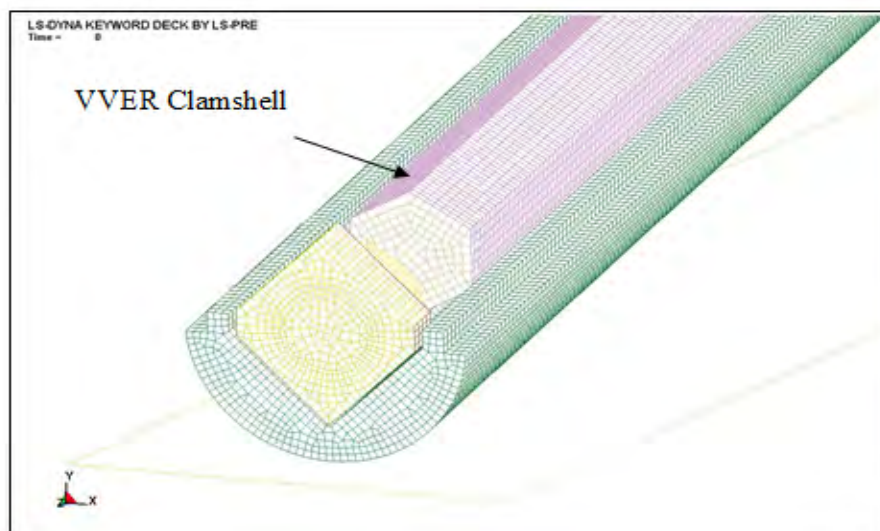


Figure 2-192 Model with Upper Outerpack Hidden to Show VVER Clamshell

The results of the low angle impact indicated robust structural performance. During the slap-down, the Outerpack and Clamshell experienced large longitudinal bending moments. The Outerpack survived this moment (peaked at 0.24 seconds) with minimal plastic deformation. As can be seen in Figure 2-193, the Outerpack survives this large bending moment with no significant structural damages other than a very slight buckle in the outer shell on the top surface. The simulated results are similar to actual slap-down tests and are consistent for the Traveller XL and Traveller VVER. The strength of an actual Outerpack is greater than the model by virtue of stiffeners, legs, hinges, etc. which were not included for simplicity and model size.

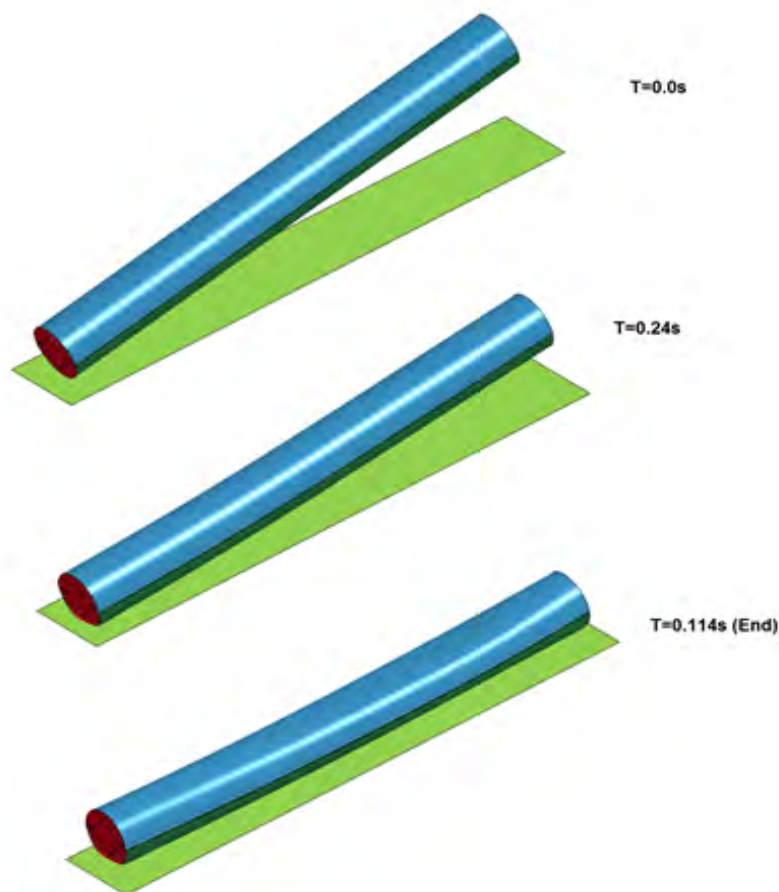


Figure 2-193 Max. Plastic Strain in the Clamshell Main Walls

Figure 2-194 shows approximately 0.12% plastic strain at peak bending, in the bottom edge, near the mid-span at the .0111 second time increment. No Clamshell damage at the first or second impact end was noted. The Clamshell extrusions including the base and wall demonstrate mechanical and geometric stability during a 30 foot slap-down impact. Based upon the robust Traveller XL Clamshell design, the VVER performed as expected. It is concluded that the VVER Clamshell has at least the structural integrity as the Traveller XL Clamshell for the slap-down event.

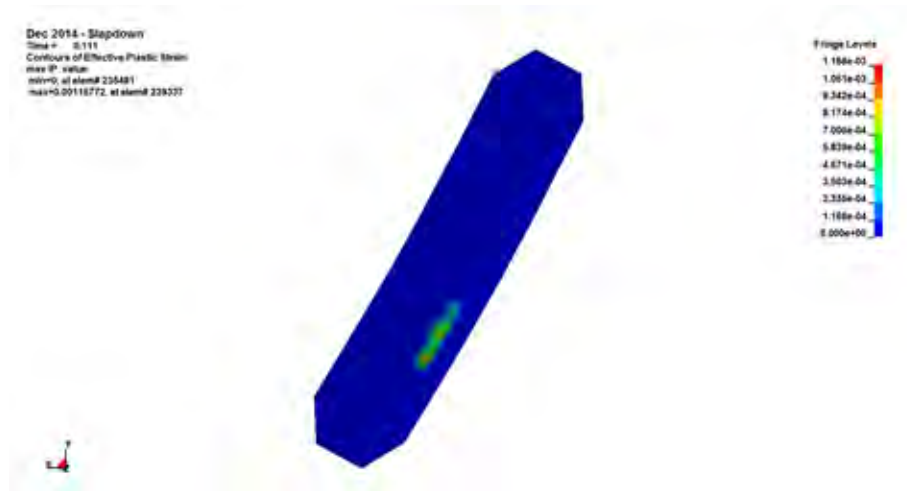


Figure 2-194 Slight Plastic Strain in Clamshell Extrusion

Figure 2-194 Slight Plastic Strain in Clamshell Extrusion

Shear Lip Strength Evaluation

During the top-down impact most of the force of the fuel assembly impact load path is directly through the top plate. Even so, the following calculation illustrates that the top plate shear lip can accommodate the entire shear load from the deceleration of the fuel assembly. The top plate shear lip is shown in Figure 2-195. The "shear lip" protrudes along 4 sides of the top plate and is engaged into the female groove on the shear lip component. When the fuel assembly collides with this top plate, the lip is loaded in shear. The calculated deceleration of the Clamshell was done above, therefore, the maximum load on the top plate cannot exceed the g's times the weight of the fuel assembly. This is an extremely conservative assumption since most of the energy of the fuel assembly collision is simply passed through the top plate and into the Pillow. The top plate is trapped between the two, and is loaded in compression. However, the calculation is still performed here to demonstrate the strength of the shear lip.

The total possible maximum load is therefore: $(72.5 \text{ g's}) \times (1850 \text{ lbs}) = 134,125 \text{ lbs}$

The allowable shear is assumed to be 60% of the yield strength of the material (6061-T6 aluminum, assume 35ksi yield per ASTM) times the shear area. Or, $(.6)(35\text{ksi})(\text{shear area})$

Where the shear area is = lip thickness x lip perimeter. The lip thickness is 0.36 inches and the perimeter is 21.60 inches.

The shear area is = $0.36 \times 21.60 = 7.78$ sq. inches.

Then, the total allowable shear lip load (with no help from the Pillow) is:

$$= (0.6) \times (35,000\text{psi}) \times (7.78\text{sq. in.})$$

$$= 163,380 \text{ lbs.}$$

This calculation shows that the shear lip alone, with no load carried from the Pillow could decelerate the fuel assembly by itself and demonstrates the robust strength of the shear lip.

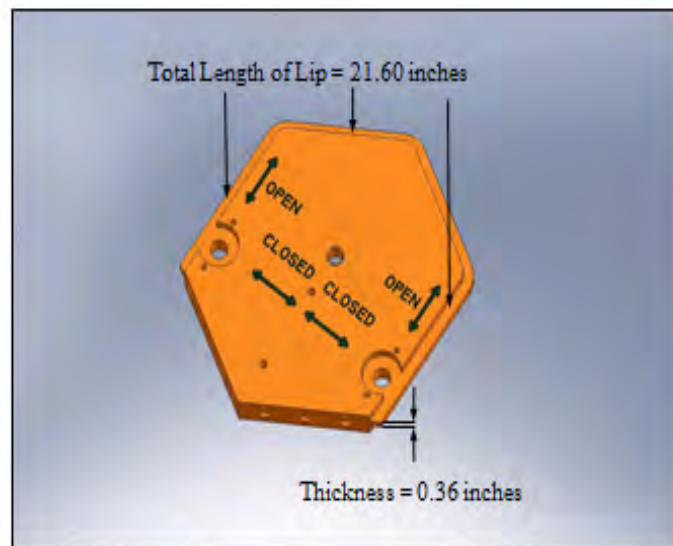


Figure 2-195 Traveller VVER Top Plate "Shear Lip"